Genetic Analysis of the Histone Chaperone Complex FACT, a Transcription Elongation Factor

by

Jennifer Rae Stevens

Submitted in partial fulfillment of the requirements
for the degree of Doctor of Philosophy

at

Dalhousie University
Halifax, Nova Scotia
August 2007

Your file Votre référence
ISBN: 978-0-494-31505-7
Our file Notre référence
ISBN: 978-0-494-31505-7

DALHOUSIE UNIVERSITY

To comply with the Canadian Privacy Act the National Library of Canada has requested that the following pages be removed from this copy of the thesis:

Preliminary Pages
- Examiners Signature Page (pii)
- Dalhousie Library Copyright Agreement (piii)

Appendices
- Copyright Releases (if applicable)

TABLE OF CONTENTS

LIST OF TABLES

LIST OF FIGURES

ABSTRACT

FACT is a highly conserved protein complex that assists in overcoming the repressive effects of chromatin for gene transcription, DNA replication, and DNA repair; however, the exact mechanisms of its actions during these processes remain unclear. FACT is found in all eukaryotes; in the budding yeast *Saccharomyces cerevisiae*, FACT is composed of two proteins: Spt16 and Pob3. My research has focused on the transcriptional involvement of the Spt16 subunit of yeast FACT, concentrating primarily on two point-mutant forms of this protein: Spt16-E857K and Spt16-E763G. These two mutations were identified by the same transcription-related dominant Spt phenotype, and affect the same region of the Spt16 polypeptide. To further understand how FACT functions in transcription, and more specifically in transcription elongation, I have identified other proteins that interact functionally with these mutant versions of Spt16. These genetic studies, in addition to my biochemical investigations, indicate that these Spt16 mutants affect FACT function in substantially different ways. My results suggest that the *spt16-E857K* mutant allele encodes a version of Spt16 protein that is impaired for its interactions with nucleosomes and/or nucleosome components, affecting the ability to reassemble nucleosomes following RNA polymerase passage. While *spt16-E857K* has a spectrum of genetic interactions that primarily involve gene deletions eliminating proteins that function in transcription, the same cannot be said about *spt16-E763G*, indicating that these two mutations affect different Spt16 protein functions. Perhaps the *spt16-E763G* mutation causes an impaired interaction between the Spt16 protein and some other protein involved in transcription, rather than a direct nucleosome reassembly defect, as suggested for Spt16-E857K. My findings further the understanding of the functional partners of FACT during transcription, and also indicate that FACT may participate in several different interactions to mediate transcription, as not all Spt16 mutant proteins demonstrate the same pattern of genetic interactions.

LIST OF ABBREVIATIONS USED

5-FOA	5-fluoro-orotic acid
CTD	C-terminal domain
DNS	downstream
EtBr	ethidium bromide
GEN	geneticin (G418)
HAT	histone acetyltransferase
HDAC	histone deacetylase
HMG	high mobility group
HRP	horseradish peroxidase
HU	hydroxyurea
NAT	nourseothricin
NTD	N-terminal domain
ORF	open reading frame
PH	pleckstrin homology
RNAPII	RNA polymerase II
SGA	synthetic genetic array
Spt	suppressor of Ty
SYNL	synthetic-lethal
UPS	upstream

Yeast Nomenclature

XYZ1	wild-type gene
xyz1	mutant gene
xyz1Δ	deleted gene
Xyz1	protein

ACKNOWLEDGEMENTS

My deepest thanks go to my supervisors, Drs. Rick Singer and Gerry Johnston. Your dedication and enthusiasm for research has made my time in their lab a wonderful learning experience. Particular thanks goes to Rick for always listening to my ideas, and for his editing and feedback during the course of writing this thesis.

To our lab technicians, Dave Carruthers, Kendra Gillis-Walker, Charlene Hubbard, and Ameer Jarrar, thank you for your assistance to this body of work. You have all contributed time and knowledge, and I appreciate your help. In particular, I would like to thank Dave Carruthers, whose expertise with tetrad analysis has been a great asset.

I would also like to thank Dr. Allyson O'Donnell, for the training and support I received upon my arrival in the Singer/Johnston lab. Without your help, this research would not have been possible.

To Rosemarie Kepkay, thank you for allowing me to be a part of your training, and for your friendship over the last few years. Thanks also to Marci Dearing, Joffre Munro, Troy Perry, Ameer Jarrar and Natalie Parks, for assistance with the experiments described here.

Thank-you to the members of my supervisory committee, Dr. Catherine Lazier, Dr. Paola Marignani, and Dr. Paul Murphy, for their advice and suggestions throughout the course of this degree. Also, thank you to all of the members, past and present, of the Dalhousie 'Yeast Group' for their time and assistance.

This research has been supported by graduate training awards from the Natural Sciences and Engineering Research Council of Canada (NSERC), and by operating grants from the Canadian Institutes for Health Research (CIHR) and NSERC, held jointly by Drs. Singer and Johnston.

Particular thanks goes to Leigh Ann Niven and Tania Wong, for your support and friendship from Day 1. It has meant so much to me. Thanks also to Jeremy Benjamin for always lightening the mood on the rough days. To all my friends and family, thank you for you love and support. Finally, to my husband Tomás, thank you for being there through the good times and the bad, and for putting up with me even when I've been at my worst.

Chapter 1 INTRODUCTION

1.1 Chromatin Structure

In eukaryotic cells, nuclear DNA is packaged with proteins into a highly compacted, tightly regulated structure known as chromatin. This chromatinization of DNA serves a two-fold purpose: it both condenses the large chromosomal DNA molecules and regulates the accessibility of DNA by other proteins such as polymerases. The basic unit of chromatin is the nucleosome, which consists of approximately 146 bp of DNA wound 1.65 times around an octameric core of histone proteins containing two each of histones H2A, H2B, H3 and H4 (Figure 1) (Luger et al. 1997, White, Suto & Luger 2001). This first level of compaction leads to an approximately 7-fold compaction in the length of the DNA molecule (Nemeth, Langst 2004). Further compaction is provided by higher-order chromatin structure. In yeast, nucleosomes are spaced approximately 160 bp apart along the DNA molecule, creating a structure sometimes referred to as a 'beads on a string' fibre, which has a diameter of approximately 10 nm (Nemeth, Langst 2004). This 10-nm fibre is then condensed into a 30-nm fibre, a process that depends on the N-terminal 'tails' of the histone proteins, and then condensed further into higher-order chromatin structures of 100-400 nm in diameter, yielding approximately a 50-fold reduction in length from the starting DNA molecule (Nemeth, Langst 2004, Peterson, Laniel 2004). While these higher-order chromatin structures most likely play a role in regulating the accessibility of the DNA molecule, these levels of organization are less well understood than is the nucleosome itself, for which the crystal structure has been solved (Luger et al. 1997, White, Suto & Luger 2001).

Within the histone octamer making up the protein core of each nucleosome, the histone proteins associate with one another in a specific fashion. Each histone protein has unstructured N- and C-terminal 'tails', and a central 'histone fold' domain, which forms a structure similar to a helix-loop-helix composed of a longer central helix flanked on each side by a shorter helix linked by a loop region (Arents et al. 1991, Luger et al. 1997). Heterodimers are formed of histones H2A and H2B, and of histones H3 and H4, through protein interactions between histone-fold domains within each histone protein (Arents et al. 1991, Luger et al. 1997). Thus, the histone octamer consists of a $(H3–H4)_2$ tetramer

A)

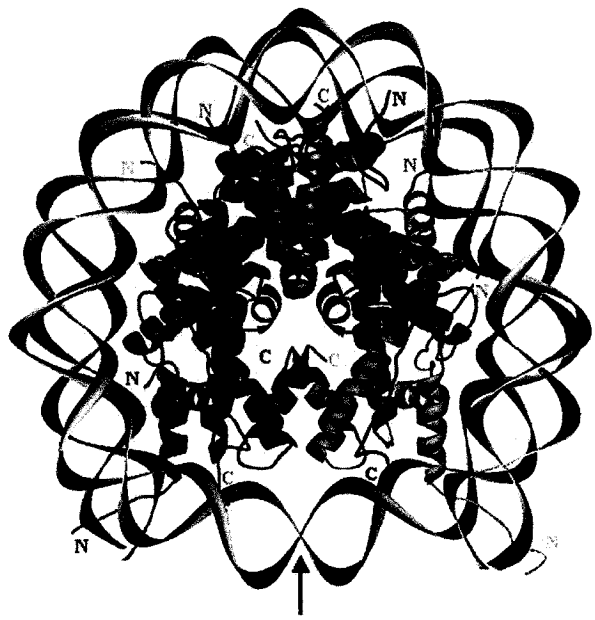

B)

Figure 1. The nucleosome. A) Nucleosome cross-section based upon crystal structure (Ramaswamy, Bahar & Ioshikhes 2005). The DNA is shown in grey, while the histones are coloured as follows (light and dark to indicate the two pairs): H2A – blue, H2B – orange, H3 – pink, H4 – green. The arrow indicates the dyad axis. B) Model of a nucleosome array (modified from Luger (2002)). The DNA is shown in dark grey, while the histones are coloured as follows: H2A – blue, H2B – green, H3 – yellow, H4 – pink. The arrows indicate locations of mutations affecting nucleosome structure.

(formed by interactions between the H3 proteins in two H3–H4 dimers), flanked on each side by an H2A–H2B dimer *via* protein interactions between histones H2B and H4 (Luger et al. 1997). Several studies have indicated that the $(H3–H4)_2$ tetramer organizes the central 121 bp of DNA, while the flanking H2A–H2B dimers organize the remainder of the nucleosomal DNA (Nemeth, Langst 2004). These observations are consistent with *in vitro* studies that have demonstrated that the deposition of H3–H4 tetramers occurs prior to the deposition of H2A–H2B dimers (Smith, Stillman 1991, Worcel, Han & Wong 1978), indicating that the H3–H4 tetramers are more stably associated with DNA than are H2A–H2B dimers. The histone 'tails' do not associate tightly with the nucleosome core, and instead protrude from the central surface of the nucleosome, where they can mediate interactions with other proteins and assist in the formation of higher-order chromatin structures (Luger et al. 1997).

Nucleosome locations within the genome appear to be at least partially dependent on DNA sequence, as certain sequences are more able to undergo the conformational changes required during nucleosome formation; nucleosome placement can therefore be predicted through analysis of DNA sequence (Ioshikhes et al. 2006, Segal et al. 2006). However, no interactions have been detected between the bases of DNA and the histone proteins (Muthurajan et al. 2003). Instead, electrostatic interactions exist between the positively charged basic amino acid side chains of the histone proteins and the negatively charged phosphate ions of the DNA backbone, and hydrogen bonding has been detected between protein amides and DNA phosphate oxygens (White, Suto & Luger 2001). Overall, approximately 120 direct protein–DNA interactions exist between the histone proteins and the DNA backbone in each nucleosome (Luger 2003, Luger 2006, Nemeth, Langst 2004), while reports of the number of indirect interactions indicate 120 to 350 water-bridged interactions for each nucleosome (Luger 2003, Nemeth, Langst 2004). This large number of interactions stabilizing nucleosome structure undoubtedly has effects on the accessibility of nucleosomal DNA; therefore, the modulation of chromatin structure is an important factor in processes that require access to DNA, such as transcription.

1.2 Modulation of Chromatin Structure

Due to the repressive nature of chromatin, multiple types of proteins modulate chromatin structure and thereby regulate chromatin-mediated processes such as transcription. Among these components are three types that directly interact with histone proteins: 1) ATP-dependent chromatin remodelling complexes, 2) enzymes that covalently modify histones, and 3) histone chaperones.

1.2.1 ATP-Dependent Chromatin Remodellers

Members of this class of protein complexes use the energy derived from ATP hydrolysis to physically move nucleosomes along a DNA molecule by weakening the interactions between the histone proteins and DNA (Saha, Wittmeyer & Cairns 2006a). This nucleosome movement is believed to regulate the accessibility of DNA sequences contained within nucleosomal regions to DNA-binding proteins. Chromatin remodelling complexes comprise a large family with at least five subgroups, but which all have catalytic subunits sharing a common ATPase domain (Saha, Wittmeyer & Cairns 2006b). These five subgroups consist of the SWI/SNF, ISW1, NURD/Mi-2/CHD, INO80, and SWR1 families of nucleosome remodellers (Saha, Wittmeyer & Cairns 2006a). During transcription, chromatin remodellers have been implicated in both the initiation stage, where they are recruited by activators to help make DNA more accessible, and the elongation stage, where they assist in overcoming nucleosomal blocks to transcription (Li, Carey & Workman 2007, Saha, Wittmeyer & Cairns 2006a, Saha, Wittmeyer & Cairns 2006b).

1.2.2 Covalent Modifications of Histone Proteins

Chromatin structure can also be affected by covalent modifications of amino acid sidechains of the histone proteins. The modifications include, but are not limited to, acetylation, methylation, ubiquitination and phosphorylation, and most modifications are reversible (Berger 2007, Kouzarides 2007, Millar, Grunstein 2006). Most histone modifications occur on residues within the unstructured 'tails' of the histone proteins, although several modified sites reside within the histone cores (Berger 2007). These modifications have various effects, both direct and indirect. Some modifications lead to alterations in chromatin structure, while others direct the recruitment of other proteins, *via* specific binding domains, to the modified nucleosomes (Berger 2007, Kouzarides

2007). Protein domains that recognize modified histones include bromodomains, which recognize acetylated lysine residues, and PHD, WD-40 and 'royal family' (chromo, tudor, and MBT) domains, which recognize methylated lysine residues (Berger 2007, Kouzarides 2007, Millar, Grunstein 2006). Various histone modifications are associated with specific chromatin states, such as transcriptionally active or silenced regions (Millar, Grunstein 2006). In general, acetylation and phosphorylation are associated with regions of active transcription, whereas methylation can be associated with either activation or repression of transcription, depending on the location of the methylation within the histone protein (Berger 2007, Kouzarides 2007, Millar, Grunstein 2006).

Several enzyme families carry out histone modifications; for example, the histone acetyltransferases carry out acetylation of lysine residues, while the histone methyltransferases carry out methylation of lysine or arginine residues (Berger 2007, Kouzarides 2007, Millar, Grunstein 2006). In addition, other protein complexes regulate the removal of these covalent modifications: histone deacetylases remove acetyl groups, while methyl groups on lysine residues, which until recently were thought to be irreversible modifications, are removed by histone demethylases (a somewhat different process appears to be used for methylated arginine residues) (Berger 2007, Kouzarides 2007).

In this thesis, I have utilized mutations affecting many of these histone modifications, specifically those with roles in the transcription process. Included in this group are mutations affecting the histone acetyltransferases Sas3, Gcn5, Elp3, Esa1, and Rtt109, the histone deacetylase complex Rpd3C(S), the histone methyltransferases COMPASS and Set2, the histone demethylase Jhd1, and the histone ubquitinase Rad6.

1.2.3 Histone Chaperones

Histone chaperones are proteins that bind histones and facilitate their deposition onto DNA (Loyola, Almouzni 2004, Tyler 2002, Workman 2006). Generally, histone chaperones have a preference for either H2A–H2B or H3–H4 dimers (Loyola, Almouzni 2004). Histone chaperones can function to deposit histones during DNA replication onto newly synthesized DNA, and/or can function in replication-independent nucleosome assembly that, for example, restores chromatin structure following transcription. Included in this group of replication-independent histone chaperones is the FACT complex, which

is the focus of my research. FACT functions as a histone chaperone *in vitro* (Belotserkovskaya et al. 2003), and is discussed in more detail in Section 1.4. Other histone chaperones discussed in this thesis include Spt6, Nap1, CAF-1, HirC, Asf1, Rtt106, and Vps75.

The Spt6 protein is thought to play a role similar to that of FACT in maintaining chromatin structure during transcription (Adkins, Tyler 2006, Kaplan, Holland & Winston 2005). Spt6 directly interacts with histones, primarily with histone H3, and thus may function as a chaperone for H3–H4 dimers or tetramers (Bortvin, Winston 1996). Another histone chaperone, the Nap1 protein, also shows preferential binding to histones H3 and H4 *in vitro*, while *in vivo* studies have also shown interactions with H2A–H2B dimers (Park, Luger 2006). For example, Nap1 is involved in the nuclear import of histones H2A and H2B (Mosammaparast, Ewart & Pemberton 2002), and *in vitro* transcription studies have shown that Nap1, like FACT, is able to disassociate one H2A-H2B dimer from a nucleosome encountered by actively transcribing RNAPII (Levchenko, Jackson 2004).

CAF-1 and HirC are two multi-subunit histone chaperones. CAF-1 (Chromatin Assembly Factor 1) participates in nucleosome assembly during DNA replication (Smith, Stillman 1989), while HirC, the yeast homologue of mammalian HIRA (Lamour et al. 1995), participates in replication-independent nucleosome assembly (Green et al. 2005, Prochasson et al. 2005). The Asf1 protein is a chaperone for histones H3 and H4 (English et al. 2005) and functions in both replication-linked and replication-independent chromatin assembly. Asf1 stimulates CAF-1 activity during replication-dependent chromatin assembly through protein interactions with the Cac2 subunit of the CAF-1 complex (Tyler et al. 1999, Tyler et al. 2001), while Asf1 function in replication-*in*dependent chromatin assembly involves protein interactions with HirC (Green et al. 2005).

Rtt106 is a recently identified histone chaperone, and although its cellular role is not fully understood, binding studies have shown that Rtt106, like the Asf1 protein, binds to histones H3 and H4 and also to one of the CAF-1 subunits, Cac1 (Huang et al. 2005). Vps75 is another recently identified histone chaperone that shows *in vitro* binding to H3–H4 tetramers, and shares sequence and structural similarity with Nap1 and its

homologues from other species (Selth, Svejstrup 2007). While little is known about the actions of Vps75 *in vivo*, it has been shown to exist in a complex with the Rtt109 histone acetyltransferase (Han et al. 2007, Selth, Svejstrup 2007, Tsubota et al. 2007).

1.3 Factor that Facilitate Transcription Through Chromatin

Many of the proteins discussed in the previous section play a role in mediating the transcription process in the context of chromatin. In addition, there are transcription elongation factors that facilitate the passage of RNAPII, but which may not easily group into any of the above three categories (Li, Carey & Workman 2007). Although these other proteins may not directly bind or modify histones, they do facilitate the transcription process, sometimes by assisting the recruitment of histone modification factors or modifying RNAPII itself. Several of these factors have been investigated in more detail in this thesis, particularly the Spt4–Spt5 complex, the Paf complex, and two protein kinases involved in transcription, Bur kinase and CTDK-1.

The Spt4–Spt5 complex is involved in transcription elongation, and is the yeast homologue of mammalian DSIF (Hartzog et al. 1998, Wada et al. 1998). The *SPT4* and *SPT5* genes were identified by the same phenotype as that used to find the histone-chaperone gene *SPT6* (Fassler, Winston 1988, Winston et al. 1984), and mutations in all three genes have similar phenotypes (Swanson, Winston 1992). The exact role of Spt4–Spt5 is unknown, but recent studies suggest that it may serve as a docking platform for the recruitment of PafC (Qiu et al. 2006). PafC is a multi-subunit complex involved in both transcription initiation and elongation (Mueller, Jaehning 2002, Squazzo et al. 2002), and has been shown to localize throughout the coding regions of ORFs, an association which requires the Spt4 protein of Spt4–Spt5 (Qiu et al. 2006).

Bur kinase and CTDK-1 have both been suggested as potential yeast orthologues of P-TEFb (Lee, Greenleaf 1997, Wood, Shilatifard 2006), a mammalian protein kinase that phosphorylates RNAPII on serine 2 of its C-terminal domain repeat during transcription (Marshall et al. 1996, Price 2000, Ramanathan et al. 2001). Phosphorylation of serine 2 is linked to the elongation phase of transcription, and allows the recruitment of proteins involved in processing the 3' end of the mRNA (Ahn, Kim & Buratowski 2004). While it is likely that CTDK-1 carries out at least some P-TEFb activities *in vivo*, it is

clear that Bur kinase is involved in transcription elongation (Yao, Neiman & Prelich 2000), although proteins other than RNAPII may be phosphorylated by Bur kinase *in vivo*. One target of Bur kinase is the Rad6 protein, which ubiquitinates histone H2B on Lys123 (Wood et al. 2005). This ubiquitination leads to another histone modification associated with actively transcribed regions, methylation of H3 lysine 4 by COMPASS (Dover et al. 2002, Sun, Allis 2002). Another potential target of Bur kinase is the Spt5 protein, which contains tandem repeats in its C terminus (Swanson, Malone & Winston 1991). In other systems, these repeats have been shown to be phosphorylation targets by Bur kinase analogs (Bourgeois et al. 2002, Ivanov et al. 2000, Kim, Sharp 2001, Pei, Shuman 2003, Yamada et al. 2006). Phosphorylation of human Spt5 is thought to mediate its transition from a repressor of transcription to a positive transcription elongation factor (Yamada et al. 2006), and thus, a similar situation may hold true for yeast Spt5.

1.4 The FACT Complex

The FACT complex (Facilitates Chromatin Transcription) was originally isolated as a component of HeLa cell extract that can overcome the blockage to *in vitro* transcription posed by nucleosomes (Orphanides et al. 1998). As described above, FACT possesses histone chaperone activity (Belotserkovskaya et al. 2003), and neither requires ATP nor covalently modifies histones in its actions (Orphanides et al. 1998, Orphanides et al. 1999). FACT homologues have been independently identified in *Xenopus* and in the budding yeast *Saccharomyces cerevisiae* as having roles in both replication and transcription. The *Xenopus* FACT homologue was identified as the DUF (DNA Unwinding Factor) complex, and was shown to unwind closed circular DNA and play a role in DNA replication (Okuhara et al. 1999), whereas yeast FACT was isolated both as a factor involved in chromatin repression (as the CP complex) (Brewster, Johnston & Singer 1998) and as a protein with a role in DNA replication (Wittmeyer, Joss & Formosa 1999).

1.4.1 FACT Composition and Conservation

The components of both yeast and human FACT are highly similar (Brewster, Johnston & Singer 2001, Orphanides et al. 1999, Wittmeyer, Formosa 1997). In yeast, FACT is composed of three protein subunits: Spt16 (also called Cdc68) and Pob3, which form a

highly stable heterodimer, along with Nhp6, which transiently associates with the Spt16–Pob3 dimer (Figure 2) (Brewster, Johnston & Singer 1998, Brewster, Johnston & Singer 2001, Formosa et al. 2001, Wittmeyer, Joss & Formosa 1999). A similar organization is present in human FACT, although human FACT contains just two subunits: hSpt16 and SSRP1 (Orphanides et al. 1999). The Spt16 subunits from yeast and human are 36% identical, and the Spt16 protein is highly conserved among many eukaryotes along its entire length (Evans et al. 1998, Orphanides et al. 1999). Yeast Pob3 is highly homologous to the N-terminal 75% of the human SSRP1 protein, having 33% identity and 45% similarity throughout this region (Wittmeyer, Formosa 1997). Interestingly, the C-terminal 25% of human SSRP1 shares homology with the third subunit of yeast FACT, the Nhp6 protein (Brewster, Johnston & Singer 2001, Formosa et al. 2001); this region corresponds to the High Mobility Group (HMG) domain of SSRP1 (Orphanides et al. 1999). Indeed, the yeast Nhp6 protein is essentially a single HMG1 motif (Costigan, Kolodrubetz & Snyder 1994), and thus Pob3 and Nhp6 together may represent the yeast analogue of SSRP1 (Brewster, Johnston & Singer 2001). The existence of Nhp6 as a separate, transiently associated, protein within yeast FACT represents a primary difference from human FACT, in which the HMG motif, as a part of SSRP1, is an integral component of the FACT complex. However, only about 5% of Nhp6 protein is found to co-purify with the Spt16–Pob3 dimer, suggesting that Nhp6 may have roles outside of its involvement in FACT functions (Brewster, Johnston & Singer 2001, Formosa et al. 2001). This hypothesis is supported by reports that have shown that Nhp6 plays a role in the regulation of transcription initiation by RNA Polymerase III (Braglia et al. 2007, Kassavetis, Steiner 2006, Kruppa et al. 2001, Martin, Gerlach & Brow 2001), and during RNAPII transcription initiation to aid in the recruitment of TATA-binding protein to promoters (Biswas et al. 2004, Biswas et al. 2006, Yu et al. 2003).

1.4.2 FACT Domain Structure

The yeast Spt16 protein is a 118-kDa, 1 035-residue protein that is essential for viability; Spt16 has a highly acidic C terminus and is encoded by an open reading frame of 3 105 bp (Malone et al. 1991, Rowley, Singer & Johnston 1991). The Pob3 protein is a 63-kDa, 552-residue protein that, like Spt16, is essential for viability; Pob3, again like Spt16, has a highly acidic C terminus and is encoded by an open reading frame of 1 659 bp

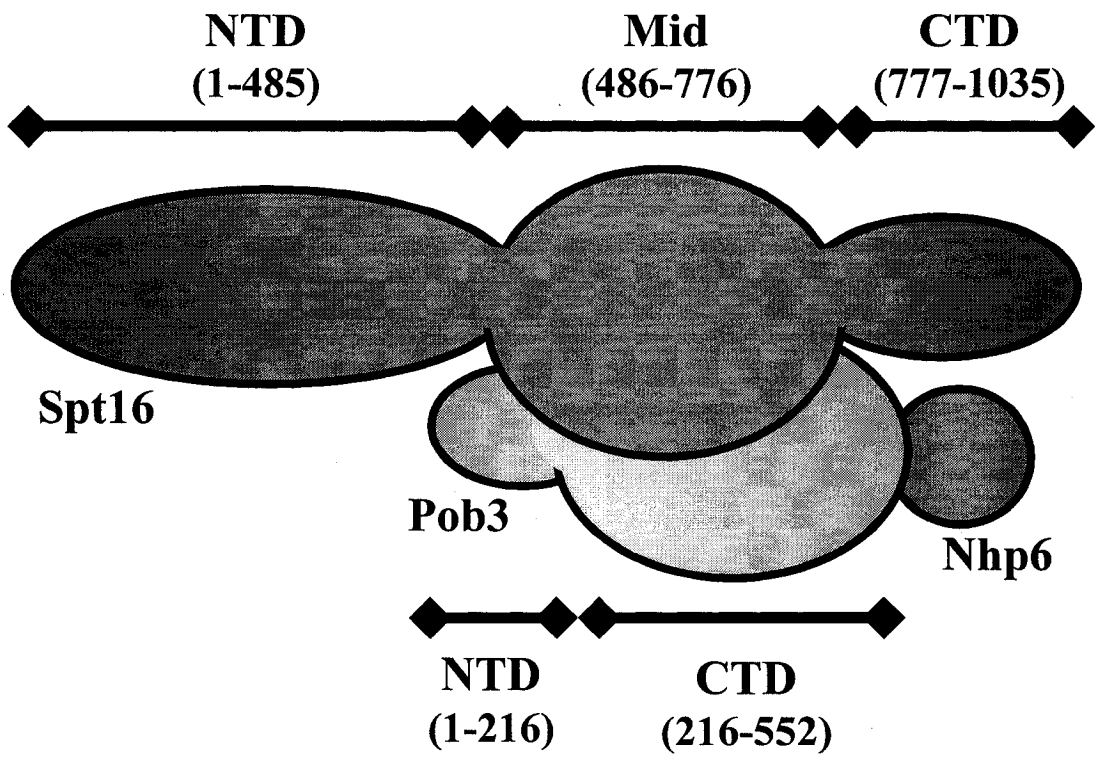

Figure 2. Domain structure of yeast FACT. The yeast FACT complex, consisting of Spt16, Pob3, and the transiently associated subunit, Nhp6 is shown here in cartoon form. The domain boundaries predicted by O'Donnell *et al.* (2004) are shown for Spt16 and Pob3.

(Wittmeyer, Formosa 1997). One recent study used partial proteolysis to suggest that Pob3 might consist of two domains: a 23-kDa NTD and a 40-kDa CTD (Figure 2) (O'Donnell et al. 2004). Similar results were obtained in a second study, although some differences in domain boundaries were reported. In this study, Pob3 was reported to contain three domains: an NTD/Dimerization domain (residues 1 to approximately 200 [the C-terminal end of this domain was not indicated]), a Mid domain (residues 237-477), and a CTD (residues 477-552) (VanDemark et al. 2006). Crystallization studies of the Pob3 Mid domain indicate that this portion of the Pob3 protein constitutes a novel subgroup within the pleckstrin homology (PH) domain family, and folds into a double PH domain (VanDemark et al. 2006). This structure is likely important for Pob3 function, as conserved residues cluster on one section of the double PH domain, and mutations in this region cause defects in Pob3 function in replication and transcription (VanDemark et al. 2006).

The same study that reported two domains for Pob3 also indicated by partial proteolysis that the Spt16 polypeptide is comprised of three independently folded domains (Figure 2): a 55-kDa N-terminal domain (NTD) consisting of residues 1-485, a 34-kDa Mid domain consisting of residues 486-776, and a 28-kDa C-terminal domain (CTD) consisting of residues 777-1 035 (O'Donnell et al. 2004). The NTD is not essential for Spt16 function, as a mutant version of Spt16 lacking the entire NTD (Spt16-ΔNTD) provides all essential functions of Spt16 (O'Donnell et al. 2004). Although the Spt16 NTD is not required for essential Spt16 functions, cells containing the Spt16-ΔNTD version instead of full-length Spt16 protein are sensitive to agents that cause replication stress, such as hydroxyurea and methylmethane sulfonate, suggesting a role for the NTD of Spt16 in overcoming replication stress (O'Donnell et al. 2004). The Mid domain of Spt16 mediates binding with Pob3, while the CTD is not required for this interaction (O'Donnell et al. 2004). The CTD of Spt16 is thought to be required for essential function, as versions of Spt16 truncated approximately at residue 764 and 915 do not support life (Evans et al. 1998). Indeed, the C-terminal region of the human Spt16 polypeptide is necessary for the *in vitro* histone-binding and histone-chaperone activity of Spt16 (Belotserkovskaya et al. 2003).

In a second study, yeast Spt16 was reported to contain four domains: an NTD (residues 1-440), a Dimerization domain (residues 527-630), a Mid domain (residues 630-959), and a CTD (959-1035) (VanDemark et al. 2006). The primary differences between this report and the previously discussed one are the boundaries of the Mid and C-terminal domains for Spt16. In the report by O'Donnell *et al.* (2004), the Mid domain of Spt16 comprises residues 486-776, while the CTD consists of residues 777-1 035. However, VanDemark *et al.* (2006) report that this portion of the Spt16 polypeptide actually consists of three domains: the Dimerization domain, the Mid domain, and the CTD, which is mainly the highly acidic C-terminal end of Spt16. This may reflect differences in experimental design in the two studies, resulting in different regions of the Spt16 polypeptide accessible to proteolysis. However, the proposed functions of the different regions of the Spt16 protein are fairly consistent between the two studies.

1.4.3 The Role of FACT in Transcription

From the original observations that mutations in the yeast *SPT16/CDC68* gene have effects on transcript abundance (Rowley, Singer & Johnston 1991) and alter the regulation of transcription from cryptic promoters (Malone et al. 1991), a role for Spt16 in gene expression has been suggested. The same mutation in *SPT16*, *spt16-G132D*, was independently identified by three different investigations (Evans et al. 1998) assessing three different effects on transcription: decreased transcript abundance for several genes, altered expression of reporter genes that rely on cryptic promoters (the Spt phenotype), and altered expression of an *HO::lacZ* reporter construct (Lycan et al. 1994, Malone et al. 1991, Rowley, Singer & Johnston 1991). Several observations from these early investigations suggested that Spt16 has a positive effect on transcription. One such line of evidence comprises the observations that *spt16* mutations cause decreased transcript abundance (Lycan et al. 1994, Rowley, Singer & Johnston 1991, Xu, Johnston & Singer 1993, Xu, Singer & Johnston 1995).

In contrast to the above findings suggesting a positive role for Spt16, other observations suggest that Spt16 negatively regulates transcription. Mutations in *SPT16* allow expression of what are termed here the Spt reporter genes, by allowing transcription to initiate from sites that are normally repressed. The Spt reporter genes *his4-912δ* (Farabaugh, Fink 1980, Roeder, Fink 1980) and *lys2-128δ* (Clark-Adams,

Winston 1987), contain DNA insertions, called δ elements, which interfere with the normal transcription of these loci (Figure 3) (Clark-Adams, Winston 1987, Silverman, Fink 1984). Thus, in otherwise normal cells, functional *HIS4* or *LYS2* transcripts fail to be produced, and consequently the cells are auxotrophic for histidine and lysine. In cells with an Spt phenotype, such as those containing *spt16* mutations, aberrant transcription from the *his4-912δ* and *lys2-128δ* loci leads to the production of functional transcripts, and as a result the cells are prototrophic for histidine and lysine (Evans et al. 1998, Malone et al. 1991). This aberrant transcription is thought to occur through loss of repression, thus suggesting a role for Spt16 in negatively regulating transcription. Several other lines of evidence support a role for Spt16 in the negative regulation of transcription. First, the *spt16-G132D* mutation allows activation of an *HO::lacZ* reporter construct when the usual activators of *HO* transcription, the Swi4 and Swi6 activators, are absent, indicative of a role for Spt16 in repression (Lycan et al. 1994). Second, mutations in *SPT16* allow expression of a mutant *SUC2* gene that is missing its upstream activation sequence (*suc2ΔUAS*) and thus cannot recruit transcriptional activators (Evans et al. 1998, Malone et al. 1991, Prelich, Winston 1993). These types of alterations in gene expression are also seen with mutations in other components that affect chromatin structure. Taken together, these findings indicate that Spt16 may play a role in both activation and repression of transcription, and may do so through modulation of chromatin structure.

The identification of human FACT as a component that promotes *in vitro* transcription through a nucleosomal template (Orphanides et al. 1998), and the subsequent identification that mammalian FACT is composed of homologues of the yeast Spt16 and Pob3 proteins (Orphanides et al. 1999), further support an involvement of FACT in transcription. In addition, the observation that human FACT is unable to promote transcription of a nucleosomal template containing covalently cross-linked histones suggests that FACT activity includes modulation of chromatin structure (Orphanides et al. 1999). Results from other systems also suggest an integral role for FACT in the transcription process: FACT co-localizes with RNAPII along polytene chromosomes in *Drosophila* (Saunders et al. 2003), and associates with actively transcribed regions in *Arabidopsis* (Duroux et al. 2004). A similar association of Spt16

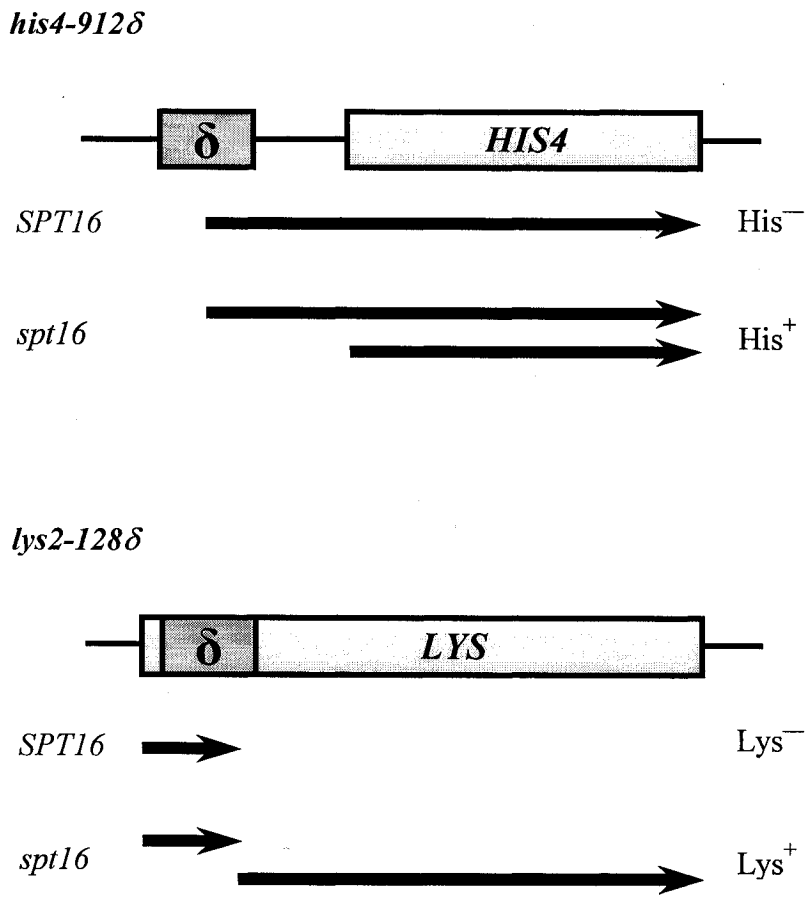

Figure 3. The Spt reporter genes *his4-912δ* and *lys2-128δ*. For each gene, the location of the δ element (the long terminal repeat of the yeast Ty transposon) insertion relative to the coding region is shown. Also, the transcripts produced in both normal (*SPT16*) and mutant (*spt16*) cells (Malone et al. 1991), and the resulting histidine and lysine auxotrophy (–) or prototrophy (+), are indicated.

along transcribed regions has been observed in yeast, where FACT has been shown to co-localize with actively transcribing RNAPII *in vivo* (Kim et al. 2004, Mason, Struhl 2003).

Also in yeast, Spt16 has been shown to physically associate with other transcription-associated proteins. Protein interactions have been observed between Spt16 and PafC components (Krogan et al. 2002, Squazzo et al. 2002), Spt5 (Lindstrom et al. 2003), histone proteins (Krogan et al. 2002), and Chd1 (Krogan et al. 2002, Simic et al. 2003), a transcription-elongation component involved in ATP-dependent chromatin remodelling (Tran et al. 2000). In addition to these protein interactions, deleterious genetic interactions have been observed when mutations in *SPT16* are combined with mutations in genes encoding PafC members (Squazzo et al. 2002) or components of the transcription initiation machinery, such as TFIIA and TBP (Biswas et al. 2005, Biswas et al. 2006). Deleterious genetic interactions are also observed in cells containing mutations affecting histones and nucleosomes, such as direct alterations of histone dosage and mutations in the genes encoding components of the HirC histone chaperone (Formosa et al. 2002). These physical and genetic interactions suggest a role for Spt16 and the FACT complex in both transcription initiation and transcription elongation.

Although early studies have linked FACT with a role in mediating chromatin structure during the transcription process, some time elapsed before a mechanism for FACT activity during transcription was suggested (Belotserkovskaya et al. 2003, Belotserkovskaya et al. 2004, Belotserkovskaya, Reinberg 2004). In this model, FACT is thought to remove one H2A–H2B dimer from the nucleosome ahead of the actively transcribing RNAPII, and the resulting modified nucleosome, or 'hexamer', somehow promotes polymerase passage along this portion of DNA (Figure 4, steps 1-3). FACT is thought to then reassemble the nucleosome and help to re-establish proper chromatin structure following RNAPII passage (Figure 4, step 4). This model is consistent with observations from genetic studies suggesting that FACT plays a role in the maintenance of proper chromatin structure, thus repressing transcription from cryptic promoters within the coding regions of several genes (Kaplan, Laprade & Winston 2003), and may explain the observation that depletion of FACT causes the deposition of components of pre-initiation complexes within coding regions (Mason, Struhl 2003).

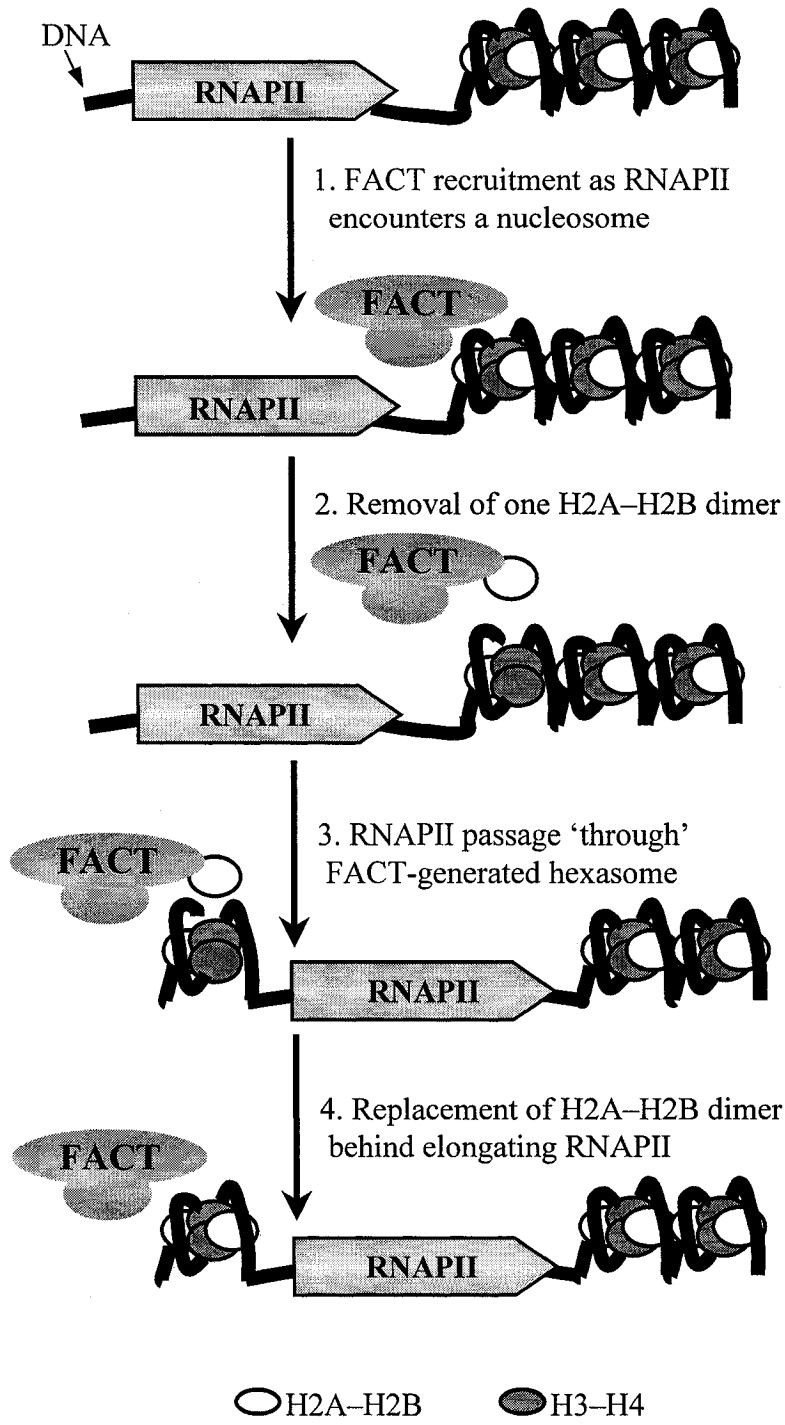

Figure 4. Model for FACT activity during RNAPII transcription. Modified from O'Donnell (2004).

Further studies have suggested a link between FACT activity and covalent histone modifications, specifically histone H2B monoubiquitination. It is thought that this monoubiquitination of histone H2B may facilitate FACT-mediated removal of a single H2A–H2B dimer from the nucleosome ahead of an actively transcribing RNAPII (Pavri et al. 2006, Reinberg, Sims 2006). Regardless of whether H2B ubiquitination actually facilitates FACT activity, or whether this histone modification works in a parallel fashion with FACT to facilitate RNAPII-mediated transcription, these results aid our understanding of how the various factors linked to transcription work together to facilitate transcription through a chromatin template.

1.5 Genetic Studies to Further Our Understanding of Spt16 Function

Previous research in our lab has focused on understanding the role of Spt16 in transcription by identifying new mutations in *SPT16* that cause a dominant Spt phenotype, indicating that these mutant alleles affect the ability of Spt16 to function normally during transcription (O'Donnell 2004, Perry 2005). The research described in this thesis focuses on one of these new mutant alleles, *spt16-E857K*, encoding a single glutamate-to-lysine substitution at residue 857 of the Spt16 polypeptide. To determine what effects this substitution has on the function of the Spt16 protein and, more generally, to understand how FACT functions during transcription, I have used this mutant allele to identify other proteins that interact functionally with the Spt16-E857K mutant protein. These investigations suggest that the *spt16-E857K* mutant allele encodes a version of the Spt16 protein that is impaired for interactions with nucleosomes, either directly or indirectly, and that this impairment affects the ability of FACT to reassemble nucleosomes following RNAPII passage during transcription.

Chapter 2 MATERIALS AND METHODS

2.1 Media and Growth Conditions

2.1.1 Yeast Growth Media

YM1 rich liquid medium contained 1% succinic acid, 0.6% sodium hydroxide, 1% peptone, 0.67% yeast nitrogen base without amino acids, and 2% dextrose (Hartwell 1967). YEPD rich solid medium contained 1% yeast extract, 2% peptone, 2% dextrose, and 2% agar (Hartwell 1967). YNB synthetic minimal medium contained 1% succinic acid, 0.6% sodium hydroxide, 0.67% yeast nitrogen base without amino acids or ammonium sulphate, and 2% dextrose (Johnston, Pringle & Hartwell 1977). This medium was supplemented with 0.1% ammonium sulphate, amino acids (40 μg/ml) and nucleoside bases (20 μg/ml) (listed below), unless the absence of one or more was required to maintain plasmid selection during growth, or to determine auxotrophies. The same recipe was utilized for solid synthetic complete (SC) medium, with the addition of 2% agar. The following amino acids and nucleoside bases were added to both types of YNB medium prior to use: arginine, aspartic acid, histidine, isoleucine, leucine, lysine, methionine, phenylalanine, serine, tryptophan, threonine, tyrosine, valine, adenine, and uracil. Except where noted otherwise, cells were grown at 30°C.

Several chemicals were added to growth media. Hydroxyurea (Sigma-Aldrich, Oakville, ON) was added to YEPD solid medium at a concentration of either 50 mM or 100 mM, to test for drug sensitivity indicating replication defects (Hampsey 1997). Nourseothricin (clonNAT) (Werner BioAgents, Germany) and geneticin (G418) (Invitrogen, Burlington, ON) were added to YEPD solid medium at concentrations of 100 mg/l and 200 mg/l, respectively, to select for resistance to these drugs, indicating presence of the *natMX4* and *kanMX4* marker, respectively (Tong et al. 2001). The analogue 5-fluoro-orotic acid (5-FOA) (BioVectra, Charlottetown, PE) was added to supplemented YNB solid medium at a concentration of 0.33 g/l, and allows counterselection against the growth of cells containing *URA3*-based plasmids.

Growth of yeast cells was often asessed by either replica-plating or serial-dilution spot testing. In both cases, the cells were grown on the indicated solid medium for durations between 1 and 7 days, depending on the type of solid medium and the growth

temperature. Generally, cells grown on YEPD solid media were incubated for durations between 1 and 3 days, while cells grown on YNB dropout solid media were incubated for durations between 3 and 7 days.

Sporulation of diploid cells was performed by first growing cells overnight in pre-sporulation liquid medium, followed by 5-7 days in sporulation liquid medium, both at 23°C. Pre-sporulation medium consisted of YM1 rich liquid medium containing 4% dextrose, rather than the 2% used in 'regular' YM1, while sporulation medium consisted of 1% potassium acetate, 0.1% yeast extract, and 0.05% dextrose (Guthrie, Fink 1991).

2.1.2 *E. coli* Growth Media

Escherichia coli (*E. coli*) cells were grown in 2xYT liquid medium, consisting of 1.6% tryptone, 1% yeast extract and 0.5% sodium chloride (Messing 1983). 2xYT solid medium was prepared by addition of 2% agar to the above mixture. To select for cells containing a plasmid (plasmids contained an ampicillin-resistance gene), ampicillin was added to 2xYT (liquid or solid) at a concentration of 50 μg/ml. *E. coli* cells of the strain TOP10 were employed for all plasmid work, except for the selection of *LEU2* plasmids, as described below. All *E. coli* growth was performed at 37°C.

To select for the presence of *LEU2* yeast plasmids, *E. coli* cells of the strain JF1754 (*lac, gal, metB, leuB, hisB436, hsdR*) were used, selecting for growth on M9 medium lacking leucine (Sambrook, Fitsch & Maniatis 1989). The yeast *LEU2* gene can complement *E. coli leuB* auxotrophy, meaning that JF1754 cells containing a *LEU2* plasmid are leucine prototrophs. M9 medium was prepared as follows: a 5X M9 salt stock solution was prepared, containing 30 g/l sodium phosphate, 15 g/l potassium phosphate, 5 g/l ammonium chloride, 2.5g/l sodium chloride, and 15 mg/l calcium chloride. For each litre of M9 medium, 200 ml of this salt solution was used, with the addition of 2% dextrose, 5 x 10^{-4}% thiamine, 1 mM magnesium sulphate, ampicillin to 50 μg/ml, amino acids to 40 μg/ml (arginine, aspartic acid, histidine, isoleucine, lysine, methionine, phenylalanine, serine, tryptophan, threonine, tyrosine, and valine), nucleoside bases to 20 μg/ml (uracil and adenine), and 2% agar. Leucine was omitted, so that the only JF1754 *E. coli* cells that are able to grow on this M9 medium are those that contain a plasmid-borne yeast *LEU2* gene.

2.2 Yeast Strains

The *Saccharomyces cerevisiae* strains used in this research are listed in Table 1.

2.2.1 BY4741-Derived Deletion Strains

All deletion strains used in this research (*hht1Δ*, *hhf1Δ*, *asf1Δ*, *nap1Δ*, *rtt106Δ*, *vps75Δ*, *ctk1Δ*, *swd1Δ*, *swd3Δ*, *rad6Δ*, *spt4Δ*, *set2Δ*, *eaf3Δ*, *rco1Δ*, *sin3Δ*, *rpd3Δ*, *jhd1Δ*, *sas3Δ*, *elp3Δ*, *gcn5Δ*, and *rtt109Δ*) were confirmed using PCR-based procedures (PCR as per Section 2.4.7; primers listed in Table 3). For these strains, primers hybridizing approximately 200 bp outside the integrated *kanMX4* drug-resistance cassette (forward and reverse) were paired with primers internal to this cassette (KanB and KanC), and the presence of a product was monitored (forward + KanB = ~500 bp; reverse + KanC = ~850 bp – Figure 5). When no product was observed, a second PCR reaction was performed using the outside forward primer, and both reverse primers. In this second reaction a product should always be formed, provided the PCR reaction is working, and the presence of the *kanMX4* cassette can be assessed by the presence of the smaller (500-bp) product, if not by a difference in size of the larger band.

Each of the deletion strains was confirmed in this manner, and all except *rpd3Δ* were found to contain the *kanMX4* cassette at the correct locus, indicating that the gene deletion/replacement is present in each strain. For the supposed *rpd3Δ* strain, PCR procedures provided no evidence of the *kanMX4* cassette at the *RPD3* locus, and the size of the amplicon using the two outside primers was consistent with full-length *RPD3*, rather than *rpd3Δ::kanMX4*. This finding suggests that the strain labelled *rpd3Δ* in our deletion collection does not, in fact, contain an *RPD3* deletion.

Upon tetrad analysis, three deletion/replacement strains, *spt4Δ*, *ctk1Δ*, and *vps75Δ*, were found to contain two *kanMX4* insertions (geneticin resistance did not segregate 2:2). For the *ctk1Δ* segregants, no deleterious genetic interaction was observed for any of the *spt16-E857K* geneticin-resistant segregants; therefore, no further steps were taken with this strain. For the *vps75Δ* segregants, different levels of growth were observed among the geneticin-resistant double mutants with both *spt16-E857K* and, to a lesser extent, *spt16-E763G*. Therefore, PCR was performed on these segregants to determine which contained the *vps75Δ::kanMX4* replacement, which allowed evaluation

Table 1. Yeast strains used in this study.

Strain	Description and Genotype	Source
BY4741-based deletions[1]	*MAT***a** *met15Δ0 his3Δ1 leu2Δ0 ura3Δ0 xyzΔ::kanMX4* (see note 1 for list)	EUROSCARF deletion collection (Tong et al. 2001)
FY362	*MAT***a** *his4-912δ ade8-104 spt5-194*	Fred Winston, Harvard University
FY1668	*MAT***a** *his4-912δ lys2-128δ spt5-4*	(Hartzog et al. 1998)
FY139	*MAT***a** *his4-192δ lys2-128δ ura3-52 ade8-104 spt6-140*	Fred Winston, Harvard University
FY2180	*MAT***a** *leu2Δ1 his4-912δ lys2-128δ FLAG-spt6-1004*	(Kaplan, Laprade & Winston 2003)
KY688	*MAT***a** *lys2Δ0 ura3Δ0 trp1Δ63 cdc73Δ::kanMX4*	Karen Arndt, University of Pittsburgh
KY690	*MAT***a** *lys2-128δ leu2Δ1 ura3-52 leo1Δ::URA3*	(Squazzo et al. 2002)
KY693	*MAT***a** *leu2Δ1 ura3Δ0 trp1Δ63 ctr9Δ::kanMX4*	Karen Arndt, University of Pittsburgh
KY802	*MAT***a** *his3Δ200 lys2-173R2 ura3(Δ0 or –52) paf1Δ::URA3*	(Braun et al. 2007)
KY957	*MAT***a** *his3Δ200 leu2Δ1 trp1Δ63 ura3-52 rtf1Δ::LEU2*	(Braun et al. 2007)
LPY3500	*MAT***a** *his3Δ200 leu2-3,112 trp1Δ1 ura3-52 esa1Δ::HIS3 esa1-L254P::URA3*	(Clarke et al. 1999)
JS34	*MAT***a** *MET15? LYS2 his3Δ1 leu2Δ0 ura3Δ0 spt4Δ::kanMX4*	*spt4Δ* X Y2454 (Tong et al. 2001)
JS35	*MAT***a** *MET15? LYS2 his3Δ1 leu2Δ0 ura3Δ0 spt4Δ::kanMX4*	*spt4Δ* X Y2454 (Tong et al. 2001)
AW11-9a[2]	*MAT*α *his4-912δ lys2-128δ leu2-3,112 trp1-Δ1 ura3-52 suc2ΔUAS*	Amy Wheeler, unpublished
FY2393[2, 3]	*MAT***a** *his3Δ200 leu2Δ1 lys2-128δ trp1Δ63 ura3-52 prGAL1-FLO8-HIS3:kanMX4*	(Prather et al. 2005)
FY631[3]	*MAT***a** *his4-917δ lys2-173R2 leu2Δ1 trp1Δ63 ura3-52*	(Roberts, Winston 1996)
RK57[3]	*MAT***a** *his4-917δ lys2-173R2 leu2Δ1 trp1Δ63 ura3-52 spt16Δ::kanMX4* [pRS316-A4] (derivative of FY632 diploid (Roberts, Winston 1996))	Rosemarie Kepkay and Ameer Jarrar (this lab), unpublished
FY1095	*MAT***a** *his4-917δ lys2-173R2 leu2Δ1 trp1Δ63 ura3-52 spt20Δ200::URA3*	(Roberts, Winston 1996)

Strain	Description and Genotype	Source
SNL-51B 314-NM3(4) WT68	*MATα ade2Δ ade3Δ his4-912δ lys2-128δ leu2-3,112 trp1-Δ1 ura3-52 spt16Δ::kanMX4* [pRS314-cdc68-E857K] [pSLCDC68]	(O'Donnell 2004)
SNL-58D 315-E857K	*MAT***a** *ade2Δ ade3Δ his4-912δ lys2-128δ leu2-3,112 trp1-Δ1 ura3-52 spt16Δ::kanMX4* [pRS315-cdc68-E857K]	(O'Donnell 2004)
JS6[4] (SYNL #1)	SNL-51B 314-NM3(4) WT68 *hir1-L259V,L760P*	UV mutagenesis derivative of SNL-51B 314-NM3(4) WT68
JS14[4] (SYNL #9)	SNL-51B 314-NM3(4) WT68 *hir3?*	UV mutagenesis derivative of SNL-51B 314-NM3(4) WT68
JS15[4] (SYNL #10)	SNL-51B 314-NM3(4) WT68 *hir2-L747R*	UV mutagenesis derivative of SNL-51B 314-NM3(4) WT68
SYNL #16[4, 5]	SNL-51B 314-NM3(4) WT68 *bur2-FS1*	Allyson O'Donnell, unpublished
SYNL #19[4]	SNL-51B 314-NM3(4) WT68 uncharacterized genomic mutation (*mut1*)	Allyson O'Donnell, unpublished
JS19[6]	SYNL #1 lacking pRS314-cdc68-E857K	Plasmid-loss derivative of JS6
JS23[6]	SYNL #9 lacking pRS314-cdc68-E857K	Plasmid-loss derivative of JS14
JS24[6]	SYNL #10 lacking pRS314-cdc68-E857K	Plasmid-loss derivative of JS15
JS26[6]	SYNL #16 lacking pRS314-cdc68-E857K	Plasmid-loss derivative of SYNL #16
JS284	SNL-51B 314-NM3(4) WT68 lacking pRS314-cdc68-E857K	Plasmid-loss derivative of SNL-51B 314-NM3(4) WT68
AJ25[2]	JS284 *hir1Δ::natMX4*	Ameer Jarrar (this lab), unpublished
bur2Δ[7]	*MAT***a** *met15Δ0 his3Δ1 leu2Δ0 ura3Δ0 bur2Δ::kanMX4*	EUROSCARF deletion collection (Tong et al. 2001)
JS113	JS284 lacking pSLCDC68 [pRS315-A4]	Plasmid-shuffle derivative of JS284
JS114	JS284 lacking pSLCDC68 [pRS315-A4-S]	Plasmid-shuffle derivative of JS284

Strain	Description and Genotype	Source
JS115	JS284 lacking pSLCDC68 [pRS315-E763G-S]	Plasmid-shuffle derivative of JS284
JS116	JS284 lacking pSLCDC68 [pRS315-E857K-S]	Plasmid-shuffle derivative of JS284
JS118	JS284 lacking pSLCDC68 [pRS315-A4-S] [pYL102]	Plasmid-shuffle derivative of JS284
JS119	JS284 lacking pSLCDC68 [pRS315-E763G-S] [pYL102]	Plasmid-shuffle derivative of JS284
JS120	JS284 lacking pSLCDC68 [pRS315-E857K-S] [pYL102]	Plasmid-shuffle derivative of JS284
JS185[8]	*MAT***a** *mat15? lys2? his3Δ0 leu2Δ0 ura3Δ0 (mfa1Δ::MFA1pr-HIS3)? can1? spt16-E857K:natMX4 asf1Δ::kanMX4*	segregant from Y2454 E857K-7 c3 X *asf1Δ*
KanB	*MAT***a**/α *his4-912δ/his4-912δ lys2-128δ/lys2-128δ leu2-3,112/leu2-3,112 trp1-Δ1/ trp1-Δ1 ura3-52/ ura3-52 ssd1-d/? SPT16/spt16Δ::kanMX4*	(O'Donnell 2004)
bur1Δ68Δ 3C	*MAT***a** *his4-912δ lys2-128δ leu2-3,112 trp1-Δ1 ura3-52 ssd1-d spt16Δ::kanMX4 bur1Δ::natMX4* [pRS316-A4] [pGP161]	*bur1Δ* haploid derivative of KanB
JS301[9]	bur1Δ68Δ 3C lacking pGP161 [pRS316-A4] [pRS315-BUR1-HA_3]	Plasmid-shuffle derivative of bur1Δ68Δ 3C
JS302[9]	bur1Δ68Δ 3C lacking pGP161 [pRS316-A4] [pRS315-bur1(1-393)-HA_3]	Plasmid-shuffle derivative of bur1Δ68Δ 3C
JS303[9]	bur1Δ68Δ 3C lacking pGP161 [pRS316-A4] [pRS315-bur1-T70A-HA_3]	Plasmid-shuffle derivative of bur1Δ68Δ 3C
JS304[9]	bur1Δ68Δ 3C lacking pGP161 [pRS316-A4] [pRS315-bur1-T240A-HA_3]	Plasmid-shuffle derivative of bur1Δ68Δ 3C
JS305[9]	bur1Δ68Δ 3C lacking pGP161 [pRS316-A4] [pRS315-bur1-80-HA_3]	Plasmid-shuffle derivative of bur1Δ68Δ 3C
JS308[9]	bur1Δ68Δ 3C lacking pGP161 [pRS316-A4] [pRS315-bur1-23-HA_3]	Plasmid-shuffle derivative of bur1Δ68Δ 3C
JS312	JS301 lacking pRS316-A4 [pRS314-A4] [pRS315-BUR1-HA_3]	Plasmid-shuffle derivative of JS301
JS313	JS301 lacking pRS316-A4 [pRS314-cdc68-E763G] [pRS315-BUR1-HA_3]	Plasmid-shuffle derivative of JS301
JS314	JS301 lacking pRS316-A4 [pRS314-cdc68-E857K] [pRS315-BUR1-HA_3]	Plasmid-shuffle derivative of JS301

Strain	Description and Genotype	Source
JS315	JS302 lacking pRS316-A4 [pRS314-A4] [pRS315-bur1(1-393)-HA_3]	Plasmid-shuffle derivative of JS302
JS316	JS302 lacking pRS316-A4 [pRS314-cdc68-E763G] [pRS315-bur1(1-393)-HA_3]	Plasmid-shuffle derivative of JS302
JS317	JS302 lacking pRS316-A4 [pRS314-cdc68-E857K] [pRS315-bur1(1-393)-HA_3]	Plasmid-shuffle derivative of JS302
JS318	JS303 lacking pRS316-A4 [pRS314-A4] [pRS315-bur1-T70A-HA_3]	Plasmid-shuffle derivative of JS303
JS319	JS303 lacking pRS316-A4 [pRS314-cdc68-E763G] [pRS315-bur1-T70A-HA_3]	Plasmid-shuffle derivative of JS303
JS320	JS303 lacking pRS316-A4 [pRS314-cdc68-E857K] [pRS315-bur1-T70A-HA_3]	Plasmid-shuffle derivative of JS303
JS321	JS304 lacking pRS316-A4 [pRS314-A4] [pRS315-bur1-T240A-HA_3]	Plasmid-shuffle derivative of JS304
JS322	JS304 lacking pRS316-A4 [pRS314-cdc68-E763G] [pRS315-bur1-T240A-HA_3]	Plasmid-shuffle derivative of JS304
JS323	JS304 lacking pRS316-A4 [pRS314-cdc68-E857K] [pRS315-bur1-T240A-HA_3]	Plasmid-shuffle derivative of JS304
JS324	JS308 lacking pRS316-A4 [pRS314-A4] [pRS315-bur1-23-HA_3]	Plasmid-shuffle derivative of JS308
JS325	JS308 lacking pRS316-A4 [pRS314-cdc68-E763G] [pRS315-bur1-23-HA_3]	Plasmid-shuffle derivative of JS308
JS326	JS308 lacking pRS316-A4 [pRS314-cdc68-E857K] [pRS315-bur1-23-HA_3]	Plasmid-shuffle derivative of JS308
JS327	JS305 lacking pRS316-A4 [pRS314-A4] [pRS315-bur1-80-HA_3]	Plasmid-shuffle derivative of JS305
JS328	JS305 lacking pRS316-A4 [pRS314-cdc68-E763G] [pRS315-bur1-80-HA_3]	Plasmid-shuffle derivative of JS305
JS329	JS305 lacking pRS316-A4 [pRS314-cdc68-E857K] [pRS315-bur1-80-HA_3]	Plasmid-shuffle derivative of JS305
Y2454 WT68 c1[10, 11]	*MATα mfa1Δ::MFA1pr-HIS3 can1Δ his3Δ1 leu2Δ0 ura3Δ0 MET15 lys2Δ0 SPT16::natMX4*	(O'Donnell 2004)
JS74[10]	Y2454 WT68 c1 [YEp24-TRT1]	Y2454 WT68 c1 transformant
Y2454 E763G-3 c3[10, 11]	*MATα mfa1Δ::MFA1pr-HIS3 can1Δ his3Δ1 leu2Δ0 ura3Δ0 MET15 lys2Δ0 spt16-E763G::natMX4*	(O'Donnell 2004)

Strain	Description and Genotype	Source
JS76[10]	Y2454 E763G-3 c3 [YEp24-TRT1]	Y2454 E763G-3 c3 transformant
Y2454 E857K-7 c3[10, 11]	*MATα mfa1Δ::MFA1pr-HIS3 can1Δ his3Δ1 leu2Δ0 ura3Δ0 MET15 lys2Δ0 spt16-E857K::natMX4*	(O'Donnell 2004)
JS78[10]	Y2454 E857K-7 c3 [YEp24-TRT1]	Y2454 E857K-7 c3 transformant
Y2454 312-8 c1[10, 11]	*MATα mfa1Δ::MFA1pr-HIS3 can1Δ his3Δ1 leu2Δ0 ura3Δ0 MET15 lys2Δ0 spt16-312::natMX4*	(O'Donnell 2004)
JS80[10]	Y2454 312-8 c1 [YEp24-TRT1]	Y2454 312-8 c1 transformant
Y2454 319-5 c1[10, 11]	*MATα mfa1Δ::MFA1pr-HIS3 can1Δ his3Δ1 leu2Δ0 ura3Δ0 MET15 lys2Δ0 spt16-319::natMX4*	(O'Donnell 2004)
JS82[10]	Y2454 319-5 c1 [YEp24-TRT1]	Y2454 319-5 c1 transformant
JS330[12]	*MATα leu2Δ0 ura3Δ0 his3Δ1 lys2? met15? (mfa1Δ::MFA1pr-HIS3)? can1? spt16-E857K:natMX4 rco1Δ::kanMX4*	segregant 2D from Y2454 E857K-7 c3 X *rco1Δ*
JS336[13]	*MATα leu2Δ0 ura3Δ0 his3Δ1 lys2? met15? (mfa1Δ::MFA1pr-HIS3)? can1? spt16-E763G:natMX4 rco1Δ::kanMX4*	segregant 8A from Y2454 E763G-3 c3 X *rco1Δ*
JS337	*MATα leu2Δ0 ura3Δ0 his3Δ1 lys2? met15? (mfa1Δ::MFA1pr-HIS3)? can1? spt16-E763G:natMX4 rco1Δ::kanMX4::Ura3MX4*	Marker-swap derivative of JS336
JS338	*MATα leu2Δ0 ura3Δ0 his3Δ1 lys2? met15? (mfa1Δ::MFA1pr-HIS3)? can1? spt16-E857K:natMX4 rco1Δ::kanMX4::Ura3MX4*	Marker-swap derivative of JS330
GRX2-1A	*MAT***a** *arg4* (*lys1* or *lys5*) *trp5 met13 ura1? cyh2*	Yeast Genetic Stock Centre
XJB3-1B	*MATα met6*	Yeast Genetic Stock Centre

Notes:

1) The following deletions were used: *hht1Δ*, *hhf1Δ*, *asf1Δ*, *nap1Δ*, *rtt106Δ*, *vps75Δ*, *ctk1Δ*, *swd1Δ*, *swd3Δ*, *rad6Δ*, *spt4Δ*, *set2Δ*, *eaf3Δ*, *rco1Δ*, *sin3Δ*, *rpd3Δ*, *jhd1Δ*, *sas3Δ*, *elp3Δ*, *gcn5Δ*, and *rtt109Δ* (in order of occurrence in Results)
2) These strains were transformed with the following plasmids: pRS315, pRS315-A4, pTF128-6, pTF128-7, pTF128-9a, pTF128-11, and (except for AJ25) pRS315-Δ922
3) These strains were transformed with the following plasmids: pRS315-A4, pRS315-cdc68-E763G, pRS315-cdc68-E857K, and (except for RK57) pRS315
4) Library screening with p366 was carried out on these strains

5) This strain was transformed with the following plasmids: pRS315, pRS315-BUR2, pRS315-BUR1-HA_3, pRS315-bur1(1-393)-HA_3, pRS315-bur1-T70A-HA_3, pRS315-bur1-T240A-HA_3, pRS315-bur1-80-HA_3, pRS315-bur1-85-HA_3, pRS315-bur1-35-HA_3, pRS315-bur1-23-HA_3, pRS315-bur1-51-HA_3, pRS315-bur1-65-HA_3, and pRS315-bur1-78-HA_3
6) These strains were transformed with the following plasmids: pRS314, pRS314-A4, pRS314-cdc68-E763G, pRS314-cdc68-E857K, pRS314-cdc68-312, pRS314-cdc68-319, p314-M68, p314-ΔNTDFLAG, p314-cdc68-1, pTF128, pTF128-4, pTF128-6, pTF128-7, pTF128-8, pTF128-9, pTF128-9a, pMS081, pMS082, pTF128-11, pTF128-12, pTF128-16ABC, pTF128-24, and pRS315
7) This strain was transformed with the following plasmids: pRS315, pRS315-BUR2, pRS315-BUR1-HA_3, pRS315-bur1(1-393)-HA_3, pRS315-bur1-T70A-HA_3, pRS315-bur1-T240A-HA_3, pRS315-bur1-80-HA_3, and pRS315-bur1-23-HA_3
8) This strain was transformed with the following plasmids: pRS316, pRS316-A4, pRS316-ASF1 and pRS316-asf1-36/37-AA
9) These strains were transformed with the following plasmids: pRS315, pRS425, pRK5, pRK6, pRK7, and pRK8
10) These strains were transformed with the following plasmids: pRS314, pRS314-A4, pRS314-cdc68-E763G, and pRS314-cdc68-E857K
11) These strains were transformed with the following plasmids: YEp24 and YEp24-TRT1
12) Segregants 3C and 5A with the same genetic makeup were also used
13) Segregants 4C, 6B and 7A with the same genetic makeup were also used

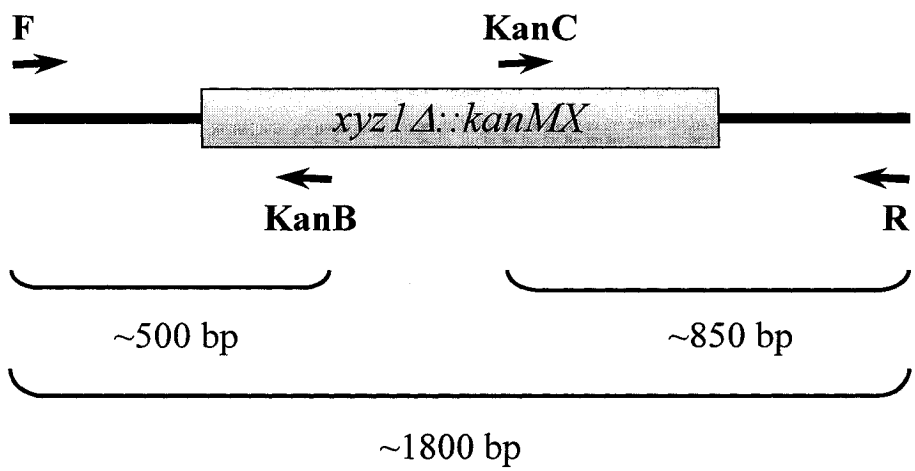

Figure 5. Schematic for confirmation of deletion strains. Forward (F) and reverse (R) primers were designed to bind approximately 200 bp beyond the ends of the integrated *kanMX4* cassette. PCR was performed using primers F and KanB (product size ~500 bp), or primers R and KanC (product size ~850 bp). When no product was observed, PCR was performed using primers F, KanB and R, as a product should be obtained using primers F and R regardless of whether the *kanMX4* cassette is present. If the cassette is present, the expected product size for this reaction is ~1800 bp.

of whether the poor growth was correlated with this gene deletion. The *spt4Δ* situation was the most elaborate. In this case, I isolated segregants to generate new *spt4Δ::kanMX4* strains. Tetrads that contained four geneticin-resistant segregants were identified, to ensure that each segregant contained a single *kanMX4* cassette. These segregants were screened for those that were *MAT*a, histidine-auxotrophic, and lysine-prototrophic (methionine prototrophy/auxotrophy was not assessed). Following this, PCR was performed, as described above, to determine which segregants contained the *spt4Δ::kanMX4* replacement. From this, two segregants were obtained that met these criteria, and are listed in Table 1 as JS34 and JS35.

2.2.2 *spt16-E857K asf1Δ* Double-Mutant Strain

To generate strain JS185, cells of strain Y2454 E857K-7 c3 (O'Donnell 2004) were crossed with cells from the *asf1Δ* strain in the EUROSCARF deletion collection (isolate location 12 D 3). These diploid cells were sporulated (Section 2.1.1), and tetrad analysis was performed, as described in Section 2.5.2. The resulting segregants were scored for growth on YEPD-NAT and YEPD-GEN media, to identify the presence of *spt16-E857K:natMX4* and *asf1Δ::kanMX4*, respectively. Mating-type testing was then performed on the double-mutant segregants, as described in Section 2.5.3; segregant 2B (*MAT***a**) was saved as strain JS185.

2.2.3 *spt16-E857K rco1Δ* and *spt16-E763G rco1Δ* Double-Mutant Strains

Strains JS330 through JS332 (*spt16-E857K rco1Δ*) and JS333 through JS336 (*spt16-E763G rco1Δ*) were generated in a manner similar to that for strain JS185. To generate strains JS330 through JS332, cells of strain Y2454 E857K-7 c3 (O'Donnell 2004) were crossed with cells from the *rco1Δ* strain in the EUROSCARF deletion collection (isolate location 2 C 10). These diploid cells were sporulated, and tetrad analysis was performed. The resulting segregants were scored for growth on YEPD-NAT and YEPD-GEN media, to identify the presence of *spt16-E857K:natMX4* and *rco1Δ::kanMX4*, respectively. Mating-type testing was then performed on the double-mutant segregants; *MAT*α segregants 2D, 3C and 5A were saved as strains JS330, JS331 and JS332, respectively.

The same procedure was used to generate strains JS333 through JS336, except that strain Y2454 E763G-3 c3 (O'Donnell 2004) was used in place of strain Y2454

E857K-7 c3. Following mating type testing, *MATα* segregants 4C, 6B, 7A and 8A were saved as strains JS333, JS334, JS335 and JS336, respectively.

2.2.4 *rco1Δ::kanMX4::Ura3MX4* Strains

For some of the analyses carried out in this work, it was desirable to have strains where the *kanMX4* cassette (replacing the *RCO1* gene) was itself replaced with a different genetic marker. To obtain such a strain, the *Ura3MX4* cassette (Voth, Jiang & Stillman 2003) was used, containing the *URA3* gene from *Candida albicans* (Goldstein, Pan & McCusker 1999). To generate strains JS337 (*spt16-E763G:natMX4*) and JS338 (*spt16-E857K:natMX4*) containing *rco1Δ::kanMX4::Ura3MX4*, a marker-swap transformation was performed on cells from strains JS336 (*spt16-E763G:natMX4 rco1Δ::kanMX4* segregant 8A) and JS330 (*spt16-E857K:natMX4 rco1Δ::kanMX4* segregant 2D). The marker-swap plasmid pAG60 (Goldstein, Pan & McCusker 1999) was digested using NotI and the resulting DNA was then purified using a Qiagen PCR Purification Kit (Qiagen, Mississauga, ON) and transformed into cells of strains JS330 and JS336 (Section 2.4.4.2). Transformants were selected on uracil-deficient medium, and replacement of the *kanMX4* cassette was confirmed by sensitivity to geneticin (G418). Because the *natMX4* and *kanMX4* cassettes contain the same promoter and terminator regions, recombination could have also occurred between *Ura3MX4* and *natMX4*. Therefore, the presence of *natMX4* was confirmed by resistance to nourseothricin (clonNAT). One isolate from each transformant population was saved as strains JS337 and JS338.

2.2.5 *spt16::kanMX4 bur1Δ::natMX4* Double Mutants and Derivatives

To generate strain bur1Δ68Δ 3C, the diploid strain KanB (O'Donnell 2004), which is heterozygous for *spt16Δ::kanMX4*, was first transformed with the *bur1Δ::natMX4* replacement cassette from plasmid pRS315-B1UTRNAT (Section 2.4.4.2). Transformants were selected on YEPD-NAT medium, and the transformants were confirmed to still contain *kanMX4* by resistance to geneticin (G418). The location of the *natMX4* cassette was verified using colony PCR with two sets of primers (Section 2.4.7.4; see Table 3 for sequences): (1) 715UPS BUR1 F and OPP1098 (internal *natMX4* reverse primer) and (2) 635DNS BUR1 R and OPP1097 (internal *natMX4* forward primer). Diploid cells containing *spt16Δ::kanMX4* and *bur1Δ::natMX4* were then

transformed with plasmids containing *BUR1* (pGP161) and *SPT16* (pRS316-A4) (Section 2.4.4.2). These transformants were then sporulated, and tetrad analysis was performed. Double-mutant haploid segregants were identified, and mating-type testing was performed as described in Section 2.5.3. One segregant with the desired markers was saved as strain bur1Δ68Δ 3C.

A plasmid-shuffle procedure was then carried out to replace plasmid pGP161 with pRS315-based *BUR1* and *bur1* plasmids (Keogh, Podolny & Buratowski 2003). Transformants containing the pRS315-based plasmids were identified, and plasmid loss of pGP161 was performed as described in Section 2.4.5. The resulting derivatives, containing pRS316-A4 and one of the pRS315-based *BUR1* or *bur1* plasmids, were saved as strains JS301 (*BUR1*), JS302 (*bur1(1-393)*), JS303 (*bur1-T70A*), JS304 (*bur1-T240A*), JS305 (*bur1-80*) and JS308 (*bur1-23*).

A further plasmid-shuffling procedure was performed on each of these strains, to replace pRS316-A4 with pRS314-based plasmids containing *SPT16*, *spt16-E763G* or *spt16-E857K* (O'Donnell 2004). This resulted in the series of strains JS312 through JS329: JS312 through JS314 (from JS301), JS315 through JS317 (from JS302), JS318 through JS320 (from JS303), JS321 through JS323 (from JS304), JS324 through JS326 (from JS305), and JS327 through JS329 (from JS308). For each set, the strain with the lowest number in the series contains pRS314-A4, the middle contains pRS314-cdc68-E763G, and the highest contains pRS314-cdc68-E857K.

2.2.6 Strains Used in Co-Immunoprecipitation Analyses

All strains created for use for co-immunoprecipitation experiments were derivatives of strain JS284. This strain was transformed with plasmids pRS315-A4, pRS315-A4-S, pRS315-E763G-S or pRS315-E857K-S, either individually or (except for pRS315-A4), in combination with pYL102 (Lorch, Kornberg 1994). The pYL102 plasmid expresses a galactose-inducible HA-tagged version of histone H2B, for use in western blotting procedures. Plasmid loss was then performed on the resulting transformants, to obtain derivatives that no longer contain the plasmid pSLCDC68. In this way, the following strains were created: JS113 (pRS315-A4), JS118 and JS114 (pRS315-A4-S with and without pYL102, respectively), JS119 and JS115 (pRS315-E763G-S with and without

pYL102, respectively), and JS120 and JS116 (pRS315-E857K-S with and without pYL102, respectively).

2.3 Plasmids

The plasmids used in this study are listed in Table 2.

2.3.1 Isolated Library Plasmids

I isolated complementing library plasmids from the centromeric yeast genomic library p366 that alleviated the deleterious genetic interaction in four of my original synthetic-lethal yeast strains (JS6 [SYNL #1], JS14 [SYNL #9], JS15 [SYNL #10] and SYNL #16), named for the yeast strain from which they were isolated (i.e. plasmids isolated from SYNL #16 were named p366 16-9 and p366 16-11). These plasmids were extracted from yeast cells (Section 2.4.2.2) and transformed into *E. coli* cells (Section 2.4.4.1) of strain JF1754 to identify the *LEU2*-based plasmids (Section 2.1.2).

2.3.2 Plasmids Used in Classical Synthetic-Lethal Screening

In my classical synthetic-lethal screen, single-gene plasmids were made containing *BUR2*, *HIR1*, and *HIR2* (pRS315-BUR2, pRS315-HIR1 and pRS315-HIR2). In addition, plasmids for gap-repair of the genomic locus were made for each of these three (pRS315-B1UTRs, pRS315-H1UTRs and pRS315-H2UTRs) (see Figure 6 for overview). For the *BUR2* plasmid pRS315-BUR2, primers (see Table 3) were designed to amplify the region from 430 bp upstream of the start codon (430 UPS BUR2, containing a NotI restriction site) to 333 bp downstream of the stop codon (333 DNS BUR2, containing a XhoI restriction site). High-fidelity PCR using Pfx Taq (Section 2.4.7.3) was performed, using the *BUR2*-containing library plasmid as template. The PCR product was digested with NotI and XhoI, and then cloned into NotI- and XhoI-digested pRS315. For the *BUR2* gap-repair plasmid, the same two primers were used, but the 430 UPS BUR2 primer was paired with a reverse primer hybridizing 25 bp upstream of the start codon (25 UPS BUR2), while the 333 DNS BUR2 primer was paired with a forward primer hybridizing 21 bp downstream of the stop codon (21 DNS BUR2). These two additional primers both contained BamHI restriction sites. Again, the *BUR2* library plasmid was used as a template for these PCR reactions. The products were digested with either NotI and

Table 2. Plasmids used in this study.

Plasmid name	Description	Source
pRS316	*URA3 CEN amp*^{R} vector	(Sikorski, Hieter 1989)
pRS315	*LEU2 CEN amp*^{R} vector	(Sikorski, Hieter 1989)
pRS314	*TRP1 CEN amp*^{R} vector	(Sikorski, Hieter 1989)
pRS425	*LEU2* 2μ *amp*^{R} vector	(Christianson et al. 1992)
YEp24	*URA3* 2μ *amp*^{R} vector	(Botstein et al. 1979)
p366	*LEU2*, *CEN* genomic library (9-12 kbp insert size)	Brenda Andrews, University of Toronto
p366 16-9	*BUR2*-containing library plasmid	This study
p366 16-11	*BUR2*-containing library plasmid	This study
p366 1-1	false positive library plasmid	This study
p366 1-3	*HIR1*-containing library plasmid	This study
p366 1-12	*HIR2*-containing library plasmid	This study
p366 1-25	false positive library plasmid	This study
p366 1-34	*HIR2*-containing library plasmid	This study
p366 9-8	*HIR3*-containing library plasmid	This study
pRS316-A4	*SPT16 URA3 CEN*	(O'Donnell 2004)
pRS316-A4-S	C-terminally S-tagged *SPT16 URA3 CEN*	(Perry 2005)
pRS315-A4	*SPT16 LEU2 CEN*	(O'Donnell 2004)
pRS315-A4-S	C-terminally S-tagged *SPT16 LEU2 CEN*	This study
pRS314-A4	*SPT16 TRP1 CEN*	(O'Donnell 2004)
pRS315-cdc68-E763G	*spt16-E763G LEU2 CEN*	(O'Donnell 2004)
pRS315-E763G-S	C-terminally S-tagged *spt16-E763G LEU2 CEN*	This study
pRS314-cdc68-E763G	*spt16-E763G TRP1 CEN*	(O'Donnell 2004)
pRS315-cdc68-E857K	*spt16-E857K LEU2 CEN*	(O'Donnell 2004)
pRS315-E857K-S	C-terminally S-tagged *spt16-E857K LEU2 CEN*	This study
pRS314-cdc68-E857K	*spt16-E857K TRP1 CEN*	(O'Donnell 2004)
pRS314-cdc68-312	*spt16-312 TRP1 CEN*	(O'Donnell 2004)
pRS314-cdc68-319	*spt16-319 TRP1 CEN*	(O'Donnell 2004)

Plasmid name	Description	Source
p314-M68	*spt16-Δ(6-435) TRP1 CEN*	(O'Donnell et al. 2004)
p314-ΔNTDFLAG	*spt16-ΔNTD-FLAG TRP1 CEN*	(O'Donnell et al. 2004)
p314-cdc68-1	*cdc68-1 TRP1 CEN*	Neil Brewster, unpublished
pTF128	*SPT16/CDC68 LEU2 CEN*	(Formosa et al. 2001)
pTF128-4	*spt16-4 LEU2 CEN*	(Formosa et al. 2001)
pTF128-6	*spt16-6 LEU2 CEN*	(Formosa et al. 2001)
pTF128-7	*spt16-7 LEU2 CEN*	(Formosa et al. 2001)
pTF128-8	*spt16-8 LEU2 CEN*	(Formosa et al. 2001)
pTF128-9	*spt16-9 LEU2 CEN*	(Formosa et al. 2001)
pTF128-9a	*spt16-9a LEU2 CEN*	(Formosa et al. 2001)
pMS081	*spt16-9b LEU2 CEN*	(Formosa et al. 2001)
pMS082	*spt16-9c LEU2 CEN*	(Formosa et al. 2001)
pTF128-11	*spt16-11 LEU2 CEN*	(Formosa et al. 2001)
pTF128-12	*spt16-12 LEU2 CEN*	(Formosa et al. 2001)
pTF128-16ABC	*spt16-16a LEU2 CEN*	(Formosa et al. 2001)
pTF128-24	*spt16-24 LEU2 CEN*	(Formosa et al. 2001)
pRS315-Δ922	*spt16-Δ922 LEU2 CEN*	Marci Dearing & Joffre Munro, Chris Barnes lab, unpublished
pRS315-B1UTRNAT	*natMX4* cassette flanked by genomic DNA sequence from upstream and downstream of the *BUR1* gene *LEU2 CEN*	This study
pRS315-BUR2	*BUR2 LEU2 CEN*	This study
pRS315-B2UTRs	*BUR2* UPS & DNS *LEU2 CEN*	This study
pRS315-HIR1	*HIR1 LEU2 CEN*	This study
pRS315-H1UTRs	*HIR1* UPS & DNS *LEU2 CEN*	This study

Plasmid name	Description	Source
pRS315-H1UTRNAT	*natMX4* cassette flanked by genomic DNA sequence from upstream and downstream of the *HIR1* gene *LEU2 CEN*	This study
pRS315-HIR2	*HIR2 LEU2 CEN*	This study
pRS315-H2UTRs	*HIR2* UPS & DNS *LEU2 CEN*	This study
pRS315-grHIR1(snl1)	*hir1-L259V,L760P LEU2 CEN*	This study
pRS315-grHIR2(snl1)	*HIR2 LEU2 CEN*	This study
pRS315-grHIR2(snl10)	*hir2-L747R LEU2 CEN*	This study
pRS315-grBUR2(snl16)	*bur2-FS1* (frameshift) *LEU2 CEN*	This study
pRS315-hir1-L259V	*hir1-L259V LEU2 CEN*	This study
pRS315-hir1-L760P	*hir1-L760P LEU2 CEN*	This study
pRS314-YNL NAT	*natMX4* cassette flanked by 167 bp upstream and 291 bp downstream of genomic DNA sequence of the YNL035c gene *TRP1 CEN*	(O'Donnell 2004)
pGAD-YNL035c	*YNL035c LEU2* 2μ	Allyson O'Donnell, unpublished
pRK5	*HHT1-HHF1 LEU2 CEN*	Rosemarie Kepkay, unpublished
pRK6	*HHT1-HHF1 LEU2* 2μ	Rosemarie Kepkay, unpublished
pRK7	*HHT2-HHF2 LEU2 CEN*	Rosemarie Kepkay, unpublished
pRK8	*HHT2-HHF2 LEU2* 2μ	Rosemarie Kepkay, unpublished
YEp24-TRT1	*HTA1-HTB1 URA3* 2μ	(Hereford et al. 1979)
pYL102	*prGAL10-HA-H2B TRP1 CEN*	(Lorch, Kornberg 1994)
pPK418	*ASF1 TRP1 CEN*	(Daganzo et al. 2003)
pPK426	*asf1-H36AD37A TRP1 CEN*	(Daganzo et al. 2003)

Plasmid name	Description	Source
pRS316-ASF1	*ASF1 URA3 CEN*	This study (from pPK418)
pRS316-asf1-36/37-AA	*asf1-H36AD37A URA3 CEN*	This study (from pPK426)
pGP161	*BUR1 TRP1 CEN*	Greg Prelich, Albert Einstein College of Medicine
pRS315-BUR1-HA_3	*BUR1 LEU2 CEN*	(Keogh, Podolny & Buratowski 2003)
pRS315-bur1(1-393)-HA_3	*bur1(1-393) LEU2 CEN*	(Keogh, Podolny & Buratowski 2003)
pRS315-bur1-T70A-HA_3	*bur1-T70A LEU2 CEN*	(Keogh, Podolny & Buratowski 2003)
pRS315-bur1-T240A-HA_3	*bur1-T240A LEU2 CEN*	(Keogh, Podolny & Buratowski 2003)
pRS315-bur1-80-HA_3	*bur1-80 LEU2 CEN*	(Keogh, Podolny & Buratowski 2003)
pRS315-bur1-85-HA_3	*bur1-85 LEU2 CEN*	(Keogh, Podolny & Buratowski 2003)
pRS315-bur1-35-HA_3	*bur1-35 LEU2 CEN*	(Keogh, Podolny & Buratowski 2003)
pRS315-bur1-23-HA_3	*bur1-23 LEU2 CEN*	(Keogh, Podolny & Buratowski 2003)
pRS315-bur1-51-HA_3	*bur1-51 LEU2 CEN*	(Keogh, Podolny & Buratowski 2003)
pRS315-bur1-65-HA_3	*bur1-65 LEU2 CEN*	(Keogh, Podolny & Buratowski 2003)
pRS315-bur1-78-HA_3	*bur1-75 LEU2 CEN*	(Keogh, Podolny & Buratowski 2003)
pAG60	*kanMX::Ura3MX4* Amp^R	(Goldstein, Pan & McCusker 1999)

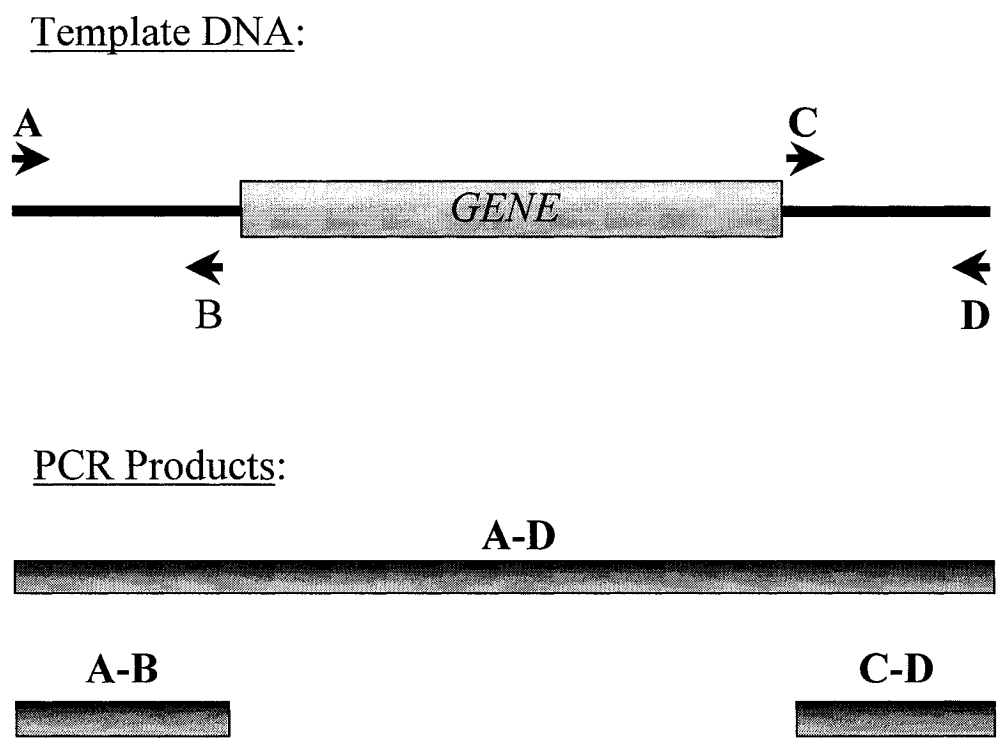

Figure 6. Schematic for creating single-gene and gap-repair plasmids for *BUR2*, *HIR1*, and *HIR2*. For single-gene plasmids, high-fidelity PCR was performed using primers A and D. The product was cloned into pRS315. For gap-repair plasmids, high-fidelity PCR was performed using primer pairs A plus B, and C plus D. Both products were then cloned into pRS315 in a three-fragment ligation. A unique restriction enzyme site at the junction between the upstream and downstream PCR amplicons allows the plasmid to be linearized and used for gap repair.

BamHI (for the upstream region) or XhoI and BamHI (for the downstream region), and were cloned into NotI- and XhoI-digested pRS315.

The plasmids for *HIR1* and *HIR2* were created in essentially the same manner. For *HIR1*, the primers used were 420 UPS HIR1 (containing a SmaI restriction site), 1 UPS HIR1 (containing a BamHI restriction site), 10 DNS HIR1 (containing a BamHI restriction site), and 402 DNS HIR1 (containing a NotI restriction site). High-fidelity PCR was performed using the *HIR1* library plasmid as a template, and the products were cloned into pRS315, as described for *BUR2*. Although the *HIR1* gap-repair plasmid was made in this manner, I had difficulty isolating the *HIR1* single-gene plasmid. Therefore, the gap-repair plasmid was used in a yeast strain containing a wild-type *HIR1* gene, thereby creating a *HIR1* plasmid by gap repair. For *HIR2*, the primers used were 377 UPS HIR2 (containing a PstI restriction site), 1 UPS HIR2 (containing a BamHI restriction site), 1 DNS HIR2 (containing a BamHI restriction site), and 367 DNS HIR2 (containing a NotI restriction site). High-fidelity PCR was performed using the *HIR2* library plasmid as a template, and the products were cloned into pRS315, as described for *BUR2*.

2.3.3 Gap-Repaired Plasmids from Synthetic-Lethal Strains

The gap-repair plasmids described in the previous section were cut at the junction between the upstream and downstream sequences, and the resulting linearized plasmid was transformed into yeast cells. To generate pRS315-grBUR2, pRS315-B2UTRs was digested using BamHI, and this linearized plasmid was transformed into SYNL #16 yeast cells. Plasmids were then isolated from the transformed yeast cells (Section 2.4.2.2), and the *LEU2*-containing plasmids were obtained using JF1754 *E. coli* cells (Section 2.1.2). A restriction digest using NotI and XhoI confirmed the presence of additional (*BUR2*) sequence in these plasmids isolated from yeast cells.

Similar protocols were used to generate pRS315-grHIR1(snl1), pRS315-grHIR2(snl1), and pRS315-grHIR2(snl10). For pRS315-grHIR1(snl1), pRS315-H1UTRs was digested using BamHI and transformed into SYNL #1 yeast cells. The presence of additional (*HIR1*) sequence in the recovered plasmid was confirmed by restriction digest using SmaI and NotI. For pRS315-grHIR2(snl1) and pRS315-grHIR2(snl10), pRS315-H2UTRs was digested using BamHI and transformed into SYNL #1 or SYNL #10 yeast

cells. The presence of additional (*HIR2*) sequence in each of the recovered plasmids was confirmed by restriction digest using PstI and NotI.

DNA sequencing was obtained (as described in Section 2.4.6) for each of these gap-repaired genes. Sequencing primers used are listed in Table 3.

2.3.4 pRS315-hir1-L259V and pRS315-L760P

The two mutations in the *hir1* gene isolated from cells of strain SYNL #1 were separated by a fragment-swap procedure. Plasmids pRS315-HIR1 and pRS315-grHIR1(snl1) were cut using PstI, which cleaves in the polylinker (5' end of *HIR1*) and approximately 2 350 bp into the *HIR1* insert, thus generating two DNA fragments: the vector and 3' end of *HIR1* (containing the mutation causing L760P) at 7.1 kbp, and the 5' end of *HIR1* (containing the mutation causing L259V) at 2.3 kbp. The two fragments from each digest were isolated, and ligations were performed (Section 2.4.1) using the large fragment from one digest with the shorter fragment from the other, thus generating plasmids pRS315-hir1-L259V and pRS315-hir1-L760P.

2.3.5 pRS315-B1UTRNAT and pRS315-H1UTRNAT

To make the *natMX4* replacement cassettes for *HIR1* and *BUR1*, a method similar to that for making the gap-repair plasmids was used. The *BUR1* gene-replacement cassette was made by a two-step process: a B1UTRs plasmid was first made, containing upstream and downstream regions of *BUR1*, and then the *natMX4* cassette was inserted between the cloned upstream and downstream sequences. To make the B1UTRs plasmid, primers were used to amplify two regions: (1) from 492 bp upstream of the *BUR1* start codon (primer contains a NotI restriction site) to 16 bp upstream of the *BUR1* start codon (primer contains a BamHI restriction site) and (2) from 10 bp downstream of the *BUR1* stop codon (primer contains a BamHI restriction site) to 495 bp downstream of the *BUR1* stop codon (primer contains a SalI restriction site). These fragments were digested with their respective enzymes and cloned into pRS315 that had been cut with NotI and SalI. Following this, both the B1UTRs plasmid and pRS314-YNL NAT (O'Donnell 2004) were digested with BamHI and the fragment containing the *natMX4* cassette from pRS314-YNL NAT was isolated. Ligations were carried out between this *natMX4* cassette and the cut B1UTRs plasmid, yielding pRS315-B1UTRNAT. The *BUR1* gene-replacement cassette was obtained from this plasmid by digestion with NotI and SalI.

A similar procedure was used to generate the *HIR1* gene-replacement cassette; however, in this case, I had already created a HIUTRs plasmid to be used in gap-repair. This plasmid was digested using BamHI to cut between the upstream and downstream *HIR1* sequences, and the cut plasmid was used in a ligation with the *natMX4* cassette isolated from pRS314-YNL NAT. This process yielded pRS315-H1UTRNAT, which in turn yields the *HIR1* gene-replacement cassette by digestion with NotI and HindIII. HindIII, which cuts both in the polylinker at the 5' end of the *HIR1* upstream fragment and 16 bp within this fragment, was used to generate the knockout cassette because SmaI, used in cloning the upstream region of *HIR1*, cuts within the *natMX4* cassette and thus cannot be used.

2.3.6 pRS316-ASF1 and pRS316-asf1-36/37-AA

These two plasmids were generated by subcloning *ASF1* and *asf1-H36AD37A* from pPK418 and pPK426 (Daganzo et al. 2003), respectively. Each of these plasmids, and also pRS316, was digested with SstI and XhoI, and the *asf1*-containing fragments were isolated. Ligations were then performed between the cut pRS316 and the *ASF1* or *asf1-H36AD37A* fragment, yielding pRS316-ASF1 and pRS316-asf1-36/37-AA, respectively.

2.3.7 Plasmids to Generate S-tagged Versions of Spt16

Plasmids were created to express versions of Spt16, Spt16-E763G and Spt16-E857K that contained the S-tag and His_6-tag at the C terminus of the Spt16 protein (pRS315-A4-S, pRS315-E763G-S and pRS315-E857K-S). The creation of these plasmids took advantage of an engineered XbaI site that is present at the 3' end of the *SPT16* coding region in pRS315-A4, pRS315-cdc68-E763G and pRS315-cdc68-E857K (O'Donnell 2004). This XbaI site is the result of a change in nucleotide 3098 from a cytosine to a thymidine, which results in the S1033F substitution but does not change the final two amino acids of the 1035 amino acid Spt16 protein (B. Smith, unpublished data). Plasmid pRS316-A4-S (Perry 2005) was digested with XbaI, and the fragment encoding the S- and His_6-tags was isolated; this fragment contains the remainder of the *SPT16* coding sequence, then the sequence for both tags, followed by a stop codon. This fragment was then cloned into XbaI-digested pRS315-A4, pRS315-cdc68-E763G and pRS315-cdc68-E857K. The orientation of this insertion was verified by PCR using a forward primer within the *SPT16* coding region (5' HindIII flank) and a reverse primer within the S-tag-encoding

sequence (S-tag reverse); a product is formed only when the S-tag insert is inserted in the correct orientation.

2.4 DNA Manipulations

2.4.1 Restriction Digests, Phosphatase Treatment, and DNA Ligations

Restriction enzymes used in this study were purchased from Invitrogen and New England Biolabs (Pickering, ON), and digests were carried out according to the supplier's recommended conditions, generally at 37°C (several enzymes were incubated at 30°C, as recommended by the supplier). When required, calf intestinal alkaline phosphatase (New England Biolabs) was added to remove 5' phosphates from digested vector DNA prior to ligation: 1 µl of phophatase was added to a 20-µl digest, and incubated for 30 minutes at 37°C. To use this digested DNA in cloning procedures, two methods were used to purify the DNA by removing the enzymes. When a DNA fragment was being cut out of one vector and subcloned into another, or when a vector was cut to be cloned into, the cut DNA was resolved using agarose gel electrophoresis to isolate the fragment of interest. This fragment was then excised from the gel and purified using either the QIAquick Gel Extraction Kit (Qiagen) or the PureLink Gel Extraction Kit (Invitrogen). However, for an isolated piece of DNA (for example, a PCR product), the enzyme(s) were removed using either the QIAquick PCR purification Kit (Qiagen) or the PureLink PCR Purification Kit (Invitrogen). Ligation reactions were performed using T4 DNA Ligase (Invitrogen). A representative reaction would be comprised of 1 µl T4 DNA ligase, 2 µl 5x ligase buffer, 5 µl of 'insert DNA', and 2 µl of vector DNA. Often, several insert-to-vector ratios were used to increase the chance of a successful ligation. Ligation reactions were incubated at 23°C for durations of one hour to overnight.

2.4.2 Plasmid Isolation

Plasmids were isolated from both *E. coli* cells and yeast cells.

2.4.2.1 Plasmid Isolation from *E. coli*

Plasmids were isolated from *E. coli* cells by alkaline lysis miniprep or by using a miniprep kit. The alkaline lysis procedure (Sambrook, Fitsch & Maniatis 1989) was performed as follows: the cells from an overnight culture of *E. coli* cells grown in 2xYT medium containing ampicillin were harvested by centrifugation at 15 000 rpm for two

minutes in a microfuge and resuspended in 100 µl TEG (25 mM Tris-Cl pH 8.0, 10 mM EDTA pH 8.0, 50 mM glucose) and lysis was carried out by the addition of 200 µl of NaOH/SDS solution (0.2 M NaOH, 1% SDS) for five minutes on ice. This mixture was then neutralized by the addition of 150 µl of 3 M KOAc and a further five minutes incubation on ice, followed by centrifugation at 15 000 rpm for ten minutes. The supernatant was transferred to a new tube and phenol/chloroform extraction was performed to remove any remaining protein from the solution. First, 500 µl of phenol/chloroform/isoamyl alcohol (25/24/1) solution was added, and the tube was vortexed and then centrifuged to separate the organic and aqueous layers. The aqueous layer was transferred to a new tube, to which 500 µl of chloroform was added; the tube was again vortexed and centrifuged, and the aqueous layer transferred to a new tube. Following this, the plasmid DNA was concentrated from the aqueous layer by ethanol precipitation: 1 ml of 95% ethanol was added, and the tubes were incubated on ice for ten minutes, followed by centrifugation for ten minutes at 15 000 rpm. The DNA pellets were then washed with 1 ml of 70% ethanol, dried, and resuspended in 50 µl TE containing 1 µg RNase A.

Alternatively, a commercial miniprep kit was used to isolate plasmid DNA. These were the GenElute Plasmid Miniprep Kit (Sigma-Aldrich), the Qiaprep Spin Miniprep Kit (Qiagen) or the PureLink Quick Plasmid Miniprep Kit (Invitrogen).

2.4.2.2 Plasmid Isolation from Yeast Cells

Plasmids were isolated from yeast cells using the glass-bead disruption method (Hoffman 1997). A 5-ml culture of yeast cells was grown overnight, then pelleted by centrifugation. The pellet was then resuspended in 300 µl of breaking buffer (100 mM NaCl, 10 mM Tris-Cl pH 8.0, 1 mM EDTA, 2% Triton X-100 and 1% SDS), to which 300 µl of phenol/chloroform/isoamyl alcohol (25/24/1) and 300 µl of acid-washed glass beads was added. This mixture was vortexed (maximum speed) for six minutes at room temperature, then centrifuged for eight minutes at 15 000 rpm. The resulting aqueous layer was transferred to a new tube, to which 1 ml of 95% ethanol was added to precipitate the DNA. This mixture was then incubated at –80°C for 20 minutes, followed by centrifugation at 4°C for 15 minutes at 15 000 rpm. The resulting DNA pellet was dried, then resuspended in 30 µl of TE containing 1 µg of RNase A.

2.4.3 Isolation of Chromosomal DNA from Yeast Cells

Chromosomal DNA was isolated from yeast cells essentially as described (Hoffman 1997). Briefly, a 10-ml culture of yeast cells was grown overnight in YM1 medium; the cell pellet was collected by centrifugation, and washed once with 500 µl of ddH_2O. The washed cells were then resuspended in 200 µl of breaking buffer (as in Section 2.4.2.2), to which 200 µl of phenol/chloroform/isoamyl alcohol and 200 µl of acid-washed glass beads was added. This mixture was vortexed (maximum speed) for three minutes at room temperature, after which 200 µl of TE buffer was added. Following this, the tubes were centrifuged for five minutes at 15 000 rpm and the aqueous layer was transferred to a new tube, to which 1 ml of 95% ethanol was added to precipitate the DNA. This mixture was then centrifuged at room temperature for 3 minutes at 15 000 rpm. The DNA pellet was dried, and then resuspended in 400 µl of TE buffer. At this point, 30 µl of RNaseA (1 µg/µl) was added, and the tubes were incubated at 37°C for 5 minutes prior to the addition of 10 µl of 4 M NH_4OAc and 1 ml of 95% ethanol. This mixture was then centrifuged at room temperature for 3 minutes at 15 000 rpm. The DNA pellet was dried, and then resuspended in 100 µl of TE buffer and stored at –20°C.

2.4.4 Plasmid Transformation

Plasmids were transformed into both *E. coli* and yeast cells.

2.4.4.1 Plasmid Transformation into, and Preparation of, Competent *E. coli* Cells

Plasmid DNA was transformed into *E. coli* cells by electroporation. Prior to transformation, 'electrocompetent' *E. coli* cells were prepared as described (Ausubel et al. 1998). Cells were grown in 2xYT liquid medium to an OD_{600} of 0.6-0.8, then placed on ice for one hour. All subsequent steps were carried out at 4°C or on ice, and all solutions, bottles and tubes were pre-chilled on ice. Cells were centrifuged at 5 000 rpm for 20 minutes, then washed twice with 125 ml ddH_2O, each followed by centrifugation for 20 minutes at 5 000 rpm. The cells were then washed once with 20 ml of 10% glycerol, centrifuged at 5 000 rpm for 10 minutes, and then resuspended in an equal volume of 10% glycerol. Following this, 80-µl portions of cell suspension were placed into microfuge tubes and stored at –80°C until use.

Electroporation was performed using a Gene Pulser (BioRad Laboratories). One portion of cells was thawed on ice, and the plasmid to be transformed (usually 2 µl of

DNA) was added. This mixture was then placed in a pre-chilled 0.2-cm electroporation cuvette (BioRad Laboratories or Invitrogen). The Gene Pulser was used to apply an electric current to the sample, according to the manufacturer's specifications (field strength of 12.5 kV/cm). Following this electroporation procedure, 800 µl of 2xYT liquid medium was added to the cells, which were then incubated at 37°C for 20 minutes, spread onto 2xYT solid medium containing ampicillin to select for plasmid-containing cells, and incubated overnight at 37°C.

2.4.4.2 Plasmid Transformation into Yeast Cells

Plasmids were transformed into yeast using three marginally different lithium acetate methods (Ito et al. 1983). Small-scale transformations were performed using a 5-ml overnight culture of yeast cells. The cells were pelleted by centrifugation, washed once with ddH_2O, once with 2 ml of TE/LiOAc (10 mM Tris-Cl pH 8.0, 1 mM EDTA pH 8.0, 0.1 M LiOAc), and resuspended in TE/LiOAc (100 µl for each transformation). The cell suspension was transferred to a microfuge tube, to which 10 µl of denatured salmon sperm carrier DNA (10 µg/ml), 2-5 µl of plasmid DNA, and 700 µl of 50% PEG (polyethylene glycol) were added. These cells were then incubated at 30°C for 30 minutes, and then at 45°C for 10 minutes. Following this, 80 µl of 95% ethanol was added and the mixture was incubated at 45°C for a further 5 minutes. The cells were then centrifuged at 5 000 x g for 10 seconds, resuspended in 300 µl of TE buffer, and spread on the appropriate solid selective medium for plasmid maintenance.

Large-scale transformations were performed using a slight modification of this protocol. A 50-ml culture of yeast cells was grown to mid-log phase, and the cells were pelleted by centrifugation, washed with 2.5 ml of ddH_2O, and resuspended in a 2:1 mixture of 50% PEG and TE/LiOAc solution (1 ml for each transformation). The cell suspension was transferred to a microfuge tube, to which 33 µl of denatured salmon sperm carrier DNA (10 µg/ml) and 2-5 µl of plasmid DNA were added. These cells were then incubated at 30°C for 30 minutes, and then at 45°C for 10 minutes. Following this, 100 µl of 95% ethanol was added and the mixture was incubated at 45°C for a further 5 minutes. The cell suspension was then centrifuged at 5 000 x g for 10 seconds, resuspended in 300 µl of TE buffer, and spread on the appropriate solid selective medium for plasmid maintenance.

A slightly modified version of the small-scale transformation protocol was used for the transformation of linear fragments containing the *natMX4* or *kanMX4* cassettes (Wach et al. 1998). Prior to incubation at 45°C, 70 µl of DMSO was added to the cell mixture, and 95% ethanol was not added following the 45°C incubation. Also, the cell pellets obtained following this incubation were resuspended in 3 ml of YM1 medium and incubated at 30°C for approximately eight hours prior to spreading onto solid selective medium.

2.4.5 Plasmid Loss

To obtain yeast cells that no longer contain a particular plasmid, a plasmid loss procedure was carried out (Cormack, Castano 2002). Briefly, cells were grown for 3 days at 30°C in 3 ml of liquid medium supplemented with the amino acid or nucleoside base of interest (i.e. for 'loss' of a *LEU2*-based plasmid, the growth medium would be supplemented with leucine). Following growth, 10 µl of this cell culture was used to inoculate 3 ml of the same supplemented liquid medium, and the cells were once again grown to stationary phase. This subculturing was performed one more time, after which 300 µl of a 1:10 000 dilution of the final cell culture was spread onto solid medium. To identify the resulting colonies that no longer contain the plasmid of interest, replica plating to solid medium lacking the amino acid or nucleoside base of interest was performed.

2.4.6 DNA Sequencing

DNA sequencing was performed by sequencing facilities (either Robarts Research Institute, London, ON, or DalGEN DNA Sequencing Facility, Halifax, NS) that employ an automated dideoxynucleotide triphosphate terminator sequencing method (Sanger, Nicklen & Coulson 1977). ChromasPro software (Technelysium Pty Ltd) was used to view, edit, align, and generate consensus sequences from the raw sequencing files provided by the sequencing facilities. Sequencing primers are listed in Table 3.

2.4.7 Polymerase Chain Reaction (PCR)

Several types of PCR were employed, depending on the application. When changes in nucleotide sequence were not detrimental, such as for verification of the presence or size of a piece of DNA, Platinum Taq DNA Polymerase (Invitrogen) that lacks proofreading capabilities was employed. However, when nucleotide sequence was important, such as for the production of DNA to be used for cloning or sequencing, high-fidelity Taq that

Table 3. Primers used in this study.

Primer	Sequence (5' → 3')	Usage	Notes
Primers to Verify Deletion Strains:			
ASF1 F	TCATTTACGCGTTTTTTCCTT	PCR	
ASF1 R	CCCTTAGCATGGGAGAGGTCT	PCR	
CTK1 F	CATATTGATTGCCAATGAGATG	PCR	
CTK1 R	CAGTTAGTGGCCAGGCTAATTT	PCR	
EAF3 F	ACCAACCGATGCTGATAGAA	PCR	
EAF3 R	ATGCGAAACGATGGATACGT	PCR	
ELP3 F	TCAAAAGTCAATACTGCCACTG	PCR	
ELP3 R	TTCGTTCCTTCCCTTCTGTT	PCR	
GCN5 F	AAACGCGTGTTAAACAGGCAT	PCR	
GCN5 R	AAAGTCCAGAAGAAGCGGATGT	PCR	
HHF1 F	TTACTTTAGCAAATGCCCGC	PCR	
HHF1 R	AAAATACGAGGCGCGTGTAA	PCR	
HHT1 F	ATTTCCTTGCTCTGCACCTT	PCR	
HHT1 R	AAGCCATAAATCTTGCCTCC	PCR	
JHD1 F	TGTGGTGGCATTCATCTTGA	PCR	
JHD1 R	GAACATGCCATTGATGAACG	PCR	
NAP1 F	ACAAGTTGGTGGGAAATGAGC	PCR	
NAP1 R	CCTTTTATAACCCTTGCTGCT	PCR	
RAD6 F	TGGTGACTACATTTCCCGGAT	PCR	
RAD6 R	AAGATACGGGTATCGGCAGTT	PCR	
RCO1 F	ATTGCTCTCTGTTGCAAGGTT	PCR	
RCO1 R	GGGCACGAAAATATTGTGATG	PCR	
RPD3 F	TGAAGCGGTGAGAGCTAATTT	PCR	
RPD3 R	TTTATCAACAGCGGTGGGA	PCR	
RTT106 F	CATTCTCCCTCCAGAATTCAA	PCR	
RTT106 R	CGAACGTATTATAGAGGCGCT	PCR	
RTT109 F	CCCGTTAAGTCGTAAACGTCAA	PCR	
RTT109 R	GCCAACCTGAGCAGTAGAGTAA	PCR	
SAS3 F	TGACATGCTATTTTGGTGGTT	PCR	
SAS3 R	ACGCAATGAGCAAGATGAAC	PCR	
SET2 F	TTGTCACGTGATCAATATCACC	PCR	
SET2 R	AGACACTTGAAACGCACGAT	PCR	
SIN3 F	TTGTCTTCCCTTTTTCGCAC	PCR	
SIN3 R	TGACGTGTAAAAAGATTCATGC	PCR	
275UPS SPT4	ACTATTTAAAGCGGTCCTCGTAG	PCR	
289DNS SPT4	TGCACGAGAATGACGCAAAA	PCR	
SWD1 F	TTTCCAAACTACAGAGGGAAGA	PCR	
SWD1 R	GCCCTTTAGGTGTACAGCTTCA	PCR	
SWD3 F	TCATAGTTGGTATGCAGGCTG	PCR	
SWD3 R	GCGAGTTCTTCGAGATGTGAA	PCR	

Primer	Sequence (5' → 3')	Usage	Notes
Primers to Verify Deletion Strains:			
VPS75 F	TGAAAAAGGAAAGGAGGAAAG	PCR	
VPS75 R	TACTATTTCCGCTTCTGGTGC	PCR	
kanMX4 Primers:			
KanB	CTGCAGCGAGGAGCCGTAAT	PCR	*kanMX4* internal reverse
KanC	TGATTTTGATGACGAGCGTAAT	PCR	*kanMX4* internal forward
natMX4 Primers:			
OPP1097	GGACTCCCGGACGTTCGTCGCG	PCR	*natMX4* internal forward (P. Poon, this lab)
OPP1098	CGCGACGAACGTCCGGGAGTCC	PCR	*natMX4* internal reverse (P. Poon, this lab)
SPT16 Primers:			
5' SpeI flank	GAAGGTTCTCCAAATTCGCT	PCR	confirm presence of *SPT16*
3' SpeI flank	TTAAAGCAGTCACCGCGTTGG	PCR	confirm presence of *SPT16*
5' HindIII flank	GATTTCAATCCCCACTAAGG	PCR and sequencing	identify E763G; confirm S-tag orientation
3' HindIII flank	TTGATGCTTCTGCGATTGCG	PCR and sequencing	identify E763G
S-Tag Primer:			
S-Tag Reverse	GCTCTAGACTACTACAGATCTGGGCTGTCC	PCR	confirm S-tag orientation
BUR1 Primers:			
492UPS BUR1	GCGGCGGCCGCTGCAACTGGATTTTTTTACCG	PCR	contains a NotI site
16UPS BUR1	CGCGGATCCTTCTGCTTGACCACGAATGT	PCR	contains a BamHI site
10DNS BUR1	CGCGGATCCTTCTCTCTTCCTTTCTGGCCT	PCR	contains a BamHI site
495DNS BUR1	CGCGTCGACCAGTGATCGTTGTATCGAGGA	PCR	contains a SalI site
715UPS BUR1	ATTTTGATCTCAGCCGCTAGG	PCR	confirm *natMX4* integration
635DNS BUR1	ACGGCGATTATTACCTGGTCA	PCR	confirm *natMX4* integration

Primer	Sequence (5' → 3')	Usage	Notes
BUR2 Primers:			
430UPS BUR2	CCCGCGGCCGCCTTTGCTCTATGATTTTTATG	PCR	contains a NotI site
25UPS BUR2	GCGGGATCCCGAAAATACTACGGCCTCCTTC	PCR	contains a BamHI site
21DNS BUR2	CGCGGATCCTTAATTGGAGGGATCAGTAAAGG	PCR	contains a BamHI site
333DNS BUR2	GCGCTCGAGCCAACTACCTAAGGTACTGTTGA	PCR	contains a XhoI site
98UPS BUR2 F	TTTCTGTTAGAAAGCAAG	Sequencing	
408 BUR2 F	AGGCCTATAGAGGCCTAT	Sequencing	
914 BUR2 F	CAACTTAAAAAGTAATAAAGG	Sequencing	
HIR1 Primers:			
420UPS HIR1 SMAI	GCGCCCGGGAAGACATCGTAGTAATAAGGTGCA	PCR	contains a SmaI site
1UPS HIR1 BAMHI	CGCGGATCCGTTATCAGAGACCTTTGGTTACTG	PCR	contains a BamHI site
10DNS HIR1 BAMHI	CGCGGATCCACCCCTTCCTTTGGACAAGTT	PCR	contains a BamHI site
402DNS HIR1	GCGGCGGCCGCAGTTTCGTACAATCTGTGCT	PCR	contains a NotI site
100UPS HIR1 F	AGGTGGCAGAAACATATA	Sequencing	
400 HIR1 F	TTGCACACGATAACGACA	Sequencing	
900 HIR1 F	AAAGACGATGACCCAGAA	Sequencing	
1412 HIR1 F	TATCTTGATTCCAAAGAG	Sequencing	
1902 HIR1 F	CCGACAACACGATGCCTT	Sequencing	
2405 HIR1 F	GGTTATTAAATGCTTTCG	Sequencing	
HIR2 Primers:			
377UPS HIR2	CGCCTGCAGTCTGCTTTTCTATCAGTTCTC	PCR	contains a PstI site
1UPS HIR2	CGCGGATCCTGTTCCGGATTGTGTAGGAA	PCR	contains a BamHI site
1DNS HIR2	CGCGGATCCTTTGGCTTTAACAATGTATAG	PCR	contains a BamHI site
367DNS HIR2	GCGGCGGCCGCTTTTGAAACAGACCGACAAAC	PCR	contains a NotI site
100UPS HIR2 F	GAATTATGAAGTCTTCAT	Sequencing	
401 HIR2 F	CTTATTTGTTCTTTTAAG	Sequencing	
900 HIR2 F	GGTACTATTTTGGTTTGG	Sequencing	
1400 HIR2 F	CAGCAAAAAGCAGAAAAA	Sequencing	
1900 HIR2 F	TAAACCCGTCATTGCGAT	Sequencing	
2400 HIR2 F	ATGATGGTTTATTGCATC	Sequencing	
Library Plasmid Primers:			
p366 F	TTGGAGCCACTATCGACTACG	Sequencing	S. Lewis, this lab
p366 R	CCACGATGCGTCCGGCGTAGA	Sequencing	S. Lewis, this lab

includes proofreading was employed: either Platinum Taq DNA Polymerase High Fidelity or Platinum *Pfx* DNA polymerase (Invitrogen). Template DNA varied depending on the application: plasmid DNA, chromosomal DNA, and whole yeast cells (colony PCR) were all used. All PCR reactions were performed in a hot-bonnet thermocycler (MJ Research, Waltham, MA). PCR primers are listed in Table 3.

2.4.7.1 PCR using Platinum Taq DNA Polymerase

A typical 50-µl PCR reaction using Platinum Taq DNA Polymerase comprised 5 µl of 10x PCR buffer, 1 µl of 10 mM dNTP mix, 1.5 µl of 50 mM $MgCl_2$, 2 µl of each primer (0.05 µg/µl stock), 5-10 µl of template DNA, and 0.5 µl of Platinum Taq DNA Polymerase, brought to 50 µl with ddH_2O. Reaction mixtures were heated for denaturation at 94°C for 2 minutes, after which the following cycle was performed 35 times: denature at 94°C for 30 seconds, anneal at 50°C to 60°C (depending on primer annealing temperature) for 45 seconds, extension at 72°C for 0.5 to 4 minutes (1 minute per kb to be amplified). A final 5-minute incubation at 72°C was performed to complete primer extension.

2.4.7.2 PCR using Platinum Taq DNA Polymerase High Fidelity

A typical 50-µl PCR reaction using Platinum Taq DNA Polymerase High Fidelity comprised 5 µl of 10x High Fidelity PCR buffer, 1 µl of 10 mM dNTP mix, 2 µl of 50 mM $MgSO_4$, 2 µl of each primer (0.05 µg/µl stock), 5-10 µl of template DNA, and 0.5 µl of Platinum Taq High Fidelity, brought to 50 µl with ddH_2O. Reaction mixtures were heated for denaturation at 94°C for 2 minutes, after which the following cycle was performed 35 times: denature at 94°C for 30 seconds, anneal at 50°C to 60°C (depending on primer annealing temperature) for 45 seconds, extension at 68°C for 0.5 to 4 minutes (1 minute per kb to be amplified). A final 5-minute incubation at 68°C was performed to complete primer extension.

2.4.7.3 PCR using Platinum *Pfx* DNA Polymerase

A typical 50-µl PCR reaction using Platinum *Pfx* DNA Polymerase comprised 5 µl of 10x *Pfx* Amplification buffer, 1.5 µl of 10 mM dNTP mix, 1 µl of 50 mM $MgSO_4$, 2 µl of each primer (0.05 µg/µl stock), 5-10 µl of template DNA, 0.5 µl of Platinum *Pfx* DNA Polymerase, and 5 µl of Enhancer Solution (used only with GC-rich templates), brought to 50 µl with ddH_2O. Reaction mixtures were heated for denaturation at 94°C for 2

minutes, after which the following cycle was performed 35 times: denature at 94°C for 30 seconds, anneal at 50°C to 60°C (depending on primer annealing temperature) for 45 seconds, extension at 68°C for 0.5 to 4 minutes (1 minute per kb to be amplified). A final 5-minute incubation at 68°C was performed to complete primer extension.

2.4.7.4 Colony PCR

Colony PCR was performed using either Platinum Taq DNA Polymerase or Platinum Taq DNA Polymerase High Fidelity according to the above protocols, with the following modifications. Rather than the addition of template DNA, a single freshly grown yeast colony was placed at the bottom of the microfuge tube. The tube was microwaved on high power for 1.5 minutes, and then placed on ice. Following this, the PCR mixture was added to the tube and thermocycling was performed as described above.

2.4.8 Agarose Gel Electrophoresis

DNA fragments were resolved using agarose gel electrophoresis, as described in Sambrook *et al.* (1989). Agarose gels were prepared in 1X TAE buffer (40 mM Tris-acetate, 1 mM EDTA), using from 0.6 to 1% agarose (depending on the sizes of the DNA bands). Ethidium bromide (0.5 μg/ml) was either added to the gel directly, or staining was performed following electrophoresis. All DNA samples and molecular markers (1 kb ladder; Invitrogen) were mixed with 10x loading buffer (50 mM EDTA pH 8.0, 50% glycerol, 0.3% bromophenol blue, 0.3% xylene cyanol) to a final concentration of 1x.

2.5 Genetic Analyses

2.5.1 Diploid Cell Construction

Diploid cells were constructed essentially as described in Guthrie and Fink (1991). Briefly, populations of two haploid cells of opposite mating types were mixed on YEPD solid medium and incubated overnight. The resultant diploids were selected using medium on which only the expected diploid cells can grow, taking advantage of drug resistance or prototrophies present only in the diploid cells. When such selection could not be employed, diploid cells were isolated manually by selection of zygotes using a micromanipulator (Singer Instrument Co., Watchet, England). The unique 'dumbell' cell shape of zygotes facilitated this selection (as shown in Sena, Radin & Fogel (1973)).

2.5.2 Tetrad Analysis

Diploid yeast cells undergo meiosis and sporulation when exposed to nutrient starvation, each cell producing four meiotic haploid progeny (called spores) inside an ascus. Sporulation of diploid cells was carried out as described in Section 2.1.1. Following sporulation, 0.2 ml of sporulation culture was diluted in 0.8 ml of phosphate-buffered saline (pH 7.4), to which 2 µl of zymolyase (MP Biomedicals, Solon, OH) was added. Zymolyase digestion was carried out for approximately 10 minutes at room temperature to weaken the walls of the asci. At this point, a sterile loop was used to spread the digested mixture onto the edge of a strip of YNB solid medium, and separation of the four spores from single asci was performed using a micromanipulator (Singer Instrument Co.). This strip of solid medium was then placed onto YEPD solid medium to accommodate any auxotrophies present in the haploid progeny and incubated for 4-5 days at 23°C to allow spore germination and colony formation. Following this, the segregants from each meiosis were patched onto YEPD medium, grown overnight, and then replica-plated to appropriate selective media to observe the segregation of markers.

2.5.3 Determination of Mating Type

To determine the mating type of segregants, or to ensure that cells are haploid rather than diploid, test crosses were performed with two strains, one each for *MAT***a** (GRX2-1A) and *MAT*α (XJB3-1B). Diploids were produced and identified as described above (Section 2.5.1), using selection medium that only diploid cells could grow on. The production of diploid cells indicated that the parental strains were of opposite mating type, whereas failure to produce diploids was an indication that the parental strains were of the same mating type.

2.6 Yeast Protein Analyses

2.6.1 Preparation of Yeast Whole Cell Extracts

Whole cell extracts were prepared in slightly different manners, depending on whether the extracted protein was to be used in co-immunoprecipitation experiments.

2.6.1.1 Whole Cell Extracts to be used in Western Blotting

Cell extracts were prepared as described in Guthrie and Fink (1991). Briefly, cell cultures (50-150 ml) were grown to mid-log phase (2-5 x 10^6 cells/ml) and the cell pellet was

recovered by centrifugation at 3 000 rpm for 2 minutes and resuspended in 500 µl of Glass Bead Disruption Buffer (20 mM Tris-Cl pH 7.9, 10 mM $MgCl_2$, 1 mM EDTA pH 8.0, 5% glycerol, 0.3 M $(NH_4)_2SO_4$), to which protease inhibitors (Sigma-Aldrich) were added to 10 µl/ml (100x protease inhibitor stock contains 62.5 µg/ml antipain, 0.05 µg/ml chymostatin, 2.5 µg/ml leupeptin, and 5µg/ml pepstatin) and PMSF added to 10 µl/ml. This suspension was transferred to a microfuge tube containing approximately 300 µl of acid-washed glass beads, vortexed at 4°C for 6 minutes, and then centrifuged at 4°C for 2 minutes. The supernatant was transferred to a new tube and stored at –20°C as whole cell extract.

2.6.1.2 Whole Cell Extracts to be used in Co-Immunoprecipitations

Slight modifications were made to the above protocol when the extracts were to be used in co-immunoprecipitation experiments. Briefly, cell cultures (50-150 ml) were grown to mid-log phase (2-5 x 10^6 cells/ml) and the cell pellet recovered by centrifugation at 3 000 rpm for 2 minutes, washed once with 2 ml ddH_2O, and resuspended in 500 µl of Co-IP Buffer (50 mM Tris-Cl pH 7.4, 50-150 mM KOAc [depending on desired stringency], 5 mM EDTA pH 8.0, 0.1% Triton X-100, 10% glycerol, 1 mM NaN_3), to which protease inhibitors (as above) were added to 10 µl/ml and PMSF added to 10 µl/ml. This mixture was transferred to a microfuge tube containing approximately 300 µl of acid-washed glass beads, vortexed at 4°C for 15 minutes, and then centrifuged at 4°C for 15 minutes. The supernatant was transferred to a new tube and stored at –20°C as whole cell extract.

2.6.2 Quantification of Total Protein

Protein concentrations in whole cell extracts were quantified using the Bradford assay (BioRad protein assay) and a bovine serum albumin (BSA) standard (New England Biolabs). Protein (BSA) standards containing 5 µg, 10 µg, 15 µg and 20 µg of total protein were mixed with Bradford Reagent (BioRad, Hercules, CA). Samples from each whole cell extract were also mixed with Bradford Reagent, and the A_{595} was recorded for each standard and sample. Using a standard curve generated from the BSA samples, the protein concentration in each whole cell extract was calculated.

2.6.3 Co-Immunoprecipitation

For co-immunoprecipitation experiments, 500 µg of total protein in co-IP buffer with the desired salt concentration was made to a total volume of 200 µl with co-IP buffer in a

microfuge tube containing 100 µl (settled volume) of S-protein agarose beads (Novagen, Madison, WI). All steps were performed either on ice or at 4°C, with pre-chilled reagents. This mixture was incubated for 2 hours with rotation, and then centrifuged for two minutes. The supernatant was discarded, and the beads were washed 3 times, each time with 1 ml co-IP buffer. Following the final wash, 50 µl of 2x Laemmli buffer (100 mM Tris-Cl pH 6.8, 10 mM EDTA, 20% glycerol, 4% SDS, 0.1 µl/ml β-mercaptoethanol, and 0.8 µl/ml bromophenol blue [0.25% solution]) was added to the beads, and the tubes were incubated at 100°C for 10 minutes. If the samples were not used immediately in SDS-PAGE, they were stored at –20°C.

For co-immunoprecipitation experiments involving the use of ethidium bromide (EtBr), the whole cell extracts were first treated with EtBr to interfere with protein-DNA interactions (Lai, Herr 1992). EtBr was added to extracts to a concentration of 50 µg/ml, followed by incubation on ice for 30 minutes. The tubes were then centrifuged for 5 min at 4°C, and the resulting supernatant was transferred to a new tube. Co-immunoprecipitation was carried out as described above, except that the buffer used to wash the beads also contained EtBr at 50 µg/ml.

2.6.4 SDS-PAGE and Transfer to PVDF Membranes

Proteins were resolved by SDS polyacrylamide gel electrophoresis (SDS-PAGE) using a mini-PROTEAN II gel apparatus (Bio-Rad), as described in Ausubel *et al.* (1998). The acrylamide percentage, 7.5%, 10% or 15%, depended on the size of the protein of interest. A typical 10% separating gel was composed of 2.5 ml 1.5 M Tris-Cl pH 8.8, 100 µl 10% SDS, 3.3 ml 30% acrylamide/bisacrylamide (30:0.8), 4.05 ml ddH_2O, 50 µl ammonium persulfate and 5 µl TEMED; for other percentages, the volumes of acrylamide/bisacrylamide and ddH_2O were adjusted as needed. For all percentages of separating gel, the stacking gel was composed of 2.5 ml 0.5 M Tris-Cl pH 6.8, 100 µl 10% SDS, 1.33 ml 30% acrylamide/bisacrylamide, 6.1 ml ddH_2O, 50 µl ammonium persulfate and 10 µl TEMED. Prior to loading, all samples were heated to 100°C for 5-10 minutes, and then centrifuged briefly to collect the sample. For samples from whole cell extracts, an equal volume of 2x Laemmli buffer was added prior to heating at 100°C. 5 µl of Rainbow Markers (Amersham Biosciences, Piscataway, NJ) (mixed with 5 µl 2x Laemmli buffer) was similarly treated and used as a molecular size marker. Running

buffer (0.3% Tris base, 1.44% glycine and 0.1% SDS) was added to the gel apparatus prior to loading samples.

Following electrophoresis, proteins were transferred to PVDF membrane (Bio-Rad) using a Trans-Blot SD Semi-Dry transfer unit (Bio-Rad). Prior to transfer, the membrane was wetted with methanol, and then by Towbin transfer buffer (0.03% Tris base, 1.44% glycine, 20% methanol); gels were soaked in Towbin buffer for 10 minutes prior to transfer, and Whatman blotting paper was soaked briefly in Towbin buffer. Transfer was carried out for approximately 60 minutes at 200 mA. Following transfer, membranes were washed twice for 10 minutes each in 0.1% TBS-T buffer (10 mM Tris-Cl pH 7.4, 140 mM NaCl, 0.1% Tween 20), and stained with India Ink (1 µl/ml; Pelikan Inc., Pembroke, MA) to assess the quality of transfer (as described in Sambrook *et al.*, 1989). Membranes were then washed three times for 10 minutes each in 0.1% TBS-T.

2.6.5 Western Blotting

Prior to western blotting, membranes were incubated overnight at room temperature in either 10% milk (Carnation non-fat milk powder) or 5% BSA (only when using antibodies against the RNAPII CTD [α-RNAPII]) in 0.1% TBS-T buffer. Membranes were then washed three times for 10 minutes each in 0.1% TBS-T. Incubation with primary antibodies was then carried out as follows (all in 0.1% TBS-T): α-HA (12CA5, Abcam, Cambridge, MA or Santa Cruz Biotechnologies, Santa Cruz, CA) at 1:2000 in 1% milk for 2 hours, α-H3 (ab1791, Abcam) at 1:5000 in 1% milk for 1.5 hours, α-H3K4triMe (ab8580, Abcam) at 1:2000 in 1% milk for 2 hours, α-RNAPII (4H8, ab5408, Abcam) at 1:15 000 in 5% BSA, and S-protein-HRP (Novagen) at 1:2000 in 1% milk for 2 hours. Membranes were then washed three times for 10 minutes each in 0.1% TBS-T, followed by incubation with secondary antibodies (all in 1% milk in 0.1% TBS-T for 2 hours): goat anti-rabbit-HRP (Kirkegaard and Perry Laboratories, Gaithersburg, MD) at 1:5000 (α-H3 and α-H3K4triMe blots) or goat anti-mouse-HRP (Santa Cruz Biotechnologies) at 1:2000 (α-HA and α-RNAPII blots). Membranes were then washed three times for 10 minutes each in 0.1% TBS-T, and bound antibody was detected using either the LumiGlo Chemiluminescent substrate system (Kirkegaard and Perry Laboratories) or Western Lightning Chemiluminescent Reagent Plus substrate system (PerkinElmer, Waltham, MA).

Chapter 3 RESULTS

3.1 Screen for Synthetic-Lethal Interactions with *spt16-E857K*

To gain further insight into the functions of the Spt16 subunit of FACT, a mutant version of this protein was used in a 'classical' screen for synthetic-lethal interactions (Bender, Pringle 1991). This screen identifies proteins that interact functionally with Spt16, by searching for genomic mutations that are lethal in combination with a point-mutant version of *SPT16*, in this case *spt16-E857K*. Synthetic lethality between mutations in two genes indicates a common function for their respective proteins. If the mutations in question result in proteins with partial function, then the identification of synthetic-lethal mutations can identify second proteins that function in the same cellular pathway, or in the same protein complex (Figure 7) (Appling 1999, Guarente 1993). In contrast, if the mutations in question are complete deletions, or result in non-functional proteins, then the identification of synthetic-lethal mutations can identify parallel pathways that carry out an overlapping function with the protein that is missing (Figure 7) (Guarente 1993). Thus, by identifying genomic mutations that are lethal in combination with *spt16-E857K*, I can begin to ascertain which functions of the Spt16 protein are impaired by this substitution, and also how Spt16 activity relates to those of other proteins.

The *spt16-E857K* mutation itself was identified in a screen for novel mutations in the *SPT16* gene that cause a dominant Spt phenotype (O'Donnell 2004). This mutant allele was chosen for further investigations for several reasons. One reason was that it contains a single point mutation, and thus any differences between the behaviour of the mutant Spt16-E857K protein and normal Spt16 can be attributed to this change alone. A second was that the Spt16-E857K protein is most likely stable, as inferred from its ability to produce an Spt phenotype that is dominant (O'Donnell 2004), unlike the products of previously characterized alleles such as *spt16-G132D* (also known as *cdc68-1*), which has been shown to produce an unstable protein (Xu, Singer & Johnston 1995). This situation means that any observations made using the *spt16-E857K* mutant allele demonstrate an effect of a change on protein function, rather than that of an altered abundance of Spt16 protein resulting from a mutation. Finally, the only phenotype observed (so far) for cells containing the *spt16-E857K* allele as the only form of *SPT16*

Figure 7. Mechanisms of synthetic-lethal interactions. This figure illustrates possible underlying mechanisms to produce deleterious genetic interactions using either null or non-null mutations. The first and second mechanisms deal with non-null mutations only, while the third can be produced by either null or non-null mutations. The situation in mechanism 1 illustrates the effects of two mutations in the same pathway, while that of mechanism 2 illustrates the effects of two mutations affecting members of the same complex. Mechanism 3 is slightly more complex: it illustrates the effects of mutations in two parallel pathways that both have the same effect on a downstream target. (modified from O'Donnell (2004))

	Function	Viable cells?

A. Single Pathway or Complex (non-null mutations)

1.

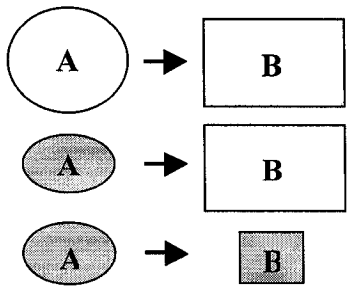

Function	Viable cells?
Yes	Yes
Impaired	Yes
No	No

2.

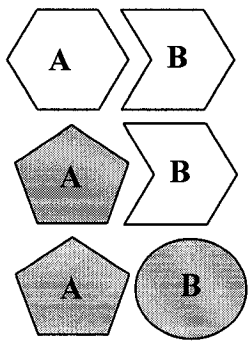

Function	Viable cells?
Yes	Yes
Impaired	Yes
No	No

B. Parallel Pathways (null or non-null mutations)

3.

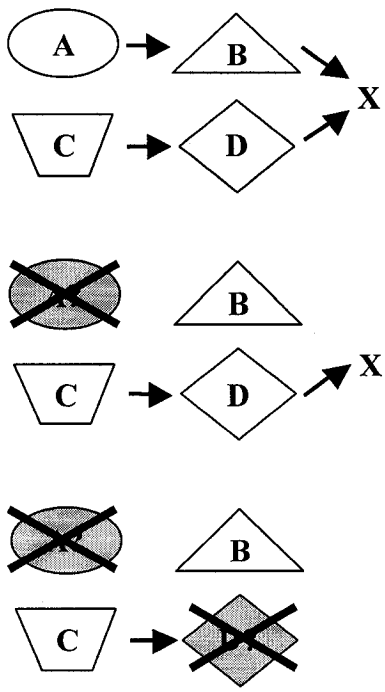

Function	Viable cells?
Yes	Yes
Impaired or Yes	Yes
No	No

had been this Spt phenotype. Thus, unlike many of the other mutant alleles of *SPT16*, which have multiple phenotypes, perhaps due to several different alterations of Spt16 or FACT function, the *spt16-E857K* mutation produces a relatively 'mild' alteration in protein function. This makes *spt16-E857K* an ideal mutant allele to use for synthetic-lethal screening, as we might expect this mutation to produce subtle changes in protein function, and thus affect a limited number of Spt16-mediated functions. These two properties of the *spt16-E857K* mutant allele increase the probability that any synthetic-lethal interactions that are identified truly reflect biological interactions of a functional nature. That is, we are likely to identify mutations in second genes that encode proteins with functions related to those of Spt16, rather than genes encoding proteins related to Spt16 protein stability, or other less immediate functions.

3.1.1 Screening Procedure

In a classical synthetic-lethal screen, mutations in the adenine biosynthesis pathway are exploited to allow a two-colour discrimination system for screening yeast colonies (Kranz, Holm 1990)(Bender, Pringle 1991). Cells that contain mutations in the *ADE2* gene accumulate an intermediate in this biosynthetic pathway, 5-phosphoribosyl 5-aminoimidazol, which causes the yeast colonies to appear red in colour, rather than the normal off-white colour. The *ADE3* gene product mediates a step in the pathway upstream of that of Ade2. Thus, cells with a mutation in the *ADE3* gene fail to produce this 'red' intermediate compound, regardless of the status of the *ADE2* gene, and therefore produce colonies with the normal off-white colour. In the synthetic-lethal screening procedure, the starting cells contain mutations in both the chromosomal *ADE2* and *ADE3* genes, and thus appear off-white in colour. However, a plasmid is introduced that contains a functioning *ADE3* gene; cells containing this plasmid are therefore blocked at only the Ade2 step of the pathway, thus accumulating the 'red' intermediate compound and forming red colonies. Colony colour for these cells therefore indicates the presence or absence of the *ADE3* plasmid, thereby also indicating the presence or absence of the *SPT16* gene found on the same plasmid, as described below.

The *ADE3* plasmid that I used, pSNLCDC68, also contains a wild-type copy of the *SPT16* gene, meaning that the colony-colour procedure can be used to determine whether cells contain this plasmid-borne copy of *SPT16* (and thus appear red) or do not

(and thus appear white). In addition, two other features of this plasmid facilitate the classical synthetic-lethal screening procedure: the *URA3* gene, and a centromere that is positioned downstream of the *GAL1* promoter. The *URA3* gene allows selection for cells containing this plasmid by growth on medium lacking uracil, and also provides a means for selecting *against* cells containing this plasmid (explained in detail below). Also, when cells containing this plasmid are grown on galactose medium, the plasmid-borne *GAL1* promoter activates transcription through the centromeric region, providing an effective mechanism for decreasing both plasmid centromere function and the efficiency of plasmid inheritance at mitosis (Barbour, Zhu & Xiao 2000). Thus, cells that no longer contain this plasmid (as a result of a failure to inherit) can be readily generated.

The haploid strain SNL-51B (*MATα spt16Δ::kanMX4 ade2Δ ade3Δ ura3-52 trp1-Δ1 leu2-3,112* [pRS316-A4]) (pRS316-A4 is a *URA3*, *SPT16* plasmid) was constructed for synthetic-lethal screening, and transformed first with a centromeric *TRP1 spt16-E857K* plasmid. Next, the *SPT16* plasmid pRS316-A4 was selected against; a resulting derivative was then transformed with the pSNLCDC68 plasmid (*URA3 ADE3 SPT16*), to create the strain SNL-51B 314-NM3(4) WT68 (all by Allyson O'Donnell, a former PhD student in the Singer/Johnston lab) (O'Donnell 2004) (Figure 8 – top). These cells contain two versions of the Spt16 protein, each able to provide all essential functions of Spt16. The presence of the wild-type version of Spt16 can be determined by observing colony colour: the *ADE3* gene on pSNLCDC68 is able to complement the *ade3Δ* deletion in the chromosome, thus allowing blockage of the adenine biosynthesis pathway at the downstream Ade2 step and allowing the red pigment to be produced. When cells are generated that do not contain this plasmid, due to a failure in plasmid inheritance at a previous mitosis, they will appear white due to the loss of the Ade3 protein and a consequent blockage of the adenine biosynthesis pathway upstream of the pigment-forming intermediate. In this situation, the Spt16-E857K protein that remains, encoded on the second plasmid, can still provide all essential Spt16 functions (Figure 8 – bottom left).

Using this strain to provide starting cultures, I carried out a synthetic-lethal screening procedure. Yeast cultures of the SNL-51B derivative containing plasmid-borne copies of both the *spt16-E857K* point-mutant and wild-type versions of the *SPT16* gene

Figure 8. Outline of synthetic-lethal screening procedure. The haploid strain SNL-51B 314-NM3(4) WT68, harbouring plasmids pSNLCDC68 (*URA3 ADE3 SPT16 GAL1p-CEN4*) and pRS314-cdc68-E857K (*TRP1 spt16-E857K*), shown at the top, forms red-coloured colonies. Screening is performed after UV mutagenesis to introduce new mutations (*mut1*) followed by growth on galactose medium to prevent efficient inheritance of pSNLCDC68. Cells that fail to inherit pSNLCDC68 grow into white-coloured colonies (shown at left), indicating that these cells do not possess a *mut1* mutation that is synthetically lethal with *spt16-E857K*. However, when a synthetic-lethal interaction exists between the *mut1* mutation and *spt16-E857K*, cells that fail to inherit pSNLCDC68 will not grow, and only red-coloured colonies are produced consisting of cells that contain pSNLCDC68 (shown at right).

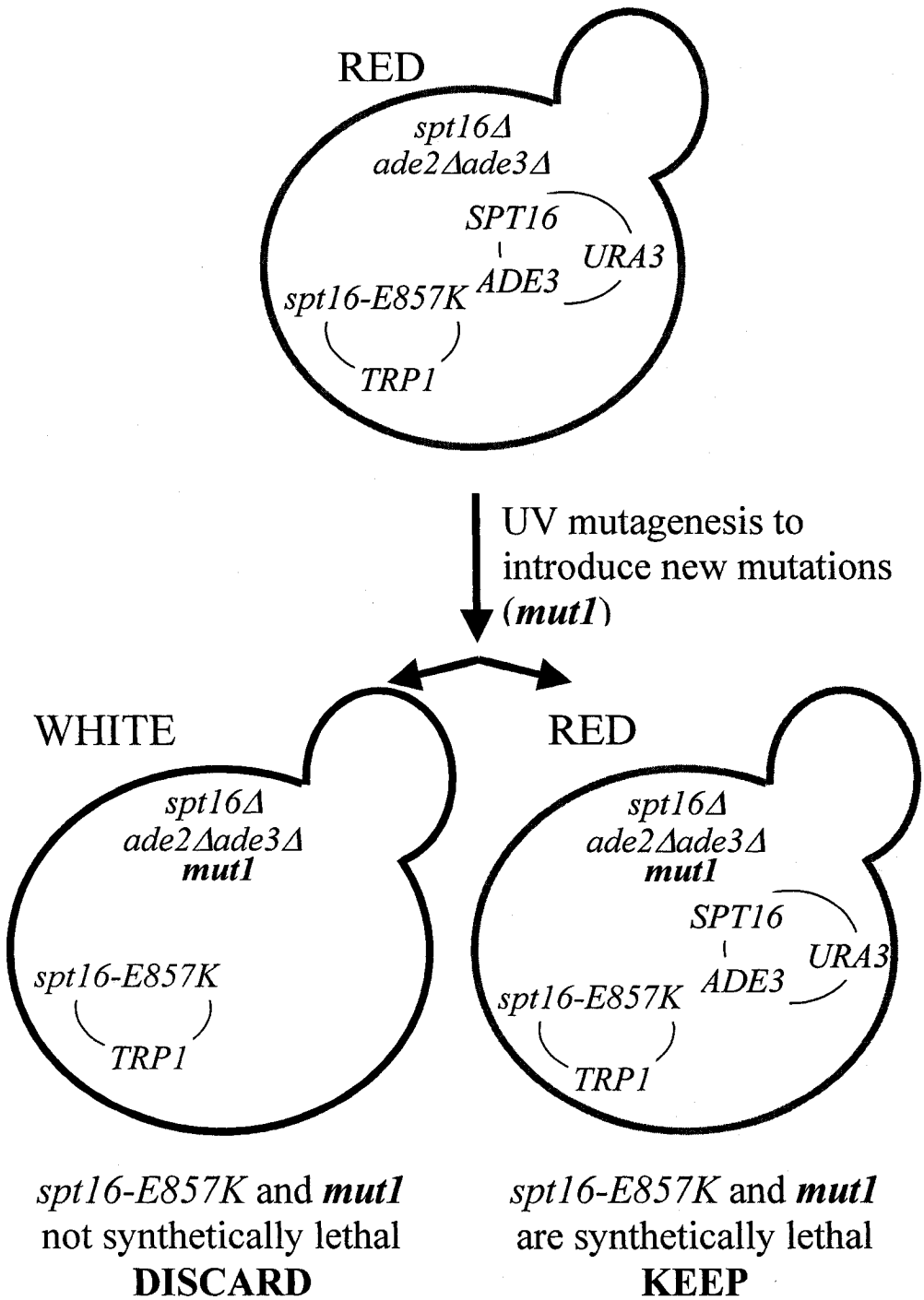

spt16-E857K and ***mut1***
not synthetically lethal
DISCARD

spt16-E857K and ***mut1***
are synthetically lethal
KEEP

were spread onto solid medium that lacked tryptophan, to select those cells containing the *spt16-E857K* plasmid, and contained galactose, to destabilize centromere function for the *SPT16* plasmid and facilitate the failure to inherit this plasmid. I then immediately introduced random mutations into the genome of these cells using UV light at a dose sufficient to kill ~40% of the cells. These treated cells were then grown in the dark, to avoid light repair of UV-induced mutagenic thymine dimers (reviewed in Sancar (2000)). Following colony growth I looked for uniformly red colonies, an indication that the cells in the colony must retain the wild-type *SPT16* plasmid for growth. As most cells will contain mutations that do not affect growth of cells with the *spt16-E857K* mutation, the majority of colonies will appear either white or with white sectors (Figure 8 – bottom left). The colonies of interest were uniform in the red colouring, as it is possible for sectors of colour to appear, resulting in a colony that has both red and white 'pie-piece shaped' regions within it. This is due to the growth pattern of the cells within a colony. Each colony began as a single yeast cell and it is possible for cells lacking the *SPT16* plasmid to be generated during any round of cell division. Any cells produced from a newly generated 'white' cell will also lack the *SPT16* plasmid, producing a white sector of progeny cells in an otherwise red colony. A white sector thus identifies good growth of cells relying on the *spt16-E857K* gene. This procedure of looking for uniformly red colonies, without white sectors, therefore identifies candidate cells that may have acquired a desired second mutation that is deleterious for a cell relying on the mutated form of Spt16 for growth (Figure 8 – bottom right).

Using this method, I screened ~70 000 colonies containing the *spt16-E857K* point-mutant allele; of these, 360 colonies remained red. Each of these colonies was then streaked onto fresh galactose medium, and allowed to generate new colonies. As described above, galactose causes transcription to occur through the plasmid-borne centromere, thus destabilizing this centromere function. This situation increases the frequency with which cells are produced that have failed to inherit the wild-type *SPT16* plasmid; colony formation on galactose-containing medium allows multiple rounds of cell division to occur under growth conditions that promote the failure to inherit the *SPT16* plasmid. Re-screening in this manner, I was able to decrease the number of

potential synthetic-lethal 'hits' from 360 to eleven that still produced uniformly red colonies.

To provide evidence that these eleven isolates may be true synthetic-lethal hits, I tested each derivative strain for the ability to grow on medium containing 5-fluoro-orotic acid (5-FOA). This compound inhibits the growth of cells with a functioning *URA3* gene, and thus selects against those cells that possess the *URA3 ADE3 SPT16* plasmid (Boeke et al. 1987). The pyrimidine biosynthesis pathway, of which Ura3 is a member, incorporates 5-FOA during the biosynthesis. This results in the production of 5-fluorodeoxy UMP (uridine-5'-monophosphate), which is an inhibitor of thymidylate synthase. Therefore, cells containing a functioning *URA3* gene will die as a result of thymine starvation when exposed to 5-FOA (Boeke, LaCroute & Fink 1984, Santoso, Thornburg 1998). Any cells that contain a desired synthetic-lethal mutation will fail to grow on medium containing 5-FOA: these cells must retain the *SPT16* plasmid to survive, yet this plasmid also carries the *URA3* gene, and thus these cells will not grow. Testing in this manner reduced the number of potential hits from eleven to five: SYNL isolates #1, #4, #7, #9, and #10 (Figure 9).

A potential, although uninteresting, way that would result in cells requiring the *SPT16* plasmid for life is that the UV-mutagenesis procedure introduced a second mutation in the *spt16-E857K* gene, rendering this now double-mutant gene unable to support life. To eliminate this possibility, I performed a plasmid-shuffle procedure with my putative hits. By growing the cells containing putative hits in medium that contained tryptophan (the amino acid synthesized through actions of the *TRP1* marker gene on the *spt16-E857K* plasmid), and then screening for derivatives that could no longer grow in the absence of tryptophan, derivative cells were isolated from each of the putative hits that no longer possessed the *spt16-E857K* plasmid. These derivatives were then transformed with either the non-mutagenized *spt16-E857K* plasmid or an *SPT16 TRP1* plasmid, as a control. The 5-FOA testing was then repeated with these new transformants, to determine which of the isolates had true synthetic-lethal interactions. Putative hits that contained additional mutations in the original *spt16-E857K* mutant allele should be able to grow on medium that contains 5-FOA, while putative hits that are true synthetic-lethal hits should remain unable to grow on medium containing 5-FOA. This testing resulted in

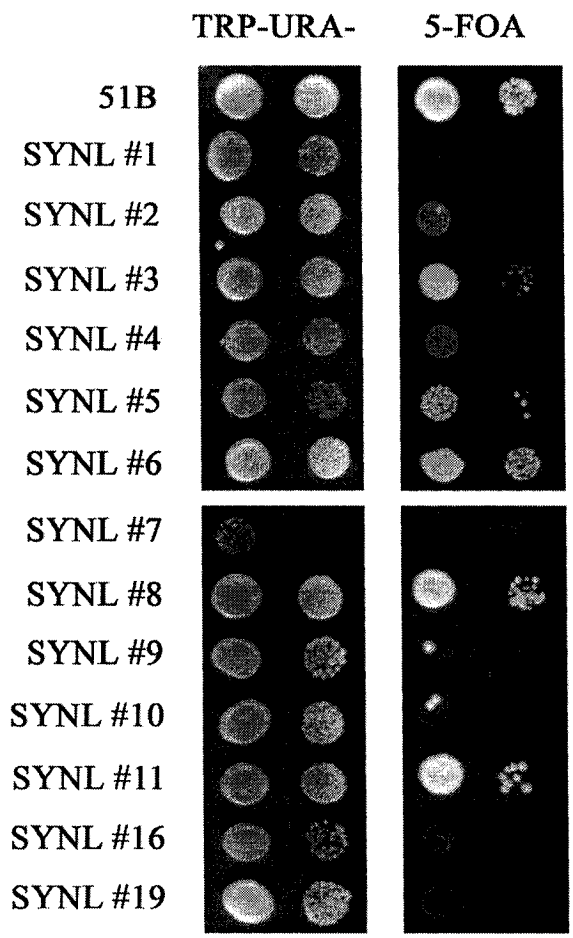

Figure 9. 5-FOA testing of putative synthetic-lethal hits. Liquid cultures of the eleven putative hits were grown to stationary phase, along with positive (51B) and negative (SYNL #16 and #19) controls. Two dilutions of each culture were spotted onto TRP-URA- and 5-FOA solid medium; the plates were incubated at 30°C for two days. The strains SYNL #1, SYNL #4, SYNL #7, SYNL #9 and SYNL #10 were chosen for further testing due to poor or no growth on solid medium containing 5-FOA, indicating a requirement for the *SPT16 URA3* plasmid. Strains SYNL #2, SYNL #3, SYNL #5, SYNL #6, SYNL #8, and SYNL #11 were discarded as false positives due to growth on the medium containing 5-FOA.

the identification of three true synthetic-lethal hits (SYNL #1, #9 and #10), from an initial pool of ~70,000 colonies (Figure 10).

A small-scale screen performed by Allyson O'Donnell using the same *spt16-E857K* starting strain identified two more synthetic-lethal hits (SYNL #16 and #19, used as controls in Figures 9 and 10) (O'Donnell 2004). These two hits were further characterized in conjunction with the three hits that arose from my screen.

3.1.2 Identification of Genomic Mutations

Following the identification of these synthetic-lethal hits, I began the process of determining what gene had been mutated in the genome to produce the synthetic-lethal interaction with *spt16-E857K*. To accomplish this goal, I employed a cloning-by-complementation strategy using a *LEU2*-based centromeric yeast genomic library (p366; ATCC #77162) (a gift from Brenda Andrews, University of Toronto). Essentially, this procedure is the reverse of the synthetic-lethality screen. Library transformations were performed, and transformed cells were grown on solid medium containing uracil but lacking both tryptophan and leucine, thereby selecting only for the *spt16-E857K* and library plasmids, respectively; the medium also contained galactose, to destabilize the centromere function of the *SPT16* plasmid and promote its failed inheritance during mitosis. The transformants were then screened for colonies that were white in colour or had sectors of white cells, indicating the ability of cells to grow in the absence of the *SPT16* plasmid (Figure 11). The likely interpretation is that these 'white' cells contain a library plasmid that alleviates the synthetic-lethal interaction by complementation (or suppression) of one of the synthetic-lethal mutations. Generally, the initial colonies obtained following a library transformation had only small sectors of white cells, with a majority of red cells. Therefore, the ability to form white colonies was confirmed by re-streaking these cells onto fresh medium for several rounds of colony formation. Additionally, the white cells were also grown on medium containing 5-FOA, to confirm that the *SPT16* plasmid (which also carries *URA3*) is no longer needed for growth.

Since a synthetic-lethal interaction is, by definition, the result of mutations in two genes, complementation of this lethality could occur when the library-plasmid insert contains either the unknown gene that is mutated in the genome or *SPT16* itself. The presence of *SPT16*-containing library inserts thus serves as a positive control that the

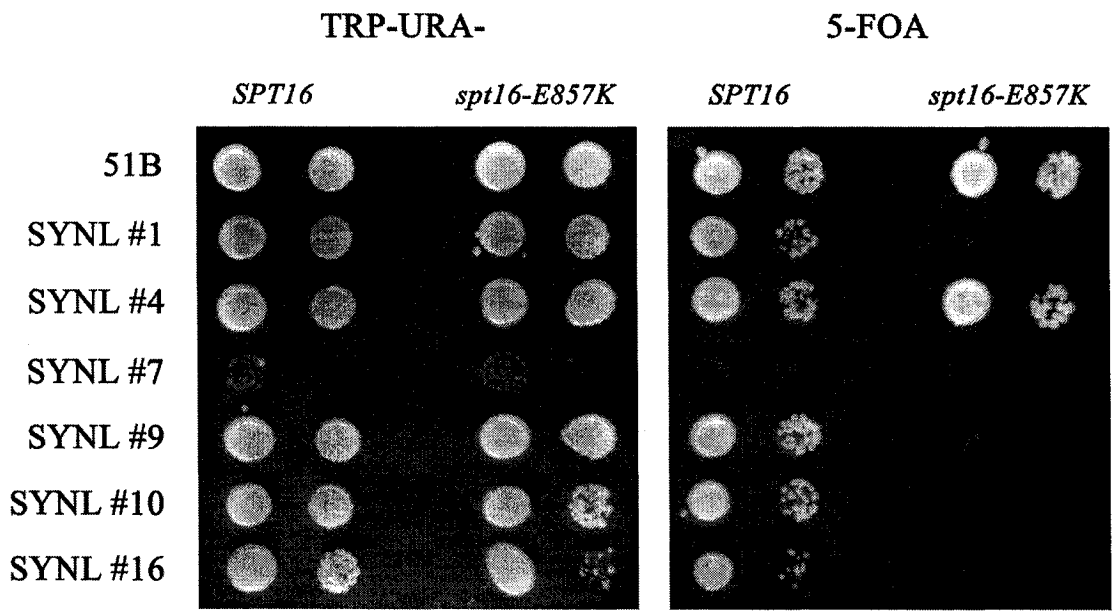

Figure 10. Plasmid-shuffling in putative synthetic-lethal hits. The original *spt16-E857K* plasmid was 'lost' from each putative synthetic-lethal hit (and control strains 51B and SYNL #16), and the resulting cells were re-transformed with either an *SPT16* plasmid or an *spt16-E857K* plasmid. Liquid cultures of these transformants were grown to stationary phase, and two dilutions were spotted onto TRP-URA- and 5-FOA solid medium. The plates were then incubated at 30°C for two days. The strains SYNL #1, SYNL #9 and SYNL #10 were all able to grow on medium containing 5-FOA when they contained an *SPT16* plasmid, but not when they contained an *spt16-E857K* plasmid, indicating that these strains contain synthetic-lethal hits. Strain SYNL #4 was able to grow on medium containing 5-FOA regardless of which plasmid it contained, while SYNL #7 did not grow on either the medium containing 5-FOA or the TRP-URA- medium; these latter two strains were therefore discarded.

Figure 11. Outline of library screening procedure. The cells containing synthetic-lethal hits (SYNL #1, #9, #10, #16 or #19) harbouring plasmids pSNLCDC68 (*URA3*, *ADE3*, *SPT16* and *GAL1p-CEN4*) and pRS314-cdc68-E857K (*TRP1 spt16-E857K*), shown at the top, form red-coloured colonies. Screening for complementation (or suppression) of the genomic mutation (*mut1*) is performed by transforming the cells with a low-copy yeast genomic library (p366 [*LEU2*, *CEN*]), followed by growth on galactose medium to prevent efficient inheritance of pSNLCDC68. Cells that continue to retain pSNLCDC68 (bottom left) grow into red-coloured colonies, indicating that these cells contain a library plasmid that does not complement the genomic mutation. However, cells that fail to inherit pSNLCDC68 (bottom right) grow into white-coloured colonies, indicating that the library plasmid contains on its insert a gene that complements (or suppresses) the genomic mutation, thereby alleviating the synthetic lethality.

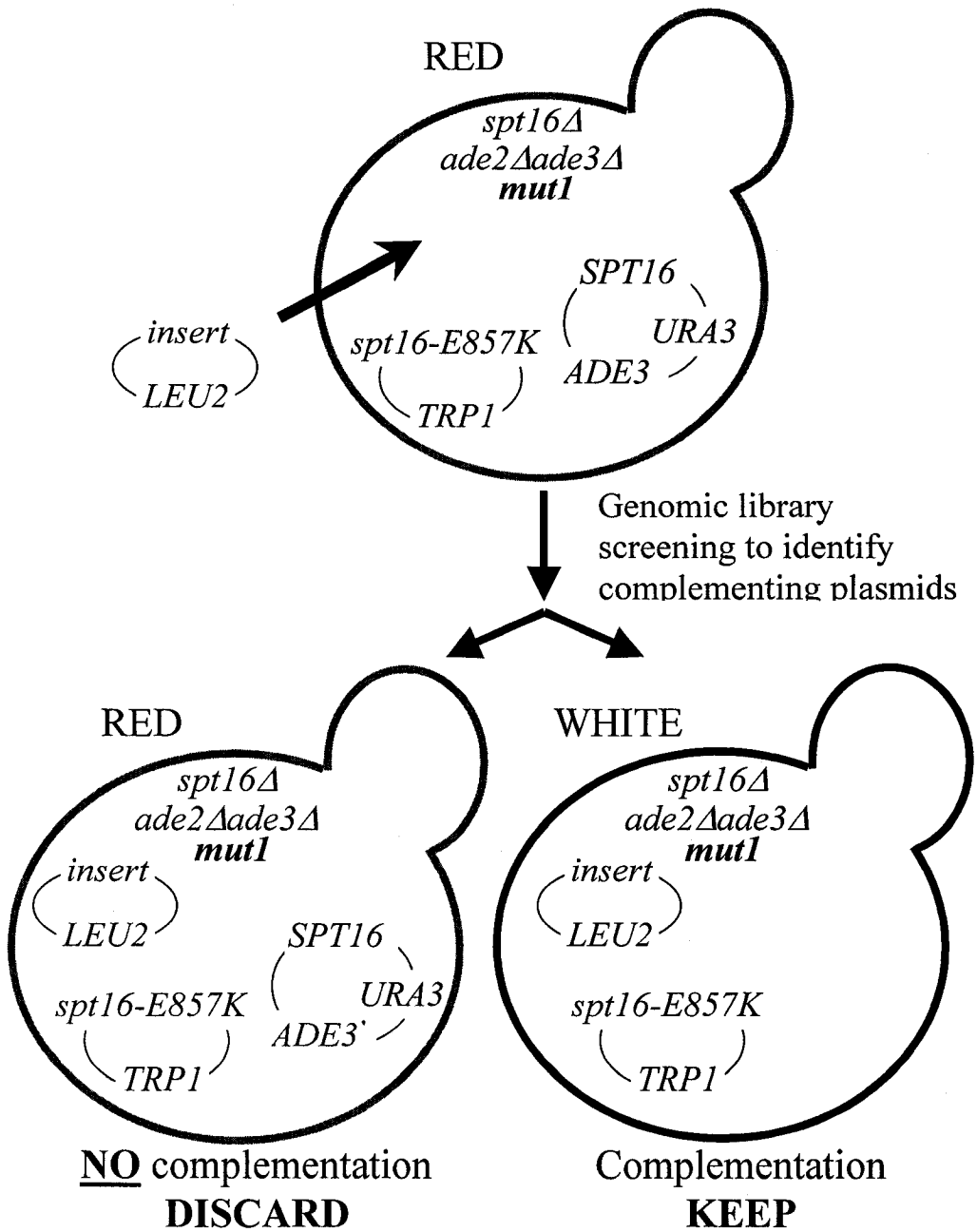
RED
spt16Δ
ade2Δade3Δ
mut1
insert
LEU2
spt16-E857K
TRP1
SPT16
URA3
ADE3
Genomic library
screening to identify
complementing plasmids
RED
spt16Δ
ade2Δade3Δ
mut1
insert
LEU2
spt16-E857K
TRP1
SPT16
URA3
ADE3
NO complementation
DISCARD
WHITE
spt16Δ
ade2Δade3Δ
mut1
insert
LEU2
spt16-E857K
TRP1
Complementation
KEEP

library transformation protocol is working as intended, but does not provide any insight into which genes are mutated to cause the synthetic-lethal interactions in these cells. To identify (and thus weed out) those transformants that contain *SPT16* on the library plasmid, I employed another plasmid-loss procedure. Isolates that contained both the *LEU2*-based library plasmid and the *TRP1 spt16-E857K* plasmid were grown for several generations in media that lacked either tryptophan or leucine, but was supplemented with the other. These conditions allow the growth of cells that have failed to inherit the plasmid containing that particular amino acid biosynthetic gene: cells that no longer contain the *spt16-E857K* plasmid will be able to grow in the medium that contains tryptophan, while those that lack the library plasmid will be able to grow in the medium containing leucine. If the library plasmid contains on its genomic insert the wild-type copy of the mutated genomic gene, then both it and the *spt16-E857K* plasmid will be required for cell survival, and we will not be able to isolate any cells that lack either of these plasmids. On the other hand, if a library plasmid contains *SPT16* on its genomic insert, then this can provide all essential functions of Spt16, and we will be able to identify cells that lack the *spt16-E857K* plasmid. For all of my synthetic-lethal hits used for library transformations, I was able to identify transformant derivatives that were able to grow without the *spt16-E857K* plasmid, indicating that the library plasmid likely contains *SPT16* on its genomic insert.

There is the slim possibility that the cells that are able to survive without the *spt16-E857K* plasmid possess a library plasmid with a gene on its insert that is able, in low-copy, to bypass the need for Spt16. While this possibility is unlikely, to confirm that this was not the case I verified that five of the library transformants that were able to survive without the *spt16-E857K* plasmid did indeed contain a copy of *SPT16*. To accomplish this, I subjected these cells to colony PCR to amplify sequence specific to *SPT16*: a product will be formed only from cells that contain the *SPT16* gene. In all five cases, a PCR product was formed, indicating that *SPT16* sequence was present in the cells, and a bypass had not occurred (Figure 12).

In this manner, I was able to identify complementing plasmids with genomic inserts that do not contain the *SPT16* gene for four of the five synthetic-lethal hits (SYNL #1, #9, #10 and #16); the identities of the complementing genes are discussed below.

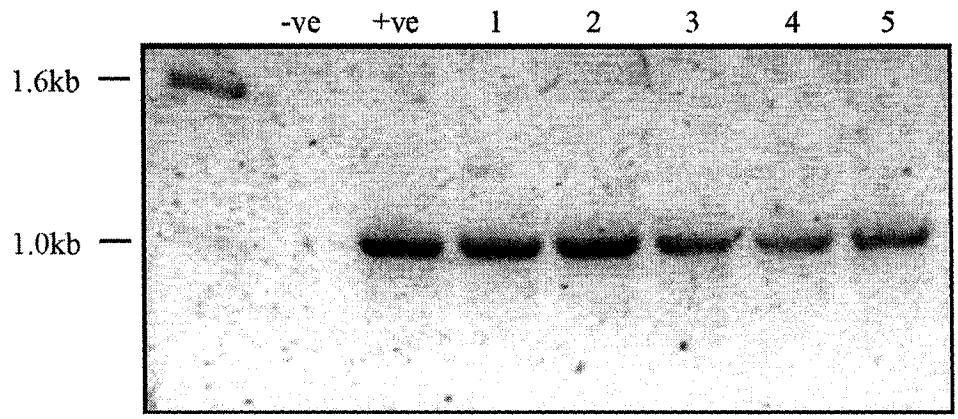

Figure 12. Colony PCR of library transformants lacking the *spt16-E857K* plasmid. Yeast cells from transformants the no longer contained pSNLCDC68 or pRS314-cdc68-E857K (samples 1 through 5) were tested to determine whether *SPT16* sequence was present by amplification using the 5'SpeI flank and 3'SpeI flank primer pair. The negative control (-ve) contained no cells, and therefore should have no template DNA, while the positive control (+ve) contained cells that maintained the *spt16-E857K* plasmid and therefore has template DNA. In all five samples from the library transformants, *SPT16* sequence was amplified, indicating the presence of the *SPT16* gene on the library insert and eliminating the possibility of a bypass mutation.

3.1.2.1 Difficulties Identifying the Synthetic-Lethal Mutation in SYNL #19

For one synthetic-lethal strain, SYNL #19, I initially screened ~17 500 library-transformant colonies without identifying any complementing plasmid (other than those containing *SPT16*). One possibility that would lead to this situation is that the mutation causing the synthetic-lethal interaction confers a phenotype that is dominant to the wild-type form of the gene. That is, that the mutation can still exert the synthetic-lethal phenotype even in the presence of the wild-type form of the gene. To ensure that the synthetic-lethal mutation in this strain does not confer a dominant phenotype, the strain (a *MAT*α haploid, one of the two yeast mating types) was mated to a similar haploid strain of the other mating type (*MAT***a**), creating a diploid strain with one normal copy of whichever gene is mutated. The same kind of colony-colour screening procedure as that described above showed that this diploid was able to survive when the only version of *SPT16* in the cells was *spt16-E857K*, indicating that the genomic synthetic-lethal mutation is recessive. Following this observation, I performed one final library transformation, screening another ~5 400 colonies without identifying a complementing plasmid. In addition, Rosemarie Kepkay, an undergraduate summer student, continued performing library transformations for this synthetic-lethal hit, screening ~32 400 colonies. Again, no complementing library plasmid (other than those containing *SPT16*) was identified. Thus, in total, ~55 000 library transformants have been screened without identifying a complementing plasmid other than those containing the *SPT16* gene. The information for this genomic library (from ATCC) states that 1 000 clones are usually sufficient for complete genome coverage; thus, we have theoretically covered the genome 50 times over without identifying the gene responsible for the synthetic-lethal phenotype.

There are several possible reasons for this negative result. One is that the gene of interest is under-represented in the genomic library, thus decreasing the chances that it will be isolated. However, unless the gene of interest is completely absent in the library, perhaps due to toxicity in *E. coli*, it is likely that we would have screened colonies containing this plasmid. A second is that the gene of interest is closely linked to *SPT16* in the genome, thus decreasing the chances that a library-plasmid insert will exist containing the gene of interest but not *SPT16*. The average size of genomic inserts in the library plasmids is 10 kbp. However, an examination of the region 10 kbp on each side of the

chromosomal *SPT16* locus does not yield any genes that are known to participate in mediating chromatin transactions. It is expected that genes causing synthetic-lethal interactions with an *spt16* mutation would be involved in similar cellular processes; that no such gene exists in the regions flanking *SPT16* in the chromosome suggests that the gene of interest is not closely linked to *SPT16*.

A third possibility is that the gene of interest is located close to a centromere, such that any genomic fragment containing this gene would also contain a centromere sequence. This situation would produce a plasmid with two centromeres – one on the vector backbone and one in the insert – which would not be maintained in yeast through mitosis (Mythreye, Bloom 2003), thus excluding these plasmids from my assessment. A survey of the centromere-proximal genes in the yeast genome yielded several possibilities for such a gene. These are genes that encode proteins functioning in processes in which the Spt16 protein is known to function, such as transcription and replication. A comparison of these genes to those identified by Allyson O'Donnell in her SGA (Synthetic Genetic Array) screening identified several centromere-proximal genes that have known deleterious genetic interactions with mutant alleles of *SPT16* (O'Donnell 2004). Among these genes are *NHP10*, which encodes a protein that may be involved in ATP-dependent chromatin remodelling (Shen et al. 2003) and is approximately 2 kbp from the Chr. IV centromere, and *HRB1*, which encodes a protein involved in the export of mRNA to the cytoplasm (Hurt et al. 2004, Shen et al. 2003) and is approximately 4 kbp from the Chr. XIV centromere. Additionally, several of the interesting centromere-proximal genes are essential, and thus would not be present in the collection of systematic gene deletions used for SGA screening. The essential gene *MCD1* encodes a protein involved in sister-chromatid cohesion (Guacci, Koshland & Strunnikov 1997), and is approximately 3 kbp from the Chr. IV centromere. *SWC4* encodes a protein involved in histone acetylation and the incorporation of the variant histone Htz1 into chromatin (Krogan et al. 2003b, Mizuguchi et al. 2004, Nourani et al. 2001), and is approximately 1.5 kbp from the Chr. VII centromere. *PAP1* encodes a protein involved in mRNA polyadenylation (Brodsky, Silver 2000, Lingner, Kellermann & Keller 1991, Preker et al. 1997), and is approximately 3 kbp from the Chr. XI centromere. *NOC3* encodes a protein involved in both ribosome synthesis and initiation of DNA replication (Milkereit et al.

2001, Zhang et al. 2002) and is approximately 3.5 kbp from the Chr. XII centromere. One centromere-linked gene that can be excluded from this list of possibilities is *RTT109*, which encodes a protein that was originally identified to help regulate Ty1 transposon transposition (Scholes et al. 2001) and has since been shown to be the histone acetyltransferase responsible for acetylation of histone H3 lysine 56 (Driscoll, Hudson & Jackson 2007, Han et al. 2007), and is approximately 3 kbp from the Chr. XII centromere. Directed testing between *spt16-E857K* and *rtt109Δ*, described below in Section 3.6.2, demonstrates that there is little growth impairment at 30°C for the double-mutant cells, which is not consistent with the lethality observed in SYNL #19.

Given this long list of centromere-linked candidates, it may well be that the gene mutated in this strain is located close to a centromere. It would therefore be unlikely that a complementing library insert exists that does not also contain a centromere, making this plasmid unable to be propagated in yeast cells. No further efforts have been undertaken to identify the mutant gene in SYNL #19.

3.1.2.2 Identification of the Synthetic-Lethal Mutation in SYNL #16

The first synthetic-lethal mutation for which a complementing library plasmid was identified was SYNL #16. Two independent library plasmids were identified and found to contain overlapping inserts. This region common to these inserts contains the complete coding sequences for *BUR2* and *ADY4*, partial sequences for the *YLR225c* and *ECM22* genes, and elements of a transposon sequence. As the only two complete genes are *ADY4* and *BUR2*, these were the most likely candidates for the gene responsible for alleviating synthetic lethality. The product of the *ADY4* gene is involved in forming the prospore membrane during meiosis (Nickas, Schwartz & Neiman 2003), whereas the *BUR2* gene encodes the regulatory subunit of the Bur1/Bur2 cyclin-dependent kinase complex that is involved in transcription elongation (Yao, Neiman & Prelich 2000). Therefore, as *BUR2* is involved in a common process with *SPT16* while *ADY4* is not, *BUR2* was considered more likely to be complementing the genomic mutation. To test this possibility, a low-copy plasmid containing only the *BUR2* gene and its flanking regions was created; this plasmid was then transformed into cells of the SYNL #16 strain and shown to alleviate synthetic lethality (Figure 13). Therefore, *BUR2* is indeed the active gene from the genomic library insert.

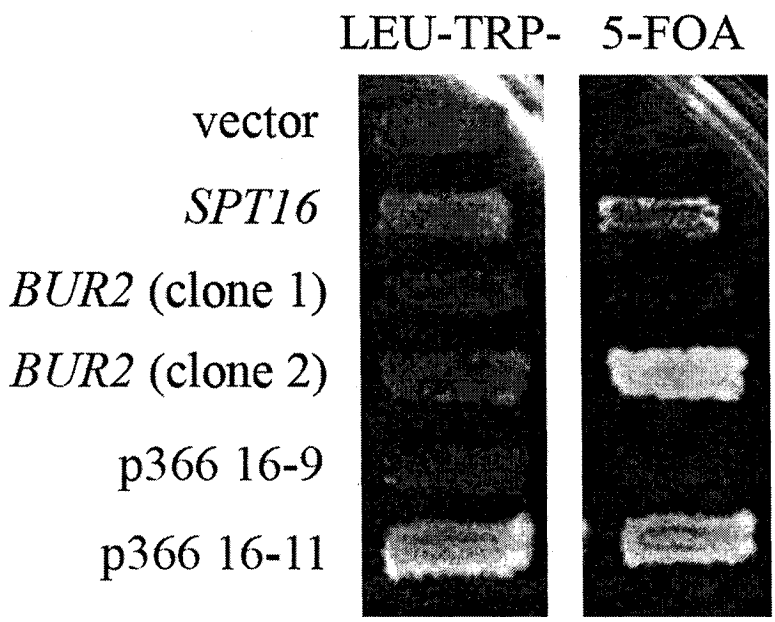

Figure 13. Alleviation of synthetic lethality in SYNL #16 by *BUR2* plasmids. SYNL #16 cells were transformed with the following *LEU2 CEN* plasmids: pRS315 (empty vector), pRS315-A4 (*SPT16*), pRS315-BUR2 (clones 1 and 2), and p366 16-9 and 16-11 (complementing library plasmids). The transformants were patched onto LEU-TRP- solid medium and replica-plated onto 5-FOA solid medium. As expected, the cells containing empty vector did not grow on 5-FOA while those with the *SPT16* plasmid did. Interestingly, only one of the two *BUR2* clones allowed growth on 5-FOA, presumably due to a PCR-induced mutation in the other. Likewise, only one of the two library plasmids reproduced the phenotype.

The chromosomal *BUR2* locus from SYNL #16 cells was gap-repaired into a plasmid, and the resulting DNA was sequenced. Sequence analysis revealed an insertion of a single G residue (coding strand) following *BUR2* ORF position 253, causing a substitution of arginine for lysine at residue 85 and a frameshift that causes a premature stop codon following residue 91, resulting in a truncated Bur2 protein of only 20% the full-length protein. This small portion of the Bur2 protein is unlikely to provide Bur2 function: SYNL #16 cells have the characteristic slow-growth phenotype of *bur2Δ* cells, which is phenotypically consistent with a non-functional *BUR2* gene in these cells.

To determine whether any of the other four synthetic-lethal hits are also complemented by *BUR2*, the two original *BUR2* library plasmids were transformed into these strains; no alleviation of the synthetic lethality was observed for any of these strains (Figure 14). Therefore, the genomic mutation in each of these strains lies within a gene other than *BUR2*.

3.1.2.3 Identification of the Synthetic-Lethal Mutations in SYNL #1 and SYNL #10

Library transformations were then performed for the SYNL #1 strain, and I found three independent library plasmids that complemented the synthetic-lethal phenotype. One of these contains on its insert the complete sequences of four genes: *SLA1*, which encodes a protein involved in the assembly of the actin cytoskeleton (Holtzman, Yang & Drubin 1993, Li, Zheng & Drubin 1995), *LDB7*, which encodes a component of the RSC chromatin remodelling complex (Cairns et al. 1996, Wilson et al. 2006), *YBL008W-A*, which encodes a putative protein of unknown function, and *HIR1*, which encodes a regulator of histone abundance (Osley, Lycan 1987, Sherwood, Tsang & Osley 1993, Spector et al. 1997); in addition, the insert contains partial sequence for *ALK2*, which encodes a protein kinase involved in DNA damage (Nespoli et al. 2006). The other two library plasmids were found to contain overlapping inserts; the overlapping region contains the complete sequences for *HIR2*, which encodes a regulator of histone abundance (Osley, Lycan 1987, Sherwood, Tsang & Osley 1993, Spector et al. 1997), *CKB2*, which encodes a subunit of casein kinase 2 (Reed, Bidwai & Glover 1994), and *GLO4*, which encodes mitochondrial glyoxylase II (Bito et al. 1997); in addition partial sequence of *CYC2*, which encodes a mitochondrial inner-membrane protein (Dumont et

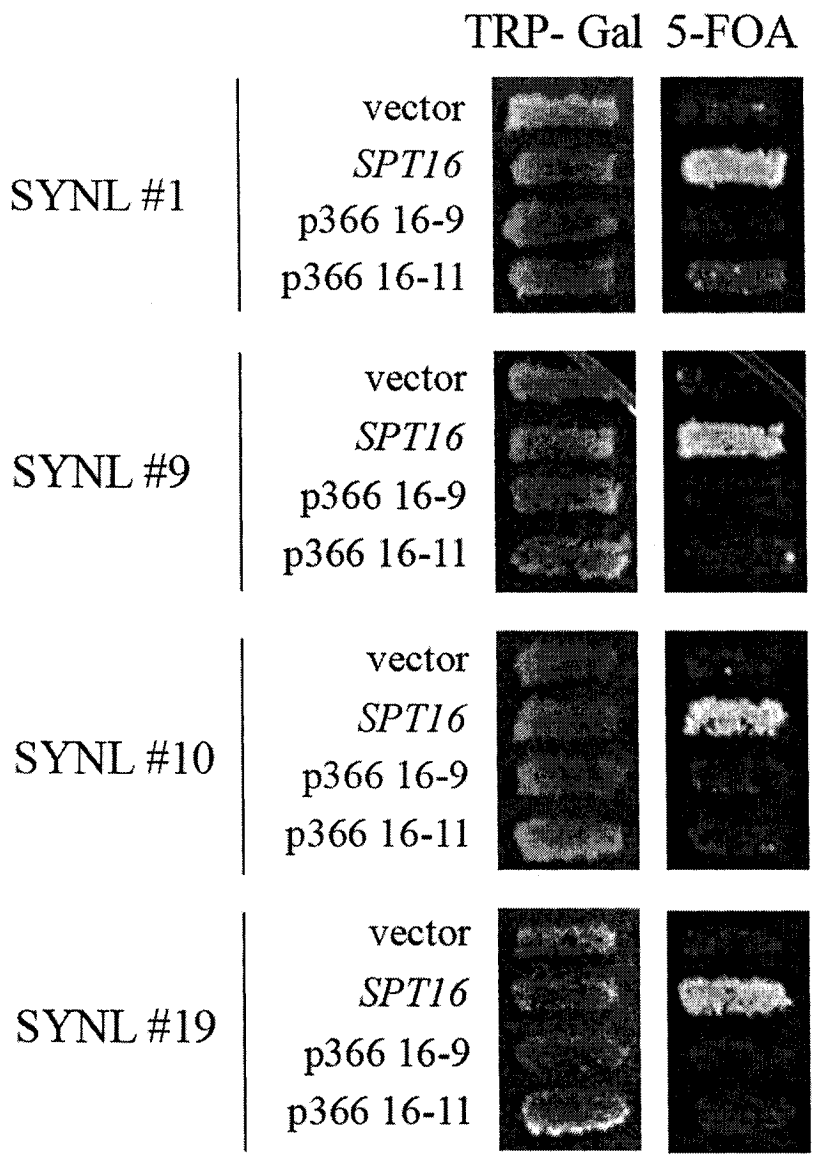

Figure 14. The library plasmids from SYNL #16 do not complement the synthetic lethality in any of the other four SYNL strains. Plasmids p366 16-9 and 16-11 (along with controls pRS315 and pRS315-A4) were transformed into cells of each of the other four synthetic-lethal strains, and transformants were patched onto Trp- Galactose solid medium, then replica-plated to 5-FOA solid medium. In no case did either library plasmid allow growth on 5-FOA, indicating that these plasmids do not contain a gene that alleviates the synthetic lethality in these strains.

al. 1993, Pearce, Cardillo & Sherman 1998), is present on the insert overlap. Although both types of insert contain more than one gene that may be responsible for alleviating synthetic lethality, the *HIR1* and *HIR2* genes were of particular interest. The Hir proteins are known to function together in a complex (Green et al. 2005, Prochasson et al. 2005), are involved in the regulation of histone abundance (Osley, Lycan 1987, Sherwood, Tsang & Osley 1993, Spector et al. 1997) and facilitate replication-independent histone deposition onto DNA (Green et al. 2005). Replication-independent histone deposition is the assembly of nucleosomes onto DNA that occurs outside of S-phase, and mainly occurs following the nucleosome disruption that takes place during transcription. This role of the Hir proteins as histone chaperones indicates a common function with Spt16, which has also been shown to function as a histone chaperone. To determine whether the active genes on these inserts are *HIR1* and *HIR2*, respectively, low-copy single-gene plasmids were created for both the *HIR1* and *HIR2* genes; these plasmids were then transformed into cells of the SYNL #1 strain. Synthetic lethality was indeed alleviated by the presence of these single-gene plasmids, indicating that these are the active genes from the library inserts (Figure 15). This situation was particularly interesting, as the synthetic-lethal interaction can be alleviated by either *HIR1* or *HIR2*. This suggests that at least one of these genes is a suppressor of the genomic mutation in SYNL #1, rather than complementing the genomic mutation.

As noted above, the Hir1 and Hir2 proteins are known to function together in a protein complex; it is therefore possible that, if the synthetic-lethal mutation affects one of these proteins and causes a decrease in the physical interaction between Hir1 and Hir2, overexpression of the other protein could restore this interaction. In this situation, either *HIR1* or *HIR2* is complementing the genomic mutation, while the other is functioning as a low-dosage copy suppressor of the same mutation. To determine whether *HIR1* or *HIR2* is in fact mutated in SYNL #1, the presumptive *HIR1* and *HIR2* chromosomal loci of SYNL #1 cells were gap-repaired onto plasmids, and these gap-repaired plasmids were then transformed back into cells of strain SYNL #1, which showed that the *HIR2* gap-repaired plasmid was able to alleviate synthetic lethality while the *HIR1* gap-repaired plasmid was not (Figure 15). This finding suggests that a mutation affecting *HIR1* is responsible for the synthetic lethality in these cells. Sequence was obtained for the

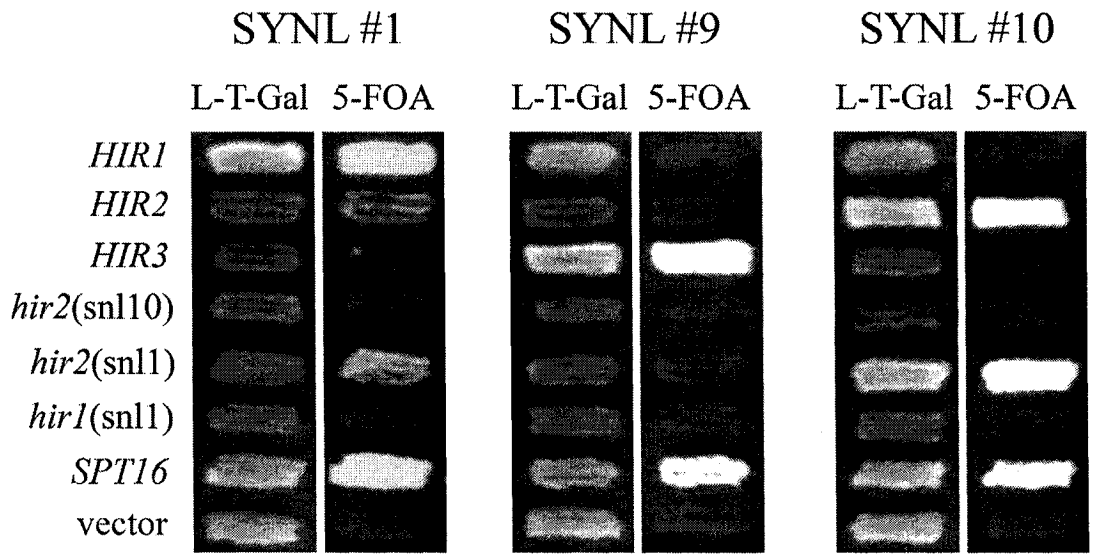

Figure 15. Alleviation of synthetic lethality by various plasmids. Cells of strains SYNL #1, #9 and #10 were transformed with pRS315-based *LEU2 CEN* plasmids containing various versions of the *HIR* genes, *SPT16* or a vector control. The *HIR1* and *HIR2* plasmids are single-gene plasmids, while the *HIR3* plasmid is the library plasmid isolate from SYNL #9; the *hir2*(snl10) plasmid was gap-repaired from the SYNL #10 strain, while the *hir2*(snl1) and *hir1*(snl1) plasmids were gap-repaired from the SYNL #1 strain. The transformants were patched onto Leu-Trp- Galactose solid medium, then replica-plated to 5-FOA solid medium. The synthetic lethality in SYNL #1 was alleviated by either the *HIR1*, *HIR2* and *hir2*(snl1) plasmids, that in SYNL #9 was alleviated only by the *HIR3* plasmid, and that in SYNL #10 was alleviated by the *HIR2* and *hir2*(snl1) plasmids. The failure of *hir2*(snl10) and *hir1*(snl1) plasmids to alleviate the synthetic lethality in any of these strains suggests that there are mutations in these cloned genes.

plasmid-borne alleles of both *HIR1* and *HIR2*. The *HIR2* allele recovered by gap-repair was found to have no mutations, while the *HIR1* allele recovered by gap-repair was found to have two substitutions at the DNA level: A778G, causing an L259V polypeptide substitution, and T2282C, causing an L760P polypeptide substitution.

The L760P substitution affects the region of the Hir1 protein that is involved in Hir2 binding (Spector et al. 1997); thus, this mutation may disrupt the physical interaction between Hir1 and Hir2. In this situation, increased amounts of Hir2 may restore the Hir1–Hir2 interaction by increasing the frequency in which a disassociated Hir1 protein encounters another Hir2 protein. If this were the case, I might expect that a mutant Hir1 protein that contains only the L760P substitution would not alleviate the synthetic-lethal interaction, while a mutant protein containing only the L259V substitution might be able to. To test this possibility, I created plasmids containing each substitution individually and transformed each one into cells of strain SYNL #1. Consistent with this hypothesis, synthetic lethality was alleviated by the L259V mutant allele, while no alleviation was observed for the L760P mutant allele (Figure 16). Thus the L259V substitution may not affect Hir1 activity, whereas the L760P substitution does have negative effects.

As I did with the library plasmids from strain SYNL #16, the library plasmids identified using synthetic-lethal strain SYNL #1 were transformed into the other synthetic-lethal hits to determine whether these genomic inserts alleviate the synthetic lethality observed in any of these strains. The *HIR1* plasmid had no effect. Interestingly, however, the *HIR2* plasmids were able to alleviate synthetic lethality in the SYNL #10 strain; no alleviation of this phenotype was observed for any of the other strains (Figure 17). To confirm that the *HIR2* gene, rather than any of the other genes on the genomic insert, is responsible for the observed effect, the low-copy *HIR2* plasmid described above was transformed into cells of strain SYNL #10 and shown to alleviate the synthetic-lethal phenotype, indicating that *HIR2* alleviates the synthetic lethality for SYNL #10 (Figure 15). The presumptive *HIR2* mutant allele from strain SYNL #10 was gap-repaired onto a plasmid. This gap-repaired plasmid was transformed into cells of strain SYNL #10, as was the gap-repaired *HIR2* plasmid that was created from strain SYNL #1 as described above, which harbours a wild-type *HIR2* gene. While the *HIR2* plasmid from SYNL #1

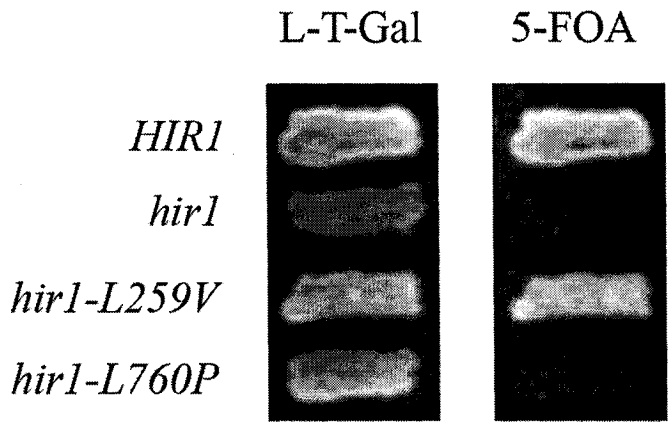

Figure 16. The L760P substitution in Hir1 is responsible for synthetic lethality with *spt16-E857K*. Cells of strain SYNL#1 were transformed with plasmids containing *HIR1*, *hir1* gap-repaired from SYNL #1 encoding both substitutions (L259V and L760P), or versions of *hir1* encoding either L259V or L760P. Transformants were patched onto Leu- Trp- Galactose solid medium, then replica-plated to 5-FOA solid medium. Both the *HIR1* and *hir1-L259V* plasmids facilitated growth on solid medium containing 5-FOA, indicating that these could complement the synthetic lethality. Conversely, the *hir1-L760P* plasmid was unable to facilitate growth, indicating that this mutation causes the synthetic-lethal phenotype in SYNL #1.

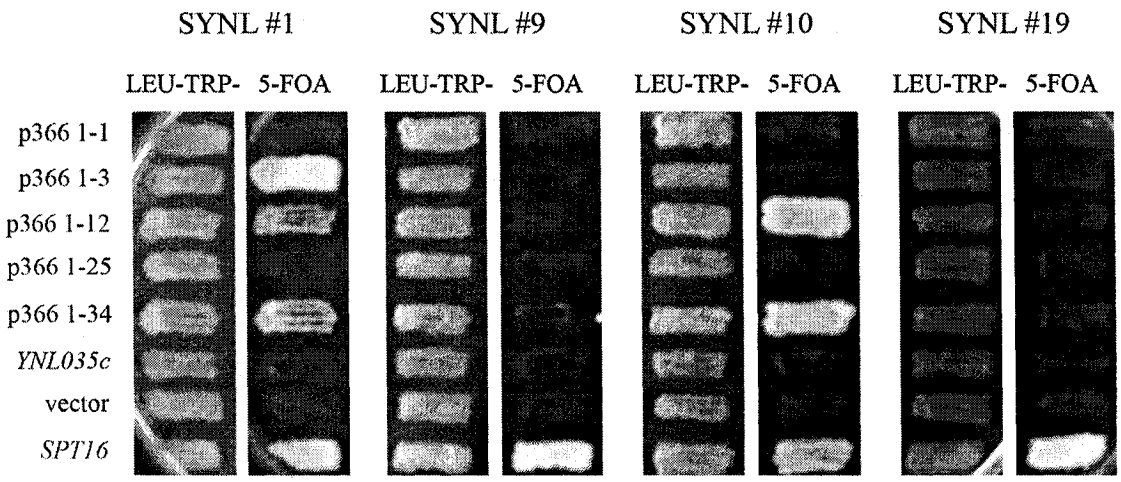

Figure 17. Library plasmids from SYNL #1 alleviate the synthetic lethality in SYNL #10. Five library plasmids isolated from SYNL #1 were transformed back into this strain, as well as the other SYNL strains. Transformants were patched onto Leu-Trp- solid medium, and then replica-plated to 5-FOA solid medium. Neither p366 1-1 or p366 1-25 were able to reproduce the phenotype in SYNL #1, although p366 1-3, p366 1-12 and p366 1-34 all allowed growth on medium containing 5-FOA, indicating that these plasmids are able to alleviate synthetic lethality in this strain. Additionally, p366 1-12 and 1-34 were able to alleviate synthetic lethality in SYNL #10, indicating that this strain has a genomic mutation that is complemented or suppressed by a gene on this plasmid. None of the plasmids were able to alleviate synthetic lethality in either SYNL #9 or SYNL #19; thus, these strains contain genomic mutations in genes that are not suppressed by these library inserts. In addition, a high-copy plasmid containing the *YNL035c* gene was transformed into these same strains; this encodes a WD-40 repeat-containing protein that interacts with Spt16 via 2-hybrid interactions (O'Donnell 2004). Since both Hir1 and Hir2 contain WD-40 repeats, perhaps this could suppress as well; however, no alleviation of any synthetic lethality was observed with this plasmid.

was able to alleviate synthetic lethality of strain SYNL #10, the plasmid from strain SYNL #10 itself was not, supporting the hypothesis that *HIR2* is mutated in this strain to cause a synthetic-lethal interaction (Figure 15). To provide evidence that the *HIR2* gene in strain SYNL #10 does harbour a mutation, sequence was obtained for the *HIR2* allele recovered by gap-repair from SYNL #10. Analysis of this sequence showed that there is a single substitution at the DNA level: T2240G, causing the amino acid substitution L747R. This substitution lies within the HIRA domain of the Hir2 protein – this domain is conserved among HIRA homologues from many species (Finn et al. 2006) and is therefore thought to be important for protein function. Thus, a mutation in this region may perturb the ability of Hir2 to function as a histone chaperone.

3.1.2.4 Identification of the Synthetic-Lethal Mutation in SYNL #9

The synthetic-lethal mutation in strain SYNL #9 was alleviated by library plasmid p366 9-8, which contains the complete coding sequences for three genes: *HIR3*, *YJR141W* and *YJR142W*, as well as the 3' end of a fourth gene, *PMT4* (Figure 18). The *PMT4* gene encodes a protein O-mannosyltransferase that transfers mannose residues from dolichyl phosphate-D-mannose to serine or threonine residues on other proteins (Girrbach, Strahl 2003, Immervoll, Gentzsch & Tanner 1995). However, since less than half of the *PMT4* coding region is present on the library insert, it is unlikely that this *PMT4* fragment is responsible for the alleviation of synthetic lethality. Both *YJR141W* and *YJR142W* remain uncharacterized, although it is known that *YJR141W* is an essential gene while *YJR142W* is not essential for viability. A genome-wide two-hybrid analysis, as part of a high-throughput study of many uncharacterized essential genes, has suggested that the *YJR141W* gene product may be involved in mRNA processing (Hazbun et al. 2003). However, the data presented in that study do not actually indicate any positive hits from their two-hybrid analysis using *YJR141W* as bait; thus there is no concrete support for this functional classification. By a process of elimination, then, the most likely candidate for the mutated gene in the SYNL #9 strain that causes synthetic lethality when combined with *spt16-E857K* is *HIR3*. This is especially probable since *HIR1* and *HIR2* have also been identified in this manner, and it is known that all three of these Hir proteins function together in a complex (Green et al. 2005, Prochasson et al. 2005).

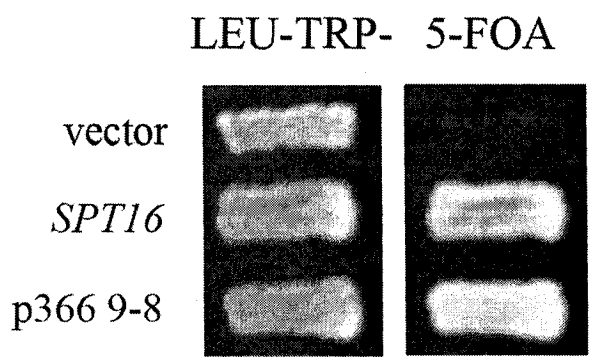

Figure 18. The library plasmid p366 9-8 alleviates synthetic lethality in SYNL #9. This plasmid was isolated from SYNL #9 yeast cells and re-transformed back into cells of strain SYNL #9. The transformants were patched onto Leu-Trp- solid medium and replica-plated onto 5-FOA solid medium. Growth on medium containing 5-FOA indicated that the genomic insert on p366 9-8 does indeed alleviate synthetic lethality in SYNL #9.

Attempts to make a *HIR3* single-gene plasmid were unsuccessful, likely due to the size of this gene (the coding region alone is 4947 bp) and the attendant difficulties in obtaining PCR amplicons of that size. Likewise, attempts at gap-repairing the presumptive mutant *hir3* allele from cells of the SYNL #9 strain were also unsuccessful. However, genome-wide synthetic genetic array analysis performed by Allyson O'Donnell identified *hir3Δ* as having deleterious genetic interactions with *spt16-E857K* (O'Donnell 2004). This finding, combined with my observations that mutations in *HIR1* and *HIR2* have deleterious genetic interactions with *spt16-E857K*, strongly suggest that the genomic mutation in SYNL #9 lies within *HIR3*.

3.2 Allele Specificity of Synthetic-Lethal Interactions

Following the identification of the four genes described above that, when mutated, have synthetic-lethal interactions with *spt16-E857K*, I decided to determine whether this synthetic lethality is common to other mutant alleles of *SPT16*. As *spt16-E857K* was identified in a screen for mutant alleles of *SPT16* that cause a dominant Spt phenotype, I tested other mutant alleles identified using this same approach. In addition, I tested alleles identified using other phenotypes, such as temperature sensitivity, that do not all demonstrate the Spt phenotype. Using a plasmid-shuffle approach, I transformed these other plasmid-borne *spt16* mutant alleles into cells of several *spt16Δ* strains containing the chromosomal synthetic-lethal mutations and kept alive by the *SPT16* plasmid pSNLCDC(3). The resulting transformants were then spread on medium containing galactose, incubated for colony growth, and assessed for cells lacking the *SPT16* plasmid using the same red-white screening procedure described above for the initial synthetic-lethal screen. First I tested several *spt16* mutant alleles that were identified in the same way as *spt16-E857K*: *spt16-E763G*, *spt16-312* and *spt16-319* (O'Donnell 2004). In addition, the original *spt16-G132D* (*cdc68-1*) allele was examined, along with two deletion mutants that are missing most, or all, of the NTD-coding sequence: *spt16-Δ(6-435)* and *spt16-ΔNTD* (O'Donnell et al. 2004). The results of these investigations (Figure 19) showed that not all of the tested *spt16* mutant alleles demonstrated the same pattern of synthetic-lethal interactions. In fact, of the alleles tested, only *spt16-319* demonstrated the same pattern of synthetic-lethal interactions as did *spt16-E857K*.

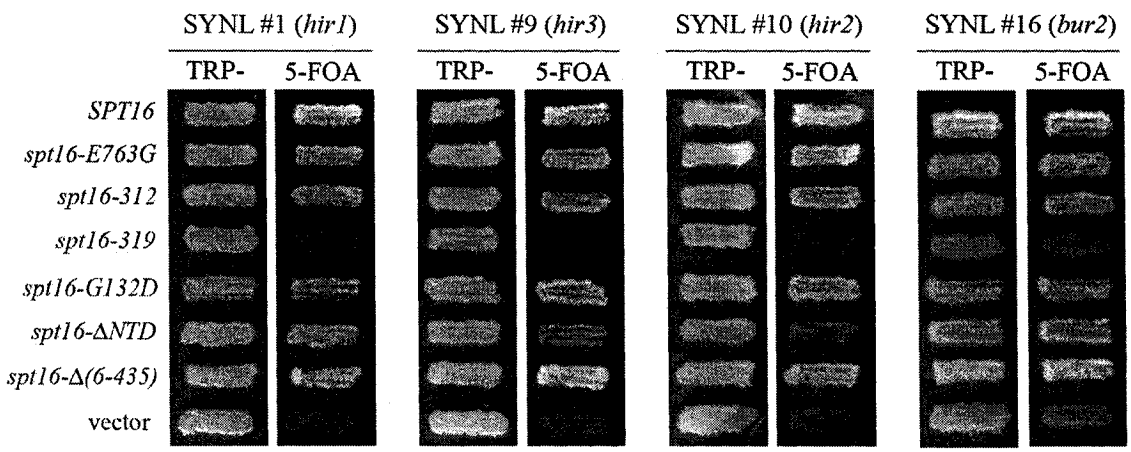

Figure 19. Synthetic lethality with mutant alleles of *spt16*. Low-copy plasmids containing various mutant alleles of *spt16* were transformed into derivatives of strains SYNL #1, #9, #10 and #16 lacking the *spt16-E857K* plasmid; transformants were patched onto Trp- solid medium and replica-plated onto 5-FOA solid medium. Only *spt16-319* was found to be synthetic-lethal in any of the four strains; no growth was observed on the 5-FOA medium for *spt16-319* transformants of any of the strains. The slight growth observed for *spt16-319* transformants of SYNL #16 was likely due to the longer incubation time required for this strain due to its slow growth; this slight growth, however, was no greater than that of empty vector, indicating a synthetic-lethal interaction with *spt16-319* in this strain.

To expand the spectrum of *spt16* mutant alleles assessed, I similarly tested several temperature-sensitive *spt16* mutant alleles from the Formosa lab: *spt16-4*, *spt16-6*, *spt16-7*, *spt16-8*, *spt16-9*, *spt16-9a*, *spt16-9b*, *spt16-9c*, *spt16-11*, *spt16-12*, *spt16-16a*, and *spt16-24* (Formosa et al. 2001). Again, several of these alleles demonstrated synthetic-lethal interactions while others did not (Figure 20). The alleles that were synthetically lethal in all four of my synthetic-lethal strains, with mutations in *bur2*, *hir1*, *hir2*, and *hir3*, are *spt16-6*, *spt16-9*, and *spt16-16a*. Additionally, *spt16-11* was found to be synthetically lethal with the *bur2* mutation, but not with any of the *hir* mutations.

Several of these *spt16* mutant alleles that were tested have point mutations that lie very close to that of *spt16-E857K*, and thus could be imagined to have a similar effect on Spt16 protein function. This group includes *spt16-7*, encoding the amino acid substitutions T848I, T849I, and D850Y; *spt16-9a*, encoding the amino acid substitutions G836S and P838S; and *spt16-11*, encoding the amino acid substitutions T828I and P859S. Yet these alleles do not demonstrate the same pattern of synthetic-lethal interactions as does *spt16-E857K*. Both the *spt16-E857K* and *spt16-319* (L804P, L946S, T1004G) alleles, which demonstrate synthetic-lethal interactions with both the *bur2* and *hir* mutations, have a dominant Spt phenotype, suggesting that this phenotype may be correlated with synthetic-lethal interactions for C-terminal mutations in the Spt16 protein.

Although the *spt16* mutant alleles from the Formosa lab (except *spt16-12*) have been shown to exhibit an Spt effect when they are the only version of *SPT16* in the cell (Formosa et al. 2001), it was not known whether the *spt16* mutant alleles from the Formosa lab have a dominant Spt effect. To assess this, I transformed the plasmid-borne *spt16* mutant alleles from the Formosa lab into cells of two different Spt-reporter yeast strains, both containing wild-type *SPT16* in the chromosome, and assessed growth of the transformants on solid medium lacking either histidine or lysine. Only those alleles with mutations affecting the C-terminal portion of the Spt16 polypeptide (*spt16-6*, *spt16-7*, *spt16-9a* and *spt16-11*) were assessed in this way for dominant Spt effects, as an unbiased screen of the entire *SPT16* open reading frame yielded mutations affecting only this portion of the protein (O'Donnell 2004). None of these *spt16* mutant alleles were found to have a dominant Spt phenotype (Figure 21). Therefore, since *spt16-6* is synthetic-lethal with mutations in *BUR2* and in the *HIR* genes, yet does not have a dominant Spt

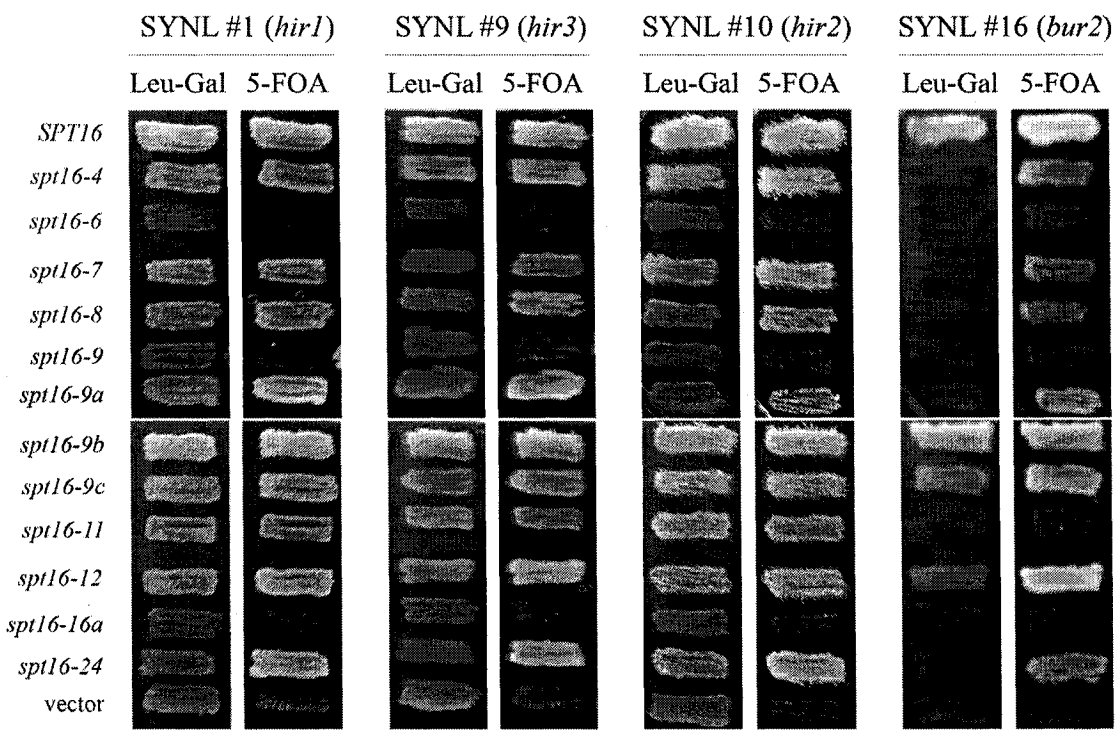

Figure 20. Synthetic lethality with the mutant *spt16* alleles from the Formosa lab. Low-copy plasmids containing various mutant alleles of *spt16* were transformed into derivatives of strains SYNL #1, #9, #10 and #16 lacking the *spt16-E857K* plasmid; transformants were patched onto Leu- Galactose solid medium and replica-plated onto 5-FOA solid medium. Only the *spt16-6*, *spt16-9* and *spt16-16a* alleles were found to cause synthetic lethality in all four strains; *spt16-11* was found to cause synthetic lethality in SYNL #16 only. In addition, cells containing many of the alleles remained red on galactose-containing medium, yet grew on 5-FOA-containing medium, a phenotype particularly evident for the transformants of SYNL #16. This may be due to a slow-growth phenotype resulting from the combination of the mutant allele of *spt16* and the genomic mutation in each strain. Thus, on galactose-containing medium, those cells which maintained the *SPT16 URA3 ADE3* plasmid grew more quickly than those cells which no longer contained this plasmid; however, on 5-FOA medium, only the cells that do not contain this plasmid were able to grow.

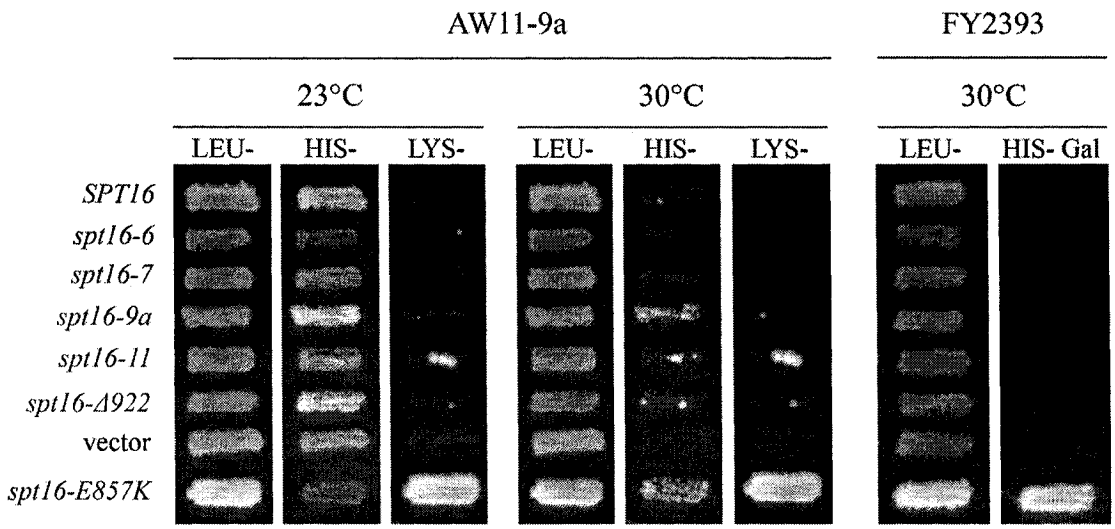

Figure 21. Dominant Spt phenotype testing of C-terminal *spt16* mutant alleles from the Formosa lab. Low-copy plasmids containing the indicated *spt16* alleles were transformed into cells of strains AW11-9a (reporter genes *his4-912δ* and *lys2-128δ*) and FY2393 (reporter gene *pGAL-FLO8-HIS3*, which contains the *HIS3* coding sequence fused downstream of the *FLO8* internal promoter, but out of frame with the *FLO8* coding sequence. Thus, *HIS3* will only be expressed as functional mRNA when the internal promoter of *FLO8* is active. In addition, the *FLO8* promoter was replaced by the *GAL1* promoter, which is activated only when galactose is used as a carbon source. Thus, transcription across the *FLO8* internal promoter can be regulated.). The resulting transformants were patched onto Leu- solid medium at 30°C, and replica-plated to the indicated medium and incubated at either 23°C or 30°C. The *spt16-E857K* plasmid was used as a positive control for a dominant Spt phenotype, and an empty vector was used as a negative control. None of the *spt16* mutant alleles from the Formosa lab with C-terminal mutations produced a dominant Spt phenotype, as evidenced by the lack of growth on medium lacking histidine or lysine for the AW11-9a transformants, or on His- Galactose medium for the FY2393 transformants.

phenotype, this Spt phenotype must not be essential for synthetic-lethal interactions involving mutations in the C-terminal portion of Spt16. Thus, mutations affecting the C-terminal portion of Spt16 may or may not demonstrate synthetic-lethal interactions regardless of their ability to cause a dominant Spt effect.

The two point mutations in *spt16-11*, causing the substitutions T828I and P859S, flank the mutation in *spt16-E857K*, and thus it is conceivable that these two different *spt16* mutant alleles may be impaired in similar processes. That *spt16-11* was found to have a synthetic-lethal interaction with the *bur2* mutation but not with the *hir* mutations was therefore interesting, because a screen for mutations synthetic-lethal with *spt16-11* that was similar to the one that I used for *spt16-E857K* identified mutations in the *HIR* genes (Formosa et al. 2002), similar to the results of my investigations using *spt16-E857K*. Therefore, why did *spt16-11* fail to show genetic interactions with the *hir1*, *hir2*, and *hir3* mutations in my experiments?

One potential explanation for this difference is that the Formosa-lab investigations used a chromosomally integrated form of *spt16-11*, while my studies used a low-copy plasmid-borne form of this allele; therefore, a modest increase in (plasmid-borne) *spt16-11* gene copy-number, and the accompanying increase in protein abundance, may account for the differences observed. Supporting this possibility, results obtained using *hpc2Δ* cells (Hpc2 is found in the same complex as the Hir proteins (Green et al. 2005, Prochasson et al. 2005)) with either a low-copy *spt16-11* plasmid or an integrated form of *spt16-11* demonstrated more severe defects in the chromosomally integrated situation (Formosa et al. 2002). A second idea is that the genetic backgrounds used for the two sets of studies are different: my strains have the commonly used S288c genetic background, while the Formosa-lab strains have the A364a genetic background. It is therefore possible that a genetic polymorphism between these two strain backgrounds accounts for the differences seen with respect to these synthetic genetic interactions. This is a reasonable possibility, as there are reported instances of differences in the effects of a different mutation assessed in these two genetic backgrounds (Schlesinger, Formosa 2000). Additionally, since the two different synthetic-lethal screens under consideration here introduced random mutations into the genome, there may be allele-dependent interactions with respect to the mutations affecting the *HIR* genes in the two screens. Indeed, while

the mutations in the *HIR* genes identified by the Formosa lab cause synthetic lethality when combined with the *spt16-11* mutation, the *HIR* mutations identified in my screen do not cause this synthetic lethality. Therefore, my *HIR* mutations may cause less severe effects for the cell than those identified by the Formosa lab. In particular, my *hir1* mutation is suppressed by low-copy *HIR2*, suggesting that the detrimental effect of this mutation is mild.

To assess this last possibility, I replaced the *HIR1* open reading frame in my synthetic-lethal starting strain with the *natMX4* cassette, creating a *hir1Δ* strain. Into these cells I then transformed the *spt16-11* mutant alleles from the Formosa lab. If the reason I did not observe synthetic lethality between *spt16-11* and my original mutant allele of *hir1* is a difference in the 'severity' of the *hir1* mutant allele, then I would expect to see deleterious genetic effects between *spt16-11* and *hir1Δ*. This is what I found: these double-mutant cells did not grow as well as *SPT16* cells, indicating a deleterious genetic interaction between *spt16-11* and *hir1Δ* (Figure 22). Therefore, the *hir1* mutation in my SYNL #1 strain is less severe than a *HIR1* deletion, as more severe genetic interactions exist in *hir1Δ* cells. However, in this test, the *spt16-11* allele did not display true synthetic lethality in combination with *hir1Δ*. This lack of synthetic lethality between *spt16-11* and *hir1Δ* indicates that the 'severity' of the *hir1* mutation does not account entirely for the differences observed between my results and those reported by the Formosa lab. Therefore, a contribution may exist from the difference in dosage between chromosomally integrated and low-copy plasmid-borne *spt16-11* alleles, and/or the difference in genetic background between A364a and S288c cells.

In addition to the *spt16-11* mutant allele, I also assessed the other alleles with mutations affecting the C-terminal portion of the Spt16 polypeptide: *spt16-6*, *spt16-7*, and *spt16-9a*. Both *spt16-6* and *spt16-7* behaved the same way in this *hir1Δ* strain as they did in my original SYNL #1 *hir1* mutant strain; that is, *spt16-6* is synthetic-lethal with *hir1Δ*, while *spt16-7* is not (Figure 22). The *spt16-9a* mutant allele also demonstrated synthetic lethality in the *hir1Δ* strain, while no synthetic-lethal interaction was observed with *spt16-9a* in my original SYNL #1 *hir1* mutant strain. Thus, *spt16-11* and *spt16-9a*

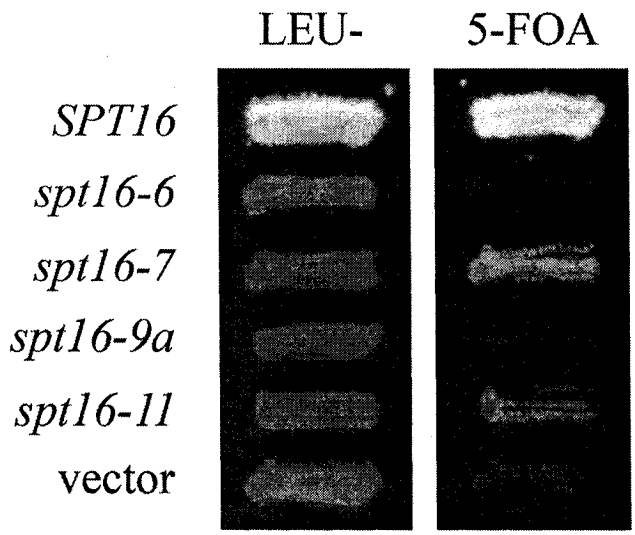

Figure 22. Synthetic lethality between the Formosa *spt16* mutant alleles and *hir1Δ*. Double-mutant *spt16Δ hir1Δ* cells containing an *SPT16 URA3* plasmid were transformed with low-copy *LEU2* plasmids containing the indicated *spt16* mutant alleles. Transformants were patched onto Leu- solid medium and replica-plated to 5-FOA solid medium to assess growth in the absence of the *SPT16 URA3* plasmid. While both *spt16-6* and *spt16-9a* were synthetic-lethal with *hir1Δ*, neither *spt16-7* nor *spt16-11* were synthetic-lethal with *hir1Δ*.

both show a more severe deleterious interaction with *hir1Δ* than with the *hir1* point mutation.

To gain a more detailed picture of mutant effects on the Spt16 protein, even more *spt16* mutant alleles were assessed for genetic interactions. A further characterization of additional dominant Spt alleles isolated by Allyson O'Donnell (O'Donnell 2004) by a former Honours student, Troy Perry, led to the identification of six novel alleles of *SPT16* that provide essential function at 30°C: *spt16-INM27* (a.k.a. *spt16-L804P*), *spt16-AM21*, *spt16-IM25*, *spt16-IM28*, *spt16-IM313*, and *spt16-ANM318* (Perry 2005). Most of these alleles have several mutational changes; however, in each case a limited subset of these mutations is responsible for the dominant Spt phenotype (Dr. Chris Barnes, Dept. of Microbiology & Immunology, Dalhousie University, personal communication). An undergraduate student whom I mentored, Rosemarie Kepkay, tested these mutant alleles for synthetic-lethal interactions with the *bur2* and *hir* mutations. All of these alleles, except for *spt16-IM25*, demonstrated synthetic lethality in combination with the mutations in *BUR2* and in each of the *HIR* genes. In contrast, the *spt16-IM25* allele behaved much like the *spt16-11* allele, in that it displayed synthetic-lethal interactions with the *bur2* mutation, but not with the *hir* mutations (Rosemarie Kepkay, unpublished observations).

A comparison of the alleles that do demonstrate synthetic-lethal interactions suggests that a limited region in the Spt16 protein may mediate some process that is impaired in most of these mutants (Figure 23). There are only four alleles with synthetic-lethal interactions that do not have mutations affecting this area: *spt16-IM25*, *spt16-IM28*, *spt16-9* and *spt16-16a*. The *spt16-IM25* and *spt16-IM28* alleles were identified in the screen for dominant Spt allele carried out by Allyson O'Donnell and characterized by Troy Perry (O'Donnell 2004, Perry 2005). In both cases, the dominant Spt phenotype is caused by the mutations in the C-terminal half of the protein, while the N-terminal mutations alone lack an Spt phenotype (Chris Barnes, personal communication). Thus, it is possible that in these two alleles the C-terminal substitutions are also responsible for the observed synthetic lethality with mutations in *BUR2* and each of the *HIR* genes.

The *spt16-9* and *spt16-16a* alleles were both identified by the Formosa lab as causing temperature sensitivity in cells where they are the only version of *SPT16*

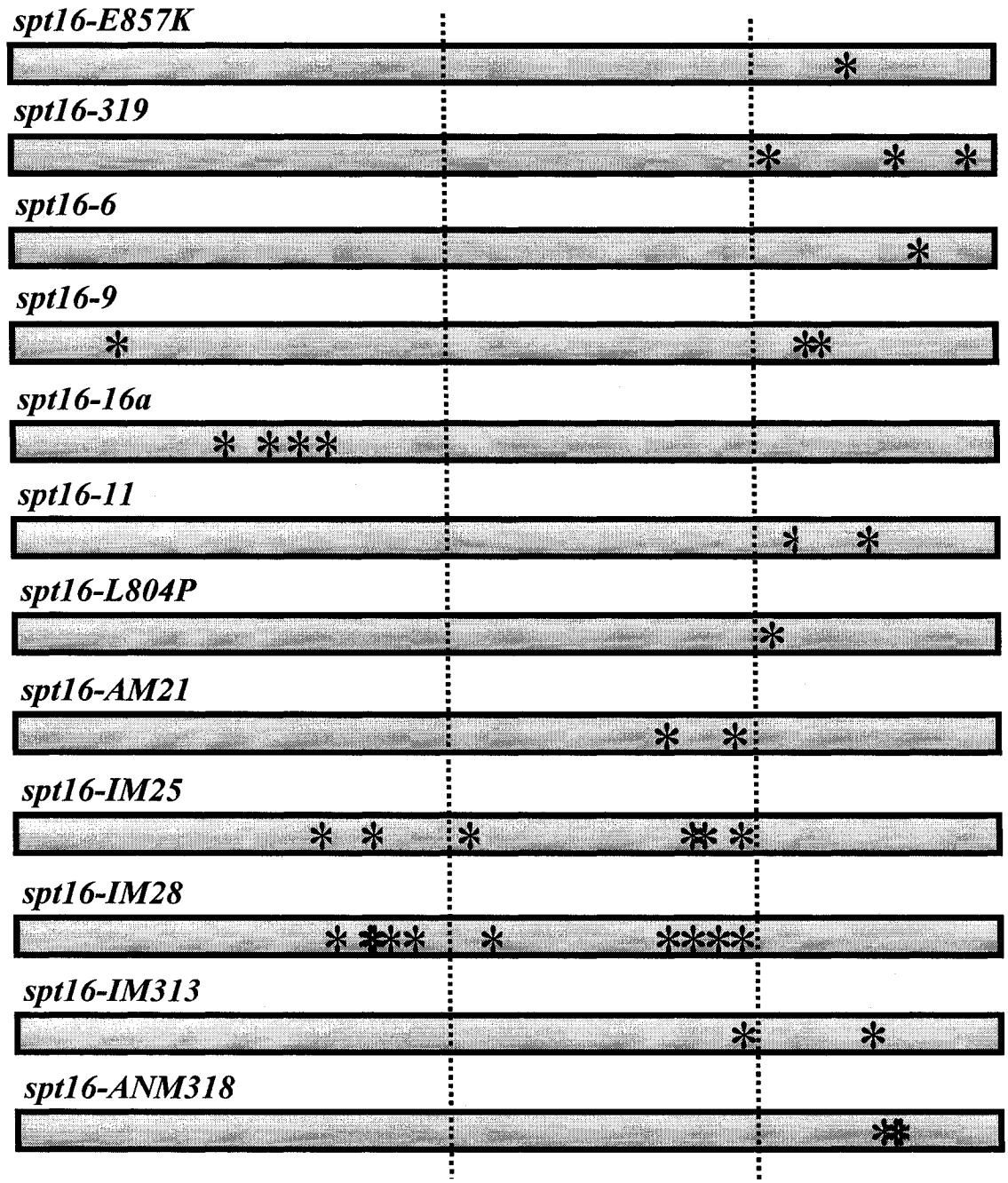

Figure 23. Schematic of *spt16* Mutant Alleles having Deleterious Genetic Interactions with *bur2* and *hir* Mutations. For each mutant, the Spt16 protein is shown as a grey box, with the approximate domain boundaries indicated by the dotted lines. The asterisks indicate the locations of the amino acid substitutions in each of the Spt16 mutant proteins encoded by each of the indicated mutant alleles.

(Formosa et al. 2001). The *spt16-16a* allele encodes four substitutions, all located within the dispensable N-terminal domain of the protein: R204W, A273V, C290V and D318N. That this allele causes synthetic lethality is unexpected, as a mutant allele missing the coding sequences for this entire domain, *spt16-ΔNTD*, does not display synthetic-lethal interactions. One possibility for the presence of synthetic-lethal interactions with *spt16-16a* is the demonstrated instability of its protein product, which appears to be a general property caused by many N-terminal point mutants of Spt16 (O'Donnell et al. 2004). However, why this particular mutant allele demonstrates synthetic-lethal interactions, while none of the other N-terminal point mutations do, is not fully explained by this reasoning. Perhaps the mutational changes in the *spt16-16a* allele do cause some impairment in Spt16 protein function as well as causing protein instability. The *spt16-9* allele contains the same mutation as *cdc68-1* (G132D), as well as two other mutations: G836S and P838S. Although the two C-terminal mutations affect the same region of the protein as do most of the other mutations that cause synthetic lethality, these two mutations alone, in the *spt16-9a* allele, do not demonstrate synthetic-lethal interactions with any of the *bur2* or *hir* mutations; similarly, the *cdc68-1* allele also does not display these synthetic-lethal interactions. Only when the three substitutions are combined does synthetic lethality occur; perhaps the two C-terminal mutations on their own do not cause a severe enough impairment to the protein, so that the additional instability provided by the G132D substitution is required to decrease the amount of Spt16 protein in the cell. This would help explain the observation that *spt16-9a* is not synthetic-lethal with a point mutation in *HIR1*, but is synthetic-lethal with the more severe situation of a *HIR1* deletion. This possibility is reinforced by the report that, while the *spt16-9a* allele is not temperature-sensitive and the *spt16-G132D* allele is temperature-sensitive only above 34°C, the *spt16-9* allele is temperature-sensitive above 32°C, suggesting that *spt16-9 is* more severely impaired than either the *spt16-G132D* allele or the *spt16-9a* allele (Formosa et al. 2001).

3.3 Interactions with Histones and Histone Chaperones

Three of my initial four synthetic-lethal interactions with *spt16-E857K* identified members of the *HIR* family of genes. The products of these genes were initially

characterized as regulators of histone gene expression (Osley, Lycan 1987, Sherwood, Tsang & Osley 1993, Spector et al. 1997), acting as both co-repressors and co-activators, and have recently been discovered to play a role as histone chaperones in replication-independent nucleosome assembly (Green et al. 2005), which occurs following processes that require the disassembly of nucleosomes, such as transcription. The synthetic lethality between *spt16-E857K* and mutations in the *HIR* genes could result from either or both of these roles of the Hir proteins.

To determine whether alterations in histone expression could be a reason for the observed synthetic lethality between *spt16-E857K* and mutations in the *HIR* genes, I decided to determine the effects of directly altering histone abundance in cells containing four mutant versions of *SPT16*. These include the *spt16-E857K* mutant allele that my work focuses on, and three other alleles that were identified in the same manner as *spt16-E857K*: *spt16-E763G*, *spt16-312* and *spt16-319* (O'Donnell 2004). These additional alleles were employed in the allele-specificity tests described above, and I have shown that *spt16-319* demonstrates synthetic-lethal interactions with mutations in the *HIR* genes, while *spt16-E763G* and *spt16-312* do not. Therefore, if synthetic lethality with mutations in the *HIR* genes is due to altered histone abundance, I may observe a similar pattern of effects when histone levels are altered directly in cells with these *spt16* mutations. In addition, due to the recently identified histone-chaperone activity of the Hir proteins (Green et al. 2005, Prochasson et al. 2005), I also decided to assess genetic interactions with other genes whose protein products have been shown to function as histone chaperones.

3.3.1 Alterations in Histone Gene Expression

Several investigations have indicated that alterations in histone gene abundance can affect the growth of cells with mutations in *SPT16*. Allyson O'Donnell's SGA analysis found that deletions in *HHT1* or *HHF1*, encoding histones H3 and H4, respectively, have deleterious genetic interactions with several mutant versions of *SPT16*, specifically *spt16-E857K* and *spt16-319* (O'Donnell 2004). Additionally, results obtained by the Formosa lab indicate that *spt16-11* causes a growth impairment when the abundance of histones H3 and H4 is decreased, or when the abundance of histones H2A and H2B is increased (Formosa et al. 2002). To test whether histone overproduction has deleterious effects on

the *spt16* mutations that I focused on, cells with chromosomal *spt16* mutations were transformed with high-copy plasmids individually expressing the following histone gene pairs: *HTA1–HTB1* (encoding histones H2A and H2B), *HHT1–HHF1* (encoding histones H3 and H4), and *HHT2–HHF2* (the other gene pair encoding histones H3 and H4). Gene expression from each of these pairs is co-ordinately regulated, and histone proteins are found *in vivo* as heterodimers, rather than as free histone monomers.

Overexpression of either of the H3–H4 gene pairs from a high-copy plasmid appeared to impair growth somewhat in a wild-type *SPT16* strain; therefore, the H3–H4 gene pairs were also tested using low-copy plasmids, which had no deleterious effects on *SPT16* cells (Figure 24). No further growth impairment, beyond that seen in *SPT16* cells, was seen for any of the H3–H4 plasmids in either *spt16-E857K* or *spt16-E763G* cells. A similar situation was observed for *spt16-312*, as overexpression of any of the H3–H4 plasmids did not significantly alter the growth of these cells. A slightly different scenario was observed with *spt16-319* cells: in these cells, overexpression of H3 and H4 appeared to provide some alleviation of the *spt16-319* temperature sensitivity. That overexpression of H3 and H4 alleviates the temperature sensitivity of *spt16-319*, but not that of *spt16-312*, indicates that the defects in these strains are due to different impairments of the Spt16 protein, much like the defects associated with the *spt16-E857K* and *spt16-E763G* mutations.

In contrast with the situation for overexpression of histones H3 and H4, overexpression of histones H2A and H2B had no deleterious effects on cells containing *SPT16*, and thus these histones were expressed from only a high-copy plasmid. This overproduction of H2A and H2B also did not cause any growth impairment for *spt16-E763G* cells; in contrast, *spt16-E857K* cells were significantly impaired for growth when H2A and H2B were overexpressed (Figure 25). This finding is yet another illustration of the differences in the behaviour between these two *spt16* mutants with respect to genetic interactions. The growth of cells containing either *spt16-312* or *spt16-319* was also impaired when the expression of H2A and H2B was increased, although the inherent temperature sensitivity of these strains meant that growth effects at 37°C could not be assessed. Even so, the effect of histone overexpression on *spt16-312* appears to be less deleterious than on *spt16-319*, as growth impairment was evident for *spt16-319* cells at

Figure 24. Effect of overexpressing histones H3 and H4 in Y2454 *SPT16*, *spt16-E763G*, *spt16-E857K*, *spt16-312* and *spt16-319* cells. Ten-fold serial dilutions of cultures of cells of *spt16* mutant derivatives of Y2454 were spotted onto Leu- solid medium and grown at the indicated temperature for 4 days. pRK5 = *HHT1-HHF1 CEN*; pRK6 = *HHT1-HHF1* 2μm; pRK7 = *HHT2-HHF2 CEN*; pRK8 = *HHT2-HHF2* 2μm. (A)-(C) High-copy expression caused slight growth impairment at all temperatures tested; low-copy expression did not have noticeable effects. (D) None of the histone-expression plasmids alleviated the temperature sensitivity, and pRK7 caused growth impairment at 35°C. (E) At 35°C, each of the H3-H4 plasmids improved growth. At 37°C, only cells containing the H3-H4 plasmids grew, with high-copy *HHT1-HHF1* and low-copy *HHT2-HHF2* plasmids allowing the most growth.

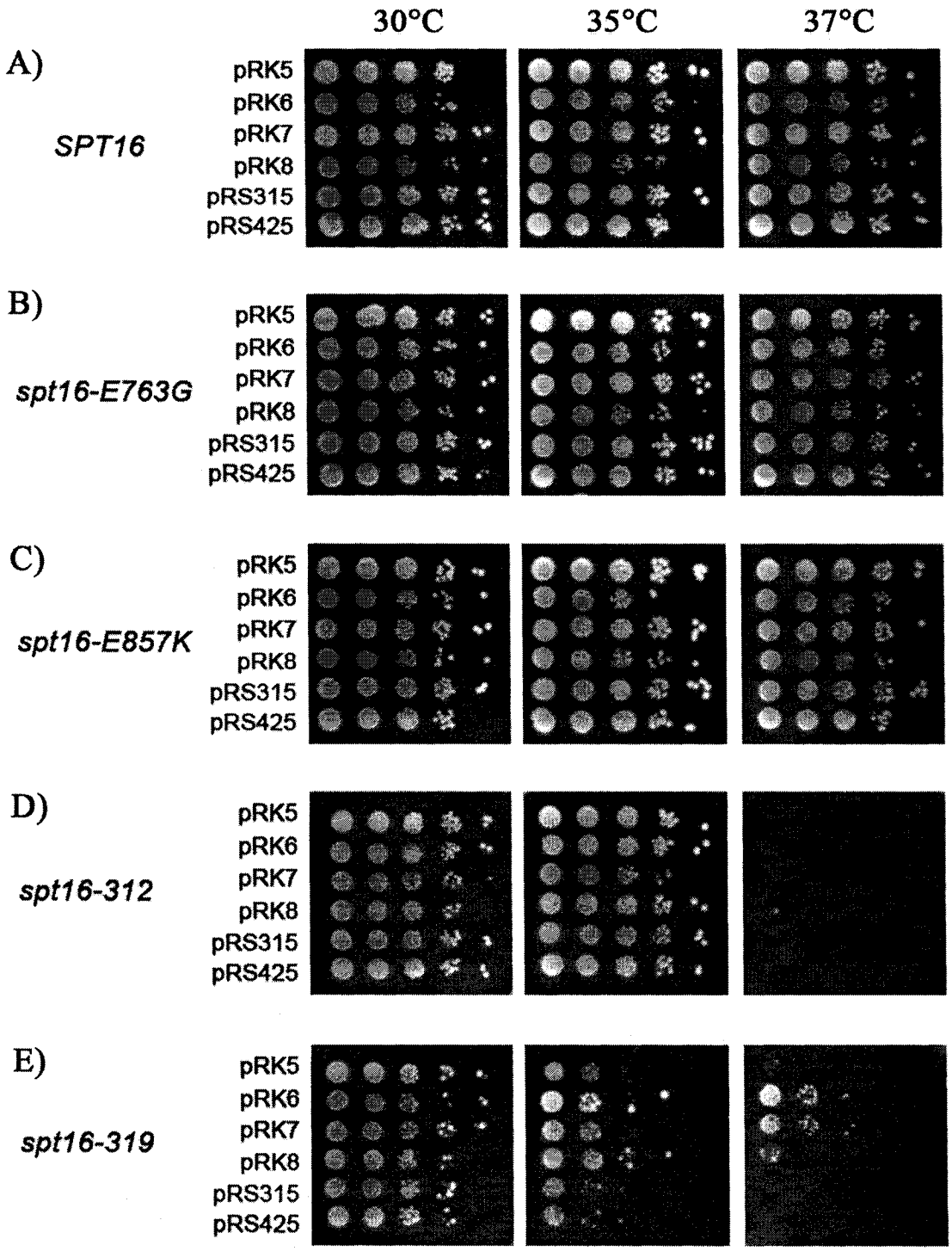
30°C
35°C
37°C
A)
SPT16
pRK5
pRK6
pRK7
pRK8
pRS315
pRS425
B)
spt16-E763G
pRK5
pRK6
pRK7
pRK8
pRS315
pRS425
C)
spt16-E857K
pRK5
pRK6
pRK7
pRK8
pRS315
pRS425
D)
spt16-312
pRK5
pRK6
pRK7
pRK8
pRS315
pRS425
E)
spt16-319
pRK5
pRK6
pRK7
pRK8
pRS315
pRS425

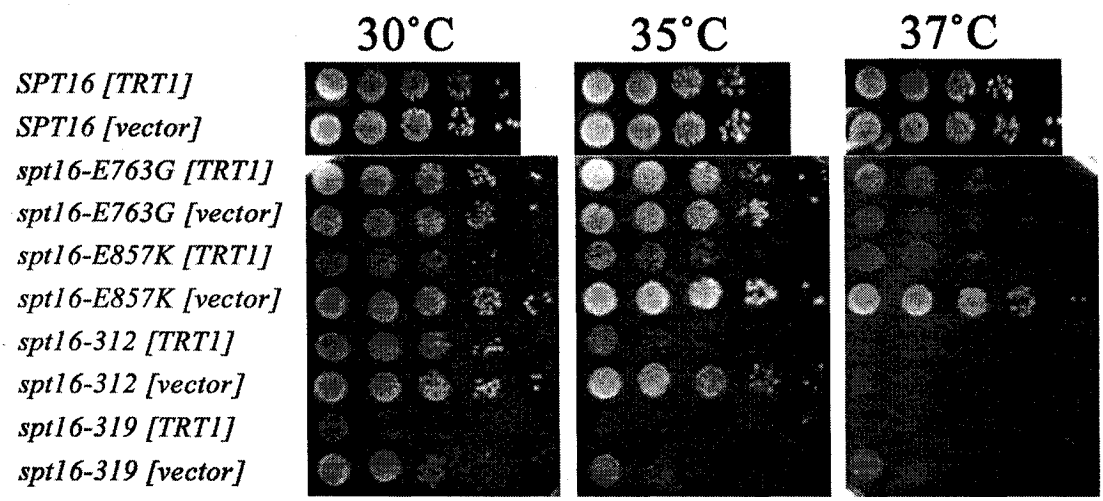

Figure 25. Functional interactions between *spt16* mutant alleles and H2A-H2B (*TRT1* locus) overexpression. Cells of strains described in Figure 24 were transformed with a high-copy *TRT1* plasmid containing the *HTA1-HTB1* locus or empty vector. Equal numbers of cells were spotted in 10-fold serial dilutions onto Ura- solid medium, and then incubated at the indicated temperature for 3 days. *HTA1-HTB1* overexpression did not cause impaired growth in cells with *SPT16* or *spt16-E763G*, but a strong deleterious genetic interaction was seen in *spt16-E857K* and *spt16-319* cells, even at 30°C. In addition, the *spt16-312* cells were growth-impaired at 35°C. Both the *spt16-312* and *spt16-319* alleles themselves cause temperature sensitivity, explaining the poor growth of these strains at high temperatures.

30°C while none was observed for *spt16-312* cells until the temperature was raised to 35°C. Thus, while the overexpression of histones H3 and H4 did not cause significant effects on cells containing any of the mutant forms of Spt16, the overexpression of H2A and H2B had detrimental effects, the magnitude of which varied depending on the mutant allele of *SPT16*.

There are several possibilities for why overexpression of the H2A–H2B gene pair causes a deleterious effect on cells containing mutant forms of *SPT16*. One is that the sheer abundance of the histone H2A–H2B heterodimer is detrimental to these cells; another is that the perturbed ratio of the histone dimers H2A–H2B to H3–H4 is detrimental. To determine which of these possibilities might explain the impaired growth, growth was assessed for cells with two plasmids: one expressing H2A and H2B and the other expressing H3 and H4. If the sheer abundance of histones H2A and H2B is detrimental, I would still expect to see impaired growth, whereas if an altered ratio of histones is detrimental, cell growth might then be improved compared to that of cells overexpressing only H2A and H2B. As shown in Figure 26, overexpression of both histone pairs did not cause any detrimental effects in cells containing *SPT16*, aside from the very mild impairment observed when H3 and H4 are expressed from a high-copy plasmid. Likewise, for *spt16-E763G* cells, which did not show any growth impairment when H2A and H2B were over-expressed, co-overexpression of all four histones had no effect on growth. In contrast, in the cases of *spt16-E857K*, *spt16-312* and *spt16-319*, overexpression of the H3–H4 gene pair alleviated the growth impairment observed when H2A and H2B are overproduced in these cells. Thus, restoring a balance between the relative expression levels of histones H2A and H2B and those of histones H3 and H4 alleviates the growth impairment observed when the expression of the H2A–H2B gene pair is increased. This finding indicates that it may be the ratio of histones that affects cells with mutations in *SPT16*, rather than the sheer abundance of the histone proteins.

To provide more evidence that it is indeed the ratio of histones that affects the growth of cells with mutations in *SPT16*, I assessed whether synthetic interactions occur in cells that contain *spt16-E857K* and a deletion of either *HHT1* or *HHF1*, which encode histones H3 and H4, respectively. Allyson O'Donnell reported a synthetic slow-growth effect between *spt16-E857K* and *hht1Δ*, as indicated by random-spore analysis

Figure 26. Effect of overexpressing all four histones in *spt16* mutant cells. Ten-fold serial dilutions of transformant cells were spotted onto Leu-Ura- solid medium and grown at the indicated temperature for 3 days. All cells contained the *HTA1-HTB1* (*TRT1*) plasmid and pRK5 (*HHT1-HHF1 CEN),* pRK6 (*HHT1-HHF1* 2μm), pRK7 (*HHT2-HHF2 CEN)*, pRK8 (*HHT2-HHF2* 2μm), or a vector control. All of the *spt16* mutant transformants containing high-copy empty vector grew better than those containing low-copy, perhaps due to increased production of leucine. However, for all of the strains that were impaired by the overexpression of histones H2A and H2B, co-overexpression of histones H3 and H4 alleviated this impairment.

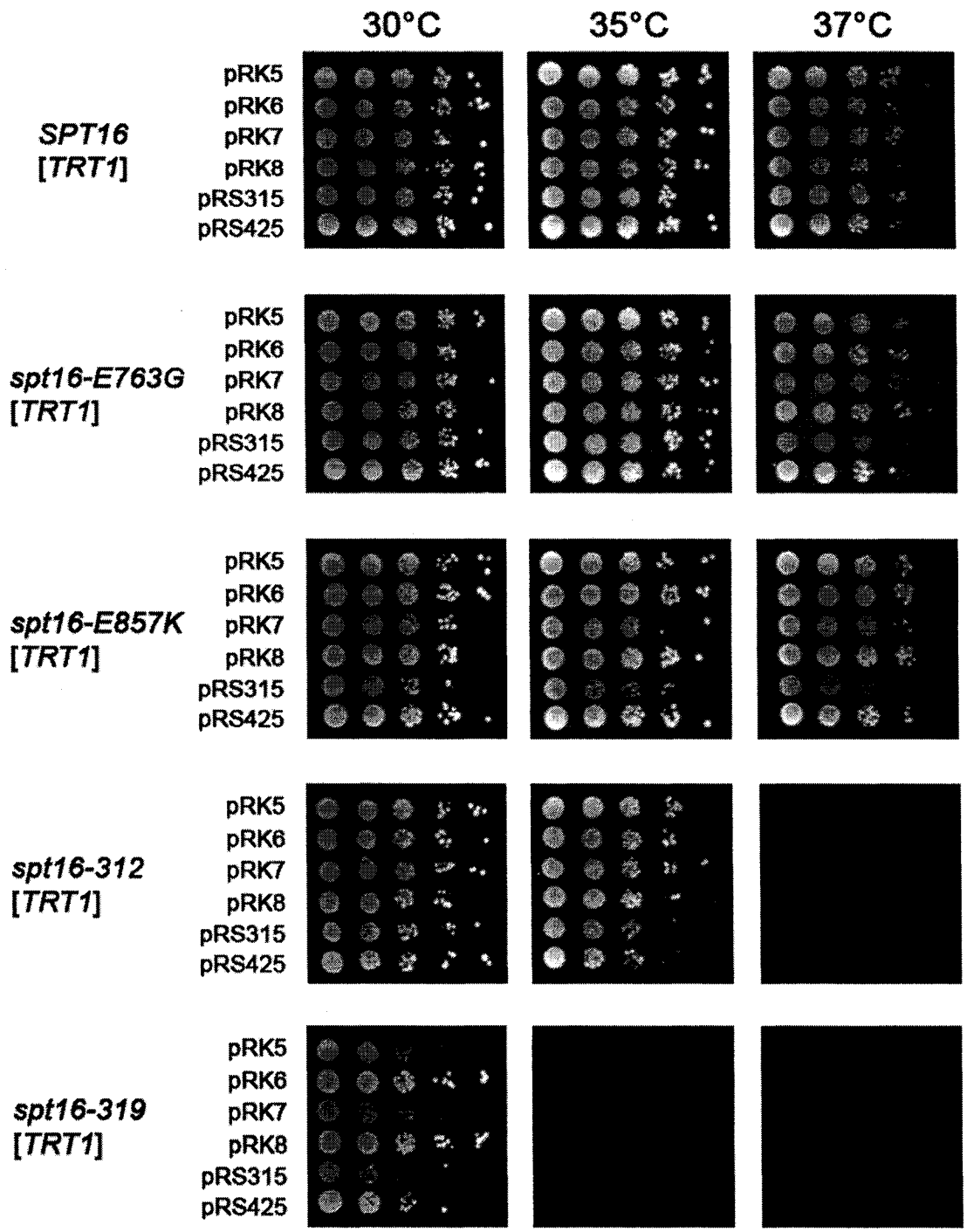
30°C
35°C
37°C
SPT16
[TRT1]
spt16-E763G
[TRT1]
spt16-E857K
[TRT1]
spt16-312
[TRT1]
spt16-319
[TRT1]
pRK5
pRK6
pRK7
pRK8
pRS315
pRS425

(O'Donnell 2004); to more fully assess these potential interactions, I decided to use tetrad analysis. The interactions between these histone-gene deletions and *spt16-E763G* were also assessed, to provide two mutant alleles of *SPT16* with which to compare the results of histone-gene deletions with histone overproduction. If the ratio of histones is the important factor, then both the *spt16-E857K* allele and the *spt16-E763G* allele should exhibit similar results when combined with H3 or H4 gene deletions as they did when histones H2A and H2B were overproduced. That is, *spt16-E857K* should show impaired growth when combined with a deletion of either *HHT1* or *HHF1*, while *spt16-E763G* should show no difference in growth in either situation. Indeed, slight growth impairment was observed for the *spt16-E857K hht1Δ* double mutants, but not for the *spt16-E857K hhf1Δ* double mutants (Figure 27). No such growth impairment was observed for either of the *spt16-E763G* double mutants. That a genetic interaction exists between *spt16-E857K* and *hht1Δ*, but not *hhf1Δ*, does not make immediate sense, as I would expect these two deletions to perturb the histone balance similarly. However, it is evident that the *HHT1* deletion affects cells differently than the *HHF1* deletion.

These results reflect those observed when histones H2A and H2B are overproduced in cells containing either *spt16-E857K* or *spt16-E763G*. However, the growth impairment seen for *spt16-E857K hht1Δ* double mutants was not as severe as that seen for overexpression of the H2A–H2B gene pair in *spt16-E857K* cells. One interpretation of these results is that the deletion of one of the two genes encoding H3 does not perturb the ratio of histones as severely as does the expression of histones H2A and H2B from a high-copy plasmid. Thus, while some alteration in the ratio of histone proteins may exist in *hht1Δ* cells, this perturbation is not as great as that which exists in cells overproducing H2A and H2B. Therefore, the deleterious effects observed between *spt16-E857K* and either of the histone-gene deletions would not be as severe as those observed when H2A and H2B are overproduced. While both situations reflect the effects of altering the ratio between H2A–H2B dimers and H3–H4 dimers, the degree of perturbation in this ratio may influence the degree of impairment observed.

There are several possibilities that could explain these observations with altered histone abundance. One such interpretation is that overproduction of histones H2A and H2B might titrate away a histone chaperone that binds to these histones, thereby

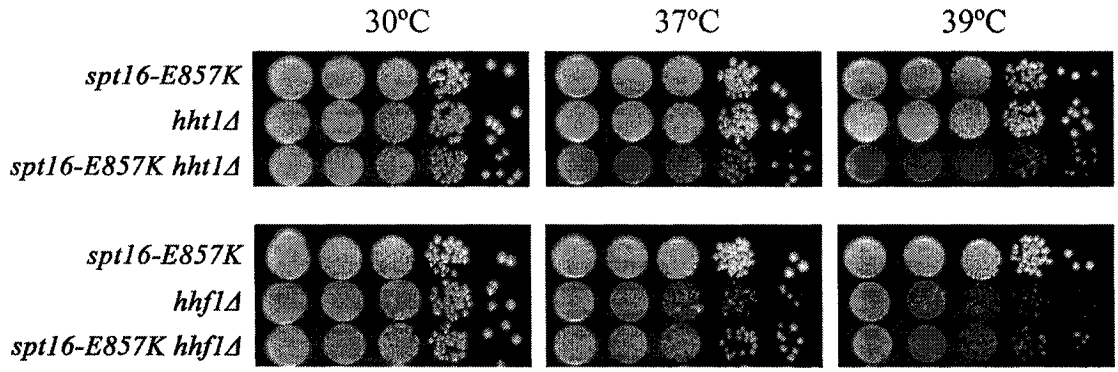

Figure 27. Deleterious genetic interactions exist between *spt16-E857K* and *hht1Δ*, but not between *spt16-E857K* and *hhf1Δ*. Single and double mutants were grown in liquid culture, and 10-fold serial dilutions were spotted onto YEPD solid medium and were incubated at the indicated temperatures for 3 days. The *spt16-E857K hht1Δ* double-mutant cells grew more poorly at high temperatures than either single mutant, indicating a deleterious genetic interaction. No such interaction was observed between *spt16-E857K* and *hhf1Δ*, indicating that these two histone-gene deletions affect cells in different ways. The *hhf1Δ* single-mutant cells were also more impaired than the *hht1Δ* single mutants, which supports the hypothesis that these two mutations have different effects on the cell.

impeding this chaperone from performing additional functions. Presumably this histone chaperone would carry out a function that partially overlaps with a function of Spt16, such that titration of this histone chaperone can be tolerated in normal Spt16 cells, but is deleterious to cells containing mutant versions of Spt16. Overproduction of all four histones would provide free H3–H4 tetramers in the nucleus, to which the excess H2A–H2B dimers could bind to form octamers, thereby freeing this putative histone chaperone to do its normal function. However, it remains unclear whether free histone octamers are formed in the cell. Another drawback to this interpretation is that it does not readily explain the detrimental effects of decreased H3, as normal levels of H2A–H2B dimers would presumably be present in these cells. Therefore, if this interpretation of the mechanism of histone-overexpression effects holds true, the effects of histone-gene deletions must be explained in a different fashion.

Another interpretation is that increased amounts of histones H2A and H2B in the cell result in an imbalance of histones in the nucleus. Like all proteins, histone proteins are made in the cytoplasm, and therefore must be imported into the nucleus. Nap1, a histone chaperone, has been shown to aid in the nuclear import of histones H2A and H2B (Mosammaparast, Ewart & Pemberton 2002), but the full picture of histone import is more complex than that. Several studies that have focused on nuclear import of histones have identified several karyopherins that mediate the import of the four histone proteins. Different mechanisms appear to exist for the import of histones H2A and H2B and for that of H3 and H4, although there is some overlap in the proteins used. There appear to be two pathways for the import of H2A and H2B, the primary pathway mediated by Kap114, and the other mediated by Kap121 and Kap123 (Greiner, Caesar & Schlenstedt 2004, Mosammaparast et al. 2001). In contrast, only one pathway appears to mediate the import of H3 and H4: that mediated by Kap121 and Kap123 (Greiner, Caesar & Schlenstedt 2004, Mosammaparast et al. 2002). In both situations, additional karyopherin proteins have been suggested to play minor roles (Greiner, Caesar & Schlenstedt 2004, Mosammaparast et al. 2001, Mosammaparast et al. 2002).

It is therefore possible that, since some of the same proteins are required to transport all four histones into the nucleus, a large increase in the amount of histones H2A and H2B might result in a decreased amount of nucleus-localized histones H3 and

H4. A large increase in the amount of H2A and H2B may overwhelm the Kap114-mediated import pathway, such that the excess H2A–H2B dimers also use the Kap121–Kap123 import pathway, thereby excluding H3 and H4 from the nucleus through competition effects. Since H3–H4 tetramers form the 'core' of nucleosomes, with two H2A–H2B dimers on either side (Luger et al. 1997, White, Suto & Luger 2001), it is possible that decreased amounts of available H3 and H4 could be more detrimental to cells than decreased amounts of H2A and H2B. Nucleosome assembly occurs in a stepwise process, with the deposition of H3–H4 tetramers occurring prior to the deposition of H2A–H2B dimers (Smith, Stillman 1991, Worcel, Han & Wong 1978). Results of *in vitro* studies indicate that it may be possible to form 'minimal' nucleosomes by wrapping DNA around an H3–H4 tetramer, but that an analogous structure is not formed by H2A–H2B dimers (Camerini-Otero, Felsenfeld 1977, Jorcano, Ruiz-Carrillo 1979, Ruiz-Carrillo et al. 1979). This potential ability to incorporate H3–H4 tetramers, but not H2A–H2B dimers, would explain the detrimental effects observed when H2A and H2B were overproduced, but not when H3 and H4 were. In addition, H3 and H4 do not appear to use the Kap114 pathway for nuclear import (Greiner, Caesar & Schlenstedt 2004, Mosammaparast et al. 2002), leaving this pathway available to import H2A–H2B dimers even when H3 and H4 are present in excess. When all four histones were overproduced, similar amounts of histone protein would be available in the cytoplasm for nuclear import, the Kap121–Kap123 pathway can again transport histones H3 and H4, and the balance of nucleus-localized histones might be restored, thereby also restoring proper chromatin structure. Thus, somehow, this decrease in nucleus-localized H3 and H4 is deleterious only to cells with certain mutations in *SPT16*. Perhaps impaired nucleosome reassembly in cells with *spt16* mutations, combined with a general decrease in the ability to form proper nucleosomes, leads to chromatin that is so improperly packaged that the cell is compromised for growth.

Unlike the first interpretation presented, this view does explain the deleterious effects of deletion of *HHT1*, as these cells would also contain decreased amounts of H3 and H4 in the nucleus and would therefore be impaired in a similar manner as cells overproducing H2A and H2B. I therefore favour the competitive-import hypothesis.

3.3.2 Genetic Interactions with Histone Chaperones

As noted above, the Hir proteins, already known to have genetic interactions with *spt16-E857K*, are components of a histone chaperone (here termed HirC) involved in replication-independent nucleosome reassembly (Green et al. 2005, Prochasson et al. 2005). In fact, a deletion of any of *HIR1*, *HIR2* or *HIR3* exhibits synthetic-lethal interactions in combination with *spt16-E857K*. However, the Hir complex is not the only histone chaperone in yeast; in fact, several other such proteins exist. FACT itself, of which Spt16 is a component, has been characterized as a histone chaperone that removes H2A–H2B dimers from nucleosomes and also reassembles intact nucleosomes (Belotserkovskaya et al. 2003, Orphanides et al. 1999, Rhoades, Ruone & Formosa 2004). Another histone chaperone is Chromatin Assembly Factor 1 (CAF-1), which participates in nucleosome assembly during DNA replication (Smith, Stillman 1989). In contrast to what is seen for the Hir complex (HirC), a deletion of any of the genes encoding CAF-1 subunits (*CAC1*, *CAC2* or *CAC3*) does not produce obvious growth effects in combination with *spt16-E857K* (O'Donnell 2004). Therefore, not all histone chaperones have genetic interactions with the *spt16-E857K* mutation. To determine whether the deleterious genetic interactions seen with mutations in the *HIR* genes are limited to this HirC histone chaperone, I assessed whether similar genetic interactions exist between *spt16-E857K* and deletions of genes encoding other histone chaperones, such as Vps75, Nap1, Spt6, Rtt106 and Asf1.

3.3.2.1 Interactions Between *spt16-E857K* and *asf1Δ*

The Asf1 protein is a chaperone for histones H3 and H4 (English et al. 2005) and is involved in many processes requiring alterations in chromatin structure. Asf1 has been shown to participate in chromatin assembly following DNA replication (Franco et al. 2005, Tyler et al. 1999) and DNA repair (Emili et al. 2001, Le et al. 1997), aids in the establishment of silenced chromatin (Le et al. 1997, Singer et al. 1998) and is involved in both chromatin disassembly and reassembly during transcription (Schwabish, Struhl 2006). High-throughput SGA analysis has suggested a genetic interaction between *spt16-E857K* and *asf1Δ* (O'Donnell 2004), but this observation was not confirmed directly using tetrad analysis. Therefore, to assess here whether a genetic interaction exists between *ASF1* and *SPT16*, tetrad analysis was carried out. Cells containing the *spt16-*

E857K mutation were crossed with *asf1Δ* cells. The resulting diploids were sporulated, and the haploid spore products assessed for growth ability. This analysis showed that the *spt16-E857K asf1Δ* double-mutant cells do indeed display a slow-growth phenotype that was not exhibited by either single mutant (Figure 28). To ensure that this slow growth was not a result of delayed germination, serial-dilution spot testing was performed for both parental strains and two of these double-mutant segregants. This analysis demonstrated that, although there was little difference in growth between *asf1Δ* cells and *spt16-E857K asf1Δ* double-mutant cells at 30°C, the *spt16-E857K asf1Δ* double mutants exhibited synthetic temperature sensitivity at the higher growth temperatures of 35°C and 37°C (Figure 28).

The role of Asf1 in replication-dependent chromatin assembly involves protein interactions with the Cac2 subunit of the CAF-1 complex, and Asf1 stimulates CAF-1 activity (Tyler et al. 1999, Tyler et al. 2001), while Asf1 function in replication-*in*dependent chromatin assembly involves protein interactions with the Hir complex (Green et al. 2005). The replication-dependent chromatin-assembly role of Asf1 is likely not important in this genetic interaction with *spt16-E857K*, as there are no genetic interactions between *spt16-E857K* and deletions of genes encoding the CAF-1 subunits. It is therefore possible that the role of Asf1 that is important for its genetic interaction with *spt16-E857K* is its role in replication-independent chromatin assembly, especially considering that all three *HIR* genes also demonstrate genetic interactions with *spt16-E857K*. One possible mechanism in the genetic interaction between *spt16-E857K* and *asf1Δ* is the absence of the Asf1–HirC interaction, and the resulting decreased activity of HirC (Green et al. 2005). The observation that a deletion of *ASF1* results in synthetic slow growth, whereas a deletion in any of the *HIR* genes results in synthetic lethality, is consistent with this explanation, as the loss of Asf1 results in decreased but measurable HirC activity rather than a completely non-functional HirC.

To test whether the loss of Asf1–HirC interaction is responsible for the observed genetic interaction with *spt16-E857K*, I used a plasmid-borne mutant form of *ASF1* (*asf1-H36AD37A*, referred to here as *asf1-36/37-AA*). This *asf1* mutant allele produces an Asf1 protein that is impaired for HirC binding, yet retains its own intrinsic histone-binding and -deposition activities (Daganzo et al. 2003, Green et al. 2005). If the synthetic impairment

A)

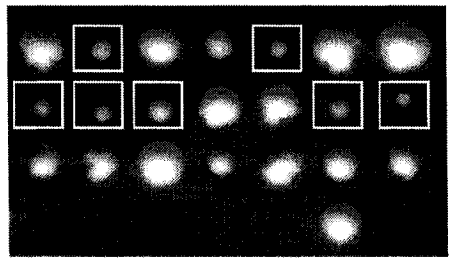

B)

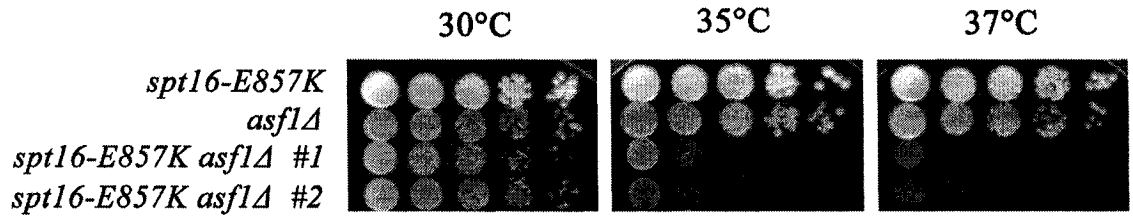

Figure 28. Deleterious genetic interactions exist between *spt16-E857K* and *asf1Δ*. A) Diploid cells heterozygous for both the *spt16-E857K* and *asf1Δ* mutations were sporulated and tetrad analysis was carried out. The *spt16-E857K asf1Δ* double-mutant segregants are highlighted by white boxes. In all cases, these segregants grew more slowly than did segregants of either parental type. B) Ten-fold serial dilutions of two different *spt16-E857K asf1Δ* double-mutant segregants were spotted onto YEPD solid medium, along with both parental strains, and incubated at the indicated temperatures. The double mutants exhibited significant inhibition of growth, particularly at 35°C and 37°C.

between *spt16-E857K* and *asf1Δ* is a result of the loss of the Asf1 contribution to HirC activity, then the presence of this plasmid-borne *asf1* mutant allele should not improve the growth of these double-mutant cells. On the other hand, if the synthetic impairment between *spt16-E857K* and *asf1Δ* is a result of some other function of Asf1, then this plasmid-borne *asf1* mutant allele might well improve the growth of these double-mutant cells. Transformants were obtained, and serial-dilution spot testing was performed to determine whether differences in growth could be observed. In fact, the *asf1-36/37-AA* plasmid was able to improve the growth of *spt16-E857K asf1Δ* cells to the same degree as an *ASF1* plasmid (Figure 29). This finding suggests that the physical interaction between Asf1 and the Hir complex is not a determining factor in the genetic interactions between *spt16-E857K* and *asf1Δ*, as the Asf1-36/37-AA mutant protein is unable to make this physical interaction, yet restores good growth to *spt16-E857K asf1Δ* double-mutant cells. Thus, another role of Asf1, outside of its roles with either CAF-1 or HirC, must be responsible for the observed genetic interactions with *spt16-E857K*.

3.3.2.2 Interactions Between *spt16-E857K* and *rtt106Δ*

The Rtt106 protein is a recently identified histone chaperone; mutations in the *RTT106* gene cause defects in transcriptional silencing and increased mobility of the Ty1 transposon (Huang et al. 2005, Scholes et al. 2001). Binding studies have shown that Rtt106, like the Asf1 protein, binds to histones H3 and H4 and also to one of the CAF-1 subunits, Cac1 (Huang et al. 2005). While little is known about the cellular functions of Rtt106, its proposed role as a histone chaperone and its Asf1-like binding properties warranted its direct testing for genetic interactions with *spt16-E857K*. High-throughput SGA analysis has suggested a genetic interaction between *spt16-E857K* and *rtt106Δ* (O'Donnell 2004); however, this result was not confirmed directly using tetrad analysis. To assess whether a genetic interaction exists between *RTT106* and *SPT16*, tetrad analysis was carried out. Cells containing the *spt16-E857K* mutation were crossed with *rtt106Δ* cells, the resulting diploids were sporulated, and the haploid spore products assessed for growth defects. The *spt16-E857K rtt106Δ* double-mutant cells did indeed display a slow-growth phenotype that was not exhibited by either single mutant (Figure 30). To ensure that this slow growth was not a result of delayed spore germination, all of the segregants were patched, and replica-plated for growth at several temperatures. This

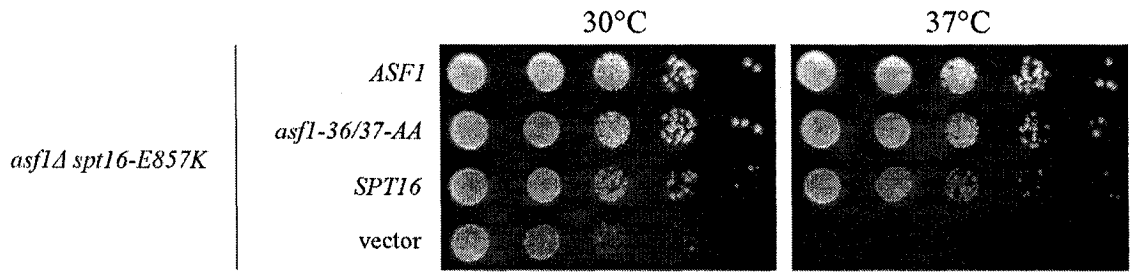

Figure 29. *asf1-36/37-AA* alleviates growth defects of *asf1Δ spt16-E857K* double-mutant cells. Ten-fold serial dilutions of double-mutant cells carrying low-copy *ASF1*, *asf1-36/37-AA*, or *SPT16* plasmids, or empty vector were spotted onto Ura- solid medium and incubated at the indicated temperatures for 3 days. All three gene-containing plasmids restored growth at high temperatures. However, both the *ASF1* and the *asf1-36/37-AA* plasmids allowed slightly better growth at 37°C than did the *SPT16* plasmid, as *asf1Δ* cells exhibit slight temperature sensitivity that is not suppressed by *SPT16*. The restoration of growth by *asf1-36/37-AA* indicates that the loss of a physical interaction between HirC and Asf1 is not involved in the deleterious genetic interaction between *asf1Δ* and *spt16-E857K*.

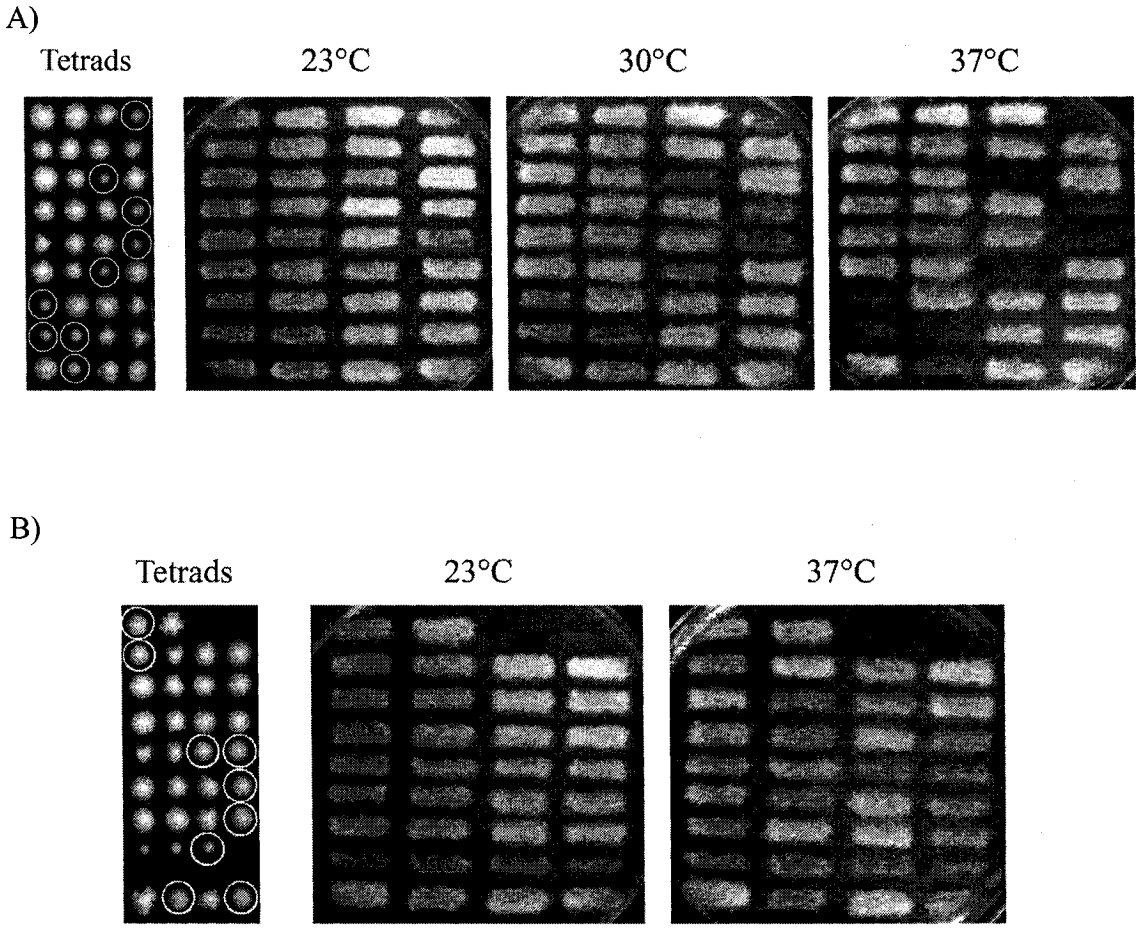

Figure 30. Deleterious genetic interactions between *spt16-E857K* and *rtt106Δ*, but not between *spt16-E763G* and *rtt106Δ*. A) Diploid cells heterozygous for *spt16-E857K* and *rtt106Δ* were sporulated, and tetrad analysis was carried out. The *spt16-E857K rtt106Δ* double-mutant segregants are outlined by the white circles. All segregants were patched in the same pattern onto YEPD solid medium at 23°C, and replica-plated to YEPD for incubation at 23°C, 30°C, and 37°C. The slow growth of the double-mutant cells was exacerbated at higher temperatures, showing virtually no growth at 37°C. Thus, a deleterious genetic interaction exists between *spt16-E857K* and *rtt106Δ*. B) Tetrad analysis and patch plating were performed for a cross between *spt16-E763G* and *rtt106Δ*, as described for *spt16-E857K* and *rtt106Δ*. In this situation, the double-mutant cells did not exhibit poor growth at 23°C or 37°C. Therefore, no synthetic genetic interaction exists between *spt16-E763G* and *rtt106Δ*.

analysis demonstrated that, although *spt16-E857K rtt106Δ* double-mutant cells grow fairly normally at 23°C, these *spt16-E857K rtt106Δ* double mutants show poor growth at 30°C, and exhibit severe temperature sensitivity at the higher temperatures of 35°C and 37°C (Figure 30). Therefore, the Rtt106 histone chaperone behaves in a manner similar to that of the Asf1 histone chaperone, at least at the level of genetic interactions between deletions of their respective genes and the *spt16-E857K* mutant allele.

In contrast, the *spt16-E763G* mutant allele gave different effects. Unlike the impaired growth observed with the *spt16-E857K* mutant allele, no genetic interaction was observed between *spt16-E763G* and *rtt106Δ*, even when the cells were grown at high temperatures (Figure 30). Thus, a deleterious genetic interaction with *rtt106Δ* is not common to all mutant alleles of *SPT16*.

3.3.2.3 Interactions Between *spt16* and *spt6*

The Spt6 protein has also been characterized as a histone chaperone, and is thought to participate in a process similar to that of FACT during transcription. Like FACT, Spt6 plays a part in maintaining chromatin structure, and mutations in the *SPT6* gene cause phenotypes consistent with impaired chromatin reassembly following transcription (Adkins, Tyler 2006, Kaplan, Holland & Winston 2005). The Spt6 protein has been shown to directly interact with histones, primarily with histone H3, and thus may function as a chaperone for H3–H4 tetramers (Bortvin, Winston 1996). Like *SPT16* itself, *SPT6* is an essential gene, and therefore the effects of a gene deletion cannot be readily analysed. Therefore, two mutant alleles of this gene, *spt6-140* and *spt6-1004*, were used in my investigations. The *spt6-140* allele was originally isolated by virtue of its Spt phenotype (Winston et al. 1984), and was found to cause temperature sensitivity for growth at 37°C (Clark-Adams, Winston 1987). While Spt6 has a role in transcription elongation, *spt6-140* causes no sensitivity to 6-azauracil, a compound that interferes with transcription elongation (Hartzog et al. 1998). The *spt6-1004* allele contains an internal deletion removing coding sequences for amino acid residues 931-994 (Kaplan, Holland & Winston 2005). Like *spt6-140*, *spt6-1004* causes an Spt phenotype and is temperature sensitive at 37°C (Kaplan, Holland & Winston 2005, Kaplan, Laprade & Winston 2003). In addition, both of these mutant alleles have been characterized to cause defects in

nucleosome reassembly following transcription (Adkins, Tyler 2006, Kaplan, Holland & Winston 2005).

Double-mutant cells were generated that contained one of these *spt6* mutations in combination with *spt16-E857K*. Both the *spt16-E857K spt6-140* double mutants and the *spt16-E857K spt6-1004* double mutants demonstrated increased temperature sensitivity compared to any of the single mutants, indicating that genetic interactions exist between the *spt6* mutations and *spt16-E857K* (Figure 31). Also, to determine whether DNA replication may also be affected by these mutations, the double mutants were examined for sensitivity to hydroxyurea. Hydroxyurea-sensitivity was observed for the *spt16-E857K spt6-1004* double-mutant cells, suggesting effects on DNA replication. However, an analogous sensitivity was not evident for the *spt16-E857K spt6-140* double mutants, indicating a difference between the two mutant alleles of *SPT6* (Figure 31).

Similar analysis using the *spt16-E763G* mutant allele also demonstrated increased temperature sensitivity among the double-mutant cells compared to any of the single mutants (Figure 31). Neither the *spt16-E763G spt6-140* double mutants nor the *spt16-E763G spt6-1004* double mutants displayed sensitivity to hydroxyurea, unlike what was observed with the *spt16-E857K spt6-1004* double mutants (Figure 31). Thus, while deleterious genetic interactions with these mutant alleles of *SPT6* are common to both mutations in *SPT16* tested, differences exist between the behaviour of *spt16-E857K* double mutants and *spt16-E763G* double mutants, indicating somewhat different effects in these cells.

3.3.2.4 Interactions Between *spt16-E763G* and *nap1Δ*

The Nap1 protein is yet another histone chaperone protein, which, like many other histone chaperones, can facilitate nucleosome assembly *in vitro* (Mazurkiewicz, Kepert & Rippe 2006). Unlike many other histone chaperones, however, Nap1 has been shown to shuttle between the nucleus and cytosol (Miyaji-Yamaguchi et al. 2003). Although *in vitro* studies using Nap1 from several species, including yeast, have shown preferential binding to histones H3 and H4, *in vivo* studies have also shown interactions with H2A–H2B dimers (Park, Luger 2006). In addition, Nap1 has been shown to be involved in the nuclear import of histones H2A and H2B through associations with the karyopherin, Kap114 (Mosammaparast, Ewart & Pemberton 2002). Thus, while the exact role(s) of

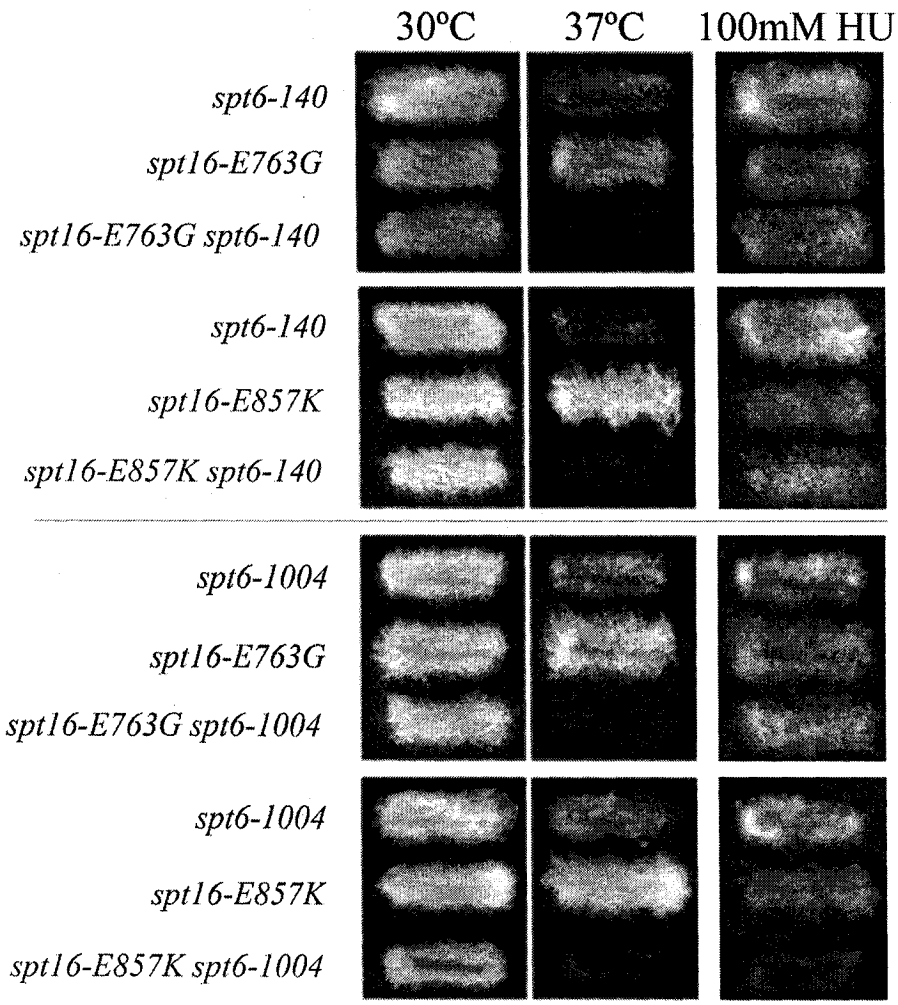

Figure 31. Deleterious genetic interactions between *spt16-E763G* or *spt16-E857K* and *spt6*. Replica plates of single and double mutants were grown under the indicated conditions overnight (2 days for hydroxyurea [HU] plates at 30°C). While both *spt16-E763G* and *spt16-E857K* have deleterious genetic interactions with both *spt6* alleles, only the *spt16-E857K spt6-1004* double mutants demonstrated synthetic hydroxyurea sensitivity. This may indicate that while different *spt16* mutations can cause deleterious genetic interactions with mutations in *SPT6*, there are differences between the *spt16-E763G* and *spt16-E857K* alleles, and between the two *spt6* mutant alleles.

Nap1 remain unclear, *in vitro* transcription studies have shown that Nap1, like FACT, is able to disassociate one H2A-H2B dimer from a nucleosome encountered by elongating RNAPII (Levchenko, Jackson 2004).

To assess whether a genetic interaction exists between *NAP1* and *SPT16*, tetrad analysis was carried out. Cells containing the *spt16-E857K* mutation were crossed with *nap1Δ* cells, the resulting diploids were sporulated, and the haploid spore products assessed for growth defects. No deleterious genetic interaction was observed between *spt16-E857K* and *nap1Δ*, even when the cells were grown at high temperatures (Figure 32). In contrast, the *spt16-E763G nap1Δ* double mutants did exhibit temperature sensitivity that was not shown by either single mutant (Figure 32). The segregants from this cross were patched, and replica-plated for growth at several temperatures. This analysis demonstrated that, although *spt16-E763G nap1Δ* double-mutant cells grow fairly normally at 23°C and 30°C, these cells exhibit severe temperature sensitivity at the higher temperatures of 37°C and 39°C (Figure 32). Therefore, a deleterious genetic interaction with *nap1Δ* is not common to all mutant alleles of *SPT16*.

This is one of the few instances where I have observed a deleterious genetic interaction using *spt16-E763G*, yet have not seen a similar interaction with *spt16-E857K*. Because of this unusual situation, allele identities were verified by sequencing the *SPT16* gene to confirm that the *spt16-E763G* mutation was indeed present in these cells. While *spt16-E763G*-specific genetic interactions have been observed using SGA analysis, most of the gene deletions in this set encode proteins involved in vesicular transport, rather than direct chromatin-related processes (O'Donnell 2004). However, of the transcription-related gene deletions identified by SGA analysis of *spt16-E763G*, only one, *cdc73Δ*, is common to the set obtained for *spt16-E857K*. My findings with *nap1Δ* therefore support the idea that while *spt16-E763G* has an effect on Spt16 function during transcription, this effect is different than that of *spt16-E857K*.

3.3.2.5 Interactions Between *spt16* and *vps75Δ*

Vps75 was recently identified as a histone chaperone that shares similarity with Nap1 and its homologues from other species (Selth, Svejstrup 2007). Unlike Nap1, which is thought to shuttle between the nucleus and cytosol, Vps75 is found primarily in the nucleus (Huh et al. 2003). In addition, *in vitro* binding experiments have demonstrated

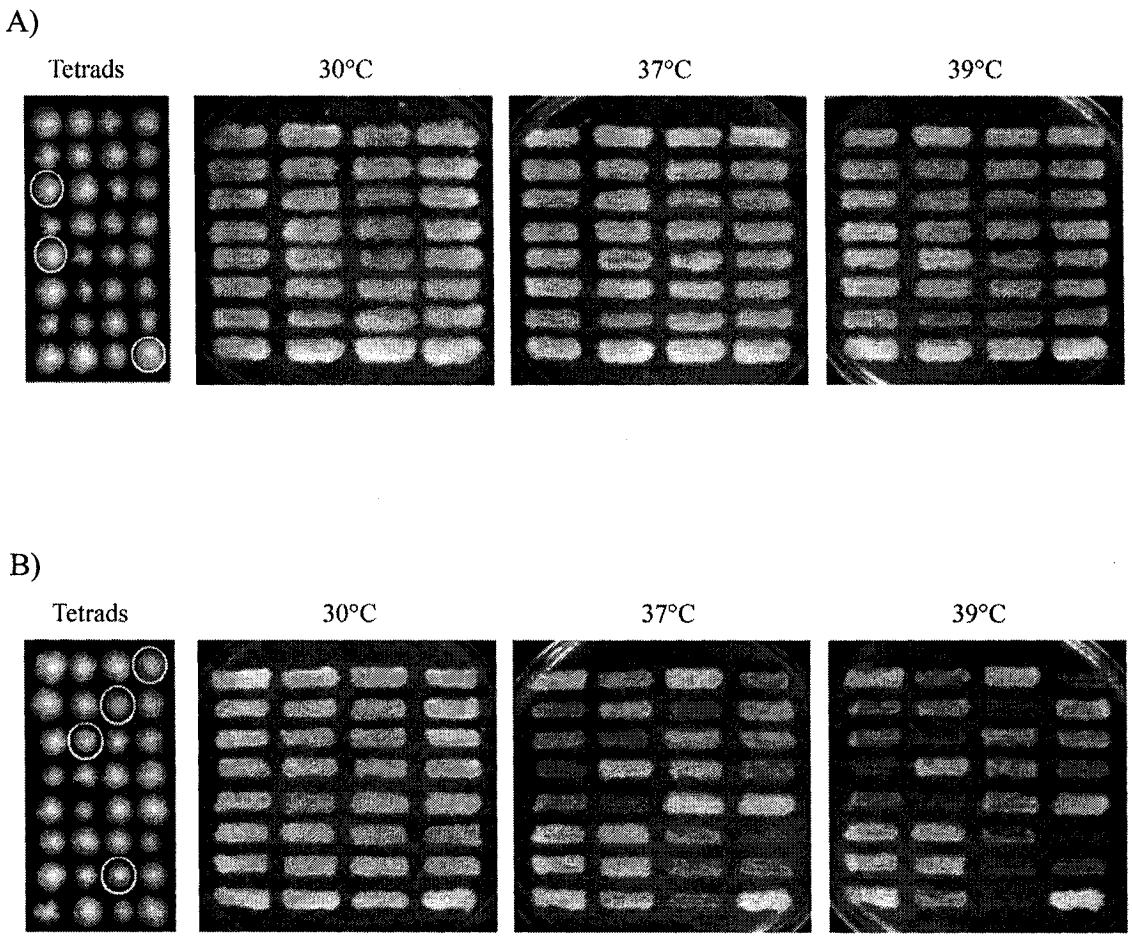

Figure 32. No deleterious genetic interaction between *spt16-E857K* and *nap1Δ*, but a deleterious genetic interaction does exist between *spt16-E763G* and *nap1Δ*. A) All segregants from tetrad analysis of a diploid heterozygous for *spt16-E857K* and *nap1Δ* were patched in the same pattern onto YEPD solid medium at 30°C, and replica-plated to YEPD for incubation at 30°C, 37°C and 39°C. The double-mutant segregants (outlined by circles) grew no differently than either single mutant at any of the temperatures. B) The same analysis was performed for the segregants of a cross between *spt16-E763G* and *nap1Δ*. The double-mutant segregants displayed temperature-sensitive growth, growing well at 30°C but poorly at 37°C and 39°C.

that Vps75 has preference for H3–H4 tetramers over H2A–H2B dimers (Selth, Svejstrup 2007). Because of the similarity to Nap1, I decided to examine whether genetic interactions exist between *VPS75* and *SPT16*.

To assess whether a genetic interaction exists, tetrad analysis was carried out. Cells containing the *spt16-E857K* mutation were crossed with *vps75Δ* cells, the resulting diploids were sporulated, and the haploid spore products assessed for growth defects. This analysis produced *spt16-E857K vps75Δ* double-mutant haploids that grew either reasonably well or quite poorly, suggesting the presence of an unmarked mutation that is affecting the growth rate (Figure 33). This prospective unmarked mutation either functions as a suppressor, masking the deleterious genetic interaction between *spt16-E857K* and *vps75Δ*, or as an enhancer, increasing the severity of the genetic interaction between *spt16-E857K* and *vps75Δ*. Thus, while a deleterious genetic interaction may exist between these two mutations, it is difficult to determine the extent of this interaction without further investigations.

A similar situation arose in the analysis of *spt16-E763G vps75Δ* double-mutant segregants, although the poorly growing double-mutant segregants from this cross were not as impaired as the poorly growing *spt16-E857K vps75Δ* double mutants (Figure 34). Thus, if there is a deleterious genetic interaction between *spt16-E763G* and *vps75Δ*, this interaction is less severe than that of *spt16-E857K*. This is in sharp contrast to the results observed with *nap1Δ* cells, which show a deleterious genetic interaction only with *spt16-E763G*. Thus, although Vps75 shares homology with Nap1 (Selth, Svejstrup 2007), deletions of *VPS75* and *NAP1* behave differently when combined with *spt16-E763G* or *spt16-E857K*, indicating different roles for the Vps75 and Nap1 proteins.

Thus, both *spt16-E857K* and *spt16-E763G* demonstrate deleterious genetic interactions with mutations in genes encoding histone chaperones, indicating a functional overlap between Spt16 and other histone chaperones. These studies have also shown that the E857K and E763G substitutions affects different aspects of Spt16 function, since *spt16-E857K* cells have deleterious genetic interactions with mutations in different histone chaperone genes than *spt16-E763G* cells. The *nap1Δ* findings are of particular interest, since Nap1 and Spt16, unlike other histone chaperones, both mediate the removal of H2A–H2B dimers during transcription (Belotserkovskaya et al. 2003,

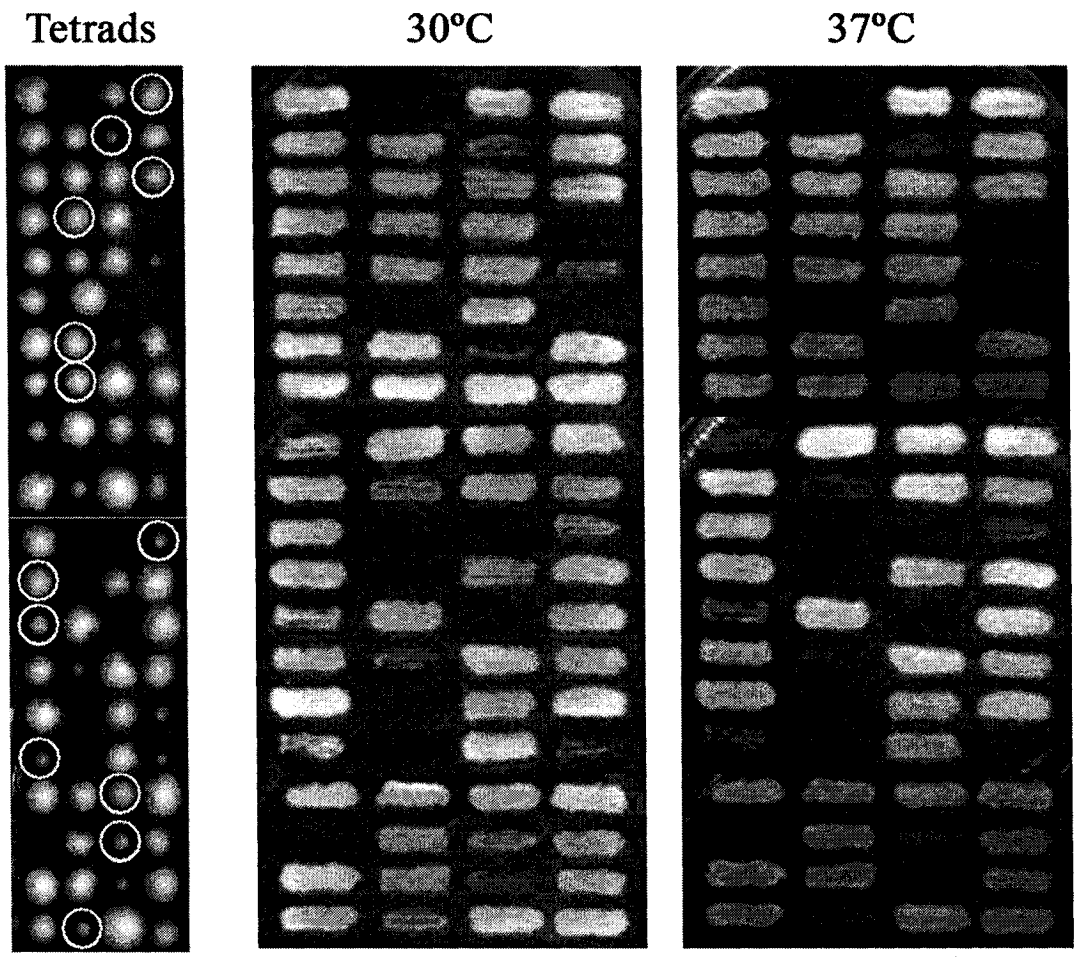

Figure 33. Lack of deleterious genetic interactions between *spt16-E857K* and *vps75Δ*. Diploid cells heterozygous for *spt16-E857K* and *vps75Δ* were sporulated, and tetrad analysis was carried out. The *spt16-E857K* G418-resistant (*kanMX4*) double-mutant segregants are outlined by the white circles, and all segregants were patched in the same pattern for analysis of growth at 30°C and 37°C. Further analysis showed that two *kanMX4* cassettes segregated in this cross; therefore, PCR analysis was performed on six of the double mutants (1D, 2C, 8B, 11D, 12A and 13A) to determine which contain *vps75Δ::kanMX4*. All six were found to have this deletion/replacement. As half of these double-mutant cells grew more poorly than either single mutant, while the other half had no observable growth defects, it is difficult to determine whether a growth impairment exists between *spt16-E857K* and *vps75Δ*.

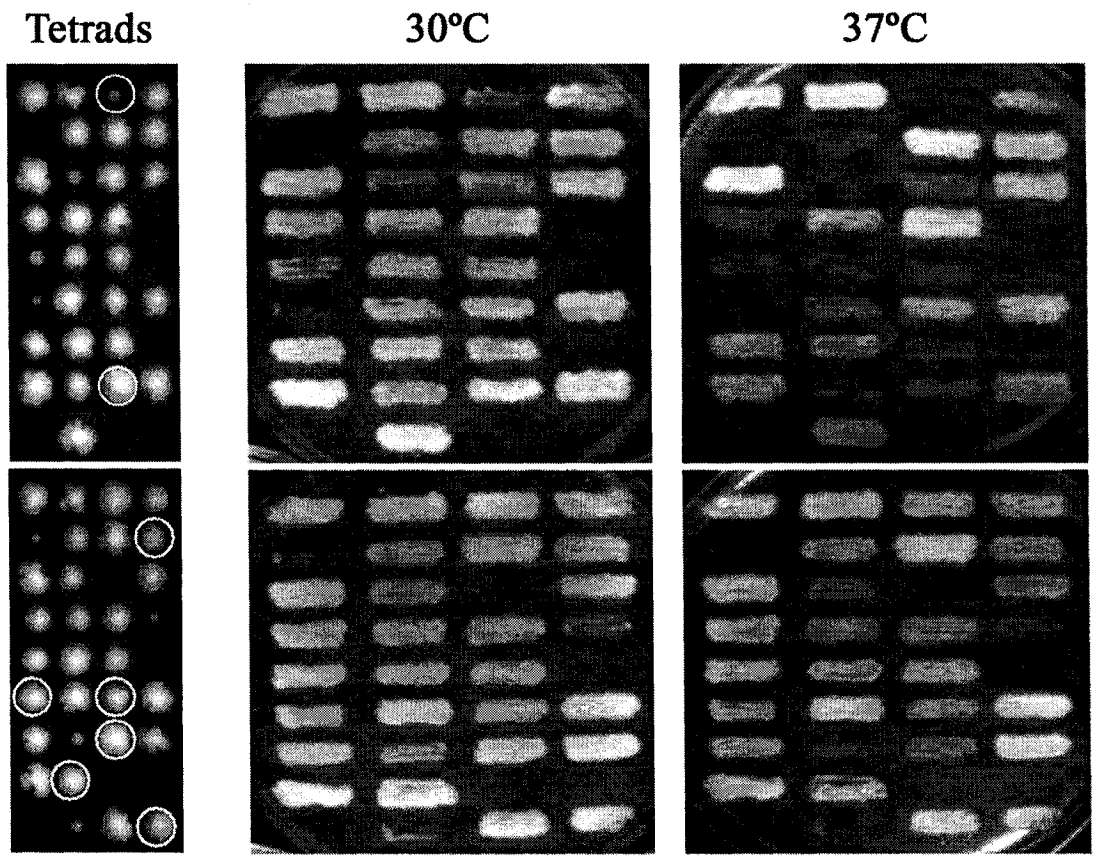

Figure 34. Lack of deleterious genetic interactions between *spt16-E763G* and *vps75Δ*. Diploid cells heterozygous for *spt16-E763G* and *vps75Δ* were sporulated, and tetrad analysis was carried out. The *spt16-E763G* G418-resistant (*kanMX4*) double-mutant segregants are outlined by the white circles, and all segregants were patched in the same pattern for analysis of growth at 30°C and 37°C. Further analysis showed that two *kanMX4* cassettes segregated in this cross; therefore, PCR analysis was performed on six of the double mutants (1C, 8C, 10D, 14A, 14C and 15C) to determine which contain *vps75Δ::kanMX4*. All six were found to have this deletion/replacement. Some of these double-mutant cells grew more poorly than either single mutant, but this poor growth is not limited to the double mutants and not all double mutants grow poorly. Therefore, there is no growth impairment between *spt16-E763G* and *vps75Δ*.

Levchenko, Jackson & Jackson 2005, Levchenko, Jackson 2004, Lorch, Maier-Davis & Kornberg 2006). That *spt16-E857K nap1Δ* cells do not exhibit any deleterious genetic interactions suggests that Spt16 and Nap1 mediate a common process, and that this process is impaired by the E857K substitution. The deleterious genetic interaction that exists between *spt16-E763G* and *nap1Δ* would therefore mean that the E763G substitution does not affect this common process. I have shown that Spt16-E857K co-immunoprecipitates histone H2B less effectively than normal Spt16, whereas Spt16-E763G shows no impairment (described below in Section 3.7.2.1). Thus, perhaps the *spt16-E857K* mutation encodes a version of Spt16 with impaired histone chaperone activity for H2A–H2B dimers, thereby affecting the same 'pathway' as a deletion of *NAP1*. This may explain the observed deleterious genetic interactions between *spt16-E857K* and deletions of genes encoding other histone chaperone such as Asf1 and Rtt106, which have binding preference for histones H3 and H4 (English et al. 2005, Huang et al. 2005), as these mutations would affect different functional pathways.

3.4 Genetic Interactions with Transcription Elongation Components

The existence of two distinct groups of *spt16* mutant alleles with respect to genetic interactions led to further investigations of two of these alleles: the *spt16-E763G* and *spt16-E857K* mutations. These mutations were chosen because they are single point mutations that represent the two 'classes' of *spt16* alleles with respect to genetic interactions with *BUR2* and the *HIR* genes.

A Synthetic Genetic Array (SGA) analysis had already been performed using chromosomally integrated forms of these alleles to obtain a more complete set of synthetic interactions (O'Donnell 2004). SGA analysis using the *spt16-E763G* allele yielded a different, virtually non-overlapping, set of genetic interactions compared to those found for *spt16-E857K*, suggesting that FACT mutations with the same initial phenotype can lead to radically different requirements for other gene products (O'Donnell 2004). However, the absence from these SGA results of certain synthetic-lethal interactions for *spt16-E857K*, such as that shown here for *hir1Δ*, indicated that there was a non-negligible incidence of false negatives associated with this high-throughput screening method. In addition, several gene deletions, among them *bur2Δ*, are routinely

false positives in SGA screening for reasons such as slow growth, poor mating, or poor sporulation (Tong et al. 2001). In all, SGA analysis is thought to miss between 17 and 41% of true genetic interactions (Tong et al. 2001, Tong et al. 2004). Thus, genes that are shown to have no interactions with the query mutation in SGA screening may demonstrate an interaction when analysed directly. In this light, I chose a number of gene deletions that did not come through the previous SGA screen for direct testing using standard genetic procedures, based on the synthetic-lethal genetic interactions for *spt16-E857K* identified here and cellular actions of the proteins encoded by these interacting genes. This directed testing was performed for both *spt16-E857K* and *spt16-E763G* to ensure that the differences observed between these two alleles in SGA analysis were due to biological reasons, rather than technical ones. Additionally, point mutations in several essential genes were assessed for genetic interactions with these *spt16* mutant alleles using this directed approach, as these genes are not represented in the deletion collection.

3.4.1 Interactions with Bur Kinase

As described above, both the 'classical' synthetic-lethal screening procedure described here and directed random-spore testing using the *bur2Δ* strain from the SGA deletion collection demonstrated that *spt16-E857K* is synthetic-lethal with the *bur2* frameshift mutant allele (*bur2-FS1*), whose identification and characterization is described above in Section 3.1.2.2, and with *bur2Δ* (as is *spt16-319*, but not *spt16-E763G* or *spt16-312*). The Bur2 protein is the regulatory subunit of the Bur kinase (Bur1 is the catalytic subunit); deletion of *BUR2* results functionally in decreased Bur1 activity (Yao, Neiman & Prelich 2000). Since the phenotype of a *bur2Δ* cell is abrogated by *BUR1* overexpression (Yao, Neiman & Prelich 2000), I decided to test whether the synthetic lethality between *spt16-E857K* and *bur2-FS1* (in cells with a chromosomal *BUR1* gene) could be alleviated by a *BUR1* plasmid. Indeed, this synthetic lethality was alleviated by additional Bur1 protein expressed from a low-copy plasmid, but not by several mutant versions (Keogh, Podolny & Buratowski 2003) of Bur1 protein expressed in the same way, indicating that significant Bur1 activity is required to abrogate these negative effects of *bur2-FS1* (Figure 35).

One possible reason for the inability of the Bur1 mutants to alleviate synthetic lethality between *spt16-E857K* and *bur2-FS1* is that these mutant alleles may not

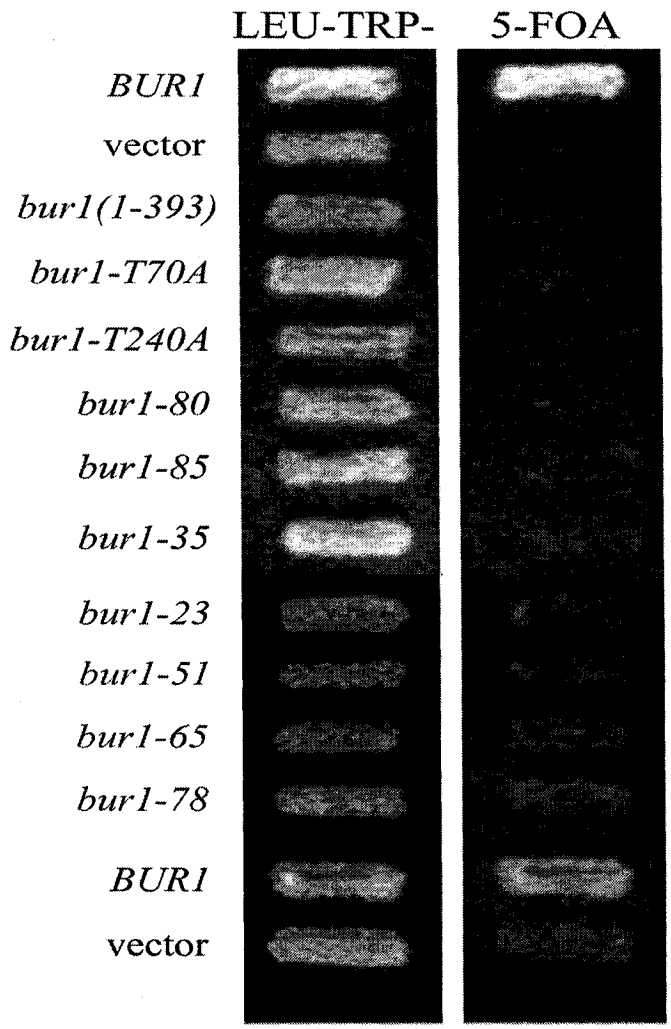

Figure 35. *BUR1*, but not *bur1* mutant alleles, suppresses the synthetic lethality between *bur2-FS1* and *spt16-E857K*. The indicated *BUR1* and *bur1* mutant alleles (on pRS315-based plasmids) were transformed into cells of strain SYNL #16 (*bur2-FS1*). Transformants were patched on Leu-Trp- solid medium, and replica-plated to Leu-Trp- and 5-FOA solid media to assess the growth of derivatives lacking pSLCDC68 (*SPT16 URA3*); growth on 5-FOA indicates alleviation of the synthetic-lethal phenotype. Only the *BUR1* plasmid suppressed the synthetic lethality in SYNL #16.

abrogate the *bur2Δ* phenotype itself. To determine whether this is the case, several of these *bur1* mutant alleles were transformed into cells of a *bur2Δ BUR1* strain, and the resulting transformants were assessed by serial-dilution spot testing to determine whether these plasmids alleviate the *bur2Δ* slow-growth phenotype (Figure 36). The effects observed here were subtle; however, they did demonstrate that several of the *bur1* mutant alleles were able to overcome the *bur2Δ* slow-growth phenotype, even though they were unable to alleviate the synthetic lethality between *bur2-FS1* and *spt16-E857K*. Therefore, while these mutant versions may provide enough Bur1 function to overcome some of the deleterious effects of a *BUR2* deletion, they are unable to compensate for the additional effects caused by the *spt16-E857K* mutation.

Interestingly, two of the *bur1* mutant alleles, *bur1(1-393)* and *bur1-T240A*, actually inhibited the growth of the *bur2Δ* cells, indicating dominance of these *bur1* mutant alleles over the chromosomal *BUR1* allele. These *bur1* mutant alleles are the only ones among the alleles tested that display a cold-sensitivity phenotype at 12°C when they are the only version of *BUR1* in the cell, with *bur1(1-393)* having a more severe growth defect than *bur1-T240A* (Keogh, Podolny & Buratowski 2003). Overproduction of Bur2 can suppress the cold sensitivity of *bur1-T240A* but not that of *bur1(1-393)* (Keogh, Podolny & Buratowski 2003). The significance of why only these *bur1* alleles inhibit growth of the *bur2Δ* cells is unclear, although it is possible that the Bur1 proteins encoded by these two mutant alleles may have some interference with the normal Bur1 present in the cell. The *bur1(1-393)* mutation eliminates the C-terminal portion of the Bur1 protein, which is of unknown function. While Bur1(1-393) causes no Spt phenotype and has been shown to have full kinase activity *in vitro*, it demonstrates decreased association with a transcribed region (Keogh, Podolny & Buratowski 2003). This observation suggests that Bur1(1-393) protein may function less effectively during transcription, although this may simply reflect decreased cross-linking of the truncated protein. Perhaps the Bur1(1-393) mutant protein, lacking its C terminus, is able to associate with some other proteins required for Bur1 function, yet be unable to associate effectively with transcribed regions. Thus, the mutant Bur1 may titrate this protein away from the normal Bur1 protein present in the cell, thereby decreasing the activity of normal Bur1. The *bur1-T240A* mutation alters a proposed activating phosphorylation site;

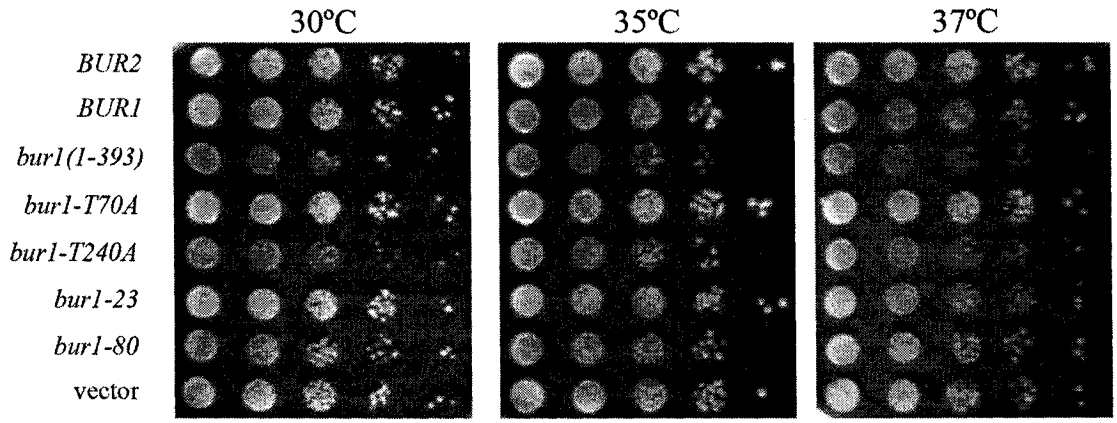

Figure 36. Effect of various *BUR1* and *bur1* mutant alleles in a *bur2Δ* strain. Cells of the deletion-collection *bur2Δ* strain (Tong et al. 2001) were transformed with the indicated *BUR1* alleles, and also *BUR2* and empty vector controls, all on *LEU2 CEN* vectors. Transformants were grown in liquid culture, and 10-fold serial dilutions were spotted onto Leu- solid medium and incubated for 4 days at the indicated temperatures. Cells harbouring the *BUR2*, *BUR1*, *bur1-T70A*, *bur1-23* and *bur1-80* plasmids grew slightly better than those with empty vector, indicating an alleviation of the *bur2Δ* growth defect. Exceptions were cells with the *bur1(1-393)* and *bur1-T240A* alleles, which actually grew somewhat worse than those with empty vector, indicating a dominant negative effect over the chromosomal *BUR1* allele. Interestingly, these two alleles are the only two with reported cold-sensitive phenotypes (at 12°C), although the functional significance of this observation is unclear.

cells containing *bur1-T240A* exhibit an Spt phenotype, and Bur1-T240A protein demonstrates decreased kinase activity *in vitro*, yet has normal association with transcribed regions (Keogh, Podolny & Buratowski 2003). The Bur1-T240A mutant protein may therefore be able to associate with phosphorylation targets of Bur1, yet be unable to phosphorylate these proteins, thus decreasing the rate at which this phosphorylation occurs.

Since the effect of a *bur2Δ* deletion is decreased Bur1 activity (Yao, Neiman & Prelich 2000), I decided to test directly several mutant versions of *BUR1* for synthetic lethality with *spt16-E857K* and *spt16-E763G*. These tests were done using a plasmid-shuffling approach. First, *spt16Δ bur1Δ* strains were created that contained *SPT16* on a *URA3* plasmid and an allele of *BUR1* on a *LEU2* plasmid (*BUR1* is an essential gene, so a functioning *BUR1* or *bur1* gene has to be present). The *spt16* mutant alleles, on *TRP1* plasmids, were then transformed in and the transformants were assessed for the ability to produce derivatives lacking the *SPT16 URA3* plasmid and therefore able to grow on medium containing 5-FOA (Figure 37). This assessment showed that in no case did actual synthetic lethality result from any of the combinations of *spt16* and *bur1* alleles. However, cells with the combination of *spt16-E857K* and *bur1-23* grew less well than did cells with any of the other combinations, suggesting a slow-growth interaction between these mutant alleles. To further investigate this possibility, and to determine whether any of the other combinations of mutations also produce subtle genetic interactions, serial-dilution spot testing was done for the double-mutant cells. By this more sensitive approach, several of the *bur1* mutant alleles showed deleterious genetic interactions with *spt16-E857K*, but not with *spt16-E763G* (Figure 38). In particular, cells carrying *bur1-T240A*, a mutation that eliminates an activating phosphorylation site, or *bur1-23*, one of the temperature-sensitive mutations of *BUR1*, are further impaired when they also contain the *spt16-E857K* allele in place of wild-type *SPT16*. Both of the *bur1* alleles that demonstrated synthetic interactions with *spt16-E857K* have been shown to result in decreased Bur kinase activity; conversely, several alleles reported to have no decrease in kinase activity (*bur1(1-393)*, *bur1-T70A* and *bur1-80*) also demonstrated no deleterious genetic interactions with *spt16-E857K*. These results, combined with the *bur2Δ* findings,

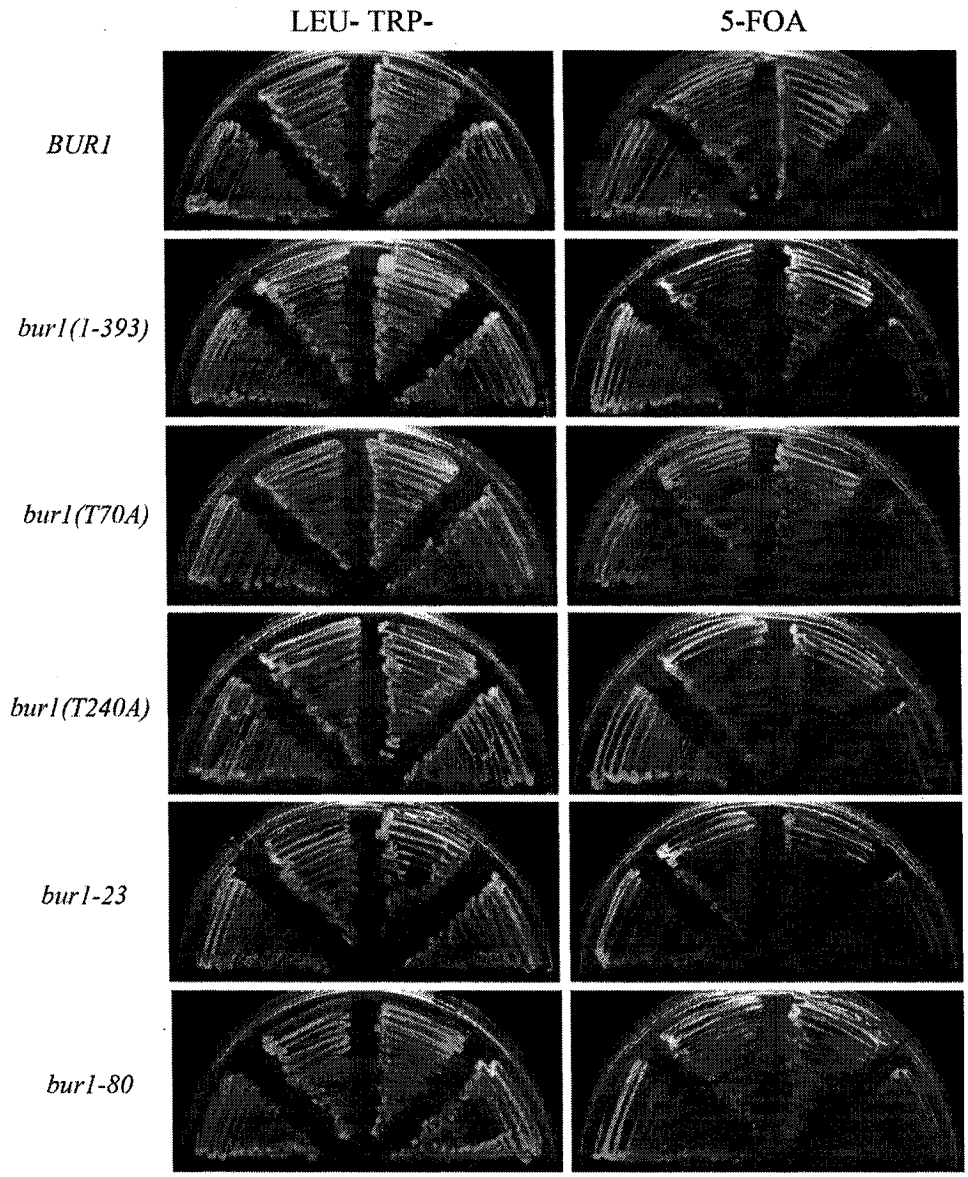

Figure 37. Deleterious genetic interactions between *spt16* and *bur1*. Cells of strains containing the indicated plasmid-borne *BUR1* or *bur1* allele and pRS316-A4 (*SPT16 URA3*) were transformed with pRS314 plasmid containing (clockwise from left for each plate) *SPT16*, *spt16-E763G*, *spt16-E857K*, or empty vector. Transformants were plated on Leu-Trp- and 5-FOA solid media and incubated at 30°C (growth on 5-FOA medium indicates the ability to survive in the absence of pRS316-A4). In all cases, both *spt16-E763G* and *spt16-E857K* permitted growth on 5-FOA, indicating a lack of severe genetic interactions between these *spt16* alleles and the mutant alleles of *BUR1*. However, the *spt16-E857K bur1-23* double-mutant cells did not grow as well on 5-FOA as did *SPT16 bur1-23* cells. Thus, there may be some synthetic impairment for this allele combination.

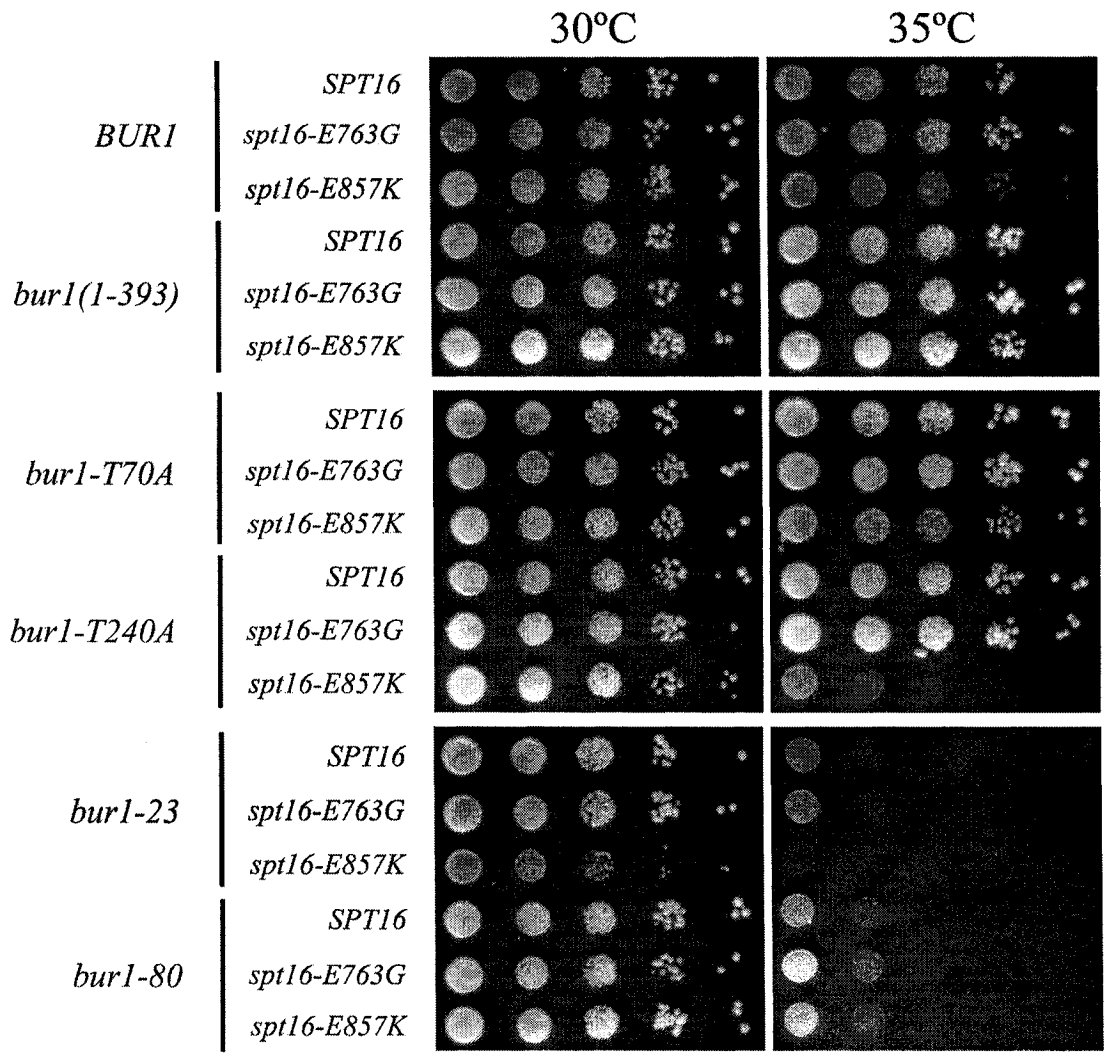

Figure 38. Deleterious genetic interactions between *spt16-E857K* and *bur1*. Cells were grown in liquid culture to stationary phase, 10-fold serial dilutions were spotted onto Leu-Trp- solid medium and incubated at the indicated temperature for 3 (35°C) or 4 (30°C) days. Deleterious genetic interactions were evident between *spt16-E857K* and *bur1-T240A* at 35°C, and between *spt16-E857K* and *bur1-23* at both temperatures. No deleterious genetic interactions are observed for any of the *bur1* alleles in combination with the *spt16-E763G* mutation.

lend support to the hypothesis that synthetic lethality is the result of decreased phosphorylation of at least one Bur-kinase target *in vivo*.

It has been suggested that Bur kinase may be a yeast orthologue of P-TEFb (Wood, Shilatifard 2006), which is a kinase that mediates transcription elongation by phosphorylation of RNAPII on serine 2 of its C-terminal domain (CTD) repeat (Marshall et al. 1996, Price 2000, Ramanathan et al. 2001). However, this possibility is complicated by the fact that another kinase, CTDK-1, has also been identified as a potential yeast P-TEFb orthologue (Lee, Greenleaf 1997, Wood, Shilatifard 2006). Although both of these kinases have been identified as possible orthologues of P-TEFb, it has been suggested that Bur kinase and CTDK-1 do not have the same phosphorylation targets *in vivo* (Cho et al. 2001, Keogh, Podolny & Buratowski 2003, Murray et al. 2001, Patturajan et al. 1999). To determine whether analogous synthetic lethality exists between alterations in Spt16 and in CTDK-1, I used cells that were missing Ctk1, the kinase subunit of CTDK-1. I crossed *spt16-E857K* cells with *ctk1Δ* cells and performed tetrad analysis on the meiotic products. Unlike the results with *bur2Δ* cells, no synthetic lethality was observed between *spt16-E857K* and *ctk1Δ*. This result provides further evidence for the idea that, while both Bur kinase and CTDK-1 phosphorylate serine 2 of the RNAPII CTD *in vitro*, they do not have the same *in vivo* targets.

3.4.2 Interactions with Potential Bur Kinase Targets

One target of Bur kinase is Rad6, an E2 ubiquitin-conjugating enzyme (Jentsch, McGrath & Varshavsky 1987), which ubiquitinates histone H2B on Lys123 (Wood et al. 2005). The PafC complex, a transcription elongation complex that associates with genes transcribed by RNAPII (Rondon et al. 2004, Rosonina, Manley 2005), aids the recruitment of Rad6, and the resulting ubiquitin mark on K123, along with PafC itself, aids in the recruitment of the COMPASS complex (Dover et al. 2002, Krogan et al. 2003a, Wood et al. 2003). The recruitment of COMPASS then leads to histone H3 trimethylation on lysine 4 (K4) (Krogan et al. 2002), a hallmark of actively transcribed regions (Ng et al. 2003, Santos-Rosa et al. 2002). Thus, one potential reason for synthetic lethality between *spt16-E857K* and *bur2Δ* would be the impairment of this histone-methylation pathway in cells lacking Bur2 or with defective Bur1 kinase.

If the impairment of this H3K4 methylation pathway is involved in the observed synthetic lethality between *spt16-E857K* and *bur2Δ*, then mutations in any of the members of the pathway should also result in analogous synthetic genetic interactions. To test this possibility, I created *spt16-E857K* strains with deletions of several genes in this ubiquitination–methylation pathway, including *rad6Δ* itself, and *swd1Δ* and *swd3Δ* (eliminating members of COMPASS). Swd1 and Swd3 form a heterodimer within COMPASS, and deletion of either one reduces the stability of the Set1 protein (the histone methyltransferase), as well as of the COMPASS complex (Dehe et al. 2006). Strains deleted for *SWD1* or *SWD3* do not exhibit methylation of H3K4, indicating that each of the gene products is required for COMPASS activity (Krogan et al. 2002, Schneider et al. 2005).

Initial investigations suggested that there might be a genetic interaction between *spt16-E857K* and *rad6Δ*, for several of the double-mutant derivatives that were obtained grew more poorly than either parental strain (Figure 39). However, not all of the double-mutant segregants behaved the same way, with these segregants displaying two levels of growth; additionally, the parental *rad6Δ* strain was not temperature-sensitive, as *rad6Δ* cells have been reported to be (Ellison et al. 1991). These observations suggested that the *rad6Δ* parental strain might contain a suppressor mutation that alleviates the temperature sensitivity. It was reasonable to expect that the *spt16-E857K* strain would not contain this suppressor mutation, and therefore the heterozygous diploid created upon mating these two strains would also be heterozygous for this supposed suppressor mutation. If this were the case, the poor growth of some of the *spt16-E857K rad6Δ* double-mutant derivatives may then simply reflect the growth effects of the *rad6Δ* deletion itself. To determine whether the putative synthetic impairment between *spt16-E857K* and *rad6Δ* simply reflected the growth of *rad6Δ* cells that were no longer suppressed for *rad6Δ* effects, I tested several *rad6Δ* single-mutant segregants from the same genetic cross. These segregants also displayed two levels of growth, with the poorly growing *rad6Δ* segregants behaving similarly to the poorly growing *spt16-E857K rad6Δ* double mutants (Figure 39). This finding suggests that the *rad6Δ* strain in the deletion collection does indeed harbour a suppressor mutation, and that the impaired growth observed for some of

A)

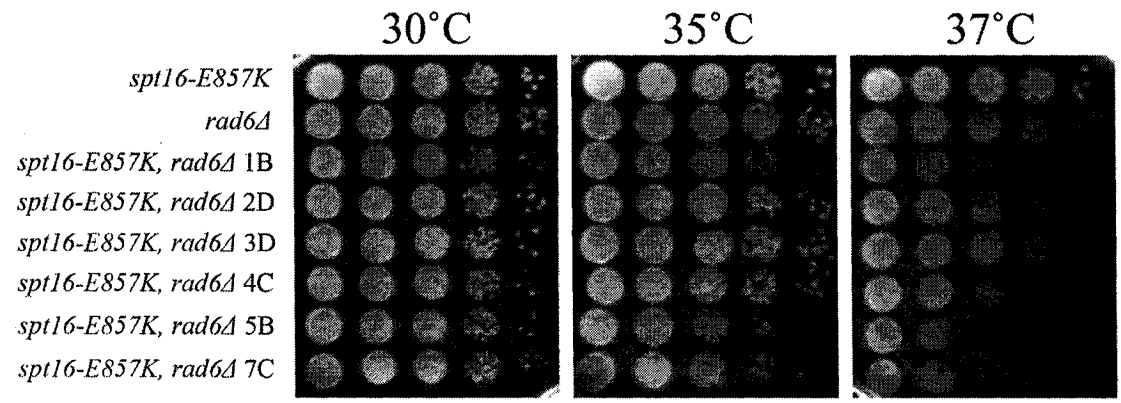

B)

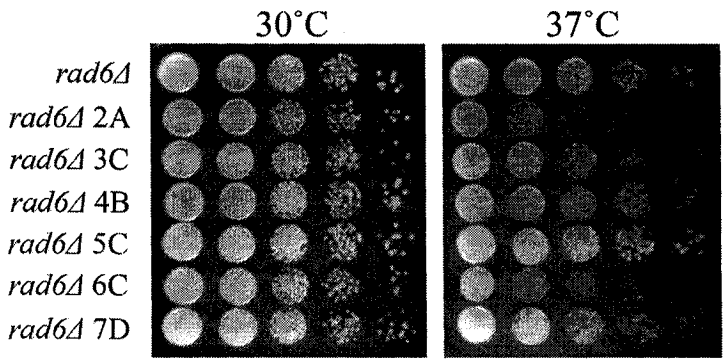

Figure 39. The apparent deleterious genetic interaction between *spt16-E857K* and *rad6Δ* is the result of a suppressor in the *rad6Δ* strain. A) 10-fold serial dilutions of *spt16-E857K rad6Δ* double mutants (and parental strains) were spotted on YEPD solid medium and incubated at the indicated temperature for two days. B) 10-fold serial dilutions of the *rad6Δ* parent and six *rad6Δ* segregants were spotted on YEPD solid medium and incubated for two days at the indicated temperatures. The distribution of poor-growing and well-growing segregants at 37°C is consistent with a single-site suppressor. Also, the growth of the poorer-growing segregants is the same as that of the unsuppressed double mutants in part A. Thus, there is no interaction between *spt16-E857K* and *rad6Δ*.

the *spt16-E857K rad6Δ* double mutants in fact results simply from the loss through genetic segregation of this suppressor mutation.

The absence of deleterious genetic interactions evident in *spt16-E857K rad6Δ* cells was mirrored by the lack of evident genetic interactions between *spt16-E857K* and the *swd1Δ* and *swd3Δ* deletions affecting the COMPASS complex (Figure 40). These findings therefore suggest that a role of the Bur kinase complex other than Rad6-mediated ubiquitination leading to H3K4 methylation is important for the deleterious genetic interactions between *spt16-E857K* and Bur-kinase mutations.

While there is no evidence to suggest that the *spt16-E857K* mutation has any effect on histone H3 lysine 4 trimethylation, another possibility for the lack of genetic interactions between *spt16-E857K* and *rad6Δ*, *swd1Δ* and *swd3Δ* is that the *spt16-E857K* mutation itself causes impairment of this histone methylation pathway. If so, then no further impairment might be expected in the double-mutant situations described above. To test the possibility that the *spt16-E857K* mutation affects histone H3K4 trimethylation, I measured the levels of H3K4 trimethylation in whole cell extracts from cells containing either normal Spt16 or the Spt16-E857K mutant protein (Figure 41). These western blots showed no difference in the levels of H3K4 trimethylation between cells containing normal or mutant Spt16, indicating that this pathway is indeed functioning properly in cells containing the *spt16-E857K* mutation. Thus, the H3K4 trimethylation function of Bur kinase is not involved in the functional interactions seen between Bur kinase and the Spt16-E857K mutant component of FACT; there must be another role of Bur kinase that is involved in this functional interaction.

Another potential target of Bur kinase is the Spt4–Spt5 complex, which is also involved in transcription elongation (Hartzog et al. 1998, Wada et al. 1998). The Spt5 protein contains tandem repeats in its C terminus (Swanson, Malone & Winston 1991), which in other systems have been shown to be targets for phosphorylation by Bur1 analogs (Bourgeois et al. 2002, Ivanov et al. 2000, Kim, Sharp 2001, Pei, Shuman 2003, Yamada et al. 2006). While a study of Spt5 protein interactions did not yield Bur1 (Lindstrom et al. 2003), it is possible that this interaction is transient and thus would not be identified in this manner. This same study did, however, identify Spt16 as co-immunopurifying with Spt5, and therefore provided an incentive to evaluate genetic

spt16-E857K X *swd1Δ*

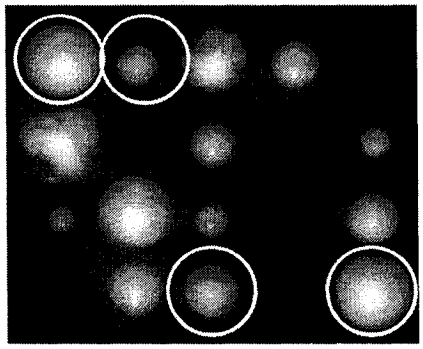

spt16-E857K X *swd3Δ*

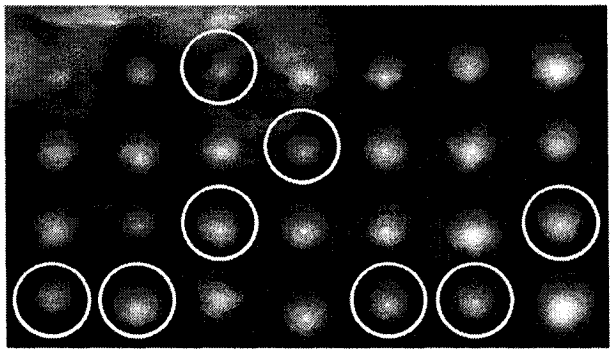

Figure 40. Lack of synthetic lethality between *spt16-E857K* and *swd1Δ* or *swd3Δ*. Diploids heterozygous for *spt16-E857K* and *swd1Δ* or *swd3Δ* were sporulated, and tetrad analysis was performed. The double-mutant segregants are outlined by the white circles. In neither cross did the double-mutant cells grow any more poorly than any single mutant.

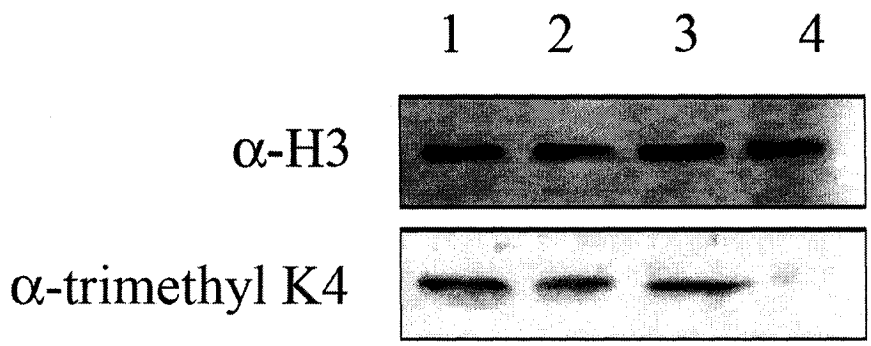

Figure 41. Neither *spt16-E763G* nor *spt16-E857K* mutant cells are impaired for trimethylation at histone H3 lysine 4. Equal amounts of whole cell extracts were resolved by 15% SDS-PAGE, transferred to PVDF, and probed with antibodies against total H3 (top panel) or H3 trimethylated at K4 (bottom panel). Lanes: 1 - *SPT16*, 2 - *spt16-E763G*, 3 - *spt16-E857K*, 4 - *swd3Δ*

interactions between *SPT16* and *SPT5*, regardless of whether Spt5 is a target of Bur kinase in *S. cerevisiae*. Therefore, I tested two mutant alleles of *SPT5* (*spt5-4* and *spt5-194*) for genetic interactions with *spt16-E857K*. The *spt5-194* allele was one of the originally isolated Spt mutations (Winston et al. 1984). The *spt5-4* allele also causes an Spt phenotype, and both *spt5-4* cells and *spt5-194* cells have demonstrated sensitivity to 6-azauracil, an analogue that interferes with transcription elongation (Hartzog et al. 1998). However, differences have also been observed between these two mutant alleles, as *spt5-4* cells produce prematurely terminated RNA from genes with internal but cryptic poly(A) sites, while *spt5-194* cells do not (Cui, Denis 2003).

Both of these *spt5* mutant alleles demonstrated genetic interactions with *spt16-E857K*, evidenced by enhanced temperature sensitivity (Figure 42). In addition, the *spt16-E857K spt5* double mutants were more sensitive to hydroxyurea than was either single mutant. Interestingly, these mutant alleles of *SPT5* also produced analogous enhanced temperature sensitivity when combined with *spt16-E763G*, although no hydroxyurea sensitivity was found for the *spt16-E763G spt5* double mutants (Figure 42). In fact, this situation is one of the few instances where these two *spt16* mutant alleles show similar genetic interactions. A possible reason for this is that both FACT and the Spt4–Spt5 complex are required for proper transcription, and that impairing both complexes, in a variety of ways, is enough to impair cell growth.

The fact that functional interactions with these *spt5* mutations exist for both *spt16-E857K* and *spt16-E763G* suggests that impairment of Spt5 function in *bur2Δ* cells may not be the reason for synthetic lethality between *bur2Δ* and *spt16-E857K*. If this were the case, then I would expect that the genetic interactions with *spt5* would be allele-specific for *spt16-E857K*, mimicking the interactions with *bur1* and *bur2* mutant genes. This interpretation does not rule out the possibility that Spt5 is a target of Bur kinase – it simply suggests that Spt5 may not be a target responsible for the observed synthetic lethality of *spt16-E857K* with *bur2Δ*.

Another interpretation, however, is that the impairment of Spt5 may indeed be responsible for the observed synthetic lethality between *bur2Δ* and *spt16-E857K*, but that the decreased phosphorylation by Bur kinase in these cells impairs a different aspect of Spt5 function than do the *spt5* mutant alleles that were directly tested. Synthetic lethality

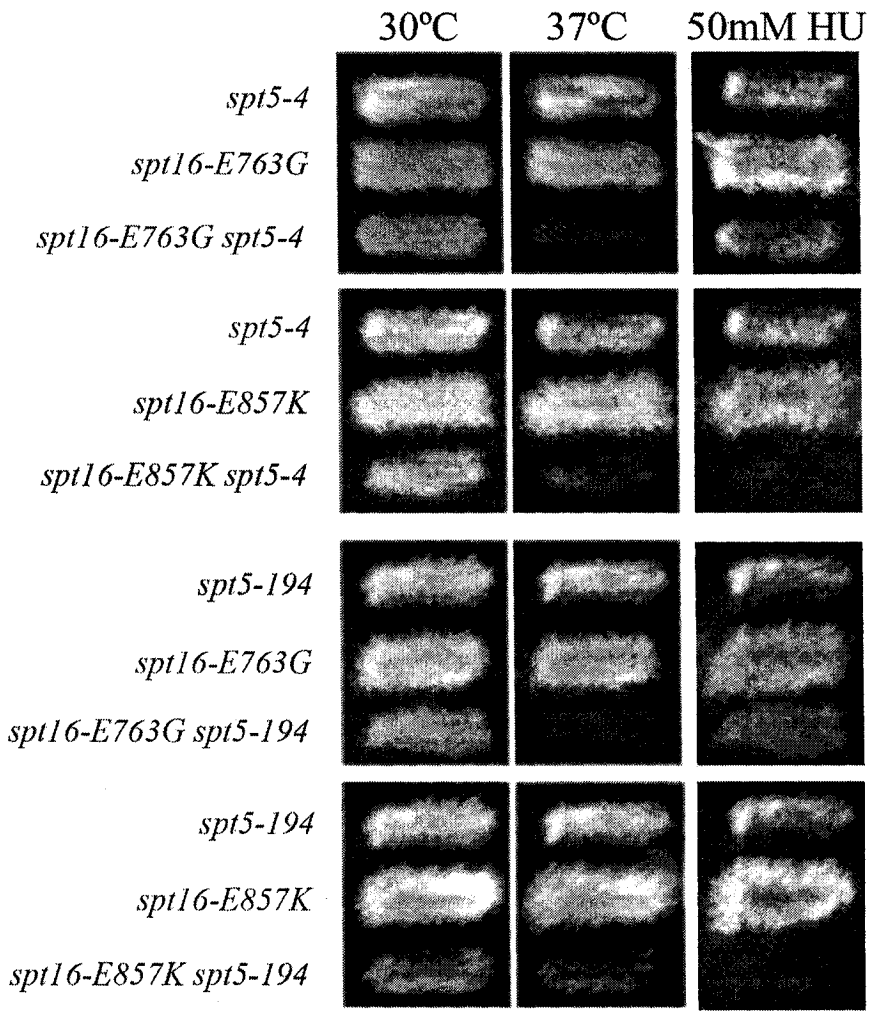

Figure 42. Deleterious genetic interactions between *spt16-E763G* or *spt16-E857K* and *spt5*. Replica plates of single and double mutants were incubated under the indicated conditions overnight (2 days for hydroxyurea [HU] plates at 30°C). While both *spt16-E763G* and *spt16-E857K* had deleterious genetic interactions with both *spt5* alleles, only the *spt16-E857K* double mutants demonstrated synthetic hydroxyurea sensitivity.

between mutations in two genes can indicate that these genes affect separate pathways. The idea here is that if a gene is deleted, its pathway is eliminated; an additional mutation affecting that pathway will not have an additive effect, whereas a mutation in a parallel pathway might. However, this interpretation may not always hold true when working with essential genes, as in this situation the effect of the absence of the gene products cannot be assessed, only that of mutated versions. Thus, while there are reported deleterious genetic interactions between *bur1-2* and *spt5-194* or *spt5-4* (Lindstrom, Hartzog 2001, Murray et al. 2001), that observation does not really help to determine whether Spt5 is a target of Bur kinase. Bur kinase and Spt5 could still mediate the same functional pathway, and decreasing the function of one or the other of these pathway components, but not both, might allow a reasonable level of activity for this pathway. Alternatively, they could mediate separate pathways and, again, decreasing the function of one or the other, but not both, might allow reasonable growth. Thus, it remains possible that impairment of Spt5 function by the effects of a *bur2Δ* deletion is responsible for the observed synthetic lethality between *spt16-E857K* and *bur2Δ*. This situation cannot be resolved without further knowledge about which aspect(s) of Spt5 function are affected by Bur kinase and which are impaired by the *spt5* mutations employed in my studies.

I also tested for genetic interactions between *spt16-E857K* and the *spt4Δ* deletion, which eliminates the binding partner of Spt5 (Hartzog et al. 1998, Wada et al. 1998), and found that there is indeed a synthetic slow-growth phenotype associated with these double mutants; additionally, these double mutants exhibited synthetic temperature sensitivity for growth (Figure 43). Synthetic temperature sensitivity was also observed between *spt16-E763G* and *spt4Δ*, yet this interaction was less severe than that for *spt16-E857K* and *spt4Δ* (Figures 44 and 45). Here again, there are differences in the effects of these two *spt16* mutant alleles. These differences may be due to the (uncharacterized) influence of Spt4 on Spt5 activity, and thus reflect the degree of impairment of Spt5 in the *spt4Δ* strains. This idea is consistent with my observations, since *spt16-E857K* causes greater genetic impairment with *spt4Δ* and the *spt5* mutations than does *spt16-E763G*.

To further pursue these investigations involving Spt4–Spt5, I created and assessed triple-mutant derivatives that contained mutations in *SPT4*, *SPT5* and *SPT16* (Figures 44

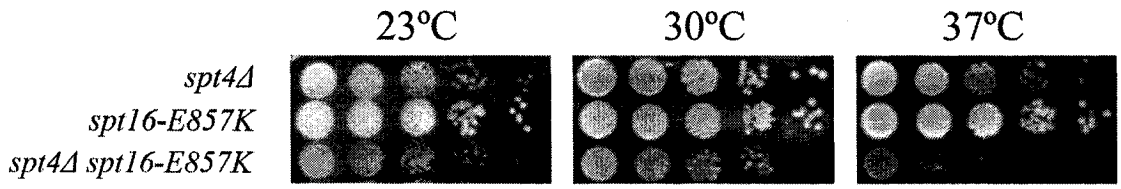

Figure 43. Deleterious genetic interactions between *spt16-E857K* and *spt4Δ*. 10-fold serial dilutions of *spt16-E857K spt4Δ* double mutants (and parental strains) were spotted on YEPD solid medium and incubated at the indicated temperature for two days. The *spt16-E857K spt4Δ* double mutants grew more poorly than either single mutant at all temperatures.

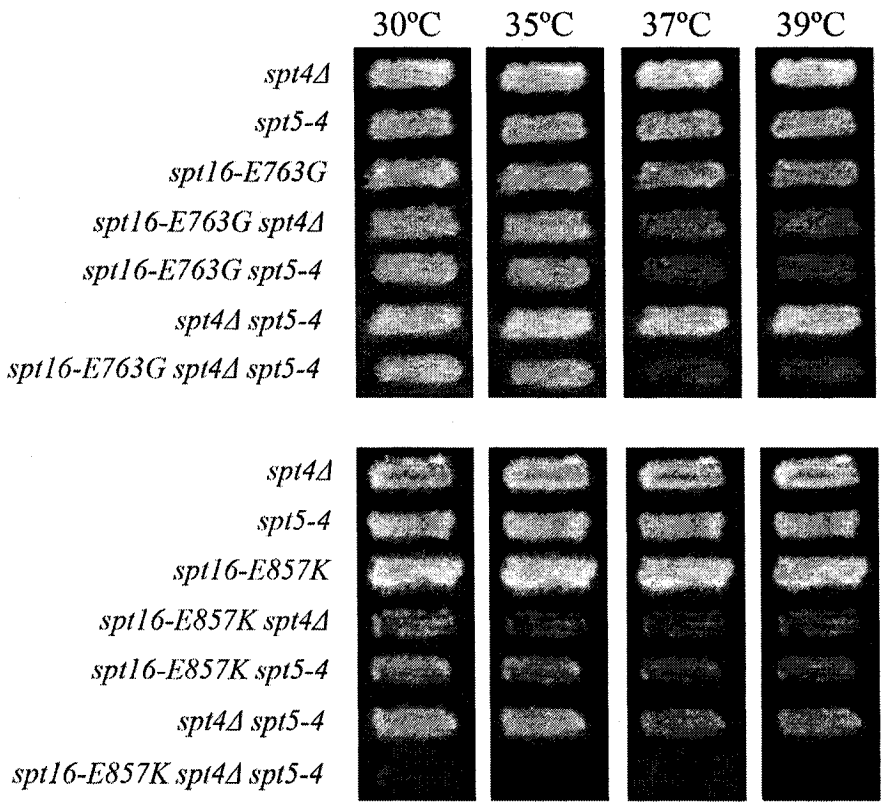

Figure 44. The deleterious genetic interaction between *spt16-E857K* and *spt5-4* is exacerbated by *spt4Δ*, but an analogous effect is not seen with *spt16-E763G*. Replica plates were incubated at the indicated temperature overnight. The *spt16-E763G spt4Δ spt5-4* triple mutants were no more impaired than either the *spt16-E763G spt4Δ* or *spt16-E763G spt5-4* double mutants. However, the *spt16-E857K spt4Δ spt5-4* triple mutants were significantly more impaired than either the *spt16-E857K spt4Δ* or *spt16-E857K spt5-4* double mutants, and grew poorly even at 30°C.

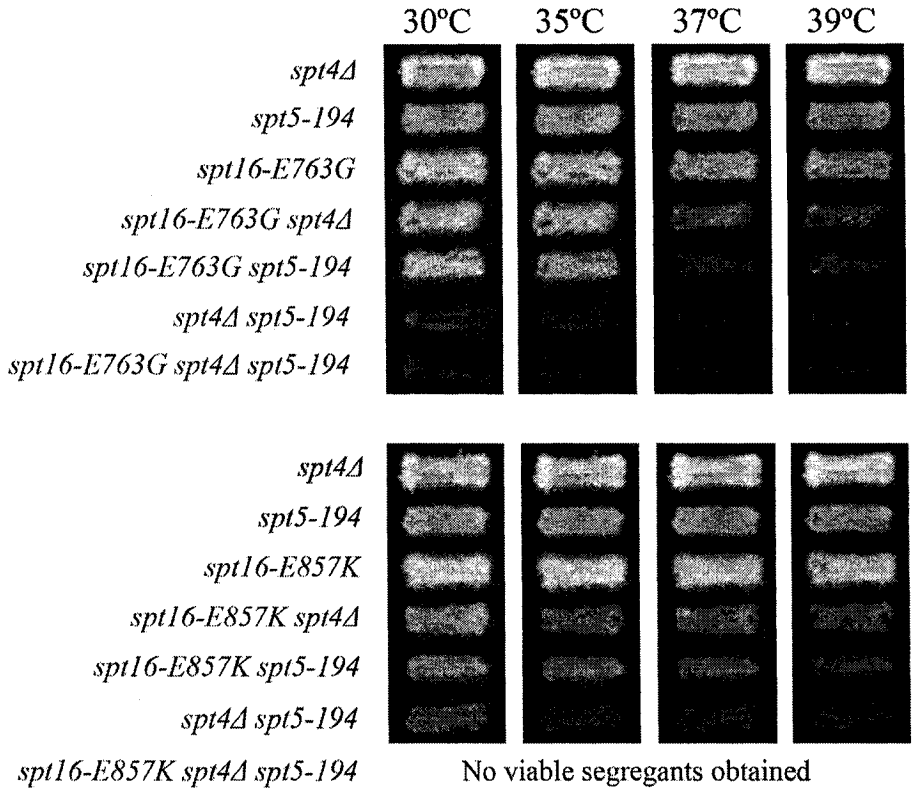

Figure 45. The deleterious genetic interaction between *spt16-E857K* and *spt5-194* is exacerbated by *spt4Δ*, but an analogous effect is not seen with *spt16-E763G*. Replica plates were incubated at the indicated temperature overnight. The *spt16-E763G spt4Δ spt5-1944* triple mutants were no more impaired than the *spt4Δ spt5-194* double mutants (these being the most severe of the double mutants). However, the *spt16-E857K spt4Δ spt5-194* triple mutants were significantly more impaired than the *spt4Δ spt5-194* double mutants. In fact, no viable triple mutants were obtained indicating lethality of these cells, whereas the *spt4Δ spt5-194* double mutant cells were merely severely growth impaired.

and 45). In neither case (with *spt5-4* or *spt5-194*) did the *spt16-E763G spt4Δ spt5* triple mutants grow more poorly than the worst combination of double mutants. In contrast, *spt16-E857K* triple mutants displayed much poorer growth with either *spt5-4* or *spt5-194* than any of the combinations of double mutants. In fact, no viable triple mutants were obtained from the *spt16-E857K spt4Δ spt5-194* combination, although every other combination of alleles yielded viable cells. The impaired growth observed for the triple mutants containing *spt16-E857K* may reflect the result of a possible decrease in Spt5 activity in these cells due to the absence of Spt4, or the absence of both Spt4-mediated and Spt5-mediated functions. If so, this situation does not appear to have any effect on the growth of the triple-mutant cells containing the *spt16-E763G* mutation, indicating that this effect is not conserved among mutations in *SPT16*. Thus, again, differences are observed between the behaviour of *spt16-E857K* and *spt16-E763G*. These differences in genetic interactions likely reflect differences in how these two alleles of *SPT16* are impaired, as the severity of genetic interactions with the same mutations in *SPT4* and *SPT5* differs between *spt16-E857K* and *spt16-E763G*.

3.4.3 Interactions with Members of PafC

Another possibility for the differences seen in *spt4Δ* and *spt5* genetic interactions between *spt16-E857K* and *spt16-E763G* may lie in the functional connection between Spt4–Spt5 and the PafC complex (Squazzo et al. 2002). PafC is a multi-subunit complex involved in both transcription initiation and elongation, consisting of the proteins Paf1, Cdc73, Leo1, Rtf1, and Ctr9 (Mueller, Jaehning 2002, Squazzo et al. 2002). PafC has been shown to localize throughout the coding regions of ORFs (Qiu et al. 2006), and the Spt4 protein is required for this PafC occupancy along ORFs and for PafC association with RNAPII (Qiu et al. 2006). Thus it has been suggested that Spt4, and perhaps also its binding partner Spt5, may serve as a platform to allow RNAPII recruitment of PafC (Qiu et al. 2006). The more severe interactions observed between *spt4Δ* and *spt16-E857K* may therefore indicate an effect on PafC rather than a direct effect on Spt5. If this were the case, I would expect that *spt16-E857K* would also display more severe genetic interactions with mutations eliminating PafC components than would *spt16-E763G*, mimicking the *spt4Δ* results.

Previous SGA analysis demonstrated deleterious genetic interactions between the *spt16-E857K* mutation and the PafC deletions *cdc73Δ* and *leo1Δ*, and between the *spt16-E763G* mutation and *cdc73Δ* (O'Donnell 2004). However, due to the limitations of performing genome-wide analyses, these were the only PafC deletions examined. In the strain collection that was used in that analysis, a *ctr9Δ* strain was not present, eliminating the ability of assessing interactions with this PafC subunit. An *rtf1Δ* strain was present, but the *RTF1* locus is located only 55 kbp away from the *SPT16* locus, and the resulting genetic linkage between these two loci decreases the frequency with which double-mutant segregants will by produced from a diploid heterozygous for mutations in these genes. Additionally, the *paf1Δ* strain is known to be a false positive in SGA analysis (Tong et al. 2001), presumably due to the poor growth of *paf1Δ* cells (Shi et al. 1996), and would therefore be difficult to assess in this manner, as both the *paf1Δ* single-mutant and the *paf1Δ spt16* double-mutant cells would be slow-growing. Nonetheless, the genetic interactions between *cdc73Δ* and both *spt16-E857K* and *spt16-E763G*, and between *leo1Δ* and *spt16-E857K*, warranted further investigation into whether such interactions exist for other members of PafC.

To characterize the genetic interactions between members of PafC and mutant versions of Spt16, I performed tetrad analysis using cells containing either *spt16-E857K* or *spt16-E763G* and a deletion of one of the genes encoding a component of PafC (*cdc73Δ*, *ctr9Δ*, *leo1Δ*, *paf1Δ* and *rtf1Δ*). In every case except *rtf1Δ*, a synthetic genetic interaction was observed, although the severity of this interaction differed between the various combinations of mutations.

The initial tetrad analysis of *cdc73Δ* cells crossed with *spt16-E857K* cells and *spt16-E763G* cells yielded double-mutant segregants that grew into colonies of several different sizes (Figure 46). Because of this variability in colony growth, it was difficult to determine whether a genetic interaction exists for either double mutant. Therefore, the segregants were patch-plated onto solid medium, and the resulting patches were replica-plated to several temperatures for further growth. This analysis confirmed that synthetic genetic interactions exist for both *spt16-E857K cdc73Δ* double-mutant cells (Figure 46) and for *spt16-E763G cdc73Δ* double-mutant cells (Figure 46). Both the *spt16-E857K*

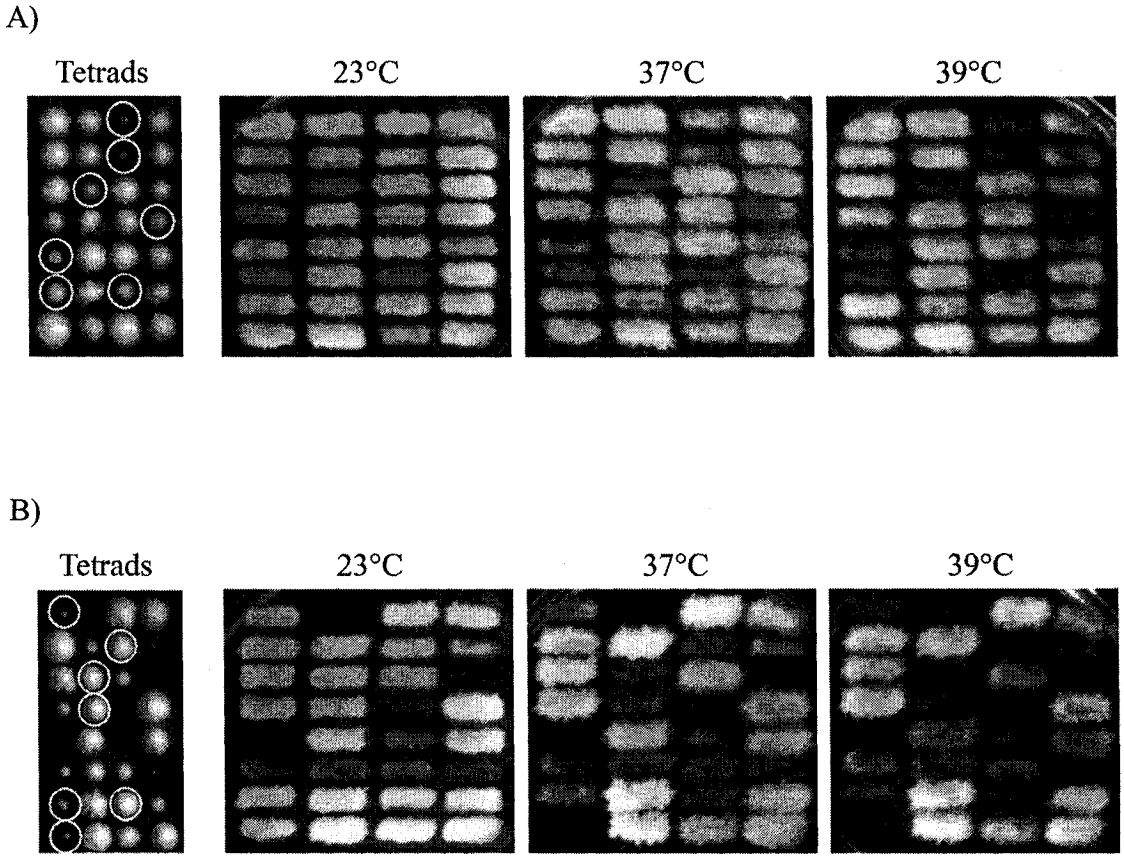

Figure 46. Deleterious genetic interaction between *spt16-E763G* or *spt16-E857K* and *cdc73Δ*. Diploids heterozygous for both mutations were sporulated, and tetrad analysis was performed. The double-mutant segregants are outlined by the white circles (*spt16-E857K* on top and *spt16-E763G* on bottom). All segregants from tetrad analysis were patched in the same pattern onto YEPD solid medium at 23°C, and replica-plated to YEPD for incubation at 23°C, 37°C and 39°C. A) Temperature sensitivity of *spt16-E857K cdc73Δ* double-mutant cells. The double-mutant cells grew well at 23°C but poorly at 37°C and 39°C. B) Temperature sensitivity of *spt16-E763G cdc73Δ* double-mutant cells. The double-mutant cells grew well at 23°C but poorly at 37°C and 39°C. Several other segregants also displayed poor growth, which was not consistent for cells of either single-mutant type.

double mutants and the *spt16-E763G* double mutants exhibited approximately the same degree of impairment, displaying temperature sensitivity at 37°C.

A similar impairment was seen for *spt16-E857K ctr9Δ* and *spt16-E763G ctr9Δ* double mutants. The results here were more straightforward than for the *cdc73Δ* crosses, with both the *spt16-E857K ctr9Δ* double-mutant segregants and the *spt16-E763G ctr9Δ* double-mutant segregants growing consistently poorly compared to the other segregants (Figure 47). In addition, the *spt16-E857K ctr9Δ* double-mutant segregants appeared to grow somewhat more poorly that the *spt16-E763G ctr9Δ* double-mutant segregants. To verify this poorer growth, both sets of segregants were assessed by patching and replica-plating. This analysis confirmed that the *spt16-E857K ctr9Δ* double mutants are more severely impaired than the *spt16-E763G ctr9Δ* double mutants, the former displaying temperature sensitivity at 30°C (Figure 47) while the latter grow reasonably well at this temperature but exhibit temperature sensitivity at 37°C (Figure 47).

The crosses involving the *spt16-E857K* and *spt16-E763G* cells and the *leo1Δ*, *paf1Δ* and *rtf1Δ* cells yielded double-mutant segregants that did not exhibit markedly different growth than any of the single-mutant segregants (Figures 48, 49, and 50). Thus, from this analysis alone it was difficult to determine whether synthetic interactions exist between any combination of these mutations. For this reason, I analysed the segregants further by patching and replica plating. This analysis showed that both the *spt16-E857K leo1Δ* double-mutant cells and the *spt16-E763G leo1Δ* double-mutant cells grow reasonably well, although they do show a mild synthetic impairment at high temperatures (Figure 48). Both the *spt16-E857K leo1Δ* double-mutants and the *spt16-E763G leo1Δ* double-mutants were impaired to approximately the same degree, growing well at 30°C and poorly at 39°C. In contrast, the *paf1Δ* double-mutant cells were less robust, likely due in part to the poor growth conferred by the *paf1Δ* mutation itself. In this case, the *spt16-E857K paf1Δ* double-mutant cells were more impaired than the *spt16-E763G paf1Δ* double-mutant cells, with the former showing temperature-sensitive growth at 30°C and above while the latter exhibited temperature sensitivity at 37°C (Figure 49). In contrast, unlike cells deleted for the other members of PafC, the *spt16-E857K rtf1Δ*

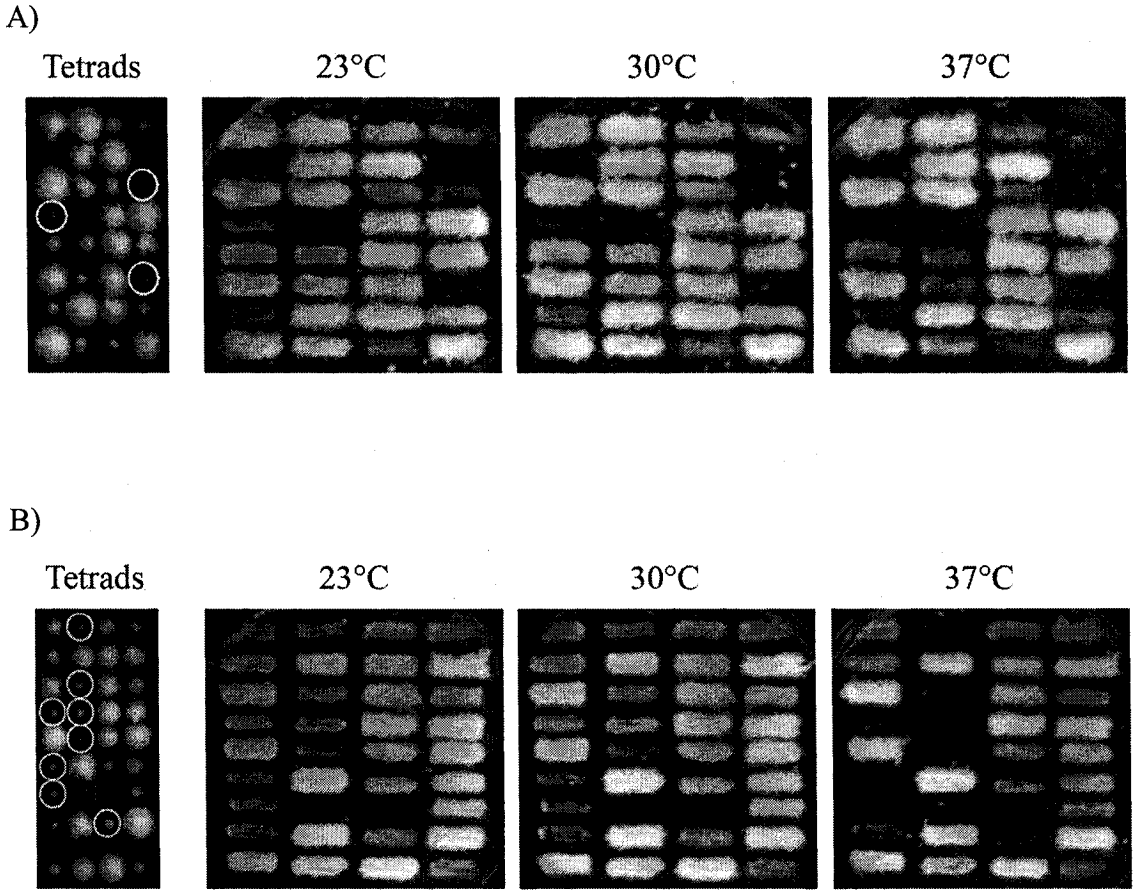

Figure 47. Deleterious genetic interaction between *spt16-E763G* or *spt16-E857K* and *ctr9Δ*. Diploids heterozygous for both mutations were sporulated, and tetrad analysis was performed. The double-mutant segregants are outlined by the white circles (*spt16-E857K* on top and *spt16-E763G* on bottom). All segregants from tetrad analysis were patched in the same pattern onto YEPD solid medium at 23°C, and replica-plated to YEPD for incubation at 23°C, 30°C and 37°C. A) Temperature sensitivity of *spt16-E857K ctr9Δ* double-mutant cells. The double-mutant cells grew well at 23°C but poorly at 30°C and 37°C. B) Temperature-sensitivity of *spt16-E763G ctr9Δ* double-mutant cells. The double-mutant cells grew well at 23°C but poorly at 30°C and 37°C. Several other segregants also displayed poor growth, which was not consistent for cells of either single-mutant type.

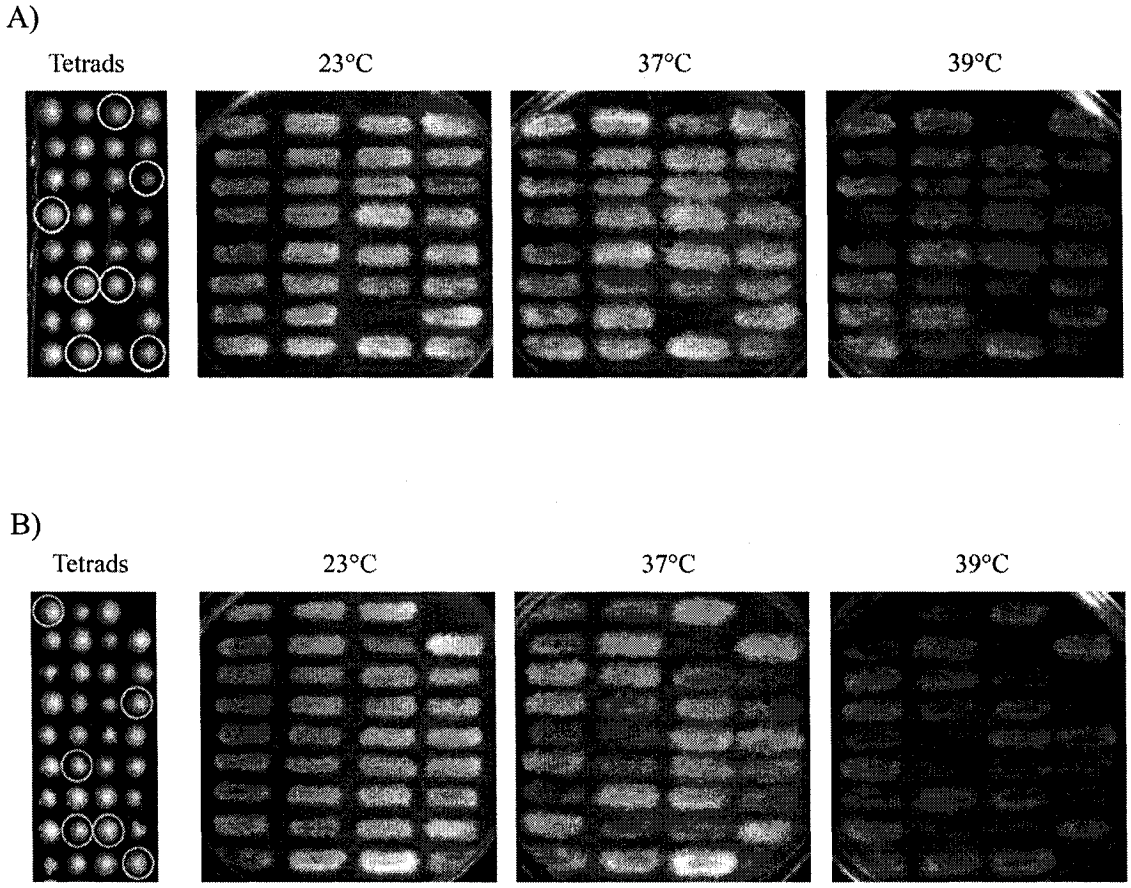

Figure 48. Deleterious genetic interaction between *spt16-E763G* or *spt16-E857K* and *leo1Δ*. Diploids heterozygous for both mutations were sporulated, and tetrad analysis was performed. The double-mutant segregants are outlined by the white circles (*spt16-E857K* on top and *spt16-E763G* on bottom). All segregants from tetrad analysis were patched in the same pattern onto YEPD solid medium at 23°C, and replica-plated to YEPD for incubation at 23°C, 37°C and 39°C. A) Temperature sensitivity of *spt16-E857K leo1Δ* double-mutant cells. The double-mutant cells grew well at 23°C but poorly at 39°C. B) Temperature sensitivity of *spt16-E763G leo1Δ* double-mutant cells. The double-mutant cells grew well at 23°C but poorly at 37°C and 39°C. Several other segregants also displayed poor growth, which was not consistent for cells of either single-mutant type.

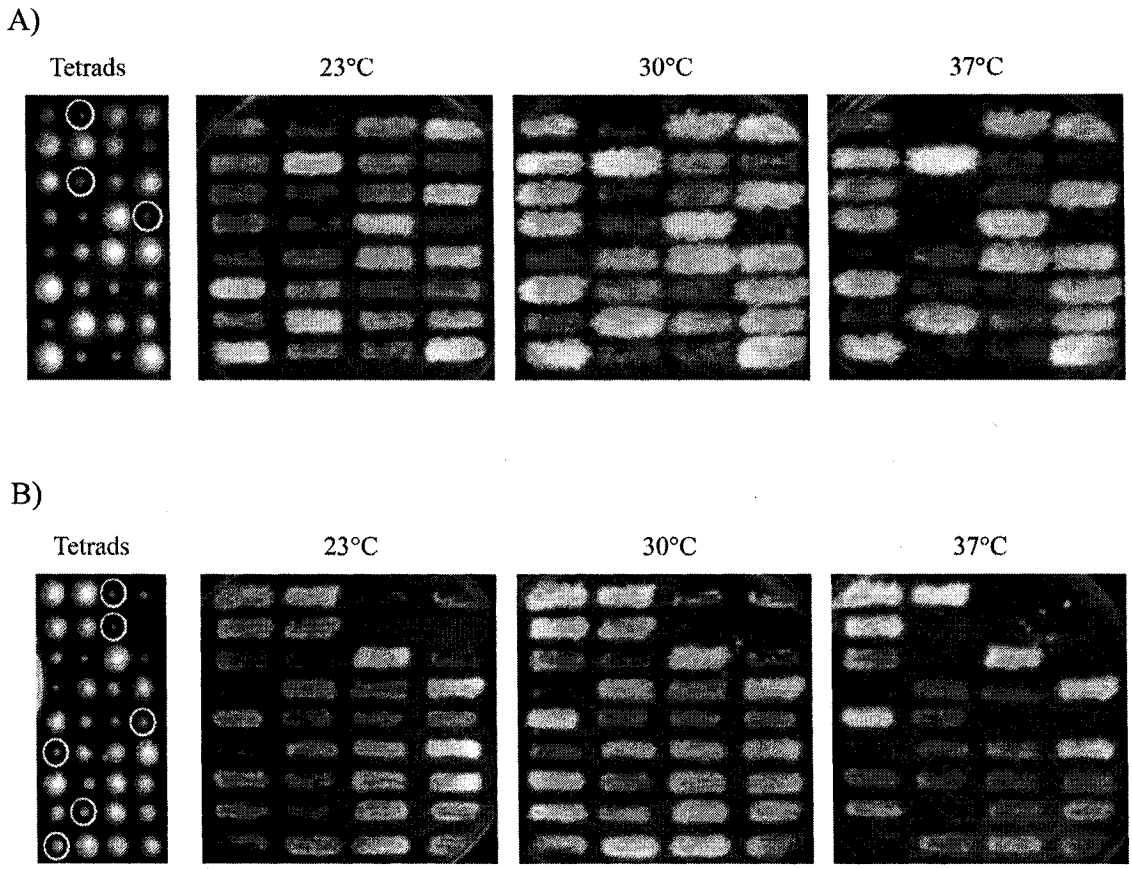

Figure 49. Deleterious genetic interaction between *spt16-E763G* or *spt16-E857K* and *paf1Δ*. Diploids heterozygous for both mutations were sporulated, and tetrad analysis was performed. The double-mutant segregants are outlined by the white circles (*spt16-E857K* on top and *spt16-E763G* on bottom). All segregants from tetrad analysis were patched in the same pattern onto YEPD solid medium at 23°C, and replica-plated to YEPD for incubation at 23°C, 30°C and 37°C. A) Temperature sensitivity of *spt16-E857K paf1Δ* double-mutant cells. The double-mutant cells grew poorly at 23°C and 30°C, but not at all at 37°C. Several other segregants also display poor growth, which was not consistent for cells of either single-mutant type. B) Temperature sensitivity of *spt16-E763G paf1Δ* double-mutant cells. The double-mutant cells grew poorly at 23°C and 30°C, but not at all at 37°C. Several other segregants also display poor growth, which was not consistent for cells of either single-mutant type.

double-mutant cells and the *spt16-E763G rtf1Δ* double-mutant cells were no more impaired than the single mutants at all temperatures tested (Figure 50).

In total, deleterious genetic interactions were seen for gene deletions eliminating four of the five subunits of PafC, with Rtf1 the only subunit without genetic interactions. It has been shown that while deletion of *RTF1* causes dissociation of the remaining PafC subunits from chromatin, Paf1 is still functional in this state (Mueller, Jaehning 2002). Therefore, perhaps the deleterious genetic interactions observed here with the other PafC deletions reflect the loss of a role for PafC independent of chromatin tethering. However, this hypothesis is not fully supported by my observations that genetic interactions exist between the *spt16* mutations and *cdc73Δ*, as elimination of this PafC component also causes dissociation of PafC from chromatin (Mueller, Jaehning 2002). It is possible that Cdc73 protein also functions in a role other than PafC tethering, and that the deleterious genetic interactions observed for *cdc73Δ* cells reflects the loss of this function, rather than loss of PafC tethering.

The degree of severity of these genetic interactions with *spt16* mutations was different for the various PafC deletions, with *ctr9Δ* cells and *paf1Δ* cells exhibiting more severe growth impairment than *cdc73Δ* cells or *leo1Δ* cells, with the *leo1Δ* interactions showing only mild growth impairment. This spectrum of effects is consistent with previous reports that the phenotypes of *ctr9Δ* and *paf1Δ* cells are much more severe than those of *rtf1Δ*, *cdc73Δ*, or *leo1Δ* cells, suggesting that Paf1 and Ctr9 form the core of PafC, and that Leo1, with the least severe growth defects, is the most peripheral subunit (Betz et al. 2002).

Severe growth impairment was seen specifically with *spt16-E857K ctr9Δ* cells and *spt16-E857K paf1Δ* cells, but not with their *spt16-E763G* counterparts. Thus, there are more severe synthetic interactions between *spt16-E857K* and deletions of PafC-subunit genes than between *spt16-E763G* and the same PafC deletions, similar to the differences observed with the genetic interactions between these two *spt16* mutant alleles and *spt4Δ*, which eliminates a protein involved in recruiting PafC for transcription (Qiu et al. 2006). Perhaps the impairment caused by the *spt16-E857K* mutation causes a greater reliance on PafC during the transcription process than does the impairment caused by the

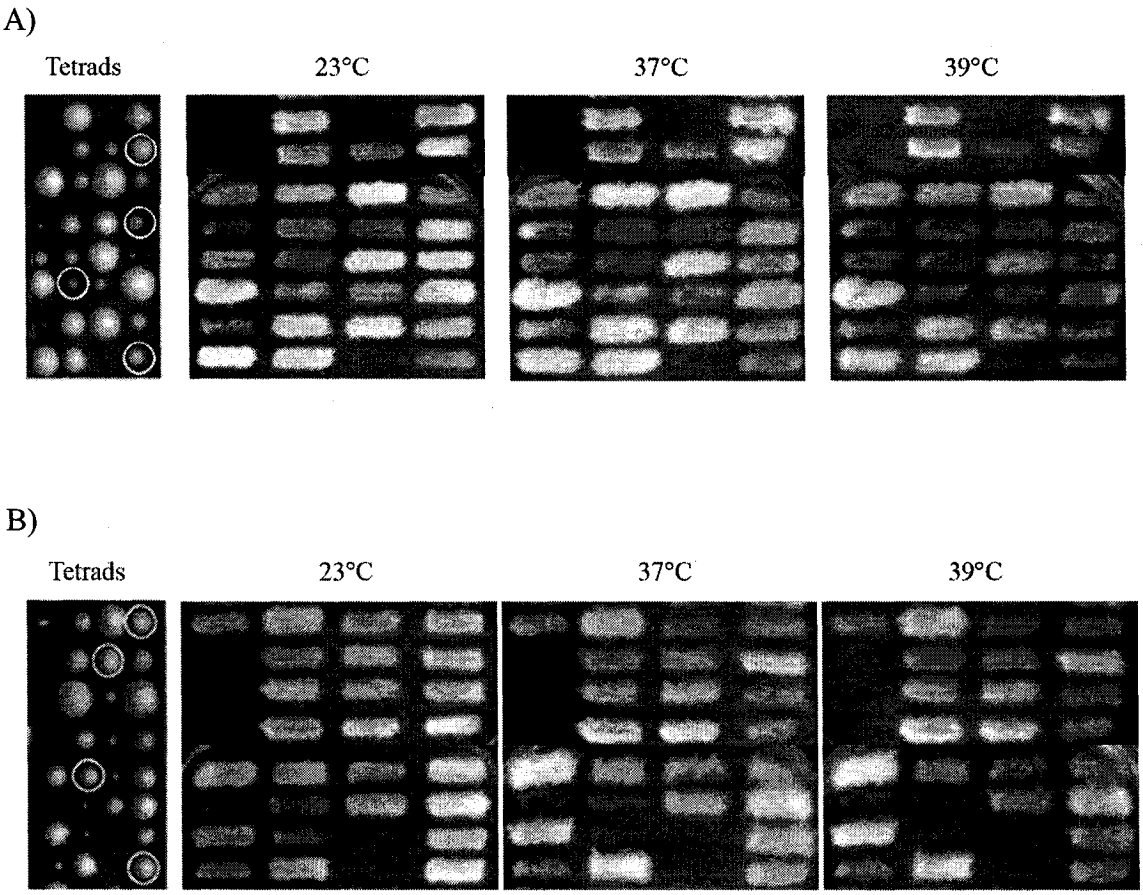

Figure 50. No deleterious genetic interaction between *spt16-E763G* or *spt16-E857K* and *rtf1Δ*. Diploids heterozygous for both mutations were sporulated, and tetrad analysis was performed. The double-mutant segregants are outlined by the white circles (*spt16-E857K* on top and *spt16-E763G* on bottom). All segregants from tetrad analysis were patched in the same pattern onto YEPD solid medium at 23°C, and replica-plated to YEPD for incubation at 23°C, 37°C and 39°C. A) Temperature sensitivity of *spt16-E857K rtf1Δ* double-mutant cells. The double-mutant cells grew well at 23° but not as well at 37°C and 39°C; this growth is no worse than that of either single mutant. B) Temperature sensitivity of *spt16-E763G rtf1Δ* double-mutant cells. The double-mutant cells grew well at 23°C, but not as well at 37°C and 39°C; this growth is no worse than that of either single mutant.

spt16-E763G mutation. Thus, deletions affecting members of PafC would cause a more deleterious genetic interaction in *spt16-E857K* cells than in *spt16-E763G* cells.

The above interpretation suggests that the more severe interaction observed between *spt4Δ* and *spt16-E857K* may indicate an effect on PafC in the *spt4Δ* cells. It has recently been shown that there is also a decreased recruitment of PafC to RNAPII in *bur2Δ* cells (Laribee et al. 2005). It is unclear whether this decrease is due to a direct effect of Bur kinase on PafC recruitment, or an indirect effect, possibly through a Bur-kinase effect on Spt4–Spt5, which in turn affects PafC recruitment. Nevertheless, this observation suggests the possibility that the lethality observed between *spt16-E857K* and *bur2Δ* could be in part due to the effects of Bur kinase on Spt4–Spt5 and PafC.

3.5 Suppression of Synthetic Lethality

Mutational suppressor analysis of a *bur1Δ* deletion mutation has identified, as mutations markedly improving the growth of *bur1Δ* cells, several gene deletions (*set2Δ*, *rpd3Δ*, *sin3Δ*, *eaf3Δ* and *rco1Δ*) eliminating members of another histone-modification pathway (Chu et al. 2006, Keogh et al. 2005). In this pathway, the Set2 protein is recruited to actively transcribed genes by RNA polymerase II that has been phosphorylated on serine 2 of its C-terminal repeats (RNAPII Ser2-P) (Li et al. 2003, Li, Moazed & Gygi 2002), and then methylates lysine 36 of histone H3 (H3K36) on the nucleosomes that are reassembled in the wake of RNAPII during the transcription process (Strahl et al. 2002, Xiao et al. 2003). This methylation then allows the recruitment, to these methylated nucleosomes, of the Rpd3C(S) complex, which contains the proteins Rpd3, Sin3, Eaf3 and Rco1; this complex deacetylates histones, leading once again to a repressive chromatin environment (Carrozza et al. 2005, Joshi, Struhl 2005, Keogh et al. 2005, Li et al. 2007).

The genetic suppression findings noted above indicate that this deacetylation activity presents a significant problem for cells that are missing the Bur kinase, suggesting that one role of Bur kinase is to provide a counterbalance to Rpd3C(S)-mediated histone deacetylation. Thus, it is reasonable to hypothesize that *spt16-E857K bur2Δ* synthetic lethality might be due to the relatively unopposed action of the Rpd3C(S) histone deacetylase (HDAC) in these cells. In this model, FACT and Bur kinase play

different but complementing roles in overcoming the repressive effects of deacetylated histones resulting from Rpd3C(S) activity. In the single-mutant case, where either FACT or Bur kinase have impaired function, the remaining normal function of Bur kinase or FACT would be enough to overcome the effects of histone deacetylation. However, when both FACT and Bur kinase are impaired there would not be enough opposing activity, and the effects of Rpd3C(S) are sufficient to impair cell growth. This hypothesis was tested genetically as described below.

Prior to testing this hypothesis, I wanted to ensure that deletions of the genes involved in this methylation–deacetylation pathway do not themselves have deleterious genetic interactions with either *spt16-E857K* or *spt16-E763G*. This assessment was carried out by tetrad analysis. Cells individually containing *set2Δ*, *sin3Δ*, *eaf3Δ* and *rco1Δ* were crossed with cells containing *spt16-E857K* or *spt16-E763G*; the resulting diploids were sporulated, and the haploid spore products were assessed for growth ability. (Cells containing *rpd3Δ* were not tested, as a *bona fide rpd3Δ* strain may not be in the deletion collection; PCR analysis of the *RPD3* locus in the so-called *rpd3Δ* strain showed that *RPD3* was intact in these cells, rather than replaced with the *kanMX4* cassette.) In all cases, no deleterious effects were observed for any of the resulting double-mutant cells, indicating no synthetic genetic interaction between deletions of members of this histone-modification pathway and either *spt16-E857K* or *spt16-E763G*. These findings therefore made it possible to assess whether the presence of the Set2–Rpd3C(S) pathway of histone methylation and deacetylation is deleterious to cells mutant for both Bur kinase and Spt16, as exemplified by the synthetic lethality between *bur2Δ* and *spt16-E857K*.

3.5.1 Suppression of the *spt16-E857K bur2Δ* Genetic Interaction

To test the above histone-methylation–histone-deacetylation hypothesis, triple-mutant cells were created using standard genetic procedures, starting with crossing a *bur2Δ* cell with an *spt16-E857K set2Δ* double-mutant cell, in which *set2Δ* eliminates the methylation mark that recruits Rpd3C(S). The resulting diploids were sporulated, and the meiotic segregants were characterized to identify the desired triple mutants (containing *spt16-E857K*, *bur2Δ* and *set2Δ*). The growth of these triple mutants showed that the *set2Δ* gene deletion does indeed suppress the synthetic lethality between *spt16-E857K* and *bur2Δ* (Figure 51).

A)

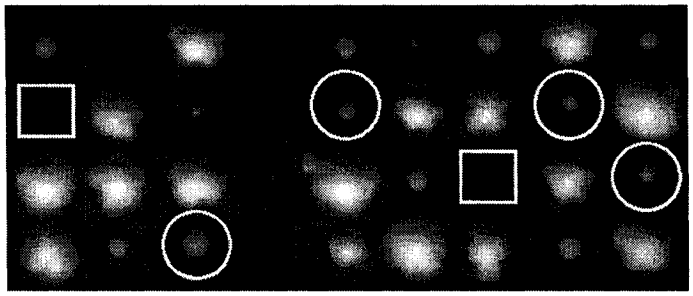

B)

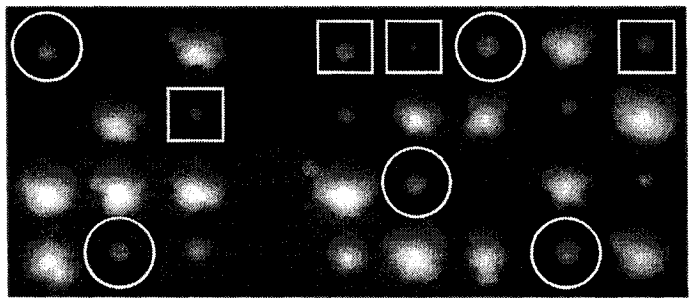

Figure 51. Suppression of *spt16-E857K bur2Δ* synthetic lethality, but not *bur2Δ* slow growth, by *set2Δ*. Diploid cells heterozygous for *spt16-E857K*, *bur2Δ* and *set2Δ* were sporulated, and tetrad analysis was performed. A) The *spt16-E857K bur2Δ* double-mutant segregants are outlined by the white squares, while the *spt16-E857K bur2Δ set2Δ* triple-mutant segregants are outlined by the white circles. The triple-mutant cells grew significantly better than the double-mutant cells. B) The *bur2Δ* single-mutant segregants are outlined by the white squares, while the *bur2Δ set2Δ* double-mutant segregants are outlined by the white circles. The double mutants grew no better than the *bur2Δ* single mutants.

The above observation does not show definitively whether the *set2Δ*-mediated suppression is due to the inability to recruit Rpd3C(S). It is possible that Set2-mediated H3K36 methylation is itself detrimental to *spt16-E857K* cells, and that the suppression observed is a reflection of the improved growth of *spt16-E857K* cells lacking this methylation due to the *set2Δ* deletion. The *spt16-E857K* mutation itself has few phenotypes that can be monitored, so it is difficult to tell whether *spt16-E857K set2Δ* double-mutant cells grow any better than *spt16-E857K* single-mutant cells. Therefore, a different approach was taken. Recently, several histone demethylases have been identified in yeast (Tu et al. 2007). Among these are two H3K36-specific demethylases: Jhd1 and Rph1 (Fang et al. 2007, Kim, Buratowski 2007, Tsukada et al. 2006, Tu et al. 2007). Rph1 appears to primarily demethylate trimethylated K36, and, to a lesser extent, dimethylated K36, whereas Jhd1 demethylates di- and mono-methylated K36 (Fang et al. 2007, Kim, Buratowski 2007, Tu et al. 2007). Overexpression of either Rph1 or Jhd1 can bypass the essential requirement for Bur1, and both are required for normal levels of RNAPII occupancy over coding regions (Kim, Buratowski 2007). These findings suggest that both Jhd1 and Rph1 remove the methyl groups that are added by Set2.

If the presence of H3K36 methylation is itself detrimental to *spt16-E857K* cells, then deleterious interactions may exist between *spt16-E857K* and *jhd1Δ*, due to the persistence of H3K36 methylation in these cells compared to cells containing normal *JHD1*. However, tetrad analysis demonstrated that no deleterious genetic interaction existed between these two mutations (Figure 52). Therefore, the mere presence of Set2-mediated H3K36 methylation is not likely to be deleterious for *spt16-E857K* cells. This observation supports the idea that the *set2Δ*-mediated suppression of *spt16-E857K bur2Δ* synthetic lethality is due to the inability to recruit the Rpd3C(S) HDAC.

To focus specifically on Rpd3C(S), a similar genetic analysis was performed by assessing the effects of a mutation eliminating the Rpd3C(S) complex. Rco1 was chosen since it is the only member of Rpd3C(S) that is specific for this complex (Carrozza et al. 2005, Keogh et al. 2005). For tetrad analysis, an *spt16-E857K rco1Δ* double-mutant cell was crossed with a *bur2Δ* cell. Analysis of the resulting haploid segregants showed that the *rco1Δ* gene deletion suppresses the synthetic lethality between *spt16-E857K* and

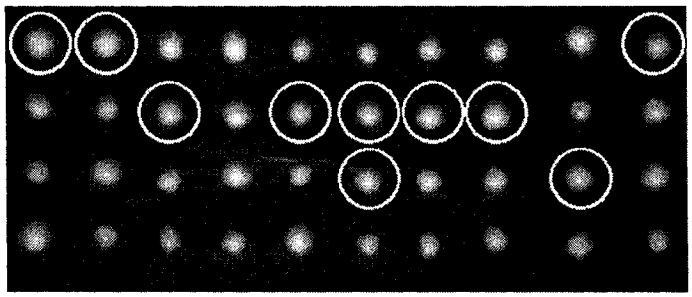

Figure 52. No deleterious genetic interaction exists between *spt16-E857K* and *jhd1Δ*. Diploid cells heterozygous for *spt16-E857K* and *jhd1Δ* were sporulated, and tetrad analysis was performed. The *spt16-E857K jhd1Δ* double-mutant segregants are outlined by white circles. These double-mutant segregants are growing no differently than either of the single-mutant cells.

bur2Δ (Figure 53), suggesting that histone deacetylation is indeed a problem for the *spt16-E857K bur2Δ* double-mutant cells.

The above *rco1Δ* finding also supports the hypothesis that the *set2Δ*-mediated suppression is due to the inability to recruit Rpd3C(S) rather than to a direct effect of the absence of Set2. If H3K36 methylation is directly inhibitory for the *spt16-E857K bur2Δ* cells, then there should have been no improvement seen in the triple mutants with *rco1Δ*, as Set2 function is presumably normal in these cells; Set2 functions upstream of Rpd3C(S) (Carrozza et al. 2005, Keogh et al. 2005). However, since there is suppression of synthetic lethality in both the *set2Δ* and *rco1Δ* triple mutants, it can be inferred that the Rpd3C(S)-mediated histone deacetylation, rather than the Set2-mediated H3K36 methylation itself, is deleterious to cells with mutations affecting both FACT and Bur kinase.

Suppression of synthetic lethality by *rco1Δ* could result from suppression of the *bur2Δ* effects or the *spt16-E857K* effects (or both). However, if *rco1Δ* suppresses the effects of *bur2Δ*, then I would expect the *rco1Δ bur2Δ* double mutants that were identified through tetrad analysis to grow better than *bur2Δ* single mutants. However, neither *set2Δ* nor *rco1Δ* improved the slow growth of *bur2Δ* cells (Figures 51 and 53), and even though *rco1Δ* does suppress the synthetic lethality of *spt16-E857K bur2Δ* cells, the *spt16-E857K rco1Δ bur2Δ* triple-mutant cells also exhibited slow growth (Figure 53), much like that of a *bur2Δ* single-mutant cell (the same holds true for *set2Δ* – Figure 51). These observations suggest that the suppression of synthetic lethality is a result of *rco1Δ* suppression of the deleterious effects of the *spt16-E857K* mutation in *bur2Δ* cells.

The above conclusion leads to the question of how *rco1Δ* suppresses the deleterious effect of *bur1Δ* (Keogh et al. 2005) when it has no effect on *bur2Δ* cells. One possible interpretation of those observations holds that FACT would be a target of Bur kinase activity (either directly or indirectly). In this scenario, *bur1Δ* cells would be unable to 'activate' FACT or a FACT-pathway component and thus would be unable to overcome the effects of histone deacetylation by Rpd3C(S). However, eliminating the Rpd3C(S) HDAC would allow the un-activated FACT to perform its job better and the cells would be able to survive. FACT could still be 'activated' by Bur kinase in *bur2Δ* cells, although not as well as in *BUR2* cells, and would therefore be able to overcome the effects of

A)

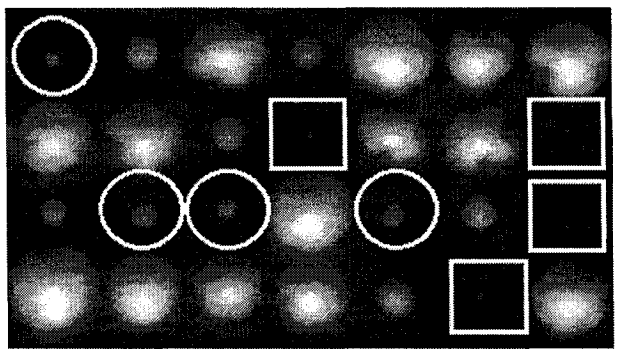

B)

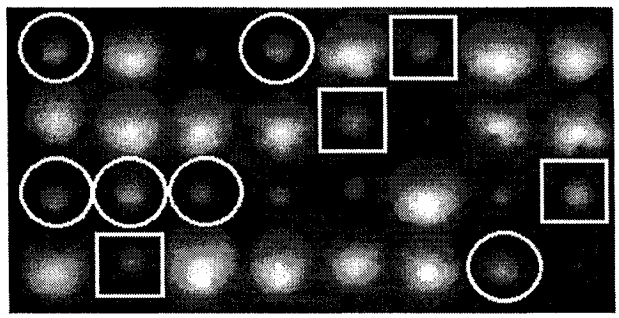

Figure 53. Suppression of *spt16-E857K bur2Δ* synthetic lethality, but not *bur2Δ* slow growth, by *rco1Δ*. A) Diploid cells heterozygous for *spt16-E857K*, *bur2Δ* and *rco1Δ* were sporulated, and tetrad analysis was performed. The *spt16-E857K bur2Δ* double-mutant segregants are outlined by the white squares, while the *spt16-E857K bur2Δ rco1Δ* triple-mutant segregants are outlined by the white circles. The triple mutants grew significantly better than the double mutants. B) Diploid cells heterozygous for *bur2Δ* and *rco1Δ* were sporulated, and tetrad analysis was performed. The *bur2Δ* single-mutant segregants are outlined by the white squares, while the *bur2Δ rco1Δ* double-mutant segregants are outlined by the white circles. The double mutants grew no better than the *bur2Δ* single mutants.

Rpd3C(S). Thus, in these *bur2Δ* cells, eliminating the HDAC would have no effect. However, cells that are both *bur2Δ* and *spt16-E857K* would have an poorly activated version of FACT that was already mutant, a situation that would severely compromise FACT activity, to the point that this mutant FACT would be unable to overcome the effects of Rpd3C(S). Eliminating the negative effects of the Rpd3C(S) HDAC would improve the growth of these cells.

An alternative interpretation has it that FACT and Bur kinase mediate parallel but non-redundant pathways, and that Bur kinase has two levels of activation of its pathway, with low kinase activity, such as that present in *bur2Δ* cells, providing enough function for life, but full activity being needed for robust growth. In this situation, the Rpd3C(S) HDAC counteracts a common function carried out by both FACT and Bur kinase. Thus, elimination of the Rpd3C(S) HDAC could overcome lethality caused by complete loss of Bur kinase function, but could not replace the need for Bur kinase for robust growth; the *bur1Δ rco1Δ* cells would be viable, but would not grow robustly. In this scenario, *rco1Δ* would have no effect on *bur2Δ* cells, as the impaired Bur kinase in these cells is able to provide life, yet does not have enough kinase activity to support robust growth. However, if an impaired version of FACT, such as that produced from the *spt16-E857K* mutation, is also present in these *bur2Δ* cells, then both the FACT-mediated pathway and the Bur kinase-mediated pathway are impaired. These *spt16-E857K bur2Δ* double mutants are therefore unable to support life, and *rco1Δ* is able to suppress the synthetic lethality. This could result from *rco1Δ* acting solely on the Bur kinase-mediated or FACT-mediated pathway, or on both of these pathways.

3.5.2 Suppression of Other Genetic Interactions by *rco1Δ*

If the maintenance of acetylated histones through inactivation of Rpd3C(S) is able to overcome the impairment of a FACT-mediated pathway, it may be possible to overcome other instances of synthetic lethality for *spt16-E857K* by introducing a deletion of *RCO1* into these cells. To determine whether the actions of the Rpd3C(S) histone deacetylase complex are, in fact, detrimental to cells containing an *spt16* mutation in combination with mutations in genes other than *BUR2*, I tested whether *rco1Δ* suppresses other *spt16* synthetic-lethal interactions that are characterized above.

3.5.2.1 Suppression of the *spt16 spt5* Genetic Interaction

This potential suppression by *rco1Δ* was initially tested using *spt16 spt5* double mutants. As described above, both *spt16-E857K* and *spt16-E763G* cause synthetic temperature sensitivity when combined with the *spt5-4* and *spt5-194* mutant alleles. Using tetrad analysis to produce and identify triple mutants, I found that both the *spt16-E857K spt5-4 rco1Δ* and the *spt16-E857K spt5-194 rco1Δ* triple mutants grew better at high temperatures compared to their respective *spt16-E857K spt5* double mutants, indicating that Rpd3C(S)-mediated histone deacetylation is indeed inhibitory for these *spt16 spt5* cells (Figure 54). In contrast, as shown in Figure 54, analogous suppression of temperature sensitivity by *rco1Δ* was not seen for the *spt16-E763G spt5-4* or *spt16-E763G spt5-194* situations, indicating at least some allele specificity for *rco1Δ*-mediated suppression of synthetic effects. However, since Spt5 may well be a target for Bur kinase activity (Bourgeois et al. 2002, Ivanov et al. 2000, Kim, Sharp 2001, Pei, Shuman 2003, Yamada et al. 2006), this particular observation may not be the best indication to see if *rco1Δ* can suppress other FACT-related deleterious genetic interactions that are unrelated to Bur kinase.

3.5.2.2 Suppression of Genetic Interactions between *spt16* and Histone Chaperones

To expand the spectrum of *spt16* genetic interactions assessed, I determined the *rco1Δ* effects on the deleterious genetic interactions with mutations in histone chaperones. While some of these interactions are specific for *spt16-E857K* or *spt16-E763G*, others are common to both mutations. The genetic interaction with a deletion of *HIR2*, which encodes a component of HirC, is specific for *spt16-E857K*, while that with a deletion of *NAP1* is specific to *spt16-E763G*. In contrast, the genetic interactions with mutations in *SPT6*, which encodes a histone chaperone involved in transcription elongation, are common to both *spt16-E857K* and *spt16-E763G*.

Assessing the triple-mutant cells generated using tetrad analysis showed that the *spt16-E857K hir2Δ rco1Δ* triple mutants were able to form colonies (Figure 55), indicating that the absence of Rpd3C(S) HDAC activity suppresses the synthetic lethality between *spt16-E857K* and *hir2Δ*. This result provides more evidence in favour of the idea that the Rpd3C(S) complex performs a function that opposes that of FACT, as Bur kinase is not likely to be impaired in this situation. Thus, the observed suppression can be

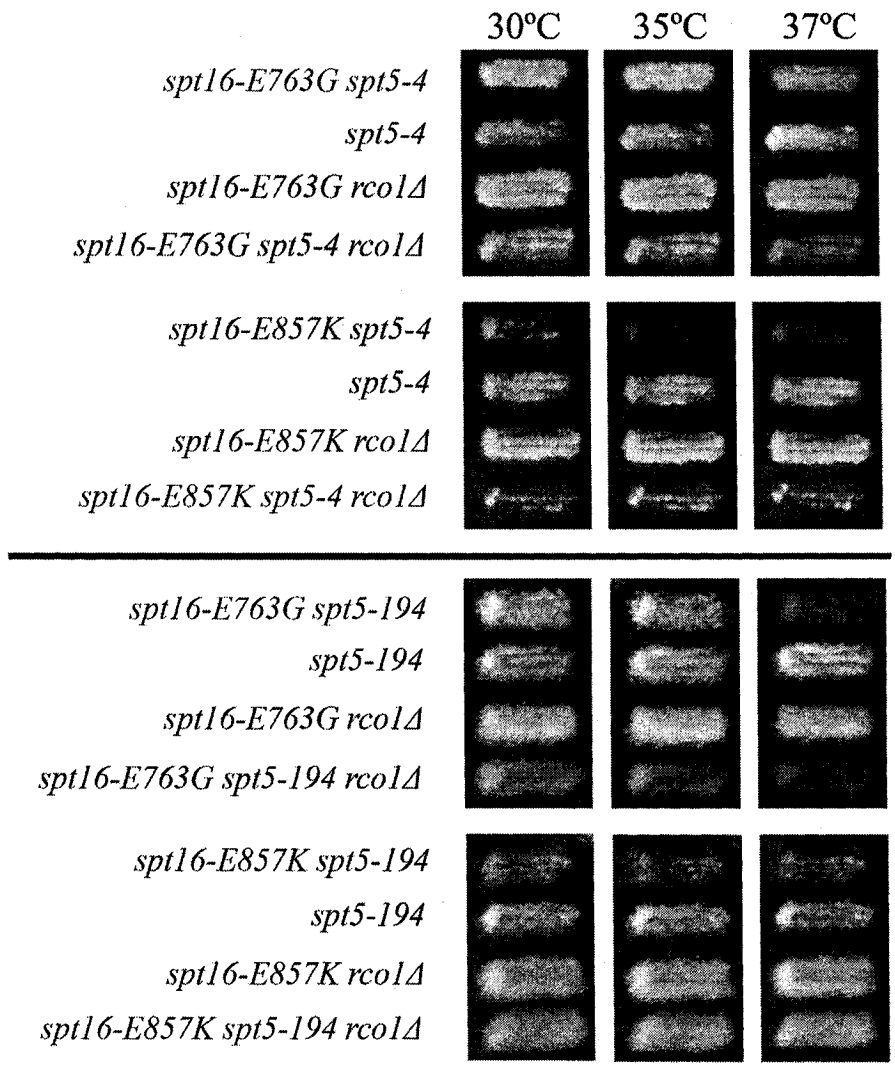

Figure 54. *rco1Δ*-mediated suppression of the deleterious genetic interactions between mutations in *SPT16* and *SPT5*. Segregants from tetrad analysis were patched on YEPD solid medium, and then replica-plated for incubation at the indicated temperature overnight. The temperature sensitivity of both the *spt16-E857K spt5-4* and *spt16-E857K spt5-194* double mutants was alleviated in the *spt16-E857K spt5 rco1Δ* triple mutants; this suppression was not seen for either of the *spt16-E763G* triple mutants.

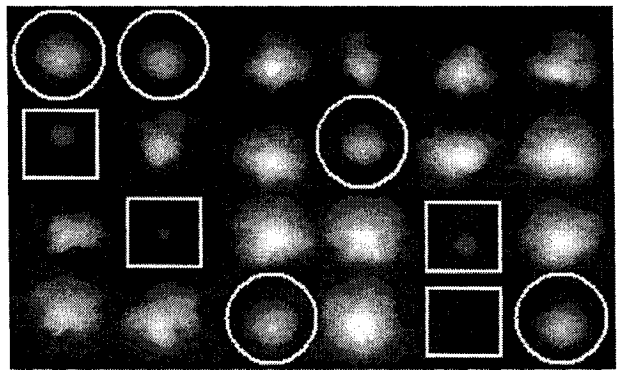

Figure 55. Suppression of *spt16-E857K hir2Δ* synthetic lethality by *rco1Δ*. Diploid cells heterozygous for *spt16-E857K*, *hir2Δ* and *rco1Δ* were sporulated, and tetrad analysis was performed. The *spt16-E857K hir2Δ* double-mutant segregants are outlined by the white squares, while the *spt16-E857K hir2Δ rco1Δ* triple-mutant segregants are outlined by the white circles. The triple mutants grew significantly better than the double mutants.

interpreted as a result of mitigating the consequences of the FACT defect in *spt16-E857K* cells. This suppression also suggests that the basis for this *spt16-E857K hir2Δ* synthetic lethality may be loss of the nucleosome-assembly activity of Hir2 rather than histone gene expression effects, as the Rpd3C(S) HDAC functions during transcription. Also supporting this interpretation are the observations that alterations in histone abundance only cause temperature sensitivity of *spt16-E857K* cells, whereas mutations in HirC cause synthetic lethality, indicating that the HirC mutations have a more severe effect on cells relying on the Spt16-E857K mutant protein.

While I observed *rco1Δ*-mediated suppression of the synthetic lethality between *spt16-E857K* and *hir2Δ*, this was not the case for the synthetic interactions with *spt6* mutations. As there are synthetic interactions between the mutant alleles of *SPT6* and both *spt16-E857K* and *spt16-E763G*, the effects of the *RCO1* deletion were determined for all of these combinations. Unlike that seen for the genetic interactions tested thus far, no *rco1Δ*-mediated suppression was observed for any of the genetic interactions involving mutations in *SPT6* (Figure 56). A similar situation was observed for the genetic interaction between *spt16-E763G* and *nap1Δ*. In this situation, like that for the *spt6* mutations, no *rco1Δ*-mediated suppression was observed (Figure 57).

Thus, while the absence of Rpd3C(S)-mediated histone deacetylation is able to alleviate the lethality of the *spt16-E857K hir2Δ* genetic interaction, it cannot overcome the deleterious genetic interactions between *spt16* and either *spt6* or *nap1Δ*. Even though all of these proteins function as histone chaperones, the mechanisms underlying the deleterious genetic interactions between mutations in the various genes must be different, as the absence of Rpd3C(S) activity is beneficial only for the deleterious genetic interaction between *spt16-E857K* and *hir2Δ*.

3.5.2.3 Suppression of Genetic Interactions between *spt16* and PafC

Since many of the deleterious genetic interactions involving *spt16-E857K* can be suppressed by *rco1Δ*, I decided to also examine the interactions with members of PafC. Both *spt16-E857K* and *spt16-E763G* displayed deleterious genetic interactions with deletions of each member of PafC except Rtf1. Thus, the genetic interactions with PafC provide an opportunity to determine whether similar suppression patterns can be seen for

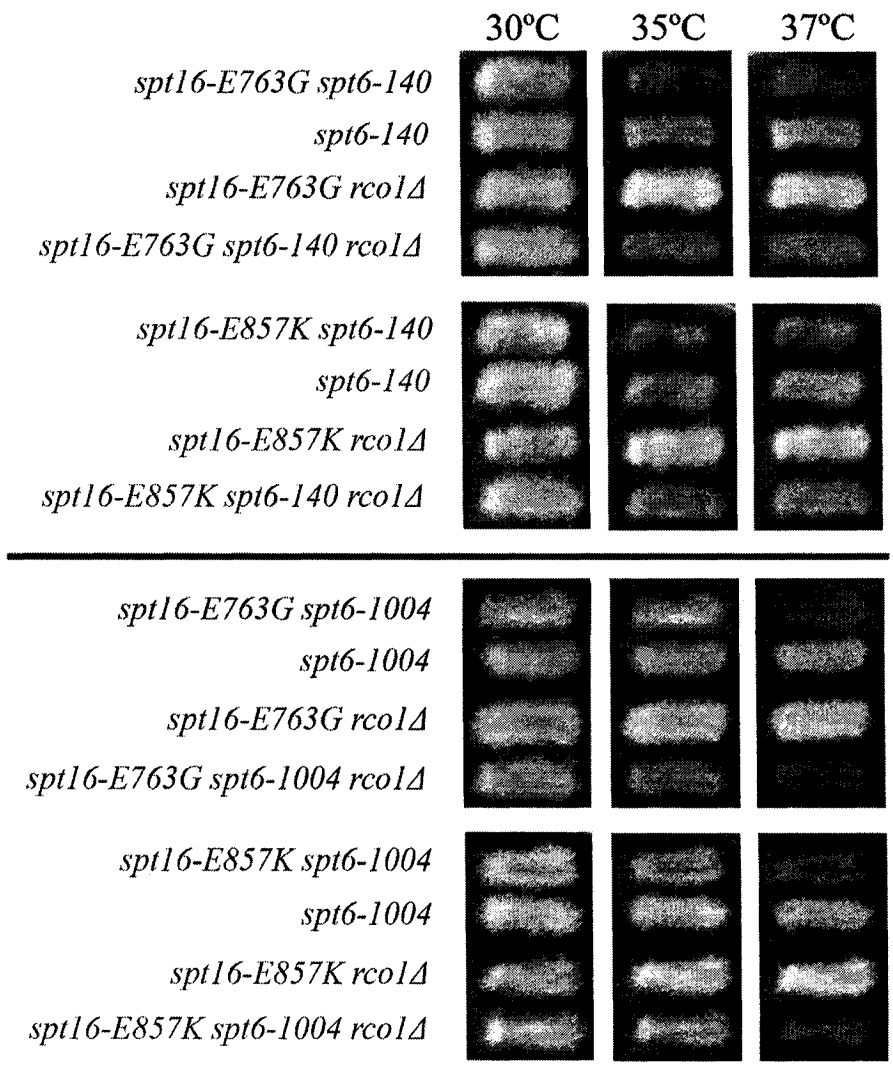

Figure 56. No *rco1Δ*-mediated suppression of the deleterious genetic interactions between mutations in *SPT16* and *SPT6*. Segregants from tetrad analysis were patched on YEPD solid medium, and then replica-plated for incubation at the indicated temperature overnight. In no case did *rco1Δ* alter the temperature sensitivity of *spt16 spt6* double-mutant cells.

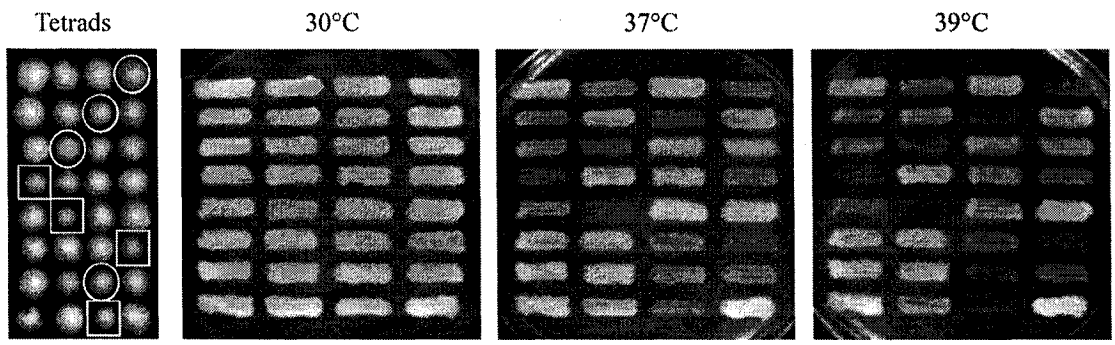

Figure 57. No *rco1Δ*-mediated suppression of the deleterious genetic interactions between *spt16-E763G* and *nap1Δ*. Diploid cells heterozygous for *spt16-E763G*, *nap1Δ* and *rco1Δ* were sporulated, and tetrad analysis was performed. All segregants from tetrad analysis were patched onto YEPD solid medium at 30°C, and replica-plated to YEPD for incubation at 30°C, 37°C and 39°C. Both the *spt16-E763G nap1Δ* double mutants (outlined by circles) and *spt16-E763G nap1Δ rco1Δ* triple mutants (outlined by squares) displayed temperature-sensitive growth, growing poorly at 37°C and 39°C.

both the *spt16-E857K* and *spt16-E763G* mutations. Using tetrad analysis to produce and identify triple mutants, I determined whether the *rco1Δ* deletion was able to suppress any of the deleterious genetic interactions between deletions of PafC members and either *spt16-E857K* or *spt16-E763G*.

Neither the *spt16-E857K ctr9Δ rco1Δ* nor the *spt16-E857K cdc73Δ rco1Δ* triple-mutant segregants exhibited any better growth than their respective double mutants, indicating that there is no *rco1Δ*-mediated suppression of these deleterious genetic interactions (Figures 58 & 59). In contrast, *rco1Δ*-mediated suppression was observed for the genetic interaction between *spt16-E857K* and *paf1Δ*. While the *spt16-E857K paf1Δ* double mutants grew extremely poorly at 30°C, *spt16-E857K paf1Δ rco1Δ* triple mutants grew fairly well at this temperature (Figure 60). This suppression is not complete, however, as neither the double mutants nor the triple mutants are able to grow at 37°C.

While it was easy to assess suppression effects with the above three PafC deletions, the situation with *leo1Δ* cells was somewhat more complicated. With the original strains used, *spt16-E857K leo1Δ* double mutants are somewhat impaired for growth at 39°C, but do not show significant growth defects even at this temperature (see Figure 61). Thus, when *spt16-E857K leo1Δ rco1Δ* triple mutants were generated, it appeared that these segregants were growing slightly better at 39°C than their *spt16-E857K leo1Δ* double-mutant counterparts (Figure 61); however, the relatively mild growth defect of the double mutants made this difficult to assess. That suppression is observed for several of the PafC genetic interactions, but not for others, suggests that the PafC deletions do not all have the same effect. This interpretation is supported by several previous studies of PafC deletions, which have shown that deleting different members of PafC have different effects on the cell (Betz et al. 2002, Mueller, Jaehning 2002, Porter, Penheiter & Jaehning 2005, Rondon et al. 2004).

In contrast to the suppression observed for several of the genetic interactions between PafC component deletions and *spt16-E857K*, no such suppression was observed for the genetic interactions involving *spt16-E763G*. Although both *spt16* mutations demonstrate genetic interactions with *ctr9Δ*, *cdc73Δ*, *paf1Δ* and *leo1Δ*, there was no *rco1Δ*-mediated suppression for any of the *spt16-E763G* interactions (Figures 58, 59, 60

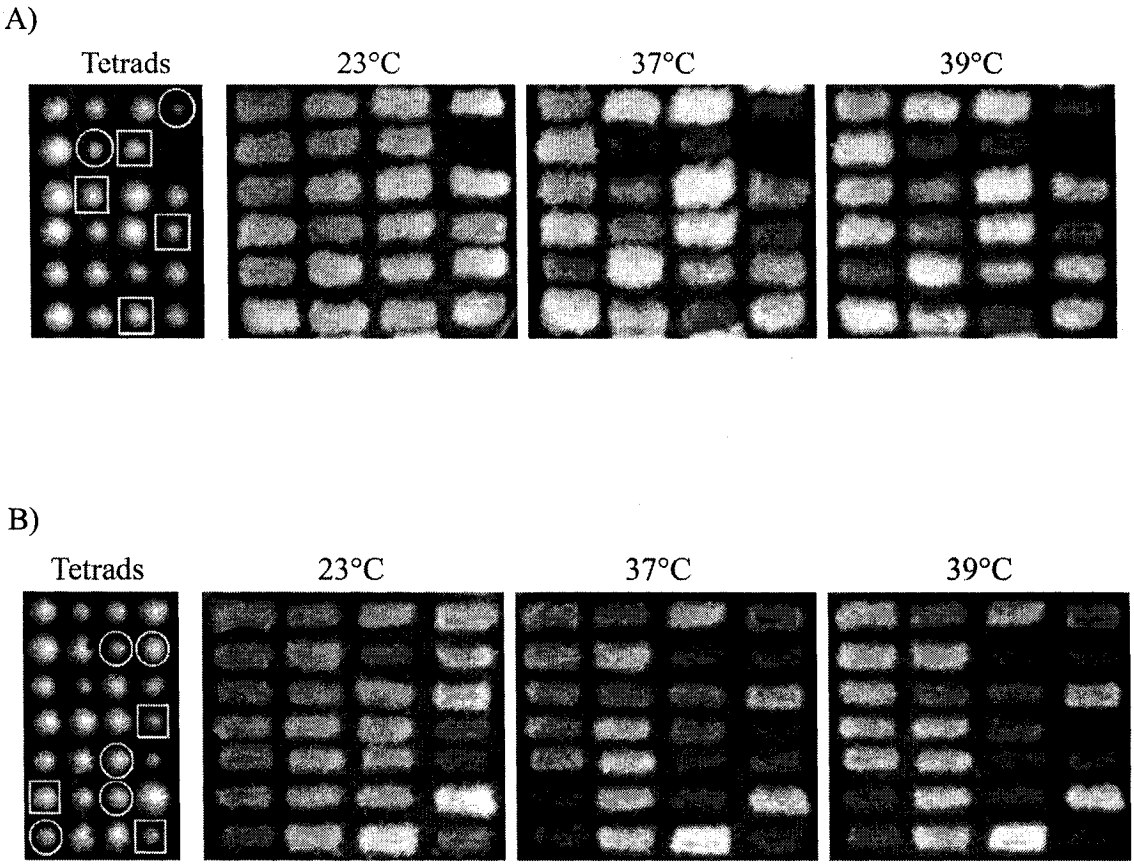

Figure 58. No *rco1Δ*-mediated suppression of the deleterious genetic interactions between *spt16-E857K* or *spt16-E763G* and *cdc73Δ*. Diploid cells heterozygous for *spt16-E857K* or *spt16-E763G*, *cdc73Δ* and *rco1Δ* were sporulated, and tetrad analysis was performed. All segregants from tetrad analysis were patched onto YEPD solid medium at 23°C, and replica-plated to YEPD for incubation at 23°C, 37°C and 39°C. A) Both the *spt16-E857K cdc73Δ* double mutants (outlined by circles) and *spt16-E857K cdc73Δ rco1Δ* triple mutants (outlined by squares) displayed temperature-sensitive growth, growing poorly at 37°C and 39°C. B) Both the *spt16-E763G cdc73Δ* double mutants (outlined by circles) and *spt16-E763G cdc73Δ rco1Δ* triple mutants (outlined by squares) displayed temperature-sensitive growth, growing poorly at 37°C and 39°C.

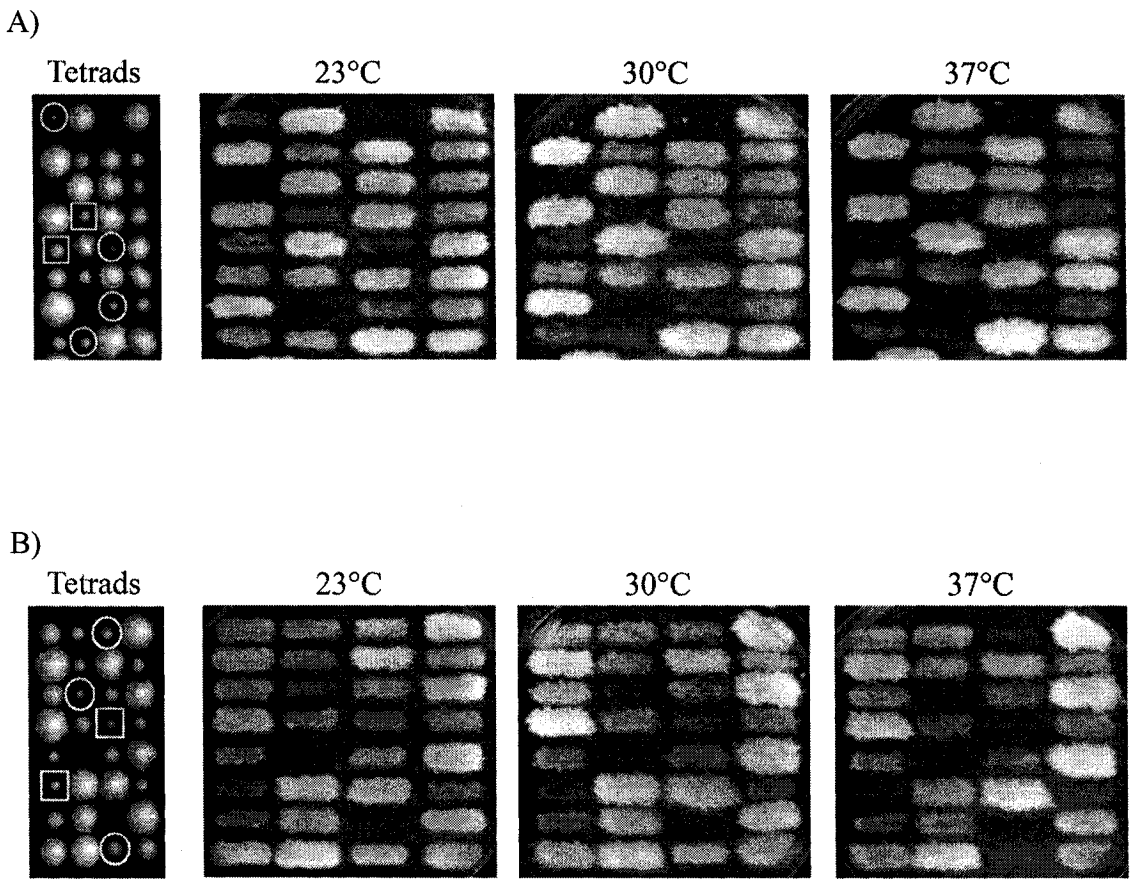

Figure 59. No *rco1Δ*-mediated suppression of the deleterious genetic interactions between *spt16-E857K* or *spt16-E763G* and *ctr9Δ*. Diploid cells heterozygous for *spt16-E857K* or *spt16-E763G*, *ctr9Δ* and *rco1Δ* were sporulated, and tetrad analysis was performed. All segregants from tetrad analysis were patched onto YEPD solid medium at 23°C, and replica-plated to YEPD for incubation at 23°C, 30°C and 37°C. A) Both the *spt16-E857K ctr9Δ* double mutants (outlined by circles) and *spt16-E857K ctr9Δ rco1Δ* triple mutants (outlined by squares) display temperature-sensitive growth, growing poorly at 30°C and 37°C. B) Both the *spt16-E763G ctr9Δ* double mutants (outlined by circles) and *spt16-E763G ctr9Δ rco1Δ* triple mutants (outlined by squares) display temperature-sensitive growth, growing poorly at 30°C and 37°C.

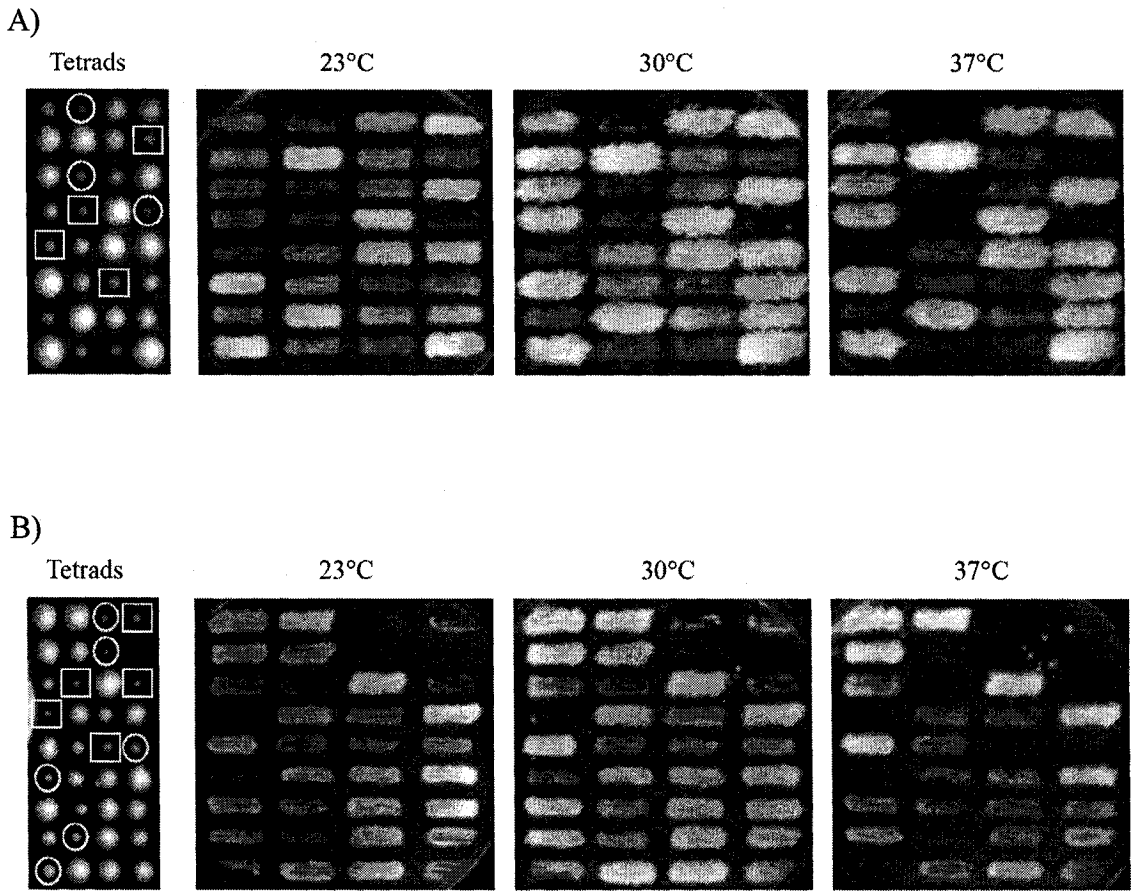

Figure 60. *rco1Δ*-mediated suppression of the deleterious genetic interaction between *spt16-E857K* and *paf1Δ*, but not between *spt16-E763G* and *paf1Δ*. Diploid cells heterozygous for *spt16-E857K* or *spt16-E763G*, *paf1Δ* and *rco1Δ* were sporulated, and tetrad analysis was performed. All segregants from tetrad analysis were patched onto YEPD solid medium at 23°C, and replica-plated to YEPD for incubation at 23°C, 30°C and 37°C. A) Both the *spt16-E857K paf1Δ* double mutants (outlined by circles) and *spt16-E857K paf1Δ rco1Δ* triple mutants (outlined by squares) display temperature-sensitive growth, growing poorly at 23°C and 30°C, but not at all at 37°C. The triple-mutant cells appear to grow somewhat better than the double-mutant cells at 30°C, although this suppression does not extend to growth at 37°C. B) Both the *spt16-E763G paf1Δ* double mutants (outlined by circles) and *spt16-E763G paf1Δ rco1Δ* triple mutants (outlined by squares) display temperature-sensitive growth, growing poorly at 23°C and 30°C, but not at all at 37°C.

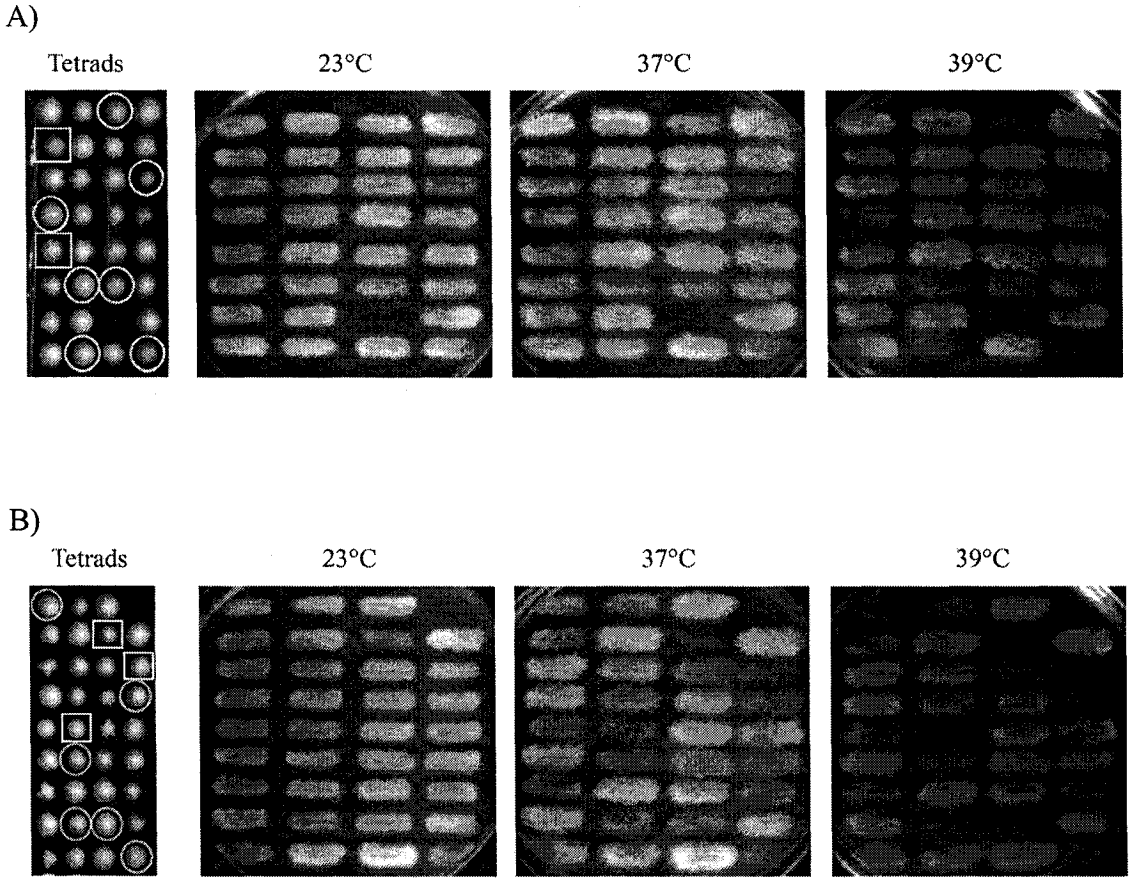

Figure 61. *rco1Δ*-mediated suppression of the deleterious genetic interaction between *spt16-E857K* and *leo1Δ*, but not between *spt16-E763G* and *leo1Δ*. Diploid cells heterozygous for *spt16-E857K* or *spt16-E763G*, *leo1Δ* and *rco1Δ* were sporulated, and tetrad analysis was performed. All segregants from tetrad analysis were patched onto YEPD solid medium at 23°C, and replica-plated to YEPD for incubation at 23°C, 37°C and 39°C. A) Both the *spt16-E857K leo1Δ* double mutants (outlined by circles) and *spt16-E857K leo1Δ rco1Δ* triple mutants (outlined by squares) display temperature-sensitive growth, growing poorly at 39°C. The triple-mutant cells appear to grow somewhat better than the double-mutant cells at 39°C. B) Both the *spt16-E763G leo1Δ* double mutants (outlined by circles) and *spt16-E763G leo1Δ rco1Δ* triple mutants (outlined by squares) display temperature-sensitive growth, growing poorly at 37°C and 39°C.

and 61). This general finding is consistent with the hypothesis that the genetic interactions between *spt16-E857K* and the PafC deletions involve both the chromatin-associated and the chromatin-independent roles of PafC, while the genetic interactions with *spt16-E763G* involve only the chromatin-independent role. As Rpd3C(S), and therefore Rco1, act on transcribed regions of DNA, it follows that *rco1Δ*-mediated suppression would only exist for genetic interactions that involve transcription elongation components. It has been noted that Spt16 abundance within transcribed regions is increased in *paf1Δ* strains (Mueller et al. 2004), perhaps indicating an increased requirement for Spt16 to overcome transcription defects caused by the loss of Paf1. If this idea is correct, then perhaps the Spt16-E857K mutant is impaired for the ability to overcome the effects of a *PAF1* deletion. In this model, normal levels of Rpd3C(S)-mediated histone deacetylation are inhibitory to Spt16 activity, and Spt16-E857K is particularly sensitive to the presence of deacetylated histones. In this model, Spt16-E763G is impaired differently than Spt16-E857K, and thus the presence or absence of Rpd3C(S)-mediated histone deacetylation has no effect on cells carrying the *spt16-E763G* mutation.

Thus, while the absence of Rpd3C(S)-mediated histone deacetylation is able to alleviate the lethality of several of the genetic interactions tested, it cannot overcome all of them. While Rpd3C(S) activity can be inhibitory when Spt16 is mutated, the absence of this activity is beneficial only for a subset of situations with deleterious *spt16* genetic interactions, and only in those involving the *spt16-E857K* mutation rather than the *spt16-E763G* mutation. Thus, there is a fundamental difference between how these two mutations in the *SPT16* gene affect Spt16 protein function. Both the *spt16-E857K* mutation and the *spt16-E763G* mutation have effects on the ability of the Spt16 protein to function during transcription, as evidenced by the ability of both mutations to produce an Spt phenotype. However, the specific perturbation of Spt16 protein function is likely different in each situation, as the absence of Rpd3C(S)-mediated histone deacetylation is beneficial only for genetic interactions involving the *spt16-E857K* mutant allele.

3.6 Interactions with Histone Acetyltransferases

The above results suggest that FACT does indeed have an activity that aids in overcoming the repressive effects of deacetylated histones that result from the activity of Rpd3C(S). One possibility is that FACT may interact with, or recruit, a histone acetyltransferase (HAT) complex to re-acetylate the histones that were previously deacetylated by Rpd3C(S). Alternately, FACT may simply work better in an environment where histones are acetylated, particularly when FACT activity is impaired due to mutations such as *spt16-E857K*.

There are many HAT complexes in yeast; however, NuA3 is a likely candidate for a HAT activity that facilitates FACT, because the HAT catalytic subunit of NuA3, Sas3, is known to interact physically with the N-terminal domain of Spt16 (John et al. 2000). This NuA3–Spt16 interaction may not be essential in otherwise wild-type cells, since cells containing either a ΔNTD form of Spt16 or a deletion of *SAS3* are alive and do not display severely impaired growth (O'Donnell et al. 2004, Reifsnyder et al. 1996). However, the loss of this NuA3–FACT interaction may account for the impaired growth of a ΔNTD form of Spt16 that also contains the E857K point mutation (O'Donnell et al. 2004). These observations suggest that the absence of a Sas3 interaction with Spt16, in combination with the impaired function of the *spt16-E857K* version of FACT, may lead to defects in cell growth. To assess this possibility, cells containing both *spt16-E857K* and *sas3Δ* were assessed for growth at a variety of temperatures; no synthetic growth impairment was observed (Figure 62). These negative results suggest that, although there may be a physical interaction between Spt16 and Sas3, the loss of this interaction is not responsible for the impaired growth observed with an *spt16-E857K* allele that is also missing its NTD. Genetic interactions between *spt16-E763G* and *sas3Δ* were also assessed; no synthetic growth impairment was observed for this combination of mutations (Figure 62). Since there are no obvious genetic interactions between *spt16-E857K* and *sas3Δ*, NuA3 is likely not a HAT complex that aids FACT significantly in opposing Rpd3C(S)-mediated histone deacetylation.

3.6.1 Interactions with *elp3Δ*, *gcn5Δ*, and *esa1-L254P*

The absence of a genetic interaction between FACT and NuA3 does not rule out the possibility that FACT has functional interactions with another HAT complex. Several

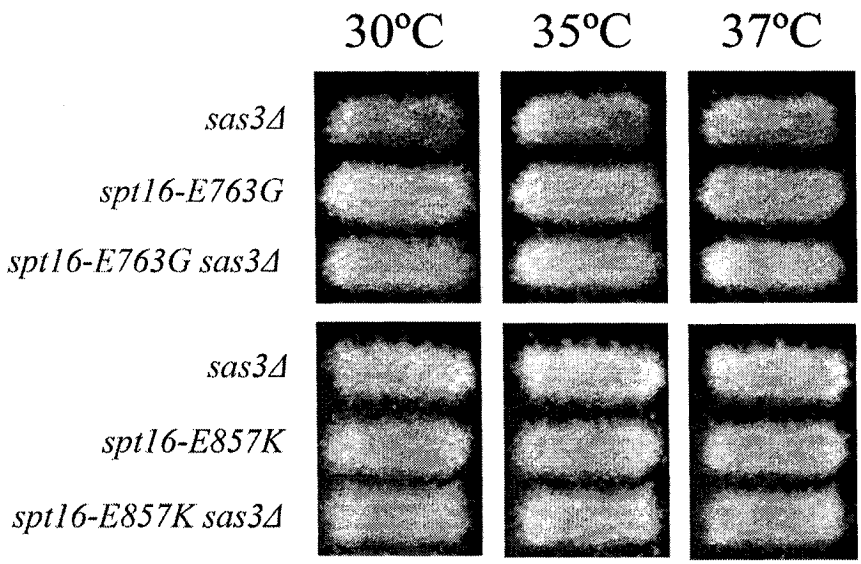

Figure 62. No deleterious genetic interactions exist between *spt16-E857K* or *spt16-E763G* and *sas3Δ*. Diploid cells heterozygous for *spt16-E857K* or *spt16-E763G* and *sas3Δ* were sporulated, and tetrad analysis was performed. Replica plates with patches of single and double mutants were incubated overnight on YEPD solid medium at the indicated temperatures. Both the *spt16-E857K sas3Δ* double mutants and the *spt16-E763G sas3Δ* double mutants grew as well as the single-mutant cells.

other HAT complexes have been identified with roles in transcription (Brown et al. 2000, Doyon, Cote 2004, Timmers, Tora 2005) – among these are ADA, SAGA, SLIK/SALSA, Elongator, NuA4, and Piccolo. ADA, SAGA, and SLIK/SALSA share the same catalytic subunit, Gcn5 (Grant et al. 1997, Pray-Grant et al. 2002, Sterner, Belotserkovskaya & Berger 2002), while Elongator has a different catalytic subunit, Elp3 (Wittschieben et al. 1999). Previous work has indicated that while Rpd3 does not appear to affect histone acetylation by Elp3, it may play a role in removing Gcn5-mediated histone acetylation (Vogelauer et al. 2000). Cells containing *elp3Δ* or *gcn5Δ* were crossed with cells containing *spt16-E857K* or *spt16-E763G* and tetrad analysis was carried out to assess genetic interactions between these genes. No significant synthetic growth impairment was observed for either the *spt16 gcn5Δ* double-mutant cells or the *spt16 elp3Δ* double-mutants cells (Figure 63). These results indicate that, as found for NuA3, the HAT complexes ADA, SAGA, SLIK and Elongator likely do not aid FACT significantly in opposing the effects of Rpd3C(S)-mediated histone deacetylation.

The catalytic subunit of NuA4 (Allard et al. 1999) and Piccolo (Boudreault et al. 2003), Esa1, is an essential protein, and thus a null allele of the *ESA1* gene cannot readily be used to assess genetic interactions (Clarke et al. 1999, Smith et al. 1998). While the Piccolo HAT complex has been suggested to mediate non-targeted histone acetylation by Esa1, the NuA4 HAT complex is thought to be involved in gene-specific histone acetylation (Boudreault et al. 2003). In addition, the NuA4 HAT complex has been shown to promote transcription from a nucleosomal template (Allard et al. 1999), further suggesting a role for Esa1 in transcription. Furthermore, Esa1 and Rpd3 have been shown to mediate opposing histone acetylation and deacetylation of the same lysine residue (H4K12) (Vogelauer et al. 2000), making Esa1 a likely target for aiding FACT to overcome Rpd3C(S)-mediated histone deacetylation. Because the *ESA1* gene is essential, I assessed genetic interactions using a point mutant form of this HAT, *esa1-L254P* (Clarke et al. 1999). The *esa1-L254P* mutation causes temperature sensitivity, and encodes a version of Esa1 that is both defective for HAT activity *in vitro* and causes decreased levels of acetylated H4 at the restrictive temperature (37°C) *in vivo* (Clarke et al. 1999).

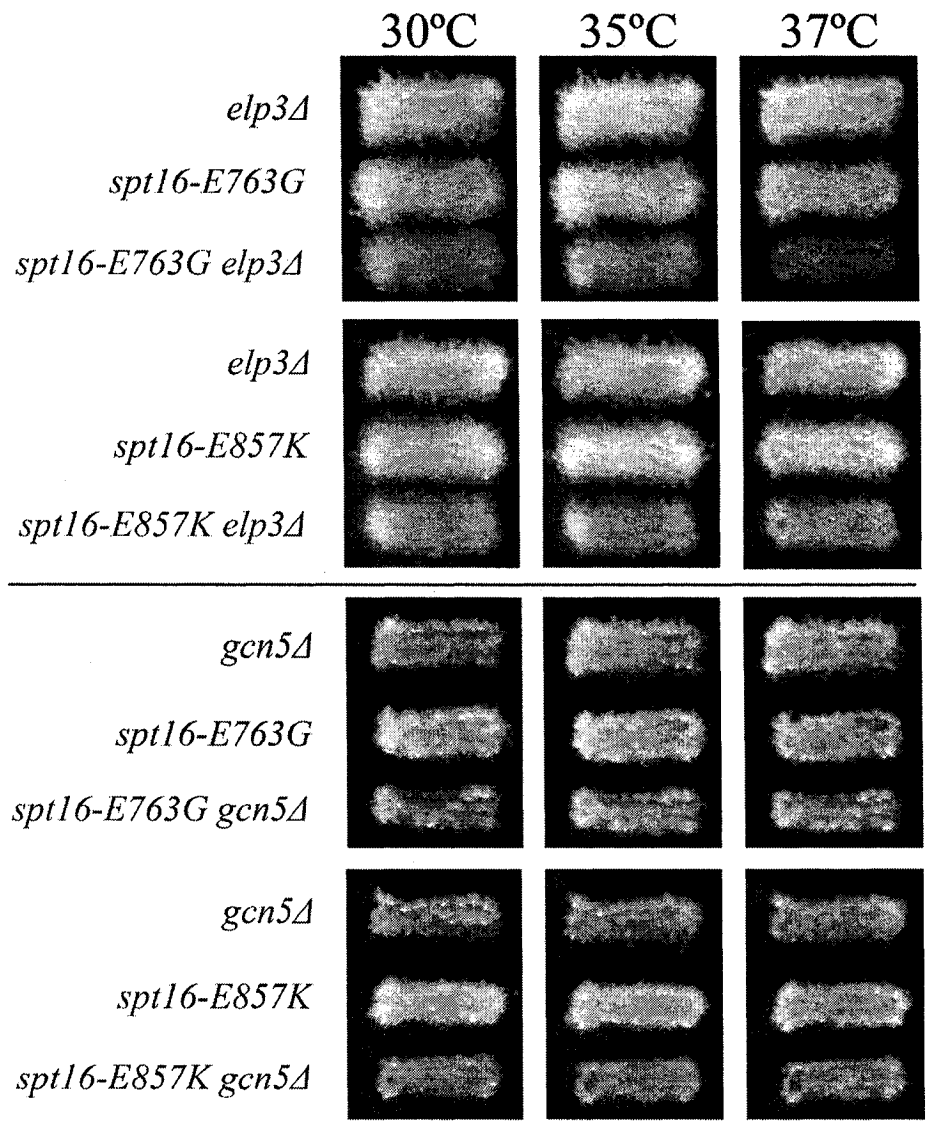

Figure 63. No deleterious genetic interactions exist between *spt16-E763G* or *spt16-E857K* and either *elp3Δ* or *gcn5Δ*. Diploid cells heterozygous for *spt16-E857K* or *spt16-E763G* and *elp3Δ* or *gcn5Δ* were sporulated, and tetrad analysis was performed. Replica plates with patches of single and double mutants were incubated overnight on YEPD solid medium at the indicated temperatures. All four double mutants grew as well as the single-mutant cells.

To assess whether a genetic interaction exists between *SPT16* and *ESA1*, tetrad analysis was carried out. Cells containing either the *spt16-E857K* mutation or the *spt16-E763G* mutation were crossed with *esa1-L254P* cells, the resulting diploids were sporulated, and the haploid spore products assessed for growth defects. This initial assessment produced many spores that failed to germinate, thereby making it difficult to analyse whether genetic interactions exist between these two genes. Therefore, one of the *esa1-L254P* segregants that did germinate was backcrossed to the *spt16*-mutant parental strains, and tetrad analysis was again carried out.

This second round of tetrad analysis of *esa1-L254P* cells crossed with *spt16-E857K* cells yielded double-mutant segregants that grew into colonies of several different sizes (Figure 64). In addition, in each cross there were still a substantial number of spores that failed to germinate, and other spore products that grew quite poorly, regardless of whether they carried a particular mutation. Because of this variable growth, it was difficult to determine whether a genetic interaction exists for either double mutant. Therefore, the segregants from these crosses were patch-plated onto solid medium, and the resulting patches were replica-plated to several temperatures for further growth. This type of analysis suggested that a deleterious genetic interaction does exist between *spt16-E857K* and *esa1-L254P* (Figure 64). However, these double-mutant cells were not all impaired to the same degree, making it difficult to determine the extent of the deleterious interaction between these two mutations. In an attempt to eliminate this variability, one of the better-growing *spt16-E857K esa1-L254P* double-mutant segregants was crossed with cells of a strain containing neither mutation, and tetrad analysis was once again carried out. Satisfyingly, the *spt16-E857K esa1-L254P* double-mutant segregants from this cross all demonstrated a similar degree of impairment, exhibiting temperature-sensitive growth at 35°C (Figure 64).

This deleterious genetic interaction between *spt16-E857K* and *esa1-L254P* may mean that NuA4 and/or Piccolo is a HAT complex that aids FACT in opposing Rpd3C(S)-mediated histone deacetylation. Based on previous results implicating NuA4 in gene-specific histone acetylation (Boudreault et al. 2003) showing that NuA4 facilitates transcription from a nucleosomal template (Allard et al. 1999, Galarneau et al. 2000), NuA4 is a more likely candidate for this function. Supporting this idea is the

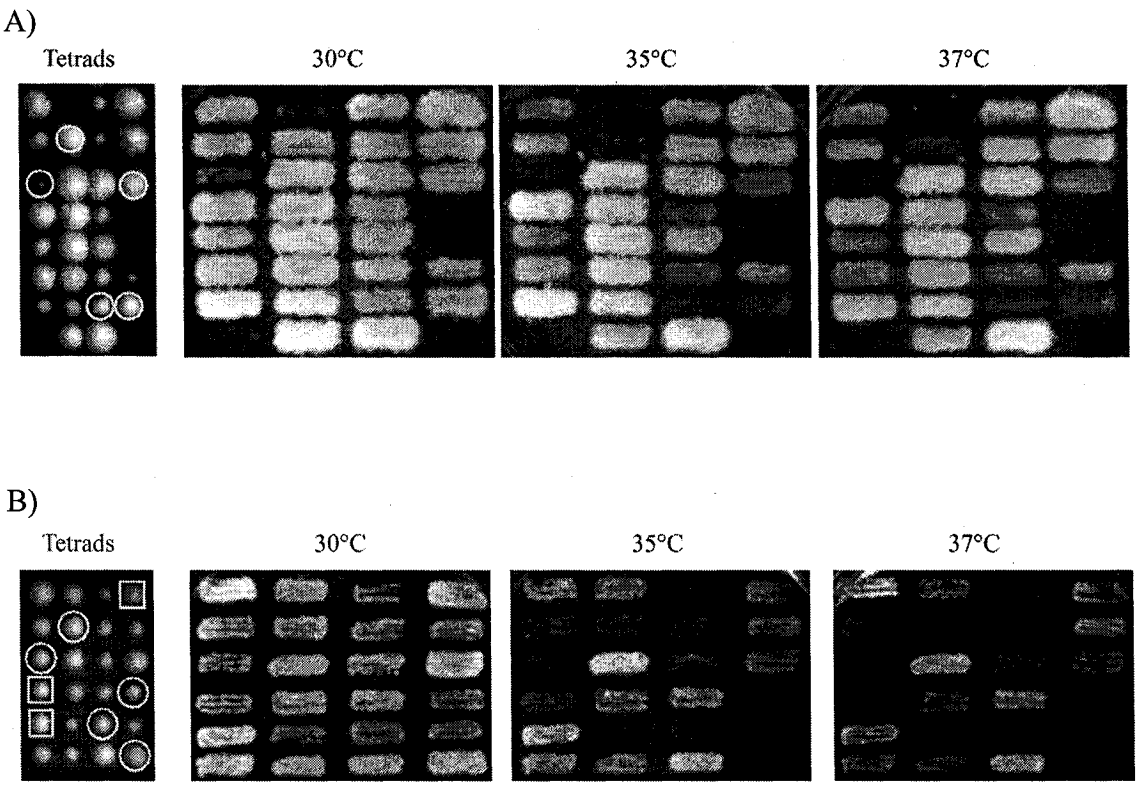

Figure 64. Deleterious genetic interactions between *spt16-E857K* and *esa1-L254P*. Diploid cells heterozygous for *spt16-E857K* and *esa1-L254P* were sporulated, and tetrad analysis was performed. All segregants from tetrad analysis were patched onto YEPD at 30°C, and replica-plated to YEPD for incubation at 30°C, 35°C and 37°C. A) The *spt16-E857K esa1-L254P* double mutants displayed temperature-sensitive growth, growing poorly at 35°C and 37°C. However, the double-mutant segregants are not all impaired to the same degree. B) One of the better-growing double mutants from (A) was backcrossed to a related strain carrying neither mutation, yielding the segregants shown here. The *spt16-E857K esa1-L254P* double mutants (outlined by circles) displayed temperature-sensitive growth, growing poorly at 35°C and 37°C. The *esa1-L254P* single mutants (outlined by squares) also display temperature-sensitive growth, but were not as impaired as the double mutants.

observation that DNA replication itself appears to occur normally in *esa1-L254P* cells (Clarke et al. 1999). In addition, Esa1 and Rpd3 have been shown to mediate opposing histone acetylation and deacetylation of the same lysine residue (H4K12) (Vogelauer et al. 2000). This possibility warrants further investigation: if histone acetylation by Esa1 is important in cells containing the *spt16-E857K* mutation, perhaps a mutant form of histone H4 that cannot be acetylated on lysine 12 would show similar deleterious interaction as does the *esa1-L254P* mutation. Also of note is the observation that the *esa1-L254P* single-mutant segregants from this cross were also uniform in behaviour, but did not display the same degree of temperature sensitivity as had been previously reported (Clarke et al. 1999), likely due to differences in the genetic background between the original *esa1-L254P* strain that I used for these studies and the *spt16* mutant strain. This possibility might also explain the poor spore germination observed for my original crosses and tetrad analyses involving *esa1-L254P*.

In contrast, the *spt16-E763G* mutant allele gave different effects. Unlike the impaired growth observed with the *spt16-E857K* mutant allele, no deleterious genetic interaction was observed between *spt16-E763G* and *esa1-L254P*, even when the cells were grown at high temperatures (Figure 65). Thus, a deleterious genetic interaction with *esa1-L254P* is not common to all mutant alleles of *SPT16*. The lack of any genetic interaction between *esa1-L254P* and *spt16-E763G* is consistent with the absence of *rco1Δ*-mediated suppression for this mutant allele of *SPT16*. Thus, unlike the *spt16-E857K* mutation, the *spt16-E763G* mutation is likely not impaired in overcoming the repressive effects of deacetylated histones that result from the activity of Rpd3C(S).

3.6.2 Interactions with *rtt109Δ*

Recently, the Rtt109 protein was shown to be required for acetylation of histone H3 lysine 56 (H3K56ac), a modification that occurs during S phase and during DNA-damage repair (Hyland et al. 2005, Masumoto et al. 2005, Ozdemir et al. 2005, Recht et al. 2006). This acetylation is also found along transcribed regions of DNA, suggesting a possible link between this histone modification and transcription elongation (Schneider et al. 2006, Xu, Zhang & Grunstein 2005). Further investigations have shown that while Rtt109 is the HAT that catalyses this acetylation of H3K56 (Driscoll, Hudson & Jackson 2007, Han et al. 2007), to perform this action Rtt109 forms separate complexes with Asf1

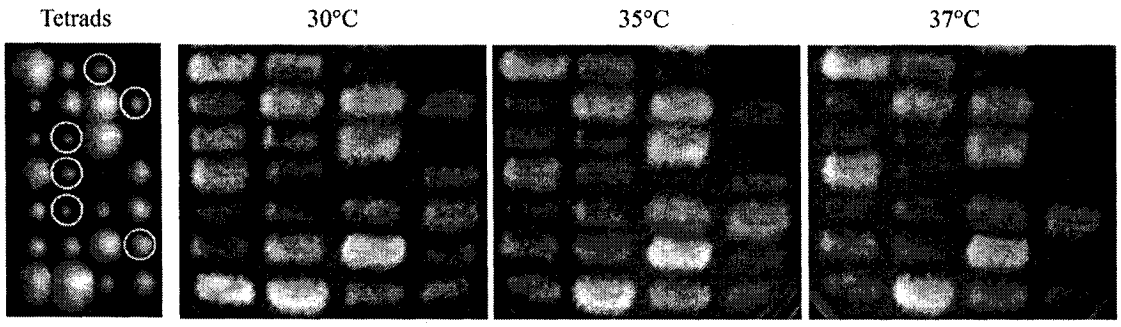

Figure 65. No deleterious genetic interaction between *spt16-E763G* and *esa1-L254P*. Diploid cells heterozygous for *spt16-E763G* and *esa1-L254P* were sporulated, and tetrad analysis was performed. All segregants from tetrad analysis were patched onto YEPD at 30°C, and replica-plated to YEPD for incubation at 30°C, 35°C and 37°C. The *spt16-E763G esa1-L254P* double mutants displayed temperature-sensitive growth, growing poorly 35°C and 37°C; however, this growth was no worse than that of the *esa1-L254P* single mutants.

and Vps75, two histone chaperones (Han et al. 2007, Selth, Svejstrup 2007, Tsubota et al. 2007). These two Rtt109 complexes appear to be functionally distinct, as cells lacking Asf1 exhibit severely decreased levels of total H3K56ac (Schneider et al. 2006) whereas cells lacking Vps75 do not (Selth, Svejstrup 2007). In addition, the Rtt109–Asf1 complex is important for genome stability, while the Rtt109–Vps75 complex is not (Selth, Svejstrup 2007, Tsubota et al. 2007). It has been further demonstrated by *in vitro* experiments that both the Rtt109–Asf1 and the Rtt109–Vps75 complex acetylate only non-nucleosomal histone H3, and cannot perform acetylation of nucleosomal H3 (Han et al. 2007, Tsubota et al. 2007). The correlation of the H3K56ac modification with S phase, and the ability of both Rtt109 HAT complexes to acetylate only non-nucleosomal H3, suggest that this HAT may not aid in overcoming transcription-related Rpd3C(S)-mediated histone deacetylation. However, the physical association between Rtt109 and both Asf1 and Vps75 suggested that further investigation into the Rtt109 HAT was warranted. I have shown above that *asf1Δ* has deleterious genetic interactions with *spt16-E857K*, yet have not determined which role(s) of Asf1 is important for this interaction. Perhaps it is the absence of the Rtt109–Asf1 complex, and the resulting decrease in H3K56ac levels, that causes the synthetic interaction between *spt16-E857K* and *asf1Δ*. If this were the case, I would expect to see a similar genetic interaction between *spt16-E857K* and *rtt109Δ*. In addition, I have also shown above that a slight deleterious genetic interaction may exist between *spt16-E857K* and *vps75Δ*. It is therefore also possible that a genetic interaction observed between *spt16-E857K* and *rtt109Δ* may reflect the loss of the Rtt109–Vps75 complex, rather than the Rtt109–Asf1 complex.

To assess whether a genetic interaction exists between *spt16-E857K* and *rtt109Δ*, tetrad analysis was performed to obtain double-mutant segregants. These segregants were patched and subsequently replica-plated to assess growth at a variety of temperatures. While there was some suggestion of synthetic growth impairment in the *spt16-E857K rtt109Δ* double-mutant cells at high temperatures, these patch tests were not sensitive enough to measure the degree of this impairment. Therefore, serial dilutions and spot testing was performed on the *spt16-E857K* and *rtt109Δ* single mutants, as well as five of the *spt16-E857K rtt109Δ* double-mutant segregants (Figure 66). This analysis indicated that the *spt16-E857K rtt109Δ* double-mutant cells grow more poorly at high temperatures

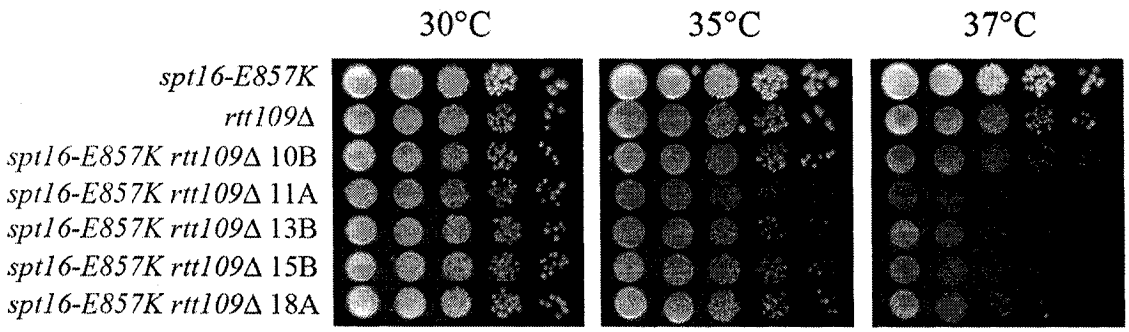

Figure 66. Deleterious genetic interaction between *spt16-E857K* and *rtt109Δ*. Following tetrad analysis, ten-fold serial dilutions of cells were spotted onto YEPD solid medium and incubated at the indicated temperatures for three days. The *spt16-E857K rtt109Δ* double mutants grew poorly at 37°C. One of the five double-mutant segregants (10B) grew better than the other four at the high temperature, likely due to the presence of a suppressor mutation. However, this improved growth is still less robust than that of the single-mutant cells.

(37°C and 39°C) than does either single mutant. Therefore, a deleterious genetic interaction does exist between *spt16-E857K* and *rtt109Δ*. This finding may indicate that the absence of the Rtt109–Asf1 protein complex is a reason for the deleterious genetic interactions between *spt16-E857K* and *asf1Δ*. However, the deleterious interaction observed between *spt16-E857K* and *rtt109Δ* is not as severe as that observed between *spt16-E857K* and *asf1Δ* (see Figure 28), which suggests that the absence of the Rtt109–Asf1 complex is not the only reason for the deleterious genetic interactions between *spt16-E857K* and *asf1Δ*. In addition, while a deleterious genetic interaction between *spt16-E857K* and *vps75Δ* has yet to be confirmed, the possibility exists that the reason behind this deleterious genetic interaction is the absence of the Rtt109-Vps75 complex.

3.7 Differences between *spt16-E857K* and *spt16-E763G*

The results of the genetic interactions described above indicate that the *spt16-E857K* and *spt16-E763G* mutations affect Spt16 function in different ways. Initial investigations performed with these two alleles on low-copy plasmids, however, did not identify any significant differences. Both mutant alleles produce proteins that are present at normal levels of abundance, and neither of them causes sensitivity to a wide variety of conditions, such as high temperature, inositol starvation, or the presence of hydroxyurea or 6-azauracil, among others (O'Donnell 2004). The first indication that the E763G substitution and the E857K substitution are somehow functionally different came out of studies that placed these substitutions in a version of Spt16 protein that was missing its N-terminal domain (Spt16-ΔNTD). While cells containing the Spt16-ΔN,E857K mutant form of Spt16 display impaired growth compared to cells with Spt16-ΔNTD or Spt16-E857K, the Spt16-ΔN,E763G mutant form of the protein confers no additional impairment (O'Donnell 2004, O'Donnell et al. 2004). This result, combined with the markedly different patterns of genetic interactions observed for the two alleles encoding these substitutions, both through SGA (O'Donnell 2004) and by directed testing as described above, indicates that there is something different about the effects of these two mutations. Thus, while *spt16-E857K* and *spt16-E763G* were identified by the same dominant Spt phenotype, they may produce this phenotype by different actions on Spt16 protein function during transcription. Therefore, I decided to examine these two

mutations in more detail, to determine whether additional differences between them could be identified.

3.7.1 Additional Spt Phenotypes of *spt16-E857K* and *spt16-E763G*

The initial Spt reporter alleles used to identify the *spt16-E857K* and *spt16-E763G* mutations, *his4-912δ* and *lys2-218δ*, have been widely used. However, these Spt reporter alleles can be activated by mutations in genes involved in either transcription elongation or transcription initiation (Winston 1992). As Spt16 has been reported to play a role in transcription initiation (Biswas et al. 2005, Biswas et al. 2006) as well as transcription elongation (Brewster, Johnston & Singer 2001, Orphanides et al. 1999), the *spt16-E857K* and *spt16-E763G* mutations may activate these two Spt reporter alleles through effects on different aspects of FACT function. To assess whether this may be the case, I examined the effects of *spt16-E857K* and *spt16-E763G* in yeast strains containing several additional Spt reporter genes.

One of these additional Spt reporters is the engineered *pGAL1-FLO8-HIS3* reporter gene (Prather et al. 2005), which takes advantage of an internal 'cryptic' promoter within the *FLO8* gene. It has been reported that *FLO8* contains an internal promoter that is only activated in cells with mutations in transcription elongation factors (Kaplan, Laprade & Winston 2003). This conclusion suggests that the internal promoter is only accessible by transcription machinery when there has been faulty chromatin reassembly following transcription of the full-length *FLO8* gene, thereby exposing the internal promoter region. The *pGAL1-FLO8-HIS3* reporter was designed to take advantage of this situation, by fusing the *HIS3* coding sequence downstream of this internal promoter, but out of frame with the *FLO8* coding sequence. This ensures that these *HIS3* sequences will only be expressed as functional mRNA when the internal promoter of *FLO8* is active. In addition, the endogenous *FLO8* promoter was replaced by the *GAL1* promoter, which is activated only when galactose is used as a carbon source. This situation provides a means by which transcription across the *FLO8* internal promoter can be regulated.

To determine whether the *spt16-E857K* or *spt16-E763G* mutations have a dominant effect on the expression of the *pGAL-FLO8-HIS3* reporter, I transformed cells containing this reporter gene, and normal chromosomal *SPT16*, with low-copy plasmids

containing either *spt16-E857K* or *spt16-E763G*. Transformants were patched onto solid medium and then replica-plated to medium lacking histidine and containing either glucose or galactose. Both *spt16-E857K* and *spt16-E763G* caused activation of the *pGAL-FLO8-HIS3* internal promoter, as evidenced by growth on the histidine-deficient, galactose-containing medium (Figure 67). In contrast, no growth was observed on the histidine-deficient, glucose-containing medium, indicating that, in both cases, transcription of *FLO8* from the *GAL1* promoter is required for activation of the internal promoter. This observation implies that the activation of the *FLO8* internal promoter is dependent on faulty chromatin reassembly during transcription of the upstream *FLO8* sequences. Thus, *spt16-E857K* and *spt16-E763G* produce a similar dominant effect over normal *SPT16* in the context of this reporter gene.

Two other Spt reporter genes used in my investigations were *his4-917δ* and *lys2-173R2*; these particular genes have been reported to be affected only by mutations affecting transcription initiation, such as mutations in the genes encoding TATA-binding protein (TBP) or components of the SAGA HAT complex, and not by mutations in *SPT6* or the genes encoding histones H2A and H2B (Winston 1992). The *his4-917δ* gene behaves in a manner similar to the other reporter genes, in that normal cells do not express a transcript of this gene that is functional, while cells containing the appropriate kind of Spt mutation do (Winston 1992, Winston et al. 1984). Therefore, while normal *his4-917δ* cells are unable to grow on medium that lacks histidine, cells containing an initiation type of Spt mutation can grow on histidine-deficient medium. The *lys2-173R2* reporter gene behaves in the converse manner. Normal cells containing this reporter gene express this gene in a functional manner and thus are able to grow on medium lacking lysine, while cells containing an initiation type of Spt mutation have altered transcription of this *lys2* mutant gene and cannot grow on lysine-deficient medium (Winston 1992). These two reporter genes were used to indicate whether *spt16-E857K* or *spt16-E763G* might have an effect on transcription initiation.

Since both of these mutant versions of *SPT16* have dominant effects on the other Spt reporter alleles used here, I first tested whether such a dominant effect exists using the initiation-type *his4-917δ* or *lys2-173R2* reporter genes. I transformed cells containing these reporter genes and normal chromosomal *SPT16* with low-copy plasmids containing

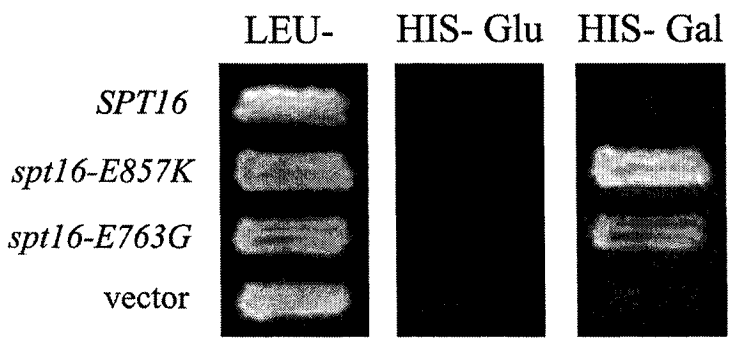

Figure 67. Both *spt16-E857K* and *spt16-E763G* activate the *pGAL1-FLO8-HIS3* cryptic promoter in a dominant fashion. Cells of the *pGAL1-FLO8-HIS3* strain FY2393 were transformed with the indicated alleles on *LEU2 CEN* vectors; transformants were patched on Leu- solid medium, and then replica-plated to both His- Glucose and His- Galactose solid medium and incubated for two days to assess activation of the *FLO8* internal cryptic promoter (growth on His- Galactose medium). Both *spt16-E857K* and *spt16-E763G* cells are able to grow on the His- Galactose solid medium, but not on the His- Glucose solid medium. While both alleles permit growth on His- Galactose medium, *spt16-E857K* appears to allow more robust growth than *spt16-E763G*, although the reason for this is unclear.

spt16-E857K or *spt16-E763G*. Transformants were patched onto solid medium and then replica-plated to medium lacking histidine or lysine to test for growth. Neither *spt16-E857K* nor *spt16-E763G* caused a dominant Spt phenotype using the *his4-917δ* and *lys2-173R2* reporters, as evidenced by lack of growth on histidine-deficient medium, and continued growth on lysine-deficient medium (Figure 68). Thus, neither *spt16-E857K* nor *spt16-E763G* produces a dominant effect over normal *SPT16* in the context of these reporter genes.

I also determined whether *spt16-E857K* or *spt16-E763G* alter expression of these Spt reporter alleles when they encode the only version of Spt16 in the cell. To do this, I first transformed *spt16Δ* cells (kept alive with a low-copy *SPT16* plasmid) containing *his4-917δ* and *lys2-173R2* with low-copy plasmids containing *spt16-E857K* or *spt16-E763G*. The original *SPT16* plasmid was then selected against, and the resulting derivatives, containing only *spt16-E857K* or *spt16-E763G*, were patched onto solid medium and replica-plated to medium lacking histidine or lysine to assess growth. While *spt16-E763G* did not cause an Spt phenotype using the *his4-917δ* and *lys2-173R2* reporters, as evidenced by lack of growth on histidine-deficient medium, and continued growth on lysine-deficient medium, cells containing *spt16-E857K* were able to grow on medium lacking histidine (Figure 68). Thus, although *spt16-E857K* does not alter expression of the *lys2-173R2* reporter gene to an extent measurable by growth effects on lysine-deficient medium, this *spt16* mutation does allow functional transcription of the *his4-917δ* reporter gene.

The production of a functional *HIS4* transcript from the *his4-917δ* reporter gene is thought to occur through a change in the transcription start site from the upstream delta element to the normal *HIS4* start site (Eisenmann, Dollard & Winston 1989). Transcription of the *his4-917δ* gene is normally initiated within the upstream delta element, producing a 5'-extended but non-functional transcript. In contrast, *his4-917δ* cells that have a mutation causing an Spt phenotype initiate transcription at the normal *HIS4* start site, and therefore produce functional *HIS4* transcripts. Thus, one possibility for the functional transcription of *his4-917δ* observed in *spt16-E857K* cells is that the Spt16-E857K protein allows use of an alternative transcription start site for the *his4-917δ* reporter gene. A recent report has suggested that Spt16 has a role in the formation of

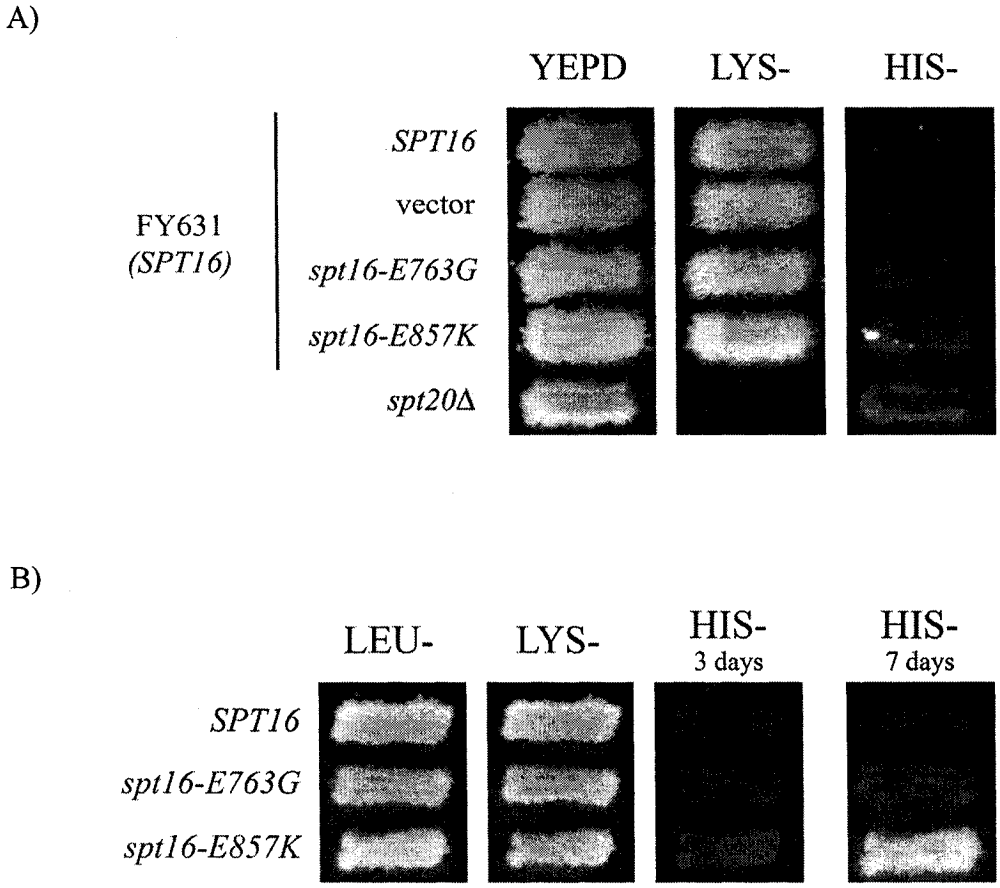

Figure 68. *spt16-E857K* has a recessive, but not a dominant, initiation Spt effect. A) Cells of the *his4-917δ* and *lys2-173R2* reporter strain FY631 were transformed with various *SPT16* plasmids; transformants were patched onto YEPD solid medium and replica plated to Lys- and His- solid media. Cells with an *spt20Δ* mutation were also patched as a positive control. Neither *spt16-E763G* nor *spt16-E857K* inhibited transcription from the *lys2-173R2* reporter, and although some background growth was observed indicating activation of the *his4-917δ* reporter, this was not significantly more than that of the vector control. B) Cells of the *his4-917δ* and *lys2-173R2* reporter strain RK57 was transformed with various *SPT16* plasmids; derivatives lacking the *SPT16 URA3* plasmid were identified and patched onto Leu- solid medium and replica plated to Lys- and His- solid media. Cells relying on *spt16-E857K* activated the *his4-917δ* reporter, although growth was not significant until 7 days after replica plating.

initiation complexes at promoters (Biswas et al. 2005), so it is not unreasonable to suggest that mutations in *SPT16* may affect the ability of the Spt16 protein to mediate initiation complex formation at various sites.

These experiments showed that *spt16-E857K* and *spt16-E763G* have different effects on the expression of Spt reporter genes, with *spt16-E857K* apparently having effects on both transcription initiation and elongation, while *spt16-E763G* affects only transcription elongation. Thus, the original effects on the *his4-912δ* and *lys2-128δ* reporter genes could result from either the initiation or elongation defects of the *spt16-E857K* mutation, but only from an elongation defect for the *spt16-E763G* mutation. These results support the hypothesis, suggested by the different patterns of genetic interactions, that these two *spt16* mutations affect different aspects of Spt16 function.

3.7.2 Protein Interactions of Spt16-E857K and Spt16-E763G

To help determine whether the *spt16-E857K* and *spt16-E763G* mutations have different effects on Spt16 protein function during the transcription process, I performed co-immunoprecipitation experiments using the Spt16-E857K and Spt16-E763G mutant proteins. Previous studies of various transcription components have identified Spt16 in complexes with numerous proteins involved in transcription (Krogan et al. 2002, Lindstrom et al. 2003, Simic et al. 2003, Squazzo et al. 2002), and thus it is possible that the E857K or the E763G substitution affects binding to certain proteins in a way that would be detectable by co-immunoprecipitation.

For these experiments, specific reagents directed against Spt16 were needed for immunoprecipitation. As our polyclonal anti-Spt16 antibody strongly detects a non-specific band at 40 kDa (O'Donnell 2004), I decided to use a tagged version of the Spt16 protein for these experiments. In these studies, the C terminus of Spt16 was fused to the S-tag (Novagen), a small fifteen-residue peptide that is part of the bovine RNase S ribonuclease enzyme (amino acids 1-15). Much like an epitope-antibody interaction, the S-tag binds to the S-protein (amino acids 21-124 of RNase S) with high affinity (K_d = 1.1 x 10^{-7} M) (Raines et al. 2000). Thus, S-protein, rather than an anti-S antibody, is used for detection and precipitation of S-tagged fusion proteins. Troy Perry, a former Honours student, had previously used the S-tag with Spt16. He has shown that C-terminal S-tag fusions do not interfere with normal Spt16 function, and that S-protein-HRP, used for

western blot detection, does not cross-react with other yeast proteins (Perry 2005). Therefore, I chose to use S-tagged forms of Spt16 in my analyses of mutant Spt16 protein interactions.

Following construction of the C-terminally S-tagged versions of Spt16-E857K and Spt16-E763G, I transformed plasmids containing the two alleles into yeast, and confirmed through a plasmid-shuffling procedure that the S-tag does not interfere with the ability of these two mutant proteins to provide essential Spt16 function. To ensure that these S-tagged forms of Spt16 can be detected by western blot, I prepared whole cell extracts from cells containing S-tagged Spt16, Spt16-E857K, or Spt16-E763G and from cells containing untagged Spt16. Indeed, the S-tagged form of Spt16 was detected in two independent extracts of each S-tagged cell type, while no signal was detected for the extracts prepared from untagged Spt16 cells (Figure 69). Therefore, I proceeded to use these S-tagged versions for Spt16 for my co-immunoprecipitation analyses.

3.7.2.1 Interactions with Histones H2B and H3

Because the primary function of Spt16 is thought to be its role as a histone chaperone, and since altered chromatin reassembly can cause an Spt phenotype using the elongation-type Spt reporters (a phenotype of both of these mutations), I first decided to examine whether these mutations caused an altered co-immunoprecipitation of histone proteins. First, I assessed whether histone H2B could be pulled down with any of the three versions of Spt16. As the interaction between Spt16 and histones is likely to be transient, the protein extractions were performed using several different salt concentrations and using potassium acetate, rather than sodium chloride. Previous work assessing the binding between Spt16 and Nhp6, a transiently associated subunit of FACT, showed that this interaction could be observed using potassium acetate, but not using sodium chloride (Brewster, Johnston & Singer 2001). The whole cell extracts were treated with S-protein agarose beads to pull down Spt16, and this precipitated material was then resolved using SDS-PAGE. This analysis showed that all three forms of Spt16 – Spt16, Spt16-E763G, and Spt16-E857K – were able to pull down histone H2B under all three salt conditions tested (Figure 70). For all three Spt16 proteins, substantially more H2B was recovered from the 50 mM pull-down than from the 100 mM or 150 mM pull-downs. However, the difference was more noticeable for the Spt16-E857K mutant, which pulled down less

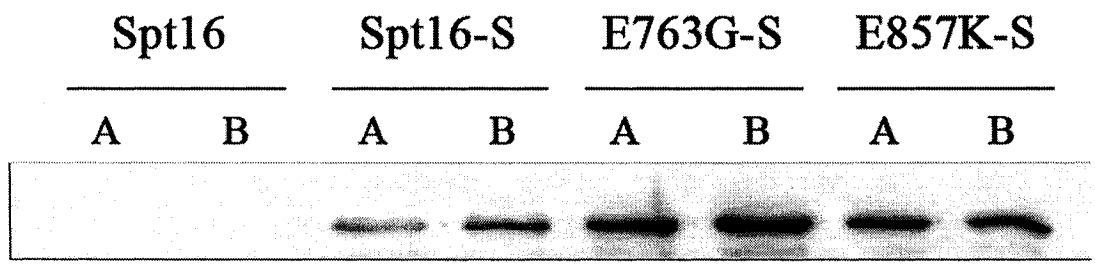

Figure 69. Detection of S-tagged Spt16. Whole cell extracts were prepared from two different cultures of cells containing either untagged Spt16, Spt16-S, Spt16-E763G-S or Spt16-E857K-S. Equal amounts of total protein were resolved by SDS-PAGE, transferred to PVDF, and probed using S-protein HRP.

A)

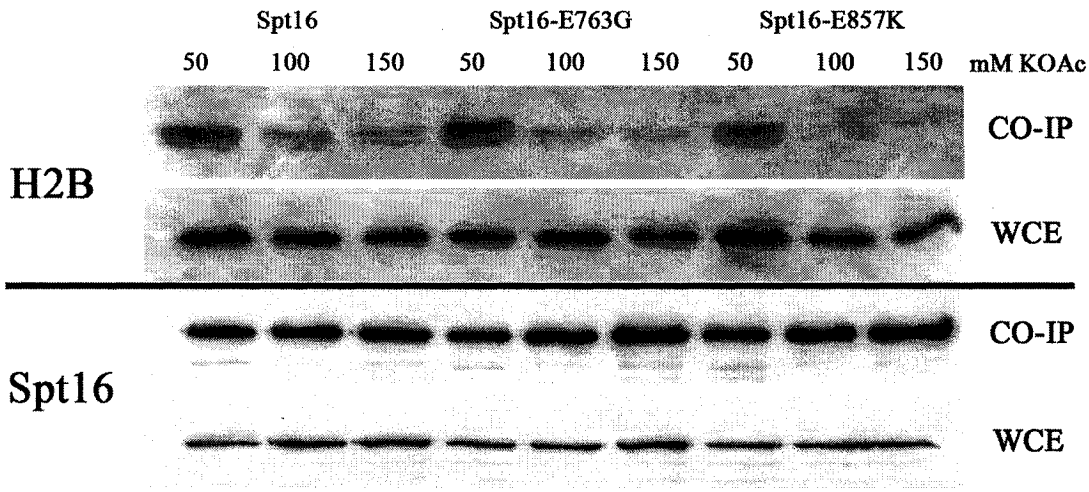

B)

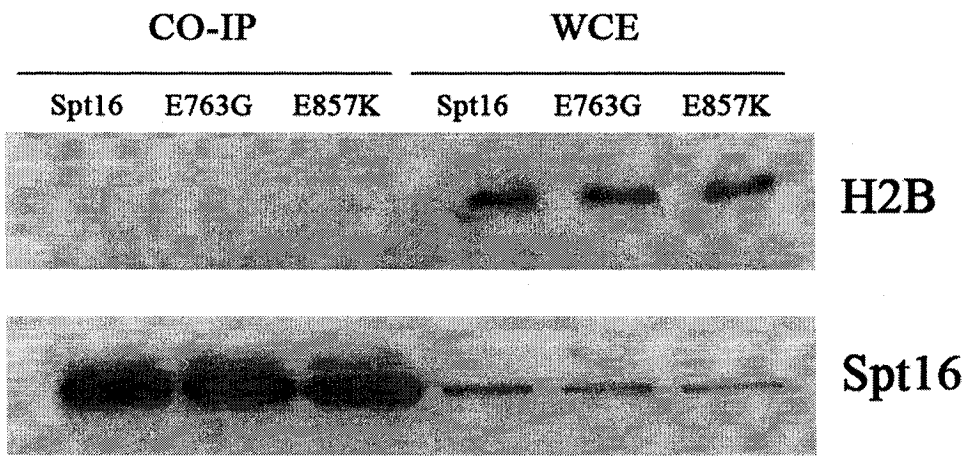

Figure 70. Spt16-E857K shows decreased pull-down of histone H2B, and DNA mediates the interaction between Spt16 and H2B. A) Whole cell extracts were prepared from cells containing S-tagged versions of the indicated form of Spt16, and Spt16 was pulled down using S-protein agarose beads (50 mM, 100 mM, or 150 mM KOAc buffer). The immunoprecipitated material was resolved by SDS-PAGE and transferred to PVDF. H2B was detected using α-HA (1:2000) and Spt16 using S-protein HRP (1:2000). H2B was polled fown by all three forms of Spt16. B) Whole cell extracts were prepared (100 mM KOAc buffer), precipitated and analysed as in (A), except that EtBr was present to disrupt protein-DNA interactions. H2B was not pulled down by any of the three forms of Spt16.

H2B at the higher salt concentrations than did either Spt16 or Spt16-E763G. Thus, the interaction between Spt16-E857K and histone H2B is weaker, compared to that of normal Spt16, while that of Spt16-E763G is not.

The E857K and E763G substitutions change a negatively charged amino acid to either a positively charged one (E857K), or a neutral one (E763G), and thus this change in charge could have an effect on protein-protein interactions. The impaired H2B pull-down in Spt16-E857K extracts could mean that the negative-to-positive change is more detrimental to the ability of Spt16 to pull down H2B than is the negative-to-neutral change. This hypothesis seems reasonable, as the histone proteins are basic, and therefore positively charged. Another possibility is that the E857K and E763G affect different portions of the Spt16 protein, and only the E857K change lies in a region that affects H2B pull-down.

Regardless, the ability to pull-down histone H2B leads to the question of whether Spt16 is pulling down H2A–H2B dimers, or is interacting with whole nucleosomes. To assess this question, the pull-downs were repeated and the western blots probed for the presence of histone H3. This time, only the 100 mM salt concentration was used, as this is where a difference was observed between Spt16 and Spt16-E857K on the H2B blots. Unlike what was observed for histone H2B, no detectable levels of histone H3 were observed from any of the pull-downs (Figure 71). This finding suggests that Spt16 is interacting primarily with free H2A–H2B dimers, rather than whole nucleosomes. This interpretation is consistent with the proposed role for Spt16 as a histone chaperone that removes one H2A–H2B dimer to allow passage of the elongating polymerase, then reassembles the nucleosome following polymerase passage (Belotserkovskaya et al. 2003).

Another question was whether protein–DNA interactions are required for the interaction between Spt16 and histone H2B. It is possible that the interaction between Spt16 and H2B is facilitated by the presence of nucleosomal DNA, and that Spt16 does not bind well to free histones. To assess this possibility, I treated the whole cells extracts with ethidium bromide (EtBr) to disrupt DNA structure, and maintained the same level of EtBr throughout the incubation with S-protein agarose beads and subsequent washes. This protocol has been previously shown to discriminate between protein interactions that

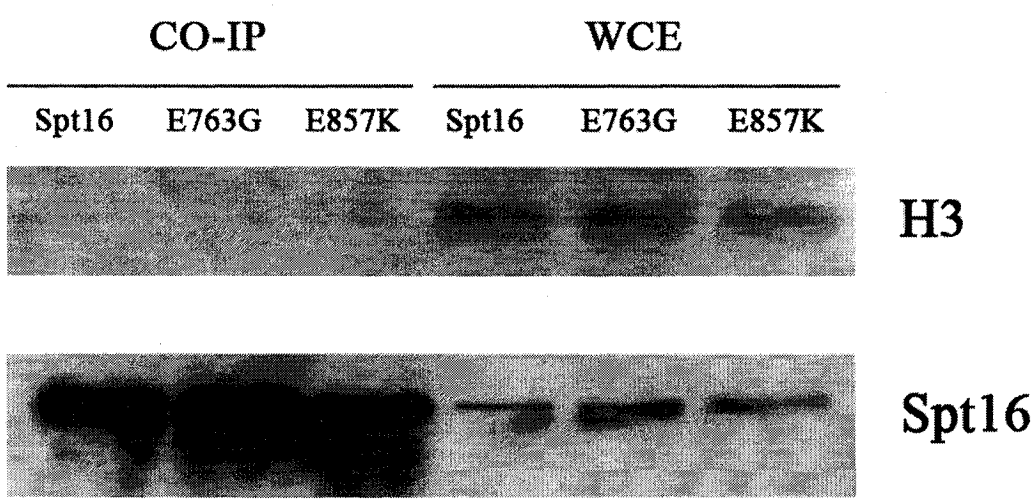

Figure 71. Histone H3 does not co-immunoprecipitate with Spt16. Whole cell extracts were prepared from cells containing S-tagged versions of the indicated mutant form of Spt16 (100 mM KOAc), and Spt16 was pulled down using S-protein agarose beads. The immunoprecipitated material was resolved by SDS-PAGE and transferred to PVDF. Histone H3 was detected using α-H3 (1:5000) and Spt16 using S-protein HRP (1:2000). No detectable levels of H3 were present in any of the pull-downs.

are mediated through DNA and those that are DNA-independent (Lai, Herr 1992). Unlike the result obtained when EtBr was absent, no detectable levels of H2B were observed when the Spt16 pull-down was performed in the presence of EtBr (Figure 70). This observation suggests that the interaction between Spt16 and histone H2B is mediated by DNA-protein interactions. However, it is also possible that the addition of EtBr and the subsequent removal of DNA from solution may affect the solubility of the histone proteins and cause them to precipitate out of solution, thus decreasing the amount of soluble H2B. To examine this possibility, I resolved equivalent amounts of EtBr-treated and untreated whole cell extracts, and probed for total levels of H2B. This experiment showed that, indeed, levels of total H2B were decreased in the EtBr-treated samples (Figure 72). Thus, the decreased pull-down of H2B by Spt16 in the EtBr samples may simply be due to a decrease in total H2B levels, rather than an absolute requirement for DNA to mediate this interaction.

3.7.2.2 Interactions with RNA Polymerase II

Since the Spt phenotype, as demonstrated by both Spt16-E857K and Spt16-E763G, is associated with altered patterns of transcription, I also determined whether either of these mutants displayed altered pull-down of RNAPII, compared to normal Spt16. Pull-downs were performed as described above for H2B and H3, and the western blot probed for the presence of RNAPII. This work showed that RNAPII was pulled down by all three versions of Spt16 (Figure 73). In addition, unlike what was seen for H2B, no decrease in RNAPII pull-down was observed for either mutant form. Thus, although Spt16-E857K is impaired in its interaction with histone H2B, no analogous impairment is observed for its interaction with RNAPII. Therefore, the E857K substitution does not cause a general defect in protein interactions related to transcription elongation.

Similar to that performed for the histone H2B pull-down, the interaction between Spt16 and RNAPII was also examined in the presence of EtBr. While the detection of RNAPII in this western blot was poor, this procedure suggested that RNAPII can still be pulled down by Spt16, even in the presence of EtBr. There also appeared to be no significant differences between normal Spt16 and either mutant version in this interaction (Figure 73). Thus, the interaction between Spt16 and RNAPII is not mediated exclusively through DNA. Again, to establish whether total levels of RNAPII were similar in the

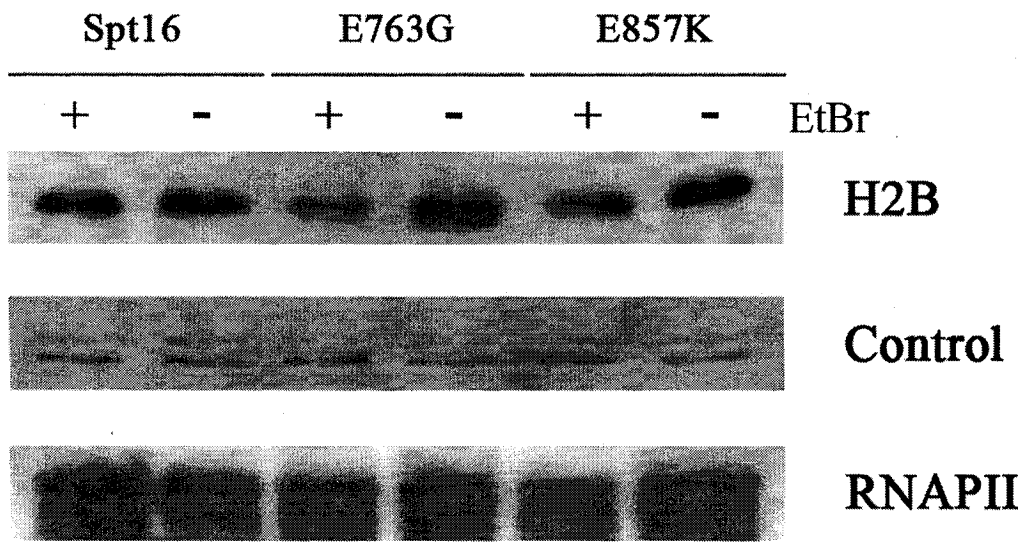

Figure 72. The amount of H2B, but not of RNAPII, in whole cell extract is affected by EtBr treatment. Whole cell extracts were prepared from cells containing S-tagged versions of the indicated mutant form of Spt16 (100 mM KOAc buffer), and either treated with EtBr to disrupt protein-DNA interactions or left untreated. The material was resolved by SDS-PAGE and transferred to PVDF. RNAPII was detected using α-RNAPII-CTD (1:15000) and H2B using α-HA (1:2000). The control is a non-specific band detected by the α-HA antibody. The amount of RNAPII is unaffected by EtBr treatment (the lower mobility band in the RNAPII blot appears in all blots with this antibody, which might be detecting a less phosphorylated form of RNAPII). In contrast, the amount of H2B is decreased in the extracts treated with EtBr.

A)

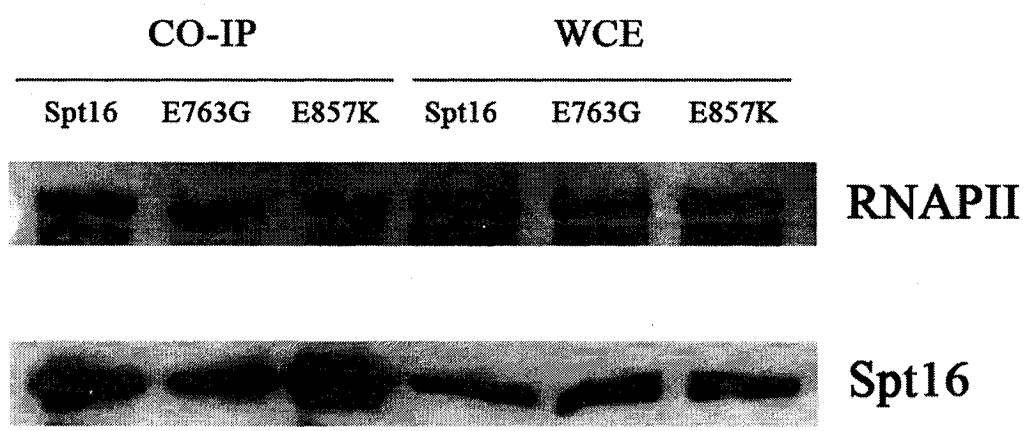

B)

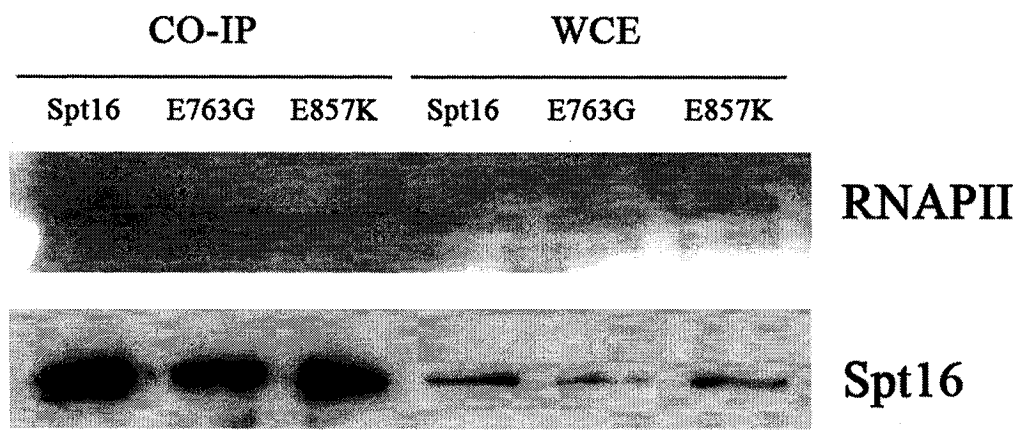

Figure 73. RNAPII co-immunoprecipitates with Spt16, and this interaction is not mediated by DNA. A) Whole cell extracts were prepared from cells containing S-tagged versions of the indicated form of Spt16 (100 mM KOAc buffer), and Spt16 was pulled down using S-protein agarose beads. The immunoprecipitated material was resolved by SDS-PAGE and transferred to PVDF. RNAPII was detected using α-RNAPII-CTD (1:15000) and Spt16 using S-protein HRP (1:2000). RNAPII was pulled down by all three forms of Spt16. B) Whole cell extracts were prepared, precipitated and analysed as in (A), except that EtBr was present to disrupt protein-DNA interactions. RNAPII was pulled down by all three forms of Spt16.

EtBr-treated and untreated extracts, I ran equivalent amounts of EtBr-treated and untreated whole cell extracts, and probed for RNAPII. Unlike the result obtained for histone H2B, total levels of RNAPII appeared unchanged by treatment with EtBr (Figure 72).

These investigations have shown that the Spt16 protein co-immunoprecipitates with both histone H2B and RNAPII, consistent with a role for Spt16 in mediating nucleosome dynamics during transcription. Although these experiments do not resolve whether these interactions are a result of direct protein interactions or are mediated through other proteins in a larger complex, the E857K substitution does lead to impaired interactions with histone H2B. In contrast, the relatively normal interaction of the Spt16-E857K mutant protein with RNAPII suggests that this substitution does not result in a general decrease in transcription-related protein interactions.

Chapter 4 DISCUSSION

4.1 FACT as a Transcription Elongation Complex

The FACT complex, composed of Spt16 and Pob3 (in yeast cells), is thought to modulate chromatin structure during processes such as transcription, DNA replication, and DNA repair (reviewed in (Belotserkovskaya et al. 2004, Formosa 2003, Neves-Costa, Varga-Weisz 2006)). Of these processes, the role of FACT in transcription has been the most studied; FACT has a well-documented role in transcription elongation (reviewed in (Belotserkovskaya, Reinberg 2004, Reinberg, Sims 2006), as well as a more recently identified role in transcription initiation (Biswas et al. 2005, Biswas et al. 2006). During transcription elongation, FACT is thought to function as a histone chaperone, removing one H2A–H2B dimer from nucleosomes ahead of elongating RNAPII and then reassembling the nucleosomes following RNAPII passage to help restore chromatin structure (Belotserkovskaya, Reinberg 2004, Reinberg, Sims 2006). Little remains known, however, about the other functional interactions engaged in by FACT in its roles in transcription, replication, and repair. My studies, as described in this thesis, have identified proteins engaged in processes functionally related to those carried out by Spt16 by determining genetic interactions for point-mutant versions of Spt16.

4.2 Genetic Studies can Improve our Understanding of FACT Function

Previous genetic studies of the Spt16 component of FACT relied on temperature-sensitive mutations that have multiple effects on Spt16 protein function; the two most widely used mutations in these studies have been the alleles *spt16-G132D* (Lycan et al. 1994, Malone et al. 1991, Prendergast et al. 1990) and *spt16-11* (Formosa et al. 2001). However, there are several drawbacks to the usage of these particular alleles in genetic screens. The *spt16-G132D* allele has been shown to produce an unstable protein (Xu, Singer & Johnston 1995), thereby making it difficult to interpret whether observations made with this allele reflect the effects of altered Spt16 protein function, rather than the demonstrably altered protein abundance. The *spt16-11* allele, on the other hand, produces an Spt16 protein impaired for DNA replication, for transcription initiation and for transcription elongation (Biswas et al. 2005, Formosa et al. 2001), thereby making it

difficult to determine which of these roles is involved in genetic interactions with mutations affecting other genes whose protein products are similarly involved in multiple processes.

As an attempt to avoid these ambiguities, and to gain a more complete picture of the functional interactions with proteins that are involved in processes similar to those carried out by Spt16 during transcription, I have focused on the *spt16-E857K* mutant allele. This allele was identified in a search for mutations in *SPT16* that give rise to a dominant Spt phenotype, and has also been shown to cause an Spt phenotype when present as the only version of *SPT16* in the cell (O'Donnell 2004). In addition, *spt16-E857K* has been shown to lack many other phenotypes (O'Donnell 2004), suggesting that this mutational change may specifically affect the transcriptional role of Spt16. My genetic studies using *spt16-E857K* shed more light on which other proteins are involved in similar processes during transcription, and which roles of Spt16 are affected by the E857K substitution. My investigations using other mutant alleles of *SPT16* indicate that not all mutations in *SPT16* have the same effect on Spt16 protein function, and that Spt16 is likely to have several different roles during the transcription process.

The genetic interactions that I identified in my work are listed in Tables 4 and 5.

4.3 Genetic and Physical Interactions Suggest that the Spt16-E857K Mutant Protein has Impaired Nucleosome Interactions

Using the *spt16-E857K* mutant allele, I identified other mutations that have deleterious genetic interactions with this *spt16* allele, and determined which of these deleterious genetic interactions can be alleviated by inactivation of the Rpd3C(S) histone deacetylase, suggesting that these deleterious interactions reflect transcriptional defects. I also showed that Spt16-E857K is impaired for the ability to co-immunoprecipitate histone H2B (Figure 70), suggesting that interactions between Spt16-E857K and the H2A–H2B dimer are weakened. Taken together, these results suggest that the *spt16-E857K* mutant allele encodes a version of Spt16 protein that is impaired for its interactions with nucleosomes and/or nucleosome components, affecting the ability to reassemble nucleosomes following RNA polymerase passage.

This hypothesis can explain many of the observations that have been made using the *spt16-E857K* allele. Central among these is the Spt phenotype, which can be created

Table 4. Allele-Specificity of Synthetic Lethality in my SYNL Yeast Strains

	bur2	***hir1***	***hir2***	***hir3***
spt16-E857K	Yes	Yes	Yes	Yes
spt16-E763G	No	No	No	No
spt16-312	No	No	No	No
spt16-319	Yes	Yes	Yes	Yes
spt16-G132D	No	No	No	No
spt16-Δ(6-435)	No	No	No	No
spt16-ΔNTD	No	No	No	No
spt16-4	No	No	No	No
spt16-6	Yes	Yes	Yes	Yes
spt16-7	No	No	No	No
spt16-8	No	No	No	No
spt16-9	Yes	Yes	Yes	Yes
spt16-9a	No	No	No	No
spt16-9b	No	No	No	No
spt16-9c	No	No	No	No
spt16-11	Yes	No	No	No
spt16-12	No	No	No	No
spt16-16a	Yes	Yes	Yes	Yes
spt16-24	No	No	No	No
spt16-INM27	Yes	Yes	Yes	Yes
spt16-AM21	Yes	Yes	Yes	Yes
spt16-IM25	Yes	No	No	No
spt16-IM28	Yes	Yes	Yes	Yes
spt16-IM313	Yes	Yes	Yes	Yes
spt16-ANM318	Yes	Yes	Yes	Yes

Table 5. Summary of *spt16-E857K* and *spt16-E763G* Genetic Interactions

Gene Tested	*spt16-E857K*	*spt16-E763G*
ASF1	SS	No
BUR1	SS	No
BUR2	SL - S	No
CDC73	SS - NS	SS - NS
CTK1	No	NT
CTR9	SS - NS	SS - NS
EAF3	No	No
ELP3	No	No
ESA1	SS	No
GCN5	No	No
HHF1	No	No
HHT1	SS	No
HIR1	SL	No
HIR2	SL - S	No
HIR3	SL	No
JHD1	No	NT
LEO1	SS - S ?	SS - S ?
NAP1	No	SS - NS
PAF1	SS - S	SS - NS
RAD6	No	No
RCO1	No	No
RTF1	No	No
RTT106	SS	No
RTT109	SS	NT
SAS3	No	No
SET2	No	No
SIN3	No	No
SPT4	SS	SS
SPT5	SS - S	SS - NS
SPT6	SS - NS	SS - NS
SWD1	No	No
SWD3	No	No
VPS75	M	M

SL = Synthetic-Lethal
SS = Synthetic-Sick
No = No Deleterious Genetic Interaction
M = Potential Deleterious Genetic Interaction – needs verification
NT = Not Tested
Where *rco1Δ*-mediated suppression was tested:

- S = Suppression
- NS = No Suppression

by the ability to access and initiate transcription from sequences that are not normally used for transcription initiation because they are repressed by chromatin structure. One possible mechanism by which these so-called 'cryptic' promoters, specifically those that lie within a transcribed region, can be made accessible to RNAPII is the impaired reassembly of the nucleosomes that have been disassembled during transcription from the upstream promoter (Kaplan, Laprade & Winston 2003). In this light, the decreased physical interaction linking Spt16-E857K and histone H2B as suggested by my co-immunoprecipitation studies may provide a mechanism to explain the Spt phenotype observed in these mutant cells. The Spt16-E857K protein is probably able to mediate the disassembly of nucleosomes during transcription, because cells relying on the Spt16-E857K protein grow fairly normally. However, the decreased interaction between this mutant Spt16 protein and the histone H2A–H2B dimer extracted from the nucleosome may result in a loss of this histone dimer before the nucleosome can be reassembled, leading to improperly reassembled histones. This improper nucleosome reassembly, in turn, impairs chromatin repression, which leads to initiation of transcription from 'cryptic' promoters that are normally repressed by chromatin structure.

The dominant Spt phenotype of spt16-E857K can be understood in a similar manner. In this situation, where there are approximately equal amounts of normal Spt16 and mutant Spt16-E857K protein present in the cells, each version of Spt16 will be found in roughly half of the total amount of FACT complex. Thus, competition will exist between the normal and mutant FACT complexes for this disassembly and reassembly of nucleosomes encountered by the elongating RNAPII. Therefore, the nucleosomes that would otherwise occlude a 'cryptic' promoter will be improperly reassembled some of the time, when the Spt16-E857K-containing FACT is responsible for reassembly of that nucleosome. This degree of poor assembly would thereby allow transcription to occur from this promoter.

Several recent studies have suggested that exchange of histones within nucleosomes occurs more frequently than previously thought, with exchange of histone H2B occurring at both active and inactive genes, while that of histone H3 is localized primarily to active promoter regions, in addition to chromatin boundary elements (Dion et al. 2007, Jamai, Imoberdorf & Strubin 2007). These high rates of histone exchange

identified in these studies suggests that during transcription it is unlikely that a nucleosome is reassembled with the same H2A–H2B dimer that was displaced from the nucleosome. This inference may mean that, although Spt16 plays a role in the reassembly of nucleosomes following polymerase passage, there is exchange of the displaced histone dimers with a pool of non-nucleosomal histone dimers. Perhaps one Spt16 molecule is responsible for the removal of the histone dimers ahead of the elongating RNAPII, while another Spt16 molecule reassembles the nucleosomes following polymerase passage, using H2A–H2B dimers from the histone pool. In this model, if Spt16-E857K is impaired for interactions with H2A–H2B dimers, perhaps nucleosome disassembly remains possible, but Spt16-E857K may be less able to shuttle an H2A–H2B dimer from the histone pool to the site of nucleosome reassembly, and therefore cannot properly reassemble nucleosomes.

The *spt16-E857K* mutation also causes deleterious consequences upon alterations in histone-gene dosage, particularly those which increase the relative expression of histones H2A and H2B compared to that of histones H3 and H4 (Figure 25). Increased amounts of H2A–H2B may result in an imbalance of histones in the nucleus, with a relative decrease in the amounts of H3 and H4. This hypothesis is based on the proposed mechanisms for nuclear import of histones, with H2A–H2B dimers able to use both a unique nuclear-import pathway as well as the primary H3–H4 import pathway (Greiner, Caesar & Schlenstedt 2004, Mosammaparast et al. 2001), whereas H3 and H4 cannot use the H2A–H2B import pathway (Greiner, Caesar & Schlenstedt 2004, Mosammaparast et al. 2002). Thus, an increase in the amount of H2A and H2B would result in a decreased nuclear import of H3 and H4, as a competition for the H3–H4 import pathway would exist. Somehow, this hypothesized decrease in nucleus-localized H3–H4 is deleterious to cells relying on *spt16-E857K*. Perhaps the proposed impairment of nucleosome reassembly in *spt16-E857K* cells, combined with a general decrease in the ability to form proper nucleosomes resulting from a scarcity of histones H3 and H4, leads to chromatin that is so improperly packaged that the cell is compromised for growth.

The deleterious genetic interactions between *spt16-E857K* and mutations in other genes involved in transcription also support the hypothesis that the E857K substitution affects the ability of Spt16 protein to function during the transcription process. Some of

these results also suggest that the acetylation state of nucleosomes is important to cells containing the *spt16-E857K* mutation. Two observations that support this hypothesis are the deleterious genetic interaction between *spt16-E857K* and *esa1-L254P* (encoding a mutant histone acetyltransferase) (Figure 64), and the ability of a deletion of *RCO1* (encoding a component of the Rpd3C(S) histone deacetylase complex) to suppress other deleterious genetic interactions for *spt16-E857K*. Esa1, as a component of the NuA4 HAT, is required for transcriptional regulation (Allard et al. 1999, Galarneau et al. 2000, Nourani et al. 2004), and cells relying on *esa1-L254P* exhibit decreased levels of histone acetylation, particularly after incubation at a restrictive temperature (Clarke et al. 1999). In contrast, cells lacking the Rco1 protein show an increase in histone acetylation within coding regions of genes (Carrozza et al. 2005, Keogh et al. 2005), suggesting that Rpd3C(S) activity removes acetyl groups from histones that have been acetylated during transcription, thereby restoring nucleosomes to a less acetylated state (Carrozza et al. 2005, Keogh et al. 2005). Thus, both *esa1-L254P* and *rco1Δ* would alter the acetylation properties of nucleosomes encountered by the Spt16 protein (and thus also FACT), and may thereby affect how effectively the FACT complex can process these nucleosomes. This idea suggests that one function of the Spt16-E857K mutant protein is facilitated by acetylated histones (as maintained in *rco1Δ* cells), but impaired when histone acetylation levels are decreased (as in *esa1-L254P* cells). One possibility is that poorly acetylated histones due to the *esa1-L254P* mutation are not reassembled by the Spt16-E857K version of FACT as effectively as are properly acetylated histones, thus leading to severely dysfunctional chromatin. An alternative possibility is that the *spt16-E857K* mutation might impair nucleosome disassembly, as triggered by RNAPII, in addition to impairing nucleosome reassembly, and that poorly acetylated nucleosomes are not disassembled effectively in cells with the Spt16-E857K version of FACT, thus preventing effective transcription by RNAPII.

4.4 Other *spt16* Mutant Alleles have Deleterious Genetic Interactions Similar to those of *spt16-E857K*

To gain a more complete understanding of the kinds of mutations in *SPT16* that cause deleterious genetic interactions similar to those of *spt16-E857K*, I assessed the genetic

interactions of numerous other *spt16* mutant alleles. These investigations were carried out using my four original synthetic-lethal strains, containing mutations in *BUR2*, *HIR1*, *HIR2* and *HIR3*. I found that, of the large number of *spt16* mutant alleles tested, only a subset exhibited deleterious genetic interactions with these *bur2* or *hir* mutations. Interestingly, all of the *spt16* mutant alleles in this subset (except *spt16-16a*) contain point mutations that alter the same region of the C terminus of the Spt16 protein (Figure 23). These observations suggest that only a small portion of the Spt16 protein mediates whichever common function is impaired in all of these mutant alleles.

As suggested for *spt16-E857K*, these other *spt16* mutant alleles may also impair the nucleosome reassembly function of Spt16. In support of this hypothesis, all of the *spt16* alleles that displayed deleterious genetic interactions similar to those of *spt16-E857K* also cause an Spt phenotype (Formosa et al. 2001, O'Donnell 2004, Perry 2005). In addition, many (but not all) of these *spt16* mutant alleles also cause a dominant Spt phenotype, similar to that of *spt16-E857K* (O'Donnell 2004, Perry 2005). These observations suggest that all of these alleles encode versions of Spt16 that are impaired for nucleosome reassembly.

4.5 Mutant Alleles of *SPT16* lacking the Genetic Interactions of *spt16-E857K*: *spt16-E763G* as an Example

While many of the *spt16* mutant alleles that I assessed had deleterious genetic interactions similar to those of *spt16-E857K*, many others were unlike *spt16-E857K* and did not demonstrate deleterious genetic interactions with the mutations in *BUR2*, *HIR1*, *HIR2* or *HIR3*. This difference suggests that these alleles encode versions of Spt16 that are not impaired in the same way as Spt16-E857K is, and would therefore possess normal nucleosome reassembly activity. However, several of these *spt16* mutant alleles that do not display these deleterious genetic interactions do cause an Spt phenotype (Formosa et al. 2001, O'Donnell 2004). Among this set, two mutant alleles – *spt16-E763G* and *spt16-312* (E763G, R784G, S819P) – also cause a dominant Spt phenotype (O'Donnell 2004). That these alleles cause an Spt phenotype, particularly for those that cause an Spt phenotype that is dominant, seems contrary to the hypothesis that these mutations do not affect the ability of Spt16 protein to properly reassemble nucleosomes.

To determine whether the lack of deleterious genetic interactions with the *bur2* and *hir* mutations is a misleading anomaly, and to better understand the effects of this type of *spt16* mutation, I experimented with the *spt16-E763G* mutant allele in more detail. This allele was chosen because it is one of the two mutant alleles with a dominant Spt phenotype that lack deleterious genetic interactions with the *bur2* and *hir* mutations, and the E763G substitution is also present in *spt16-312*, the other allele with a dominant Spt phenotype lacking *bur2* and *hir* genetic interactions. Genome-wide assessment of deleterious genetic interactions for *spt16-E763G* resulted in a set of interactions that is almost completely different from that for *spt16-E857K* (O'Donnell 2004). While, by that analysis, *spt16-E857K* has a spectrum of genetic interactions that primarily involve gene deletions eliminating proteins that function in transcription, the same cannot be said about *spt16-E763G*. These findings suggest that the effects of these two mutations on Spt16 protein function are, in fact, different and that the lack of deleterious genetic interactions between *spt16-E763G* and the *bur2* and *hir* mutations is not simply an anomalous result.

The deleterious genetic interaction between *spt16-E763G* and *nap1Δ* (Figure 32) provides some insight into the defects associated with this mutant Spt16 protein. Cells lacking Nap1 protein show decreased levels of nucleus-localized reporters for H2A and H2B (Mosammaparast, Ewart & Pemberton 2002), suggesting that Nap1 plays a role in the import of these histones into the nucleus. The same study suggested that *nap1Δ* cells demonstrate decreased transcription from the Ty1 promoter, presumably due to decreased deposition of H2A–H2B dimers onto chromatin, and might therefore exhibit an Spt phenotype (Mosammaparast, Ewart & Pemberton 2002). Thus, perhaps the Spt16-E763G mutant protein does not function well in an environment where chromatin assembly is impaired (due to the lack of Nap1 and its nucleosome-assembly function). My histone pull-down studies using Spt16-E857K and Spt16-E763G demonstrated that, while there is a weakened interaction linking Spt16-E857K to histone H2B, this interaction appears normal for Spt16-E763G. I found that, unlike *spt16-E763G*, *spt16-E857K* does not have deleterious genetic interactions with *nap1Δ* (Figure 32). If *nap1Δ* cells are already impaired for histone H2A–H2B assembly into chromatin, perhaps the weakened interaction linking these histones to Spt16-E857K does not impair the cells any further. That is, impaired chromatin reassembly in *spt16-E857K* cells may not produce a more

deleterious situation when chromatin structure has already been impaired (in the same way) by *nap1Δ*. In contrast, if *spt16-E763G* affects a different Spt16 function, cells containing this mutation may be further impaired by the impaired nucleosome assembly caused by *nap1Δ*. Perhaps the *spt16-E763G* mutation causes an impaired interaction between the Spt16 protein and some other protein involved in transcription, rather than a direct nucleosome reassembly defect. The Spt phenotype observed in *spt16-E763G* cells may therefore reflect a more direct effect on transcription, rather than an indirect effect manifested through nucleosome structure.

It remains possible that histone interaction with Spt16 is subtly impaired by the E763G substitution, but not to the same degree as by the E857K substitution, leading to only occasional failure to reassemble nucleosomes and consequent activation of cryptic promoters. The observation that growth resulting from activation of the internal promoter in the *pGAL1-FLO8-HIS3* reporter gene is less for *spt16-E763G* cells than for *spt16-E857K* cells (Figure 67) supports this hypothesis, as activation of this internal promoter almost certainly depends on faulty nucleosome reassembly following transcription from the upstream promoter. Another possibility is that the E763G substitution impairs Spt16 interactions with another, non-histone, protein that is involved in mediating transcription. Perhaps the Spt16-E763G mutant protein interacts poorly with another histone chaperone, thus indirectly impairing nucleosome reassembly, but in a manner distinct from that when Spt16 itself is impaired for its nucleosome reassembly activity. In this scenario, an interaction between Spt16 and this histone chaperone would be required for the nucleosome reassembly activity of the second histone chaperone, but not of FACT itself. The E763G substitution, by impairing the interaction with this second histone chaperone, impairs its ability to reassemble nucleosomes, thereby causing an Spt phenotype by an indirect mechanism. If this were the case, then deletion of this second histone chaperone may cause no additional deleterious phenotypes in an *spt16-E763G* cell. Therefore, based on my investigations, possible candidates for this second histone chaperone are Asf1, Rtt106, or HirC, as deletions of the genes encoding any of these proteins do not have deleterious genetic interactions with *spt16-E763G*.

In spite of these differences, some similarity exists between the genetic interactions of *spt16-E857K* and *spt16-E763G*. In particular, both *spt16* mutations show

deleterious genetic interactions with mutations in *SPT4*, *SPT5* or *SPT6*, or when genes encoding various members of PafC are deleted. All of those mutations affect important elements in transcription elongation, which is particularly evident by the facts that both *SPT5* and *SPT6* encode essential genes (Clark-Adams, Winston 1987, Swanson, Malone & Winston 1991), and that *paf1Δ* cells grow poorly (Shi et al. 1996). This genetic similarity between *spt16-E857K* and *spt16-E763G* suggests that, although these mutations may have different effects on Spt16 protein function, there must be some similarities in how these mutations affect the ability of Spt16, and therefore FACT, to carry out its roles during the transcription process.

4.6 Functional Differences between Spt16-E857K and Spt16-E763G

From my studies it is clear that, although *spt16-E857K* and *spt16-E763G* were both identified by virtue of the same dominant Spt phenotype, the two encoded substitutions cause different alterations of Spt16 function in many aspects. These differences are evident in the patterns of genetic interactions, the abilities to produce an Spt effect using various reporter genes, and the physical linkage to histone H2B. Both of these Spt16 protein substitutions alter an acidic amino acid residue; however, the E857K substitution causes a change to a basic residue whereas E763G causes a change to a neutral residue. Thus, one possible explanation for the differences observed with these two alleles is that the change from a negatively charged amino acid to a positively charged one (E857K) causes a more significant effect on Spt16 function than does the negative-to-neutral change (E763G). Many histone-chaperone proteins contain regions of acidic residues that are thought mediate interactions with the basic histone proteins. Thus, a change from an acidic amino acid to a basic residue, such as that in *spt16-E857K*, could affect binding to histone proteins more severely than an acidic-to-neutral change, such as that in *spt16-E763G*.

It has previously been shown that the C-terminal portion of Spt16, in which both of these substitutions are located, is required for essential function. In fact, a mutant form of Spt16 that terminates at the HindIII site, the same site altered in the E763G substitution, does not support life (Evans et al. 1998). In addition, *in vitro* studies using a version of human Spt16 missing its C terminus demonstrated that this portion of the

Spt16 protein is required for interactions with mononucleosomes and for the facilitation of transcription (Belotserkovskaya et al. 2003). In terms of protein structure, both the E763G and E857K substitutions lie within a predicted double pleckstrin-homology (PH) domain in the Spt16 polypeptide (Dr. Richard Singer, personal communication, http://toolkit.tuebingen.mpg.de/hhpred), a motif that might mediate protein-protein interactions. However, the substituted residues are located nearly 100 amino acids apart, and thus may have different effects on protein function. It is possible that, if this region of the Spt16 protein mediates multiple protein interactions, the E857K substitution may affect different protein interactions than does the E763G substitution.

Regardless of the molecular basis for the functional differences observed between *spt16-E857K* and *spt16-E763G*, it is important to note that *spt16-E857K* is not simply a more severe version of the same kind of mutation. If this were the case, then I would expect that *spt16-E763G* cells would simply exhibit a subset of the *spt16-E857K* deleterious genetic interactions. This is clearly not the case, as these two mutant alleles have nearly non-overlapping sets of deleterious genetic interactions when analysed by genome-wide SGA analysis (O'Donnell 2004), and a limited overlap of deleterious genetic interactions in my investigations. Although mutations in a few genes do have similar genetic interactions with both *spt16* mutations, most of these exhibit some differences in phenotype between *spt16-E857K* and *spt16-E763G*. One such difference is the ability of *rco1Δ* to mediate suppression of deleterious genetic interactions for *spt16-E857K*, but not for *spt16-E763G* (for example, Figure 54). These observations suggest that these deleterious genetic interactions are, at least partially, manifested for different reasons.

4.7 The C-terminal Domain of Spt16 Mediates Multiple Protein Interactions

As noted above, Spt16 is predicted to contain a double-PH domain, which is affected by many of the point mutations I have studied. Interestingly, the only protein that has actually been demonstrated to possess a double-PH domain is Pob3, the other subunit of yeast FACT (VanDemark et al. 2006). Although PH domains are generally considered to be lipid-binding modules, this specificity is not always the case. In fact, some PH domains mediate binding to peptides or proteins, indicating a diverse function for this

structural feature (Lemmon 2004). All of the known mutations affecting Spt16 that give rise to a dominant Spt phenotype alter the predicted double-PH domain, suggesting that this portion of the polypeptide is important for the activities of Spt16 in transcription, and may well be responsible for the interactions between Spt16 and histone proteins.

Despite the possible linkage between histone interactions and the double-PH domain, the patterns of deleterious genetic interactions that I have found suggest that mutations affecting this predicted domain do not all have the same effect on Spt16 protein function. Several mutant alleles encoding Spt16 proteins altered in this predicted domain, such as *spt16-E763G* and *spt16-312*, although producing a dominant Spt phenotype suggestive of alterations in nucleosome reassembly, do not have synthetic-lethal interactions with mutations in *BUR2* or the *HIR* genes. Conversely, other mutant alleles altering this portion of Spt16, such as *spt16-6*, *spt16-7*, *spt16-9a* and *spt16-11*, do not cause a dominant Spt phenotype, yet all but *spt16-7* show deleterious genetic interactions with one or all of the transcription and histone-related mutations tested here. Taken together, these findings indicate that not all mutations affecting the predicted double-PH domain have the same effect on Spt16 protein function, suggesting that this portion of the Spt16 protein may mediate several different interactions.

In support of this hypothesis are certain observations using a second mutation affecting residue 857 of the Spt16 polypeptide. This mutation, in the mutant allele *spt16-E857Q*, changes the glutamic acid residue at position 857 to glutamine, rather than to lysine as in *spt16-E857K*. The *spt16-E857Q* mutation has been identified by Dr. Andrea Duina (personal communication) as a suppressor of defects caused by a substitution mutation altering histone H3 (H3-L61W) (Duina, Winston 2004). A second mutation, *spt16-E790K*, was also found to have the same suppressive effect in cells containing H3-L61W (Andrea Duina, personal communication). These two *spt16* mutations were the focus of the B.Sc. Honours research carried out in our lab by Rosemarie Kepkay, and her results have shown that these two alleles also have different phenotypes than those of *spt16-E857K* (Kepkay 2007). While growth inhibition is observed for both *spt16-E857Q* and *spt16-E790K* mutant cells upon histone H2A–H2B overexpression, similar to the inhibition seen for *spt16-E857K* cells, neither of these two *spt16* mutant alleles exhibits deleterious genetic interactions with my mutations in *BUR2* or the *HIR* genes, and neither

causes an Spt phenotype ((Kepkay 2007)and unpublished observations). In addition, the inhibition observed for *spt16-E857Q* cells upon H2A–H2B overexpression is less severe than that observed for *spt16-E857K* cells, suggesting that the E-to-Q substitution may cause less of a perturbation to Spt16 function than the E-to-K substitution. This idea is reasonable, as one could expect a negative-to-neutral change (E857Q) to be less disruptive than a negative-to-positive change (E857K) at the same position. If this were the case, one might expect that *spt16-E857K* would exhibit the same phenotypes as *spt16-E857Q*, as *spt16-E857K* would be a more 'severe' version of the same kind of mutation. However, *spt16-E857K* does not suppress the defects associated with H3-L61W, making it less likely that *spt16-E857Q* is simply a less severe version of the *spt16-E857K* mutation (Andrea Duina, personal communication). Thus, mutations at the same residue of the Spt16 polypeptide can have different effects on Spt16 function, further evidence that the region of the Spt16 protein surrounding position 857 may have several binding partners.

The multifaceted nature of the *spt16* mutant alleles studied here makes it difficult to define a particular region of the Spt16 protein that is responsible for the function(s) affected by the *spt16-E857K* mutation. Among the many mutant alleles of *SPT16* that I examined, there is no group of alleles that possesses all the same phenotypes in every test. Not all alleles with a dominant Spt phenotype demonstrate the same pattern of genetic interactions as *spt16-E857K*, and not all alleles with the same genetic interactions exhibit a dominant Spt phenotype. Even *spt16-E857K* and *spt16-E763G*, while having nearly non-overlapping sets of deleterious genetic interactions when analysed by genome-wide SGA analysis (O'Donnell 2004), behave similarly in some instances. Overall, it appears that the C-terminal region of Spt16 may mediate interactions with several different proteins, and that different mutations affecting this region have effects on specific subsets of these interactions. Thus, different alterations of Spt16 affect different functions of the Spt16 protein. This hypothesis rationalizes how the various mutations analysed here, and elsewhere, have such varied phenotypes.

4.8 Overall Conclusions

My studies, focusing mainly on the *spt16-E857K* mutation, shed more light on the role of Spt16, and therefore FACT, during the transcription process. I have shown that this mutation has deleterious genetic interactions with mutations in other genes encoding proteins that participate in transcription elongation, and that many of these deleterious interactions can be alleviated by inactivation of the Rpd3C(S) histone deacetylase complex. In these *rco1Δ* cells, histones in transcribed regions remain acetylated following RNAPII passage; this situation may mediate easier passage of the next RNAPII elongation complex, which would not require renewed acetylation of these nucleosomes. This view suggests that the Spt16-E857K mutant protein is impaired in its ability to overcome the impediment to transcription provided by deacetylated nucleosomes. Supporting this idea, *spt16-E857K* also has deleterious genetic interactions with mutations in *ESA1*, which encodes a histone acetylase that has been shown to act on the same amino acid as the Rpd3 histone deacetylase. The Esa1-L254P mutant protein shows poor acetylation of histones, and the NuA4 HAT complex that contains the Esa1 enzyme has been suggested to be required for effective transcription. The poor acetylation of histones in *esa1-L254P* cells, combined with the suggested impairment caused by Spt16-E857K in overcoming the impediment to transcription provided by deacetylated nucleosomes, may lead to an inability of RNAPII to effectively transcribe genes. In addition, I have shown that *spt16-E857K* cells are impaired when combined with mutations in genes coding for other histone chaperones, when the ratio of histone proteins is altered such that histone H2A–H2B levels are increased compared to those of H3–H4, and that the Spt16-E857K protein shows decreased immunoprecipitation of histone H2B compared to normal Spt16. These results may indicate that nucleosome reassembly is impaired in *spt16-E857K* cells. When this deficiency is combined with a general decrease in the ability to form proper nucleosomes resulting from impairments in other histone chaperones or a scarcity of histones H3 and H4, it leads to chromatin that is so improperly packaged that the cell is compromised for growth.

A detailed comparison was carried out using a second mutation, *spt16-E763G*, showing that this mutant allele demonstrates genetic effects different than those for *spt16-E857K*. These differences exist despite the fact that both of these *spt16* mutant

alleles were isolated by virtue of the same dominant Spt phenotype, a marker of altered nucleosome reassembly during transcription. Furthermore, many other mutant alleles of *SPT16* were tested for deleterious genetic interactions similar to those for *spt16-E857K*, with nearly equal numbers having these deleterious genetic interactions and not having such interactions. Thus, my findings indicate that FACT may participate in several different interactions to mediate transcription. Among these interactions would be those with histones H2A and H2B, and with proteins such as RNAPII, other histone chaperones, HAT complexes, and transcription elongation factors.

REFERENCES

Adkins, M.W. and Tyler, J.K. 2006. Transcriptional activators are dispensable for transcription in the absence of Spt6-mediated chromatin reassembly of promoter regions. *Mol. Cell.* 21: 405-416.

Ahn, S.H., Kim, M. and Buratowski, S. 2004. Phosphorylation of serine 2 within the RNA polymerase II C-terminal domain couples transcription and 3' end processing. *Mol. Cell.* 13: 67-76.

Allard, S., Utley, R.T., Savard, J., Clarke, A., Grant, P., Brandl, C.J., Pillus, L., Workman, J.L. and Cote, J. 1999. NuA4, an essential transcription adaptor/histone H4 acetyltransferase complex containing Esa1p and the ATM-related cofactor Tra1p. *EMBO J.* 18: 5108-5119.

Appling, D.R. 1999. Genetic approaches to the study of protein-protein interactions. *Methods.* 19: 338-349.

Arents, G., Burlingame, R.W., Wang, B.C., Love, W.E. and Moudrianakis, E.N. 1991. The nucleosomal core histone octamer at 3.1 A resolution: A tripartite protein assembly and a left-handed superhelix. *Proc. Natl. Acad. Sci. U. S. A.* 88: 10148-10152.

Ausubel, F.M., Brent, R., Kingston, R.E., Moore, D.D., Seidman, J.G., Smith, J.A. and Struhl, K. 1998. Current protocols in molecular biology.

Barbour, L., Zhu, Y. and Xiao, W. 2000. Improving synthetic lethal screens by regulating the yeast centromere sequence. *Genome.* 43: 910-917.

Belotserkovskaya, R., Oh, S., Bondarenko, V.A., Orphanides, G., Studitsky, V.M. and Reinberg, D. 2003. FACT facilitates transcription-dependent nucleosome alteration. *Science.* 301: 1090-1093.

Belotserkovskaya, R. and Reinberg, D. 2004. Facts about FACT and transcript elongation through chromatin. *Curr. Opin. Genet. Dev.* 14: 139-146.

Belotserkovskaya, R., Saunders, A., Lis, J.T. and Reinberg, D. 2004. Transcription through chromatin: Understanding a complex FACT. *Biochim. Biophys. Acta.* 1677: 87-99.

Bender, A. and Pringle, J.R. 1991. Use of a screen for synthetic lethal and multicopy suppressee mutants to identify two new genes involved in morphogenesis in saccharomyces cerevisiae. *Mol. Cell. Biol.* 11: 1295-1305.

Berger, S.L. 2007. The complex language of chromatin regulation during transcription. *Nature.* 447: 407-412.

Betz, J.L., Chang, M., Washburn, T.M., Porter, S.E., Mueller, C.L. and Jaehning, J.A. 2002. Phenotypic analysis of Paf1/RNA polymerase II complex mutations reveals connections to cell cycle regulation, protein synthesis, and lipid and nucleic acid metabolism. *Mol. Genet. Genomics.* 268: 272-285.

Biswas, D., Dutta-Biswas, R., Mitra, D., Shibata, Y., Strahl, B.D., Formosa, T. and Stillman, D.J. 2006. Opposing roles for Set2 and yFACT in regulating TBP binding at promoters. *EMBO J.* 25: 4479-4489.

Biswas, D., Yu, Y., Prall, M., Formosa, T. and Stillman, D.J. 2005. The yeast FACT complex has a role in transcriptional initiation. *Mol. Cell. Biol.* 25: 5812-5822.

Biswas, D., Imbalzano, A.N., Eriksson, P., Yu, Y. and Stillman, D.J. 2004. Role for Nhp6, Gcn5, and the Swi/Snf complex in stimulating formation of the TATA-binding protein-TFIIA-DNA complex. *Mol. Cell. Biol.* 24: 8312-8321.

Biswas, D., Yu, Y., Mitra, D. and Stillman, D.J. 2006. Genetic interactions between Nhp6 and Gcn5 with Mot1 and the Ccr4-not complex that regulate binding of TATA-binding protein in saccharomyces cerevisiae. *Genetics.* 172: 837-849.

Bito, A., Haider, M., Hadler, I. and Breitenbach, M. 1997. Identification and phenotypic analysis of two glyoxalase II encoding genes from saccharomyces cerevisiae, GLO2 and GLO4, and intracellular localization of the corresponding proteins. *J. Biol. Chem.* 272: 21509-21519.

Boeke, J.D., LaCroute, F. and Fink, G.R. 1984. A positive selection for mutants lacking orotidine-5'-phosphate decarboxylase activity in yeast: 5-fluoro-orotic acid resistance. *Mol. Gen. Genet.* 197: 345-346.

Boeke, J.D., Trueheart, J., Natsoulis, G. and Fink, G.R. 1987. 5-fluoroorotic acid as a selective agent in yeast molecular genetics. *Methods Enzymol.* 154: 164-175.

Bortvin, A. and Winston, F. 1996. Evidence that Spt6p controls chromatin structure by a direct interaction with histones. *Science.* 272: 1473-1476.

Botstein, D., Falco, S.C., Stewart, S.E., Brennan, M., Scherer, S., Stinchcomb, D.T., Struhl, K. and Davis, R.W. 1979. Sterile host yeasts (SHY): A eukaryotic system of biological containment for recombinant DNA experiments. *Gene.* 8: 17-24.

Boudreault, A.A., Cronier, D., Selleck, W., Lacoste, N., Utley, R.T., Allard, S., Savard, J., Lane, W.S., Tan, S. and Cote, J. 2003. Yeast enhancer of polycomb defines global Esa1-dependent acetylation of chromatin. *Genes Dev.* 17: 1415-1428.

Bourgeois, C.F., Kim, Y.K., Churcher, M.J., West, M.J. and Karn, J. 2002. Spt5 cooperates with human immunodeficiency virus type 1 tat by preventing premature RNA release at terminator sequences. *Mol. Cell. Biol.* 22: 1079-1093.

Braun, M.A., Costa, P.J., Crisucci, E.M. and Arndt, K.M. 2007. Identification of Rkr1, a nuclear RING domain protein with functional connections to chromatin modification in saccharomyces cerevisiae. *Mol. Cell. Biol.* 27: 2800-2811.

Brewster, N.K., Johnston, G.C. and Singer, R.A. 2001. A bipartite yeast SSRP1 analog comprised of Pob3 and Nhp6 proteins modulates transcription. *Mol. Cell. Biol.* 21: 3491-3502.

Brewster, N.K., Johnston, G.C. and Singer, R.A. 1998. Characterization of the CP complex, an abundant dimer of Cdc68 and Pob3 proteins that regulates yeast transcriptional activation and chromatin repression. *J. Biol. Chem.* 273: 21972-21979.

Braglia, P., Dugas, S.L., Donze, D. and Dieci, G. 2007. Requirement of Nhp6 proteins for transcription of a subset of tRNA genes and heterochromatin barrier function in saccharomyces cerevisiae. *Mol. Cell. Biol.* 27: 1545-1557.

Brodsky, A.S. and Silver, P.A. 2000. Pre-mRNA processing factors are required for nuclear export. *RNA.* 6: 1737-1749.

Brown, C.E., Lechner, T., Howe, L. and Workman, J.L. 2000. The many HATs of transcription coactivators. *Trends Biochem. Sci.* 25: 15-19.

Cairns, B.R., Lorch, Y., Li, Y., Zhang, M., Lacomis, L., Erdjument-Bromage, H., Tempst, P., Du, J., Laurent, B. and Kornberg, R.D. 1996. RSC, an essential, abundant chromatin-remodeling complex. *Cell.* 87: 1249-1260.

Camerini-Otero, R.D. and Felsenfeld, G. 1977. Supercoiling energy and nucleosome formation: The role of the arginine-rich histone kernel. *Nucleic Acids Res.* 4: 1159-1181.

Carrozza, M.J., Li, B., Florens, L., Suganuma, T., Swanson, S.K., Lee, K.K., Shia, W.J., Anderson, S., Yates, J., Washburn, M.P. and Workman, J.L. 2005. Histone H3 methylation by Set2 directs deacetylation of coding regions by Rpd3S to suppress spurious intragenic transcription. *Cell.* 123: 581-592.

Cho, E.J., Kobor, M.S., Kim, M., Greenblatt, J. and Buratowski, S. 2001. Opposing effects of Ctk1 kinase and Fcp1 phosphatase at ser 2 of the RNA polymerase II C-terminal domain. *Genes Dev.* 15: 3319-3329.

Christianson, T.W., Sikorski, R.S., Dante, M., Shero, J.H. and Hieter, P. 1992. Multifunctional yeast high-copy-number shuttle vectors. *Gene.* 110: 119-122.

Chu, Y., Sutton, A., Sternglanz, R. and Prelich, G. 2006. The BUR1 cyclin-dependent protein kinase is required for the normal pattern of histone methylation by SET2. *Mol. Cell. Biol.* 26: 3029-3038.

Clark-Adams, C.D. and Winston, F. 1987. The SPT6 gene is essential for growth and is required for delta-mediated transcription in saccharomyces cerevisiae. *Mol. Cell. Biol.* 7: 679-686.

Clarke, A.S., Lowell, J.E., Jacobson, S.J. and Pillus, L. 1999. Esa1p is an essential histone acetyltransferase required for cell cycle progression. *Mol. Cell. Biol.* 19: 2515-2526.

Cormack, B. and Castano, I. 2002. Introduction of point mutations into cloned genes. *Methods Enzymol.* 350: 199-218.

Costigan, C., Kolodrubetz, D. and Snyder, M. 1994. NHP6A and NHP6B, which encode HMG1-like proteins, are candidates for downstream components of the yeast SLT2 mitogen-activated protein kinase pathway. *Mol. Cell. Biol.* 14: 2391-2403.

Cui, Y. and Denis, C.L. 2003. In vivo evidence that defects in the transcriptional elongation factors RPB2, TFIIS, and SPT5 enhance upstream poly(A) site utilization. *Mol. Cell. Biol.* 23: 7887-7901.

Daganzo, S.M., Erzberger, J.P., Lam, W.M., Skordalakes, E., Zhang, R., Franco, A.A., Brill, S.J., Adams, P.D., Berger, J.M. and Kaufman, P.D. 2003. Structure and function of the conserved core of histone deposition protein Asf1. *Curr. Biol.* 13: 2148-2158.

Dehe, P.M., Dichtl, B., Schaft, D., Roguev, A., Pamblanco, M., Lebrun, R., Rodriguez-Gil, A., Mkandawire, M., Landsberg, K., Shevchenko, A., Shevchenko, A., Rosaleny, L.E., Tordera, V., Chavez, S., Stewart, A.F. and Geli, V. 2006. Protein interactions within the Set1 complex and their roles in the regulation of histone 3 lysine 4 methylation. *J. Biol. Chem.* 281: 35404-35412.

Dion, M.F., Kaplan, T., Kim, M., Buratowski, S., Friedman, N. and Rando, O.J. 2007. Dynamics of replication-independent histone turnover in budding yeast. *Science.* 315: 1405-1408.

Dover, J., Schneider, J., Tawiah-Boateng, M.A., Wood, A., Dean, K., Johnston, M. and Shilatifard, A. 2002. Methylation of histone H3 by COMPASS requires ubiquitination of histone H2B by Rad6. *J. Biol. Chem.* 277: 28368-28371.

Doyon, Y. and Cote, J. 2004. The highly conserved and multifunctional NuA4 HAT complex. *Curr. Opin. Genet. Dev.* 14: 147-154.

Driscoll, R., Hudson, A. and Jackson, S.P. 2007. Yeast Rtt109 promotes genome stability by acetylating histone H3 on lysine 56. *Science.* 315: 649-652.

Duina, A.A. and Winston, F. 2004. Analysis of a mutant histone H3 that perturbs the association of Swi/Snf with chromatin. *Mol. Cell. Biol.* 24: 561-572.

Dumont, M.E., Schlichter, J.B., Cardillo, T.S., Hayes, M.K., Bethlendy, G. and Sherman, F. 1993. CYC2 encodes a factor involved in mitochondrial import of yeast cytochrome c. *Mol. Cell. Biol.* 13: 6442-6451.

Duroux, M., Houben, A., Ruzicka, K., Friml, J. and Grasser, K.D. 2004. The chromatin remodelling complex FACT associates with actively transcribed regions of the arabidopsis genome. *Plant J.* 40: 660-671.

Eisenmann, D.M., Dollard, C. and Winston, F. 1989. SPT15, the gene encoding the yeast TATA binding factor TFIID, is required for normal transcription initiation in vivo. *Cell.* 58: 1183-1191.

Ellison, K.S., Gwozd, T., Prendergast, J.A., Paterson, M.C. and Ellison, M.J. 1991. A site-directed approach for constructing temperature-sensitive ubiquitin-conjugating enzymes reveals a cell cycle function and growth function for RAD6. *J. Biol. Chem.* 266: 24116-24120.

Emili, A., Schieltz, D.M., Yates, J.R.,3rd and Hartwell, L.H. 2001. Dynamic interaction of DNA damage checkpoint protein Rad53 with chromatin assembly factor Asf1. *Mol. Cell.* 7: 13-20.

English, C.M., Maluf, N.K., Tripet, B., Churchill, M.E. and Tyler, J.K. 2005. ASF1 binds to a heterodimer of histones H3 and H4: A two-step mechanism for the assembly of the H3-H4 heterotetramer on DNA. *Biochemistry.* 44: 13673-13682.

Evans, D.R., Brewster, N.K., Xu, Q., Rowley, A., Altheim, B.A., Johnston, G.C. and Singer, R.A. 1998. The yeast protein complex containing cdc68 and pob3 mediates core-promoter repression through the cdc68 N-terminal domain. *Genetics.* 150: 1393-1405.

Fang, J., Hogan, G.J., Liang, G., Lieb, J.D. and Zhang, Y. 2007. The saccharomyces cerevisiae histone demethylase Jhd1 fine-tunes the distribution of H3K36me2. *Mol. Cell. Biol.* 27: 5055-5065.

Farabaugh, P.J. and Fink, G.R. 1980. Insertion of the eukaryotic transposable element Ty1 creates a 5-base pair duplication. *Nature.* 286: 352-356.

Fassler, J.S. and Winston, F. 1988. Isolation and analysis of a novel class of suppressor of ty insertion mutations in saccharomyces cerevisiae. *Genetics.* 118: 203-212.

Finn, R.D., Mistry, J., Schuster-Bockler, B., Griffiths-Jones, S., Hollich, V., Lassmann, T., Moxon, S., Marshall, M., Khanna, A., Durbin, R., Eddy, S.R., Sonnhammer, E.L. and Bateman, A. 2006. Pfam: Clans, web tools and services. *Nucleic Acids Res.* 34: D247-51.

Formosa, T. 2003. Changing the DNA landscape: Putting a SPN on chromatin. *Curr. Top. Microbiol. Immunol.* 274: 171-201.

Formosa, T., Eriksson, P., Wittmeyer, J., Ginn, J., Yu, Y. and Stillman, D.J. 2001. Spt16-Pob3 and the HMG protein Nhp6 combine to form the nucleosome-binding factor SPN. *EMBO J.* 20: 3506-3517.

Formosa, T., Ruone, S., Adams, M.D., Olsen, A.E., Eriksson, P., Yu, Y., Rhoades, A.R., Kaufman, P.D. and Stillman, D.J. 2002. Defects in SPT16 or POB3 (yFACT) in saccharomyces cerevisiae cause dependence on the Hir/Hpc pathway: Polymerase passage may degrade chromatin structure. *Genetics.* 162: 1557-1571.

Franco, A.A., Lam, W.M., Burgers, P.M. and Kaufman, P.D. 2005. Histone deposition protein Asf1 maintains DNA replisome integrity and interacts with replication factor C. *Genes Dev.* 19: 1365-1375.

Galarneau, L., Nourani, A., Boudreault, A.A., Zhang, Y., Heliot, L., Allard, S., Savard, J., Lane, W.S., Stillman, D.J. and Cote, J. 2000. Multiple links between the NuA4 histone acetyltransferase complex and epigenetic control of transcription. *Mol. Cell.* 5: 927-937.

Girrbach, V. and Strahl, S. 2003. Members of the evolutionarily conserved PMT family of protein O-mannosyltransferases form distinct protein complexes among themselves. *J. Biol. Chem.* 278: 12554-12562.

Goldstein, A.L., Pan, X. and McCusker, J.H. 1999. Heterologous URA3MX cassettes for gene replacement in saccharomyces cerevisiae. *Yeast.* 15: 507-511.

Grant, P.A., Duggan, L., Cote, J., Roberts, S.M., Brownell, J.E., Candau, R., Ohba, R., Owen-Hughes, T., Allis, C.D., Winston, F., Berger, S.L. and Workman, J.L. 1997. Yeast Gcn5 functions in two multisubunit complexes to acetylate nucleosomal histones: Characterization of an ada complex and the SAGA (Spt/Ada) complex. *Genes Dev.* 11: 1640-1650.

Green, E.M., Antczak, A.J., Bailey, A.O., Franco, A.A., Wu, K.J., Yates, J.R.,3rd and Kaufman, P.D. 2005. Replication-independent histone deposition by the HIR complex and Asf1. *Curr. Biol.* 15: 2044-2049.

Greiner, M., Caesar, S. and Schlenstedt, G. 2004. The histones H2A/H2B and H3/H4 are imported into the yeast nucleus by different mechanisms. *Eur. J. Cell Biol.* 83: 511-520.

Guacci, V., Koshland, D. and Strunnikov, A. 1997. A direct link between sister chromatid cohesion and chromosome condensation revealed through the analysis of MCD1 in S. cerevisiae. *Cell.* 91: 47-57.

Guarente, L. 1993. Strategies for the identification of interacting proteins. *Proc. Natl. Acad. Sci. U. S. A.* 90: 1639-1641.

Guthrie, C. and Fink, G.R. 1991. Guide to yeast genetics and molecular biology. in *Methods in enzymology* (Anonymous)Academic Press, San Diego, CA.

Hampsey, M. 1997. A review of phenotypes in saccharomyces cerevisiae. *Yeast.* 13: 1099-1133.

Han, J., Zhou, H., Horazdovsky, B., Zhang, K., Xu, R.M. and Zhang, Z. 2007. Rtt109 acetylates histone H3 lysine 56 and functions in DNA replication. *Science.* 315: 653-655.

Hartwell, L.H. 1967. Macromolecule synthesis in temperature-sensitive mutants of yeast. *J. Bacteriol.* 93: 1662-1670.

Hartzog, G.A., Wada, T., Handa, H. and Winston, F. 1998. Evidence that Spt4, Spt5, and Spt6 control transcription elongation by RNA polymerase II in saccharomyces cerevisiae. *Genes Dev.* 12: 357-369.

Hazbun, T.R., Malmstrom, L., Anderson, S., Graczyk, B.J., Fox, B., Riffle, M., Sundin, B.A., Aranda, J.D., McDonald, W.H., Chiu, C.H., Snydsman, B.E., Bradley, P., Muller, E.G., Fields, S., Baker, D., Yates, J.R.,3rd and Davis, T.N. 2003. Assigning function to yeast proteins by integration of technologies. *Mol. Cell.* 12: 1353-1365.

Hereford, L., Fahrner, K., Woolford, J.,Jr, Rosbash, M. and Kaback, D.B. 1979. Isolation of yeast histone genes H2A and H2B. *Cell.* 18: 1261-1271.

Hoffman, C.S. 1997. Preparation of yeast DNA, RNA, and proteins. in *Current protocols in molecular biology* (eds, F.M. Ausubel, R. Brent, R.E. Kingston, et al)John Wiley & Sons, Inc., New York, N.Y.

Holtzman, D.A., Yang, S. and Drubin, D.G. 1993. Synthetic-lethal interactions identify two novel genes, SLA1 and SLA2, that control membrane cytoskeleton assembly in saccharomyces cerevisiae. *J. Cell Biol.* 122: 635-644.

Huang, S., Zhou, H., Katzmann, D., Hochstrasser, M., Atanasova, E. and Zhang, Z. 2005. Rtt106p is a histone chaperone involved in heterochromatin-mediated silencing. *Proc. Natl. Acad. Sci. U. S. A.* 102: 13410-13415.

Huh, W.K., Falvo, J.V., Gerke, L.C., Carroll, A.S., Howson, R.W., Weissman, J.S. and O'Shea, E.K. 2003. Global analysis of protein localization in budding yeast. *Nature.* 425: 686-691.

Hurt, E., Luo, M.J., Rother, S., Reed, R. and Strasser, K. 2004. Cotranscriptional recruitment of the serine-arginine-rich (SR)-like proteins Gbp2 and Hrb1 to nascent mRNA via the TREX complex. *Proc. Natl. Acad. Sci. U. S. A.* 101: 1858-1862.

Hyland, E.M., Cosgrove, M.S., Molina, H., Wang, D., Pandey, A., Cottee, R.J. and Boeke, J.D. 2005. Insights into the role of histone H3 and histone H4 core modifiable residues in saccharomyces cerevisiae. *Mol. Cell. Biol.* 25: 10060-10070.

Immervoll, T., Gentzsch, M. and Tanner, W. 1995. PMT3 and PMT4, two new members of the protein-O-mannosyltransferase gene family of saccharomyces cerevisiae. *Yeast.* 11: 1345-1351.

Ioshikhes, I.P., Albert, I., Zanton, S.J. and Pugh, B.F. 2006. Nucleosome positions predicted through comparative genomics. *Nat. Genet.* 38: 1210-1215.

Ito, H., Fukuda, Y., Murata, K. and Kimura, A. 1983. Transformation of intact yeast cells treated with alkali cations. *J. Bacteriol.* 153: 163-168.

Ivanov, D., Kwak, Y.T., Guo, J. and Gaynor, R.B. 2000. Domains in the SPT5 protein that modulate its transcriptional regulatory properties. *Mol. Cell. Biol.* 20: 2970-2983.

Jamai, A., Imoberdorf, R.M. and Strubin, M. 2007. Continuous histone H2B and transcription-dependent histone H3 exchange in yeast cells outside of replication. *Mol. Cell.* 25: 345-355.

Jentsch, S., McGrath, J.P. and Varshavsky, A. 1987. The yeast DNA repair gene RAD6 encodes a ubiquitin-conjugating enzyme. *Nature.* 329: 131-134.

John, S., Howe, L., Tafrov, S.T., Grant, P.A., Sternglanz, R. and Workman, J.L. 2000. The something about silencing protein, Sas3, is the catalytic subunit of NuA3, a yTAF(II)30-containing HAT complex that interacts with the Spt16 subunit of the yeast CP (Cdc68/Pob3)-FACT complex. *Genes Dev.* 14: 1196-1208.

Johnston, G.C., Pringle, J.R. and Hartwell, L.H. 1977. Coordination of growth with cell division in the yeast saccharomyces cerevisiae. *Exp. Cell Res.* 105: 79-98.

Jorcano, J.L. and Ruiz-Carrillo, A. 1979. H3.H4 tetramer directs DNA and core histone octamer assembly in the nucleosome core particle. *Biochemistry.* 18: 768-774.

Joshi, A.A. and Struhl, K. 2005. Eaf3 chromodomain interaction with methylated H3-K36 links histone deacetylation to pol II elongation. *Mol. Cell.* 20: 971-978.

Kaplan, C.D., Holland, M.J. and Winston, F. 2005. Interaction between transcription elongation factors and mRNA 3'-end formation at the saccharomyces cerevisiae GAL10-GAL7 locus. *J. Biol. Chem.* 280: 913-922.

Kaplan, C.D., Laprade, L. and Winston, F. 2003. Transcription elongation factors repress transcription initiation from cryptic sites. *Science.* 301: 1096-1099.

Kassavetis, G.A. and Steiner, D.F. 2006. Nhp6 is a transcriptional initiation fidelity factor for RNA polymerase III transcription in vitro and in vivo. *J. Biol. Chem.* 281: 7445-7451.

Keogh, M.C., Kurdistani, S.K., Morris, S.A., Ahn, S.H., Podolny, V., Collins, S.R., Schuldiner, M., Chin, K., Punna, T., Thompson, N.J., Boone, C., Emili, A., Weissman, J.S., Hughes, T.R., Strahl, B.D., Grunstein, M., Greenblatt, J.F., Buratowski, S. and Krogan, N.J. 2005. Cotranscriptional set2 methylation of histone H3 lysine 36 recruits a repressive Rpd3 complex. *Cell.* 123: 593-605.

Keogh, M.C., Podolny, V. and Buratowski, S. 2003. Burl kinase is required for efficient transcription elongation by RNA polymerase II. *Mol. Cell. Biol.* 23: 7005-7018.

Kepkay, R. 2007. Multiple interactions regulating nucleosome dynamics by an important histone chaperone.

Kim, J.B. and Sharp, P.A. 2001. Positive transcription elongation factor B phosphorylates hSPT5 and RNA polymerase II carboxyl-terminal domain independently of cyclin-dependent kinase-activating kinase. *J. Biol. Chem.* 276: 12317-12323.

Kim, M., Ahn, S.H., Krogan, N.J., Greenblatt, J.F. and Buratowski, S. 2004. Transitions in RNA polymerase II elongation complexes at the 3' ends of genes. *EMBO J.* 23: 354-364.

Kim, T. and Buratowski, S. 2007. Two saccharomyces cerevisiae JmjC domain proteins demethylate histone H3 K36 in transcribed regions to promote elongation. *J. Biol. Chem.*

Kouzarides, T. 2007. Chromatin modifications and their function. *Cell.* 128: 693-705.

Kranz, J.E. and Holm, C. 1990. Cloning by function: An alternative approach for identifying yeast homologs of genes from other organisms. *Proc. Natl. Acad. Sci. U. S. A.* 87: 6629-6633.

Krogan, N.J., Dover, J., Khorrami, S., Greenblatt, J.F., Schneider, J., Johnston, M. and Shilatifard, A. 2002. COMPASS, a histone H3 (lysine 4) methyltransferase required for telomeric silencing of gene expression. *J. Biol. Chem.* 277: 10753-10755.

Krogan, N.J., Dover, J., Wood, A., Schneider, J., Heidt, J., Boateng, M.A., Dean, K., Ryan, O.W., Golshani, A., Johnston, M., Greenblatt, J.F. and Shilatifard, A. 2003a. The Paf1 complex is required for histone H3 methylation by COMPASS and Dot1p: Linking transcriptional elongation to histone methylation. *Mol. Cell.* 11: 721-729.

Krogan, N.J., Keogh, M.C., Datta, N., Sawa, C., Ryan, O.W., Ding, H., Haw, R.A., Pootoolal, J., Tong, A., Canadien, V., Richards, D.P., Wu, X., Emili, A., Hughes, T.R., Buratowski, S. and Greenblatt, J.F. 2003b. A Snf2 family ATPase complex required for recruitment of the histone H2A variant Htz1. *Mol. Cell.* 12: 1565-1576.

Krogan, N.J., Kim, M., Ahn, S.H., Zhong, G., Kobor, M.S., Cagney, G., Emili, A., Shilatifard, A., Buratowski, S. and Greenblatt, J.F. 2002. RNA polymerase II elongation factors of saccharomyces cerevisiae: A targeted proteomics approach. *Mol. Cell. Biol.* 22: 6979-6992.

Kruppa, M., Moir, R.D., Kolodrubetz, D. and Willis, I.M. 2001. Nhp6, an HMG1 protein, functions in SNR6 transcription by RNA polymerase III in S. cerevisiae. *Mol. Cell.* 7: 309-318.

Lai, J.S. and Herr, W. 1992. Ethidium bromide provides a simple tool for identifying genuine DNA-independent protein associations. *Proc. Natl. Acad. Sci. U. S. A.* 89: 6958-6962.

Lamour, V., Lecluse, Y., Desmaze, C., Spector, M., Bodescot, M., Aurias, A., Osley, M.A. and Lipinski, M. 1995. A human homolog of the S. cerevisiae HIR1 and HIR2 transcriptional repressors cloned from the DiGeorge syndrome critical region. *Hum. Mol. Genet.* 4: 791-799.

Laribee, R.N., Krogan, N.J., Xiao, T., Shibata, Y., Hughes, T.R., Greenblatt, J.F. and Strahl, B.D. 2005. BUR kinase selectively regulates H3 K4 trimethylation and H2B ubiquitylation through recruitment of the PAF elongation complex. *Curr. Biol.* 15: 1487-1493.

Le, S., Davis, C., Konopka, J.B. and Sternglanz, R. 1997. Two new S-phase-specific genes from saccharomyces cerevisiae. *Yeast.* 13: 1029-1042.

Lee, J.M. and Greenleaf, A.L. 1997. Modulation of RNA polymerase II elongation efficiency by C-terminal heptapeptide repeat domain kinase I. *J. Biol. Chem.* 272: 10990-10993.

Lemmon, M.A. 2004. Pleckstrin homology domains: Not just for phosphoinositides. *Biochem. Soc. Trans.* 32: 707-711.

Levchenko, V., Jackson, B. and Jackson, V. 2005. Histone release during transcription: Displacement of the two H2A-H2B dimers in the nucleosome is dependent on different levels of transcription-induced positive stress. *Biochemistry.* 44: 5357-5372.

Levchenko, V. and Jackson, V. 2004. Histone release during transcription: NAP1 forms a complex with H2A and H2B and facilitates a topologically dependent release of H3 and H4 from the nucleosome. *Biochemistry.* 43: 2359-2372.

Li, B., Carey, M. and Workman, J.L. 2007. The role of chromatin during transcription. *Cell.* 128: 707-719.

Li, B., Gogol, M., Carey, M., Lee, D., Seidel, C. and Workman, J.L. 2007. Combined action of PHD and chromo domains directs the Rpd3S HDAC to transcribed chromatin. *Science.* 316: 1050-1054.

Li, B., Howe, L., Anderson, S., Yates, J.R.,3rd and Workman, J.L. 2003. The Set2 histone methyltransferase functions through the phosphorylated carboxyl-terminal domain of RNA polymerase II. *J. Biol. Chem.* 278: 8897-8903.

Li, J., Moazed, D. and Gygi, S.P. 2002. Association of the histone methyltransferase Set2 with RNA polymerase II plays a role in transcription elongation. *J. Biol. Chem.* 277: 49383-49388.

Li, R., Zheng, Y. and Drubin, D.G. 1995. Regulation of cortical actin cytoskeleton assembly during polarized cell growth in budding yeast. *J. Cell Biol.* 128: 599-615.

Lindstrom, D.L. and Hartzog, G.A. 2001. Genetic interactions of Spt4-Spt5 and TFIIS with the RNA polymerase II CTD and CTD modifying enzymes in saccharomyces cerevisiae. *Genetics.* 159: 487-497.

Lindstrom, D.L., Squazzo, S.L., Muster, N., Burckin, T.A., Wachter, K.C., Emigh, C.A., McCleery, J.A., Yates, J.R.,3rd and Hartzog, G.A. 2003. Dual roles for Spt5 in pre-mRNA processing and transcription elongation revealed by identification of Spt5-associated proteins. *Mol. Cell. Biol.* 23: 1368-1378.

Lingner, J., Kellermann, J. and Keller, W. 1991. Cloning and expression of the essential gene for poly(A) polymerase from S. cerevisiae. *Nature.* 354: 496-498.

Lorch, Y. and Kornberg, R.D. 1994. Isolation of the yeast histone octamer. *Proc. Natl. Acad. Sci. U. S. A.* 91: 11032-11034.

Lorch, Y., Maier-Davis, B. and Kornberg, R.D. 2006. Chromatin remodeling by nucleosome disassembly in vitro. *Proc. Natl. Acad. Sci. U. S. A.* 103: 3090-3093.

Loyola, A. and Almouzni, G. 2004. Histone chaperones, a supporting role in the limelight. *Biochim. Biophys. Acta.* 1677: 3-11.

Luger, K. 2006. Dynamic nucleosomes. *Chromosome Res.* 14: 5-16.

Luger, K. 2003. Structure and dynamic behavior of nucleosomes. *Curr. Opin. Genet. Dev.* 13: 127-135.

Luger, K. 2002. The tail does not always wag the dog. *Nat. Genet.* 32: 221-222.

Luger, K., Mader, A.W., Richmond, R.K., Sargent, D.F. and Richmond, T.J. 1997. Crystal structure of the nucleosome core particle at 2.8 A resolution. *Nature.* 389: 251-260.

Lycan, D., Mikesell, G., Bunger, M. and Breeden, L. 1994. Differential effects of Cdc68 on cell cycle-regulated promoters in saccharomyces cerevisiae. *Mol. Cell. Biol.* 14: 7455-7465.

Malone, E.A., Clark, C.D., Chiang, A. and Winston, F. 1991. Mutations in SPT16/CDC68 suppress cis- and trans-acting mutations that affect promoter function in saccharomyces cerevisiae. *Mol. Cell. Biol.* 11: 5710-5717.

Marshall, N.F., Peng, J., Xie, Z. and Price, D.H. 1996. Control of RNA polymerase II elongation potential by a novel carboxyl-terminal domain kinase. *J. Biol. Chem.* 271: 27176-27183.

Martin, M.P., Gerlach, V.L. and Brow, D.A. 2001. A novel upstream RNA polymerase III promoter element becomes essential when the chromatin structure of the yeast U6 RNA gene is altered. *Mol. Cell. Biol.* 21: 6429-6439.

Mason, P.B. and Struhl, K. 2003. The FACT complex travels with elongating RNA polymerase II and is important for the fidelity of transcriptional initiation in vivo. *Mol. Cell. Biol.* 23: 8323-8333.

Masumoto, H., Hawke, D., Kobayashi, R. and Verreault, A. 2005. A role for cell-cycle-regulated histone H3 lysine 56 acetylation in the DNA damage response. *Nature.* 436: 294-298.

Mazurkiewicz, J., Kepert, J.F. and Rippe, K. 2006. On the mechanism of nucleosome assembly by histone chaperone NAP1. *J. Biol. Chem.* 281: 16462-16472.

Messing, J. 1983. New M13 vectors for cloning. *Methods Enzymol.* 101: 20-78.

Milkereit, P., Gadal, O., Podtelejnikov, A., Trumtel, S., Gas, N., Petfalski, E., Tollervey, D., Mann, M., Hurt, E. and Tschochner, H. 2001. Maturation and intranuclear transport of pre-ribosomes requires noc proteins. *Cell.* 105: 499-509.

Millar, C.B. and Grunstein, M. 2006. Genome-wide patterns of histone modifications in yeast. *Nat. Rev. Mol. Cell Biol.* 7: 657-666.

Miyaji-Yamaguchi, M., Kato, K., Nakano, R., Akashi, T., Kikuchi, A. and Nagata, K. 2003. Involvement of nucleocytoplasmic shuttling of yeast Nap1 in mitotic progression. *Mol. Cell. Biol.* 23: 6672-6684.

Mizuguchi, G., Shen, X., Landry, J., Wu, W.H., Sen, S. and Wu, C. 2004. ATP-driven exchange of histone H2AZ variant catalyzed by SWR1 chromatin remodeling complex. *Science.* 303: 343-348.

Mosammaparast, N., Ewart, C.S. and Pemberton, L.F. 2002. A role for nucleosome assembly protein 1 in the nuclear transport of histones H2A and H2B. *EMBO J.* 21: 6527-6538.

Mosammaparast, N., Guo, Y., Shabanowitz, J., Hunt, D.F. and Pemberton, L.F. 2002. Pathways mediating the nuclear import of histones H3 and H4 in yeast. *J. Biol. Chem.* 277: 862-868.

Mosammaparast, N., Jackson, K.R., Guo, Y., Brame, C.J., Shabanowitz, J., Hunt, D.F. and Pemberton, L.F. 2001. Nuclear import of histone H2A and H2B is mediated by a network of karyopherins. *J. Cell Biol.* 153: 251-262.

Mueller, C.L. and Jaehning, J.A. 2002. Ctr9, Rtf1, and Leo1 are components of the Paf1/RNA polymerase II complex. *Mol. Cell. Biol.* 22: 1971-1980.

Mueller, C.L., Porter, S.E., Hoffman, M.G. and Jaehning, J.A. 2004. The Paf1 complex has functions independent of actively transcribing RNA polymerase II. *Mol. Cell.* 14: 447-456.

Murray, S., Udupa, R., Yao, S., Hartzog, G. and Prelich, G. 2001. Phosphorylation of the RNA polymerase II carboxy-terminal domain by the Bur1 cyclin-dependent kinase. *Mol. Cell. Biol.* 21: 4089-4096.

Muthurajan, U.M., Park, Y.J., Edayathumangalam, R.S., Suto, R.K., Chakravarthy, S., Dyer, P.N. and Luger, K. 2003. Structure and dynamics of nucleosomal DNA. *Biopolymers.* 68: 547-556.

Mythreye, K. and Bloom, K.S. 2003. Differential kinetochore protein requirements for establishment versus propagation of centromere activity in saccharomyces cerevisiae. *J. Cell Biol.* 160: 833-843.

Nemeth, A. and Langst, G. 2004. Chromatin higher order structure: Opening up chromatin for transcription. *Brief Funct. Genomic Proteomic.* 2: 334-343.

Nespoli, A., Vercillo, R., di Nola, L., Diani, L., Giannattasio, M., Plevani, P. and Muzi-Falconi, M. 2006. Alk1 and Alk2 are two new cell cycle-regulated haspin-like proteins in budding yeast. *Cell. Cycle.* 5: 1464-1471.

Neves-Costa, A. and Varga-Weisz, P. 2006. The roles of chromatin remodelling factors in replication. *Results Probl. Cell Differ.* 41: 91-107.

Ng, H.H., Robert, F., Young, R.A. and Struhl, K. 2003. Targeted recruitment of Set1 histone methylase by elongating pol II provides a localized mark and memory of recent transcriptional activity. *Mol. Cell.* 11: 709-719.

Nickas, M.E., Schwartz, C. and Neiman, A.M. 2003. Ady4p and Spo74p are components of the meiotic spindle pole body that promote growth of the prospore membrane in saccharomyces cerevisiae. *Eukaryot. Cell.* 2: 431-445.

Nourani, A., Doyon, Y., Utley, R.T., Allard, S., Lane, W.S. and Cote, J. 2001. Role of an ING1 growth regulator in transcriptional activation and targeted histone acetylation by the NuA4 complex. *Mol. Cell. Biol.* 21: 7629-7640.

Nourani, A., Utley, R.T., Allard, S. and Cote, J. 2004. Recruitment of the NuA4 complex poises the PHO5 promoter for chromatin remodeling and activation. *EMBO J.* 23: 2597-2607.

O'Donnell, A.F. 2004. Mutational analysis of the yeast chromatin modulator conplex FACT.

O'Donnell, A.F., Brewster, N.K., Kurniawan, J., Minard, L.V., Johnston, G.C. and Singer, R.A. 2004. Domain organization of the yeast histone chaperone FACT: The conserved N-terminal domain of FACT subunit Spt16 mediates recovery from replication stress. *Nucleic Acids Res.* 32: 5894-5906.

Okuhara, K., Ohta, K., Seo, H., Shioda, M., Yamada, T., Tanaka, Y., Dohmae, N., Seyama, Y., Shibata, T. and Murofushi, H. 1999. A DNA unwinding factor involved in DNA replication in cell-free extracts of xenopus eggs. *Curr. Biol.* 9: 341-350.

Orphanides, G., LeRoy, G., Chang, C.H., Luse, D.S. and Reinberg, D. 1998. FACT, a factor that facilitates transcript elongation through nucleosomes. *Cell.* 92: 105-116.

Orphanides, G., Wu, W.H., Lane, W.S., Hampsey, M. and Reinberg, D. 1999. The chromatin-specific transcription elongation factor FACT comprises human SPT16 and SSRP1 proteins. *Nature.* 400: 284-288.

Osley, M.A. and Lycan, D. 1987. Trans-acting regulatory mutations that alter transcription of saccharomyces cerevisiae histone genes. *Mol. Cell. Biol.* 7: 4204-4210.

Ozdemir, A., Spicuglia, S., Lasonder, E., Vermeulen, M., Campsteijn, C., Stunnenberg, H.G. and Logie, C. 2005. Characterization of lysine 56 of histone H3 as an acetylation site in saccharomyces cerevisiae. *J. Biol. Chem.* 280: 25949-25952.

Park, Y.J. and Luger, K. 2006. Structure and function of nucleosome assembly proteins. *Biochem. Cell Biol.* 84: 549-558.

Patturajan, M., Conrad, N.K., Bregman, D.B. and Corden, J.L. 1999. Yeast carboxyl-terminal domain kinase I positively and negatively regulates RNA polymerase II carboxyl-terminal domain phosphorylation. *J. Biol. Chem.* 274: 27823-27828.

Pavri, R., Zhu, B., Li, G., Trojer, P., Mandal, S., Shilatifard, A. and Reinberg, D. 2006. Histone H2B monoubiquitination functions cooperatively with FACT to regulate elongation by RNA polymerase II. *Cell.* 125: 703-717.

Pearce, D.A., Cardillo, T.S. and Sherman, F. 1998. Cyc2p is required for maintaining ionic stability and efficient cytochrome c import and mitochondrial function in saccharomyces cerevisiae. *FEBS Lett.* 439: 307-311.

Pei, Y. and Shuman, S. 2003. Characterization of the schizosaccharomyces pombe Cdk9/Pch1 protein kinase: Spt5 phosphorylation, autophosphorylation, and mutational analysis. *J. Biol. Chem.* 278: 43346-43356.

Perry, T.E. 2005. Identification and characterization of novel Spt16 alleles: An essential subunit of yFACT.

Peterson, C.L. and Laniel, M.A. 2004. Histones and histone modifications. *Curr. Biol.* 14: R546-51.

Porter, S.E., Penheiter, K.L. and Jaehning, J.A. 2005. Separation of the saccharomyces cerevisiae Paf1 complex from RNA polymerase II results in changes in its subnuclear localization. *Eukaryot. Cell.* 4: 209-220.

Prather, D., Krogan, N.J., Emili, A., Greenblatt, J.F. and Winston, F. 2005. Identification and characterization of Elf1, a conserved transcription elongation factor in saccharomyces cerevisiae. *Mol. Cell. Biol.* 25: 10122-10135.

Pray-Grant, M.G., Schieltz, D., McMahon, S.J., Wood, J.M., Kennedy, E.L., Cook, R.G., Workman, J.L., Yates, J.R.,3rd and Grant, P.A. 2002. The novel SLIK histone acetyltransferase complex functions in the yeast retrograde response pathway. *Mol. Cell. Biol.* 22: 8774-8786.

Preker, P.J., Ohnacker, M., Minvielle-Sebastia, L. and Keller, W. 1997. A multisubunit 3' end processing factor from yeast containing poly(A) polymerase and homologues of the subunits of mammalian cleavage and polyadenylation specificity factor. *EMBO J.* 16: 4727-4737.

Prelich, G. and Winston, F. 1993. Mutations that suppress the deletion of an upstream activating sequence in yeast: Involvement of a protein kinase and histone H3 in repressing transcription in vivo. *Genetics.* 135: 665-676.

Prendergast, J.A., Murray, L.E., Rowley, A., Carruthers, D.R., Singer, R.A. and Johnston, G.C. 1990. Size selection identifies new genes that regulate saccharomyces cerevisiae cell proliferation. *Genetics.* 124: 81-90.

Price, D.H. 2000. P-TEFb, a cyclin-dependent kinase controlling elongation by RNA polymerase II. *Mol. Cell. Biol.* 20: 2629-2634.

Prochasson, P., Florens, L., Swanson, S.K., Washburn, M.P. and Workman, J.L. 2005. The HIR corepressor complex binds to nucleosomes generating a distinct protein/DNA complex resistant to remodeling by SWI/SNF. *Genes Dev.* 19: 2534-2539.

Qiu, H., Hu, C., Wong, C.M. and Hinnebusch, A.G. 2006. The Spt4p subunit of yeast DSIF stimulates association of the Paf1 complex with elongating RNA polymerase II. *Mol. Cell. Biol.* 26: 3135-3148.

Raines, R.T., McCormick, M., Van Oosbree, T.R. and Mierendorf, R.C. 2000. The S.tag fusion system for protein purification. *Methods Enzymol.* 326: 362-376.

Ramanathan, Y., Rajpara, S.M., Reza, S.M., Lees, E., Shuman, S., Mathews, M.B. and Pe'ery, T. 2001. Three RNA polymerase II carboxyl-terminal domain kinases display distinct substrate preferences. *J. Biol. Chem.* 276: 10913-10920.

Ramaswamy, A., Bahar, I. and Ioshikhes, I. 2005. Structural dynamics of nucleosome core particle: Comparison with nucleosomes containing histone variants. *Proteins.* 58: 683-696.

Recht, J., Tsubota, T., Tanny, J.C., Diaz, R.L., Berger, J.M., Zhang, X., Garcia, B.A., Shabanowitz, J., Burlingame, A.L., Hunt, D.F., Kaufman, P.D. and Allis, C.D. 2006. Histone chaperone Asf1 is required for histone H3 lysine 56 acetylation, a modification associated with S phase in mitosis and meiosis. *Proc. Natl. Acad. Sci. U. S. A.* 103: 6988-6993.

Reed, J.C., Bidwai, A.P. and Glover, C.V. 1994. Cloning and disruption of CKB2, the gene encoding the 32-kDa regulatory beta'-subunit of saccharomyces cerevisiae casein kinase II. *J. Biol. Chem.* 269: 18192-18200.

Reifsnyder, C., Lowell, J., Clarke, A. and Pillus, L. 1996. Yeast SAS silencing genes and human genes associated with AML and HIV-1 tat interactions are homologous with acetyltransferases. *Nat. Genet.* 14: 42-49.

Reinberg, D. and Sims, R.J.,3rd 2006. De FACTo nucleosome dynamics. *J. Biol. Chem.* 281: 23297-23301.

Rhoades, A.R., Ruone, S. and Formosa, T. 2004. Structural features of nucleosomes reorganized by yeast FACT and its HMG box component, Nhp6. *Mol. Cell. Biol.* 24: 3907-3917.

Roberts, S.M. and Winston, F. 1996. SPT20/ADA5 encodes a novel protein functionally related to the TATA-binding protein and important for transcription in saccharomyces cerevisiae. *Mol. Cell. Biol.* 16: 3206-3213.

Roeder, G.S. and Fink, G.R. 1980. DNA rearrangements associated with a transposable element in yeast. *Cell.* 21: 239-249.

Rondon, A.G., Gallardo, M., Garcia-Rubio, M. and Aguilera, A. 2004. Molecular evidence indicating that the yeast PAF complex is required for transcription elongation. *EMBO Rep.* 5: 47-53.

Rosonina, E. and Manley, J.L. 2005. From transcription to mRNA: PAF provides a new path. *Mol. Cell.* 20: 167-168.

Rowley, A., Singer, R.A. and Johnston, G.C. 1991. CDC68, a yeast gene that affects regulation of cell proliferation and transcription, encodes a protein with a highly acidic carboxyl terminus. *Mol. Cell. Biol.* 11: 5718-5726.

Ruiz-Carrillo, A., Jorcano, J.L., Eder, G. and Lurz, R. 1979. In vitro core particle and nucleosome assembly at physiological ionic strength. *Proc. Natl. Acad. Sci. U. S. A.* 76: 3284-3288.

Saha, A., Wittmeyer, J. and Cairns, B.R. 2006a. Chromatin remodelling: The industrial revolution of DNA around histones. *Nat. Rev. Mol. Cell Biol.* 7: 437-447.

Saha, A., Wittmeyer, J. and Cairns, B.R. 2006b. Mechanisms for nucleosome movement by ATP-dependent chromatin remodeling complexes. *Results Probl. Cell Differ.* 41: 127-148.

Sambrook, J., Fitsch, E.F. and Maniatis, T. 1989. *Molecular cloning: A laboratory manual.* Cold Spring Harbor Laboratory Press, New York, NY.

Sancar, G.B. 2000. Enzymatic photoreactivation: 50 years and counting. *Mutat. Res.* 451: 25-37.

Sanger, F., Nicklen, S. and Coulson, A.R. 1977. DNA sequencing with chain-terminating inhibitors. *Proc. Natl. Acad. Sci. U. S. A.* 74: 5463-5467.

Santoso, D. and Thornburg, R. 1998. Uridine 5'-monophosphate synthase is transcriptionally regulated by pyrimidine levels in nicotiana plumbaginifolia. *Plant Physiol.* 116: 815-821.

Santos-Rosa, H., Schneider, R., Bannister, A.J., Sherriff, J., Bernstein, B.E., Emre, N.C., Schreiber, S.L., Mellor, J. and Kouzarides, T. 2002. Active genes are tri-methylated at K4 of histone H3. *Nature.* 419: 407-411.

Saunders, A., Werner, J., Andrulis, E.D., Nakayama, T., Hirose, S., Reinberg, D. and Lis, J.T. 2003. Tracking FACT and the RNA polymerase II elongation complex through chromatin in vivo. *Science.* 301: 1094-1096.

Schlesinger, M.B. and Formosa, T. 2000. POB3 is required for both transcription and replication in the yeast saccharomyces cerevisiae. *Genetics.* 155: 1593-1606.

Schneider, J., Bajwa, P., Johnson, F.C., Bhaumik, S.R. and Shilatifard, A. 2006. Rtt109 is required for proper H3K56 acetylation: A chromatin mark associated with the elongating RNA polymerase II. *J. Biol. Chem.* 281: 37270-37274.

Schneider, J., Wood, A., Lee, J.S., Schuster, R., Dueker, J., Maguire, C., Swanson, S.K., Florens, L., Washburn, M.P. and Shilatifard, A. 2005. Molecular regulation of histone H3 trimethylation by COMPASS and the regulation of gene expression. *Mol. Cell.* 19: 849-856.

Scholes, D.T., Banerjee, M., Bowen, B. and Curcio, M.J. 2001. Multiple regulators of Ty1 transposition in saccharomyces cerevisiae have conserved roles in genome maintenance. *Genetics.* 159: 1449-1465.

Schwabish, M.A. and Struhl, K. 2006. Asf1 mediates histone eviction and deposition during elongation by RNA polymerase II. *Mol. Cell.* 22: 415-422.

Segal, E., Fondufe-Mittendorf, Y., Chen, L., Thastrom, A., Field, Y., Moore, I.K., Wang, J.P. and Widom, J. 2006. A genomic code for nucleosome positioning. *Nature.* 442: 772-778.

Selth, L. and Svejstrup, J.Q. 2007. Vps75, a new yeast member of the NAP histone chaperone family. *J. Biol. Chem.* 282: 12358-12362.

Sena, E.P., Radin, D.N. and Fogel, S. 1973. Synchronous mating in yeast. *Proc. Natl. Acad. Sci. U. S. A.* 70: 1373-1377.

Shen, X., Ranallo, R., Choi, E. and Wu, C. 2003. Involvement of actin-related proteins in ATP-dependent chromatin remodeling. *Mol. Cell.* 12: 147-155.

Sherwood, P.W., Tsang, S.V. and Osley, M.A. 1993. Characterization of HIR1 and HIR2, two genes required for regulation of histone gene transcription in saccharomyces cerevisiae. *Mol. Cell. Biol.* 13: 28-38.

Shi, X., Finkelstein, A., Wolf, A.J., Wade, P.A., Burton, Z.F. and Jaehning, J.A. 1996. Paf1p, an RNA polymerase II-associated factor in saccharomyces cerevisiae, may have both positive and negative roles in transcription. *Mol. Cell. Biol.* 16: 669-676.

Sikorski, R.S. and Hieter, P. 1989. A system of shuttle vectors and yeast host strains designed for efficient manipulation of DNA in saccharomyces cerevisiae. *Genetics.* 122: 19-27.

Silverman, S.J. and Fink, G.R. 1984. Effects of ty insertions on HIS4 transcription in saccharomyces cerevisiae. *Mol. Cell. Biol.* 4: 1246-1251.

Simic, R., Lindstrom, D.L., Tran, H.G., Roinick, K.L., Costa, P.J., Johnson, A.D., Hartzog, G.A. and Arndt, K.M. 2003. Chromatin remodeling protein Chd1 interacts with transcription elongation factors and localizes to transcribed genes. *EMBO J.* 22: 1846-1856.

Singer, M.S., Kahana, A., Wolf, A.J., Meisinger, L.L., Peterson, S.E., Goggin, C., Mahowald, M. and Gottschling, D.E. 1998. Identification of high-copy disruptors of telomeric silencing in saccharomyces cerevisiae. *Genetics.* 150: 613-632.

Smith, E.R., Eisen, A., Gu, W., Sattah, M., Pannuti, A., Zhou, J., Cook, R.G., Lucchesi, J.C. and Allis, C.D. 1998. ESA1 is a histone acetyltransferase that is essential for growth in yeast. *Proc. Natl. Acad. Sci. U. S. A.* 95: 3561-3565.

Smith, S. and Stillman, B. 1991. Stepwise assembly of chromatin during DNA replication in vitro. *EMBO J.* 10: 971-980.

Smith, S. and Stillman, B. 1989. Purification and characterization of CAF-I, a human cell factor required for chromatin assembly during DNA replication in vitro. *Cell.* 58: 15-25.

Spector, M.S., Raff, A., DeSilva, H., Lee, K. and Osley, M.A. 1997. Hir1p and Hir2p function as transcriptional corepressors to regulate histone gene transcription in the saccharomyces cerevisiae cell cycle. *Mol. Cell. Biol.* 17: 545-552.

Squazzo, S.L., Costa, P.J., Lindstrom, D.L., Kumer, K.E., Simic, R., Jennings, J.L., Link, A.J., Arndt, K.M. and Hartzog, G.A. 2002. The Paf1 complex physically and functionally associates with transcription elongation factors in vivo. *EMBO J.* 21: 1764-1774.

Sterner, D.E., Belotserkovskaya, R. and Berger, S.L. 2002. SALSA, a variant of yeast SAGA, contains truncated Spt7, which correlates with activated transcription. *Proc. Natl. Acad. Sci. U. S. A.* 99: 11622-11627.

Strahl, B.D., Grant, P.A., Briggs, S.D., Sun, Z.W., Bone, J.R., Caldwell, J.A., Mollah, S., Cook, R.G., Shabanowitz, J., Hunt, D.F. and Allis, C.D. 2002. Set2 is a nucleosomal histone H3-selective methyltransferase that mediates transcriptional repression. *Mol. Cell. Biol.* 22: 1298-1306.

Sun, Z.W. and Allis, C.D. 2002. Ubiquitination of histone H2B regulates H3 methylation and gene silencing in yeast. *Nature.* 418: 104-108.

Swanson, M.S., Malone, E.A. and Winston, F. 1991. SPT5, an essential gene important for normal transcription in saccharomyces cerevisiae, encodes an acidic nuclear protein with a carboxy-terminal repeat. *Mol. Cell. Biol.* 11: 3009-3019.

Swanson, M.S. and Winston, F. 1992. SPT4, SPT5 and SPT6 interactions: Effects on transcription and viability in saccharomyces cerevisiae. *Genetics.* 132: 325-336.

Timmers, H.T. and Tora, L. 2005. SAGA unveiled. *Trends Biochem. Sci.* 30: 7-10.

Tong, A.H., Evangelista, M., Parsons, A.B., Xu, H., Bader, G.D., Page, N., Robinson, M., Raghibizadeh, S., Hogue, C.W., Bussey, H., Andrews, B., Tyers, M. and Boone, C. 2001. Systematic genetic analysis with ordered arrays of yeast deletion mutants. *Science.* 294: 2364-2368.

Tong, A.H., Lesage, G., Bader, G.D., Ding, H., Xu, H., Xin, X., Young, J., Berriz, G.F., Brost, R.L., Chang, M., Chen, Y., Cheng, X., Chua, G., Friesen, H., Goldberg, D.S., Haynes, J., Humphries, C., He, G., Hussein, S., Ke, L., Krogan, N., Li, Z., Levinson, J.N., Lu, H., Menard, P., Munyana, C., Parsons, A.B., Ryan, O., Tonikian, R., Roberts, T., Sdicu, A.M., Shapiro, J., Sheikh, B., Suter, B., Wong, S.L., Zhang, L.V., Zhu, H., Burd, C.G., Munro, S., Sander, C., Rine, J., Greenblatt, J., Peter, M., Bretscher, A., Bell, G., Roth, F.P., Brown, G.W., Andrews, B., Bussey, H. and Boone, C. 2004. Global mapping of the yeast genetic interaction network. *Science.* 303: 808-813.

Tran, H.G., Steger, D.J., Iyer, V.R. and Johnson, A.D. 2000. The chromo domain protein chd1p from budding yeast is an ATP-dependent chromatin-modifying factor. *EMBO J.* 19: 2323-2331.

Tsubota, T., Berndsen, C.E., Erkmann, J.A., Smith, C.L., Yang, L., Freitas, M.A., Denu, J.M. and Kaufman, P.D. 2007. Histone H3-K56 acetylation is catalyzed by histone chaperone-dependent complexes. *Mol. Cell.* 25: 703-712.

Tsukada, Y., Fang, J., Erdjument-Bromage, H., Warren, M.E., Borchers, C.H., Tempst, P. and Zhang, Y. 2006. Histone demethylation by a family of JmjC domain-containing proteins. *Nature.* 439: 811-816.

Tu, S., Bulloch, E.M., Yang, L., Ren, C., Huang, W.C., Hsu, P.H., Chen, C.H., Liao, C.L., Yu, H.M., Lo, W.S., Freitas, M.A. and Tsai, M.D. 2007. Identification of histone demethylases in saccharomyces cerevisiae. *J. Biol. Chem.* 282: 14262-14271.

Tyler, J.K. 2002. Chromatin assembly. cooperation between histone chaperones and ATP-dependent nucleosome remodeling machines. *Eur. J. Biochem.* 269: 2268-2274.

Tyler, J.K., Adams, C.R., Chen, S.R., Kobayashi, R., Kamakaka, R.T. and Kadonaga, J.T. 1999. The RCAF complex mediates chromatin assembly during DNA replication and repair. *Nature.* 402: 555-560.

Tyler, J.K., Collins, K.A., Prasad-Sinha, J., Amiott, E., Bulger, M., Harte, P.J., Kobayashi, R. and Kadonaga, J.T. 2001. Interaction between the drosophila CAF-1 and ASF1 chromatin assembly factors. *Mol. Cell. Biol.* 21: 6574-6584.

VanDemark, A.P., Blanksma, M., Ferris, E., Heroux, A., Hill, C.P. and Formosa, T. 2006. The structure of the yFACT Pob3-M domain, its interaction with the DNA replication factor RPA, and a potential role in nucleosome deposition. *Mol. Cell.* 22: 363-374.

Vogelauer, M., Wu, J., Suka, N. and Grunstein, M. 2000. Global histone acetylation and deacetylation in yeast. *Nature.* 408: 495-498.

Voth, W.P., Jiang, Y.W. and Stillman, D.J. 2003. New 'marker swap' plasmids for converting selectable markers on budding yeast gene disruptions and plasmids. *Yeast.* 20: 985-993.

Wach, A., Brachat, A., Rebischung, C., Steiner, S., Pokorni, K., te Heesen, S. and Philippsen, P. 1998. PCR-based gene targeting in *saccharomyces cerevisiae.* in *Methods in microbiology* (eds, A.J.P. Brown and M.F. Tuite)Academic Press, San Diego, CA.

Wada, T., Takagi, T., Yamaguchi, Y., Ferdous, A., Imai, T., Hirose, S., Sugimoto, S., Yano, K., Hartzog, G.A., Winston, F., Buratowski, S. and Handa, H. 1998. DSIF, a novel transcription elongation factor that regulates RNA polymerase II processivity, is composed of human Spt4 and Spt5 homologs. *Genes Dev.* 12: 343-356.

White, C.L., Suto, R.K. and Luger, K. 2001. Structure of the yeast nucleosome core particle reveals fundamental changes in internucleosome interactions. *EMBO J.* 20: 5207-5218.

Wilson, B., Erdjument-Bromage, H., Tempst, P. and Cairns, B.R. 2006. The RSC chromatin remodeling complex bears an essential fungal-specific protein module with broad functional roles. *Genetics.* 172: 795-809.

Winston, F. 1992. Analysis of *SPT* genes: A genetic approach toward analysis of TFIID, histones, and other transcription factors of yeast. in *Transcriptional regulation* (eds, S.L. McKnight and K.R. Yamamoto), pp. 1271-1292. Cold Spring Harbor Laboratory Press, Cold Spring Harbor, NY.

Winston, F., Chaleff, D.T., Valent, B. and Fink, G.R. 1984. Mutations affecting ty-mediated expression of the HIS4 gene of saccharomyces cerevisiae. *Genetics.* 107: 179-197.

Wittmeyer, J. and Formosa, T. 1997. The saccharomyces cerevisiae DNA polymerase alpha catalytic subunit interacts with Cdc68/Spt16 and with Pob3, a protein similar to an HMG1-like protein. *Mol. Cell. Biol.* 17: 4178-4190.

Wittmeyer, J., Joss, L. and Formosa, T. 1999. Spt16 and Pob3 of saccharomyces cerevisiae form an essential, abundant heterodimer that is nuclear, chromatin-associated, and copurifies with DNA polymerase alpha. *Biochemistry.* 38: 8961-8971.

Wittschieben, B.O., Otero, G., de Bizemont, T., Fellows, J., Erdjument-Bromage, H., Ohba, R., Li, Y., Allis, C.D., Tempst, P. and Svejstrup, J.Q. 1999. A novel histone acetyltransferase is an integral subunit of elongating RNA polymerase II holoenzyme. *Mol. Cell.* 4: 123-128.

Wood, A., Schneider, J., Dover, J., Johnston, M. and Shilatifard, A. 2005. The Bur1/Bur2 complex is required for histone H2B monoubiquitination by Rad6/Bre1 and histone methylation by COMPASS. *Mol. Cell.* 20: 589-599.

Wood, A., Schneider, J., Dover, J., Johnston, M. and Shilatifard, A. 2003. The Paf1 complex is essential for histone monoubiquitination by the Rad6-Bre1 complex, which signals for histone methylation by COMPASS and Dot1p. *J. Biol. Chem.* 278: 34739-34742.

Wood, A. and Shilatifard, A. 2006. Bur1/Bur2 and the ctk complex in yeast: The split personality of mammalian P-TEFb. *Cell. Cycle.* 5: 1066-1068.

Worcel, A., Han, S. and Wong, M.L. 1978. Assembly of newly replicated chromatin. *Cell.* 15: 969-977.

Workman, J.L. 2006. Nucleosome displacement in transcription. *Genes Dev.* 20: 2009-2017.

Xiao, T., Hall, H., Kizer, K.O., Shibata, Y., Hall, M.C., Borchers, C.H. and Strahl, B.D. 2003. Phosphorylation of RNA polymerase II CTD regulates H3 methylation in yeast. *Genes Dev.* 17: 654-663.

Xu, F., Zhang, K. and Grunstein, M. 2005. Acetylation in histone H3 globular domain regulates gene expression in yeast. *Cell.* 121: 375-385.

Xu, Q., Johnston, G.C. and Singer, R.A. 1993. The saccharomyces cerevisiae Cdc68 transcription activator is antagonized by San1, a protein implicated in transcriptional silencing. *Mol. Cell. Biol.* 13: 7553-7565.

Xu, Q., Singer, R.A. and Johnston, G.C. 1995. Sug1 modulates yeast transcription activation by Cdc68. *Mol. Cell. Biol.* 15: 6025-6035.

Yamada, T., Yamaguchi, Y., Inukai, N., Okamoto, S., Mura, T. and Handa, H. 2006. P-TEFb-mediated phosphorylation of hSpt5 C-terminal repeats is critical for processive transcription elongation. *Mol. Cell.* 21: 227-237.

Yao, S., Neiman, A. and Prelich, G. 2000. BUR1 and BUR2 encode a divergent cyclin-dependent kinase-cyclin complex important for transcription in vivo. *Mol. Cell. Biol.* 20: 7080-7087.

Yu, Y., Eriksson, P., Bhoite, L.T. and Stillman, D.J. 2003. Regulation of TATA-binding protein binding by the SAGA complex and the Nhp6 high-mobility group protein. *Mol. Cell. Biol.* 23: 1910-1921.

Zhang, Y., Yu, Z., Fu, X. and Liang, C. 2002. Noc3p, a bHLH protein, plays an integral role in the initiation of DNA replication in budding yeast. *Cell.* 109: 849-860.